Natural genetic variation for regulation of photosynthesis response to light in *Arabidopsis thaliana*

Roxanne van Rooijen

Natural genetic variation for regulation of photosynthesis response to light in *Arabidopsis thaliana*

Roxanne van Rooijen

Thesis

submitted in fulfilment of the requirements for the degree of doctor

at Wageningen University

by the authority of the Rector Magnificus

Prof. Dr A.P.J. Mol,

in the presence of the

Thesis Committee appointed by the Academic Board

to be defended in public

on Tuesday 05 July 2016

at 11 a.m. in the Aula.

Roxanne van Rooijen

Natural genetic variation for regulation of photosynthesis response to light in *Arabidopsis thaliana*

235 pages.

Contents

Chapter 1

General Introduction

Uncovering the molecular basis of growth, development, and adaptation is a major research area in plant science, with useful applications in plant breeding. Photosynthesis is an underused resource for plant breeding because of its physiological and molecular complexity as well as its complex relationship with yield. However, it is acknowledged to have great potential for crop improvement (Lawson et al., 2012; Long et al., 2015). The light-use efficiency of photosynthesis depends on the molecular, structural and physiological state of the plant (Eberhard et al., 2008; Zhu et al., 2008; Foyer et al., 2012). The physiological state depends on many environmental factors, of which the level of irradiance has a direct relation with photosynthesis light-use efficiency as it is the driving force for photosynthesis. Sudden increases in the level of irradiance can result in a situation in which the incoming light level exceeds the capacity for photosynthetic metabolism. Acclimation to increased irradiance is crucial for plant survival, as excess incoming light levels lead to damaged photosystems and the production of reactive oxygen species (ROS). The acclimation response of photosynthesis appears to reduce the formation of ROS, especially under excess irradiance levels (Scheibe et al., 2005; Suzuki et al., 2012).

This thesis describes a study into natural genetic variation for the acclimation response of photosynthetic light use efficiency to increased growth irradiance. By identifying and characterizing genes for which different alleles affect photosynthesis responses, I could reveal some of the regulatory and physiological processes underlying natural variation for photosynthetic acclimation to a step increase in irradiance

Photosynthesis

Central to this thesis is the understanding of photosynthesis at the molecular level. When trying to identify genes, one needs to realize each gene encodes for one protein. A protein is a biological macro-molecule, consisting of a chain of amino acids folded in a specific three-dimensional structure that determines its pattern of activity. The sequence of amino acids is encoded for by the gene and one small change in the gene's DNA sequence can result in a different amino acid, which can result in different structural properties of the protein, which can result in a different biological functionality.

The process of photosynthesis has been studied for long time, with its first discovery by Jan van Helmont in the 17th century, who discovered that the mass of a growing plant came from water and carbon dioxide (and not from soil). In the next century, Jan

Ingenhousz discovered this process was powered by sunlight. Not long after that, it was discovered that both CO_2 and water are the substrates for a plant to form biomass and O_2 under the influence of light energy (Hill, 2012).

Photosynthesis is a complex process both at the physiological as well as the molecular level, involving many steps. These include the light reactions: the harvest of light energy, the transfer of excitation energy, the energy conversion, the electron transfer from water to $NADP^+$, the oxygen evolution, and the ATP generation; and the dark reactions: the Calvin cycle that fixes CO_2 to assimilate carbohydrates, catalysed by the enzyme ribulose-1,5-bisphosphate carboxylase/oxygenase (Rubisco) (Fig. 1). Proteins and cofactors, coded for by genes, execute all of these steps. Some of these genes are encoded in the nuclear genome, and some in the chloroplast genome, requiring complex cross talk between nucleus and chloroplast. The work described in this thesis is focussed the identification and characterization of genes involved in photosynthesis responses to increased light levels extending over several days, which is directly related to the primary processes of photosynthesis (light harvesting and energy conversion), the energy transduction machinery, and the metabolic processes of photosynthesis. The applied genetic methods exclusively targeted the nuclear encoded genes.
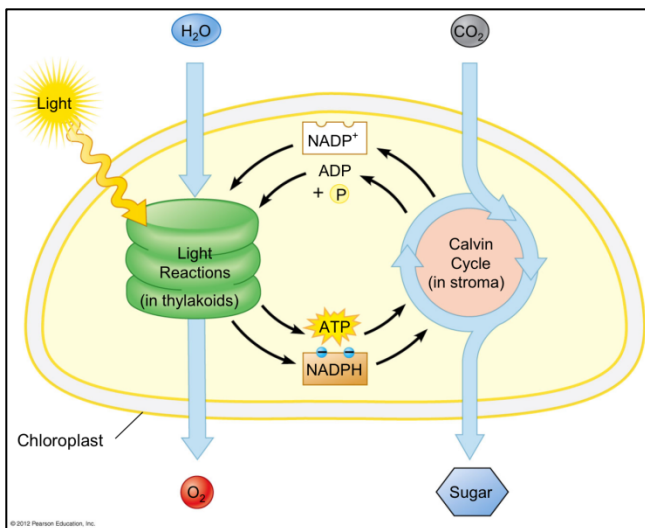

Figure 1. The light and dark reactions (Calvin Cycle) of photosynthesis.
Picture from Pearson Education, 2012.

Photosynthesis occurs in the chloroplasts, where chlorophyll molecules divided over two different photosystems harvest the incoming light. The photosystems are embedded in

9

the thylakoid membranes, which are specialized structures laying inside the chloroplast. Photosystem II (also known as PSII, Psb, and P600) absorbs light up to 600 nm wavelength and contains both chlorophyll a and chlorophyll b. Photosystem I (also known as PSI, Psa, and P700), absorbs light up to 700 nm wavelength and contains only chlorophyll a. At the molecular level, both photosystems are connected to light harvesting complexes (LHCI for PSI and LHCII for PSII). PSII is associated with the oxygen-evolving complex (also known as the water-splitting complex), which donates an electron coming from a water-molecule each time PSII is excited with light (Fig 2). This is the first reaction of the light reactions, using the high-energy state of the chlorophyll molecules associated with PSII. This energy then enters an electron transport chain involving plastoquinone (PQ), cytochrome b_6/f (Cyt b_6/f), and plastocyanin (PC), whereby the high energy molecule ATP is produced that is later needed in the dark reactions of photosynthesis (Fig. 2). The ATP is formed through an ATPase acting as a proton-pump, pumping the H^+ coming from the water molecules through the thylakoid membranes resulting in proton motive force (Fig. 2). At the end of the electron transport chain, the electron has lost its energy, and is donated to PSI. The excited electrons from PSI are then donated to ferredoxin (Fd), a soluble protein that facilitates reduction of NADP+ to NADPH, a high-energy molecule needed for the dark reactions of photosynthesis (Fig. 2).
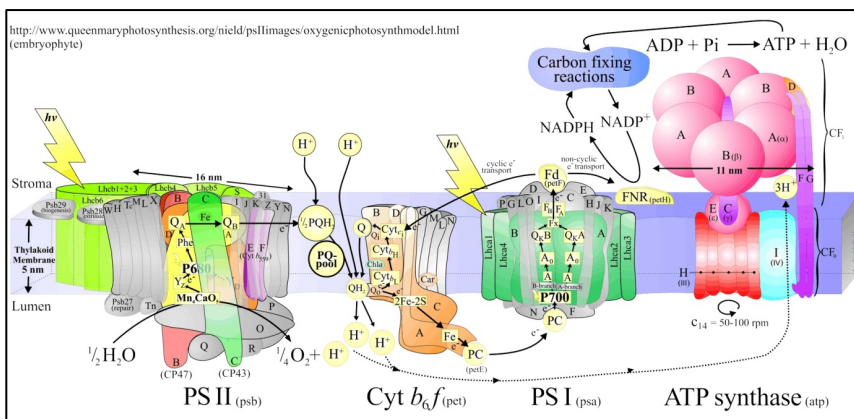

Figure 2. The light reactions of photosynthesis occurring in the thylakoid membrane showing all structural proteins forming PSII, CytB6f, PSI, and the ATP synthase, and their link to the carbon fixing dark reactions through ATP and NADPH supply.
Picture from Dr. Jon Nield (http://macromol.sbcs.qmul.ac.uk/).

10

Sensing and responding to excess light

Light is the driving force for photosynthesis, and the relationship between light and photosynthesis is complex. Light is essential for photosynthesis, but absorbed light exceeding the photosynthetic capacity of a plant gives rise to reactive intermediates and by-products that can damage the photosynthetic machinery (Powles, 1984; Asada, 2006). Protection from these damaging processes, while at the same time permitting high photosynthetic rates under high light conditions, seems to be the driving force behind the evolution of many of the regulatory processes of photosynthesis. This thesis describes discoveries on the genetic variation apparent for these regulatory processes in natural populations, explaining part of the photosynthetic acclimation process. This requires understanding of the physiological and molecular regulatory processes occurring in the plant cell when it experiences excess light stress. Excess light can arise simply when the amount of absorbed light exceeds the plant's photosynthetic capacity, but can also result from decreases in photosynthesis rates as result of chilling or water stress. This thesis only focusses on the first situation.

Plants have evolved several mechanisms for sensing increases in absorbed irradiance levels (Li et al., 2009); they sense it using several classes of photoreceptors, and they sense it through biochemical and metabolic signals. The photoreceptors involved in excess light response are: phototropins, phytochromes and cryptochromes. The biochemical and metabolic signals come from internal redox and internal pH levels (Li et al., 2009).

The photoreceptor phototropin mediates avoidance response of chloroplast, which makes these move to the sides of a plant cell to avoid excess light absorption (Kasahara et al., 2002). Changes in light quantity can come about with changes in light quality, especially when a plant is moved from a shaded environment to an exposed environment. When plants shade each other, this causes a change in the light spectrum, as the chlorophyll of the upper plants absorbs some wavelengths. Only the light that is outside the spectral range and capacity for the upper plants is transmitted to the lower plants. The changes in spectral composition of the light when a plant is moved from a shaded to exposed environment is sensed by the phytochrome photoreceptor. Phytochrome mainly influences responses unrelated to photosynthesis, such as stem- and leaf elongation, flowering time, and seed maturation (Schepens et al., 2004). The cryptochrome photoreceptor is shown to regulate a large number of genes in response to increased light, that at the end of the signalling cascade lead to formation of flavonoids and

anthocyanins that protect photosynthesis tissue from high light damage by absorbing the high energy containing blue-green and ultraviolet light, significantly reducing the amount of ROS produced (Kleine et al., 2007).

Two major biochemical signals indicate excess light, a pH-change within the chloroplast occurring within milliseconds after the induction of the stress (proton gradient dependent regulation) and a redox change via changes in thioredoxin levels and oxidized/reduced plastoquinone ratios as well as through a build-up of ROS (redox-dependent regulation). The pH-change, occurring over the thylakoid membranes, results from a decrease in the ATPase proton-pump. The extra electrons coming from the increased irradiance level will go to other acceptors than the electron transport chain, such as oxygen (producing ROS) or thioredoxin, resulting in decreased lumen pH. This is sensed by the protein PsbS (Li et al., 2004), which then activates the energy-dependent part of the photoprotection response (non-photochemical quenching, NPQ), (Demmig-Adams and Adams, 1992). NPQ is a mechanism involving the fast dissipation of the excess excitation energy as heat. It involves several molecular mechanisms, which are energy-dependent quenching (qE), quenching associated with state transitions (qT), and photoinhibitory quenching (qI), (Horton and Hague, 1988). The fastest response is qE, which is the only NPQ mechanism initiated by the protein PsbS, involves dissipating the excess energy through the xanthophyll cycle, resulting in the formation of zeaxanthin. Protonation of PsbS and binding of zeaxanthin to PSII produces conformational changes in the photosystems that result in increases in the efficient heat dissipation of the excess energy (Sylak-Glassman et al., 2014). The second NPQ response is qT, where phosphorylation of PSII associated light-harvesting complexes results in a decrease in the cross section of PSII with LHCII and an increase in that of PSI and LHCII, thereby adjusting the relative excitation energy distribution between PSII and PSI (Tikkanen et al., 2010). The last NPQ response is qI, resulting from photoinhibition of photochemistry, increasing the dissipation of excitation energy as heat, by breaking down photosynthetic proteins. NPQ is a photoprotection response occurring mainly around PSII. PSI has evolved an alternative protective mechanism for excess light, resulting in cyclic electron flow around PSI (Munekage et al., 2004). In cyclic electron flow, electrons can be recycled from either reduced ferredoxin or NADPH to plastoquinone, and subsequently to the cytochrome b_6/f complex. This generates a renewed proton motive force for ATP production, decreasing lumen pH without the accumulation of ROS, thus protecting the photosystem proteins from damage and keeping up the supply of ATP and NADPH enabling increased photosynthesis rates. A third alternative for the dissipation of excess electrons is the donation to O_2, forming H_2O_2 and ultimately water. This is known as the water-water cycle, because the initial

12

reaction in photosynthesis is the splitting of water, donating electrons to PSII for excitation. It is also known as the Mehler reaction, named after its first discoverer (Mehler and Brown, 1952). Extra advantage of the water-water cycle is it also scavenges ROS, as it binds superoxide formed by the reduction of O_2 (Asada, 1999).

When the excess light persists after a few hours when photoprotection has finished, the plant will start altering its photosynthetic proteome, via what is known as photosynthetic acclimation (Walters, 2005). This response is initiated by the photoreceptor cryptochrome (the CRY1 protein), as well as by several heat-shock proteins and heat shock transcription factors (Rossel et al., 2002; Kleine et al., 2007). Ultimately, photosynthetic acclimation will provoke changes in the cellular composition in terms of their organisation of the photosystems, proteins, pigments, lipids, and other cofactors involved in electron transport and ROS metabolism (Bailey et al., 2004; Walters, 2005). Regarding the organisation of the photosystems, in response to high irradiance PSII acclimates by decreasing its antenna size via a decrease the amount of LHCII proteins associated with the PSII supercomplex, analogous to the short-term qT response (Kouřil et al., 2013). The ratio of LHCI to PSI is not altered, but the antenna size of PSI deceases with increasing irradiance due to a decreased association of LHCII with PSI (Ballottari et al., 2007; Wientjes et al., 2013). All the changes during photosynthetic acclimation are the result of signal-induced changes in gene expression, in a tight co-ordinated regulation between nuclear and chloroplast genes. At the time when I started the project of which the results are described in this thesis, molecular understanding of photosynthetic acclimation lagged behind the understanding of photosynthesis itself as well as behind the molecular understanding of photoprotection.

Phenotyping photosynthesis

Photosynthesis is about taking up CO_2 for fixation into carbohydrates, and releasing back O_2 into the atmosphere. Therefore, its most direct measurement for photosynthesis efficiency is through gas exchange analysis (Von Caemmerer and Farquhar, 1981; Long et al., 1996b; Johnson and Murchie, 2011). Infra-red sensors for gas analysis (IRGA) are most common for CO_2 measurement and are based on an infrared emitter-photodetector of which the light beam is used to measure the concentration of gas molecules in the air of a leaf chamber (Sesták et al., 1971). In order to measure variation for photosynthesis efficiency among natural populations, the IRGA method is very laborious as for every plant at least one leaf (normally it is leaves that are measured rather than shoots or larger

parts of plants) has to be enclosed inside a leaf chamber each time photosynthesis is measured.

Besides gas-exchange, photosynthesis is about efficiently using the light energy that is absorbed by the plant. Once a photon is absorbed by the plant, it can have three fates: used for photosynthesis (photochemistry), dissipated as heat (a process facilitated by photoprotection), or re-emitted as chlorophyll fluorescence (Butler, 1978). Chlorophyll fluorescence is the light re-emitted by chlorophyll molecules during return from excited to non-excited states, and is the only one of the three fates that can easily be measured. Using a smart design of repeatedly measuring chlorophyll fluorescence in open and closed photosystems, calculations can be made of the amount of light energy going into photochemistry, and thus the photosynthetic light use efficiency, Φ_{PSII} (Baker, 2008). Because chlorophyll fluorescence can be detected using a camera, it is non-destructive and it can easily handle many plants by either automatically moving each plant to the camera, or automatically moving the camera to each plant (Harbinson et al., 2012; Flood et al., 2016).

From phenotype to genotype

The area within biology that tries to genetically explain phenotypes that vary continuously, such as photosynthetic light use efficiency, is called quantitative genetics, whereby the genetic loci explaining the phenotypes are called quantitative trait loci (QTLs), (Alonso-Blanco et al., 2009; Alonso-Blanco and Méndez-Vigo, 2014). To perform quantitative genetics in plants, *Arabidopsis thaliana* is the model species of choice, because of its well-described genetics, its wide availability of genotyped natural accessions, and the ability to exploit it in genome wide association studies (GWAS), (Atwell et al., 2010; Bergelson and Roux, 2010; Ogura and Busch, 2015). Genome-wide association studies (GWAS) analyse natural variation in populations consisting of a large number of natural isogenic lines collected from nature, called natural accessions in case of *Arabidopsis thaliana* (Arabidopsis). The accessions are collected worldwide in the native range of Arabidopsis, and as such have genetically adapted to different ecological conditions over thousands of years. In order to genetically map quantitative traits to the genome, GWAS take advantage of the recombination events that have accumulated over all those generations resulting in a high mapping resolution (Bergelson and Roux, 2010). An important aspect to consider when performing GWAS is Linkage Disequilibrium (LD), which is the non-random association of alleles at different loci, affecting the number of

14

recombination events occurring through time (Kim et al., 2007). When LD is only over short lengths in the genome, it requires a very high density of genotyping to find causal loci for a phenotypic trait in GWAS. Over the past years, GWAS have proven to be successful in Arabidopsis for identifying novel genes underlying the natural variation in several physiological (Atwell et al., 2010; Chao et al., 2012), morphological (Filiault and Maloof, 2012), cellular (Meijón et al., 2014; Verslues et al., 2014), and defence-related traits (Horton et al., 2014). The interpretation of association peaks in GWAS is not straightforward as population structure can lead to the occurrence of false positive associations, and the presence of causal alleles with low allele frequency or the presence of multiple alleles having the same phenotype can lead to hidden heritability (Korte and Farlow, 2013). One factor leading to hidden heritability is an epistatic interaction between two (or more) genes, where the allelic effect of one gene is depending on the allelic effect of another gene (Korte and Farlow, 2013).

A more traditional method to link phenotypic variation to genetics is to do family mapping (Lander and Botstein, 1989). For this, two different accessions are crossed, the heterozygous plant that arises is self-fertilized, and the segregating offspring are phenotyped for the trait of interest, and genotyped for enough molecular markers to cover the genome. In this approach, different numbers of accessions can be (inter-) crossed to vary the amount of genetic variation, and different generations of offspring can be chosen for analysis to vary the level of heterozygosity. While family mapping provides the mapping power that is lacking in GWAS, it has a very low resolution because it depends upon the limited number of recombination events that have occurred in one (or a few) generation(s). The combination of GWAS and family mapping has proven to be a successful strategy in unravelling complex plant genetics (Motte et al., 2014).

Resolving QTLs to the gene level for any biological process being studied will help the physiological and molecular understanding of that process. To study natural genetic variation for any trait, first a survey must be performed on the extent of variation present among different accessions before proceeding to the genetic analysis, as described in chapter 2 of this thesis for photosynthesis efficiency responses to increased irradiance in Arabidopsis.

Outline of thesis

In this thesis, I describe a study of natural genetic variation for photosynthesis responses to increased growth irradiance. This work was carried out within the research programme of BioSolar Cells, co-financed by the Dutch Ministry of Economic Affairs. The aim of Biosolar Cells is to optimize the photosynthesis process in plants, algae and bacteria, and to develop artifical leaves that combine biological and artificial components (www.biosolarcells.nl).

Plants are known to be able to acclimate their photosynthesis to the level of irradiance. **Chapter 2** describes which light environment reveals most natural variation and for which photosynthetic parameter this is. It shows different Arabidopsis accessions display different photosynthetic responses to various light environments, well relatable to genetic differences. A candidate gene list for the direct response to increased growth irradiance was revealed.

Acclimation of photosynthesis to changing light environment is a dynamic trait, for which at different time points, different genes are causal. **Chapter 3** describes the dynamics of the QTLs underlying photosynthetic acclimation to increased growth irradiance. This chapter shows it is possible to simplify the complexity of photosynthetic physiology as well as the genetic analysis in such way to confirm the causal underlying genes. This was confirmed for the *YS1* gene, a gene encoding a Pentatrico-Peptide-Repeat (PPR) protein involved in RNA editing of plastid-encoded genes essential for photosystems I and II.

Genetic variation for any trait can be on the transcriptional level or on the functional level (quantity versus quality). **Chapter 4** analyses the transcriptional response of three Arabidopsis accessions with distinct photosynthesis responses to increased growth irradiance. The existence of a gene activation pathway leading to the process of membrane lipid transformation was shown, whose involvement in photosynthetic acclimation is explained by the replacement of phospholipids by galactolipids for releasing extra orthophosphate (Pi) needed for photosynthetic structures and creating a charge balance to the photosynthetic membranes that is overcharged as a result of the excess light. Accession-specific differences in activation of this gene activation pathway could be associated with variation in photosynthesis efficiency response to increased irradiance.

Chapter 5 describes how genome wide association mapping (GWAS) and family mapping combine to reveal genetic epistatic interactions underlying photosynthetic

acclimation to increased growth irradiance. This chapter shows an epistatic relation between two genes, *PHOSPHATIDIC ACID PHOSPHOHYDROLASE 2 (PAH2)* and *ASPARAGINE SYNTHETASE 2 (ASN2)*. Strong indications are given for the involvement of combinations of specific *PAH2* and *ASN2* natural alleles in keeping high photosynthesis efficiencies in response to increased irradiance.

It In **Chapter 6**, the results of the preceding chapters are discussed in the context of current research on quantitative genetics and photosynthetic physiology.

Chapter 2

Natural genetic variation for acclimation of photosynthetic light use efficiency to growth irradiance in Arabidopsis thaliana

Roxanne van Rooijen[1,2], Mark G.M Aarts[1], Jeremy Harbinson[2]

[1]Laboratory of Genetics & [2]Horticulture and Product Physiology, Wageningen University, Droevendaalsesteeg 1, 6708 PB Wageningen, The Netherlands

ABSTRACT

Plants are known to be able to acclimate their photosynthesis to the level of irradiance. Here we present the analysis of natural genetic variation for photosynthetic light use efficiency (Φ_{PSII}) in response to five light environments among 12 genetically diverse *Arabidopsis thaliana* accessions. We measured acclimation of Φ_{PSII} to constant growth irradiances of four different levels (100, 200, 400, and 600 µmol m^{-2} s^{-1}) by imaging chlorophyll fluorescence after 24 days of growth, and compared these results to acclimation of Φ_{PSII} to a step-wise change in irradiance where the growth irradiance was increased from 100 to 600 µmol m^{-2} s^{-1} after 24 days of growth. Genotypic variation for Φ_{PSII} is shown by calculating heritability for short-term Φ_{PSII} response to different irradiance levels, as well as for the relation of Φ_{PSII} measured at light saturation (a measure of photosynthetic capacity) to growth irradiance level, and for the kinetics of the response to a step-wise increase in irradiance from 100 to 600 µmol m^{-2} s^{-1}. A genome-wide association study for Φ_{PSII} measured one hour after a step-wise increase in irradiance identified several new candidate genes controlling this trait. In conclusion, the different photosynthetic responses to a changing light environment displayed by different Arabidopsis accessions are due to genetic differences, and we have identified candidate genes for the photosynthetic response to an irradiance change. The genetic variation for photosynthetic acclimation to irradiance found in this study will allow future identification and analysis of the causal genes for the regulation of Φ_{PSII} in plants.

Abbreviations:

PSI – photosystem I; PSII – photosystem II; LHC – light harvesting complex; F_o – minimum fluorescence yield in dark-adapted state; F_m – maximum fluorescence yield in dark-adapted state; F_m' – maximum fluorescence yield in light-adapted state; F_v/F_m – maximum photosynthetic light use efficiency of PSII in dark-adapted state; Φ_{PSII} – operating photosynthetic light use efficiency of PSII in light-adapted state; rETR – relative electron transport rate; NPQ – non-photochemical quenching; q_P – co-efficient of photochemical quenching of chlorophyll fluorescence (PSII efficiency facor); F_v'/F_m' – photosynthetic light use efficiency of the open PSII reaction centres in light-adapted state

INTRODUCTION

Light is the driving force for photosynthesis and the relation between light and photosynthesis is complex; light is essential for photosynthesis but absorbed light naturally gives rise to reactive intermediates and by-products that can damage the photosynthetic machinery (Powles, 1984; Asada, 2006). Even at low irradiances these damaging reactions occur and they increase with increasing irradiance as photosynthesis becomes increasingly light-saturated. Protection from these damaging processes, while at the same time permitting high photosynthetic rates under high light conditions and a high light use efficiency under low light conditions, seems to be the driving force behind evolution of many of the regulatory processes of photosynthesis.

Managing the fate of absorbed light energy is regulated within a plant at the level of the chloroplast membranes. Chloroplast membranes are highly organised; the total amount of photosystems in a chloroplast, the amount of photosystem I (PSI) in relation to photosystem II (PSII), and within each photosystem the amount of light harvesting complexes (LHCs) in relation to the amount of reaction centres, are tightly organised in response to the prevailing light condition around the leaf (Dekker and Boekema, 2005; Kouřil et al., 2012; Tikkanen et al., 2012; Kouřil et al., 2013). A high growth irradiance will lead to relatively more photosystem-core protein complexes, electron transport complexes, ATP synthase and enzymes in the Calvin-Benson cycle, whereas low growth irradiances will lead to relatively more light harvesting complexes and stacking of the thylakoid membranes (Bailey et al., 2001).

With increasing irradiance, the rate of excitation of PSII and PSI exceeds the capacity of photosynthetic electron transport or metabolic capacity, resulting in excess irradiance. In the short-term this provokes a physiological, regulatory response, while in the longer term a sufficiently large excess irradiance will often result in alterations in the chloroplast proteome. Both the short-term and long-term responses have limits to their action (Foyer et al., 2012; Tikkanen et al., 2012). In the short-term, excess irradiance imposes a strain on the capacity to protect the photosystems from damage (photoprotection) (Demmig-Adams and Adams, 1992). PSII is particularly susceptible to photodamage and has evolved an active regulatory process to reduce the extent of damage combined with an active repair system to replace damaged PSII reaction centres. As a first line of defence, PSII to a certain extent is able to dissipate the excess irradiance as heat via regulated non-photochemical quenching mechanisms (NPQ) reducing the rate of reaction centre damage (Rabinowitch, 1951). This process is initiated within seconds after an increase in

light intensity (Muller et al., 2001). The mechanism of NPQ in plants has been intensively studied, with most focus on the role of lumen pH dependent, or energy-dependent, dissipation of excess light (also known as qE, (Demmig et al., 1987)) via a mechanism that involves psbS and the xanthophyll cycle, one of the major short-term regulatory responses to excess irradiance.

The long-term response of plants to excess irradiance occurs over the time scale of hours or days and results in acclimation to the excess irradiance environment (Walters, 2005). This leads to increased capacities for electron and proton transport, coupled with increased photosynthetic metabolic capacity, often combined with alterations in organisation of the photosystems. These changes in capacity are due to changes in the amounts of soluble enzymes of photosynthesis, in electron transport components and pathways, and in pigment-protein complexes (Murchie and Niyogi, 2011). Regarding the photosystem subunit stoichiometry, PSII in response to high irradiance decreases its antenna size by decreasing the amount of LHCII proteins associated with the PSII supercomplex (Kouřil et al., 2013). Though the ratio of LHCI to PSI is not altered by irradiance, the antenna size of PSI decreases with increasing irradiance due to a decreased association of LHCII with PSI (Ballottari et al., 2007; Wientjes et al., 2013) (ie decreases in the amount of LHCII seems to alter the antenna size of both photosystems). In addition to this long-term adjustment of PSI cross-section, a short-term adjustment of the relative cross-sections of PSII and PSI can be brought about by state-transitions, driven by phosphorylation of LHCII, with phosphorylation being associated with a decrease in the cross-section of PSII and an increase in that of PSI (Allen, 1992; Tikkanen et al., 2010).

In the event that the sum of the short and long-term regulatory responses are insufficient, then more persistent damage to the photosynthetic apparatus (photoinhibition), especially to PSII, results. Damage to PSII, which is conveniently measured as a reduction of the F_v/F_m parameter derived from chlorophyll fluorescence measurements (Baker, 2008), is commonly used as an indicator of decreased photosynthetic performance arising from excess irradiance, though other parameters, such as decreased leaf chlorophyll content, are also used (Björkman and Demmig, 1987). The irradiance at which this damage will become apparent is difficult to predict.

Natural genetic variation in plant photosynthesis is a valuable resource (Flood et al., 2011). Naturally occurring variation in the photosynthetic acclimation response to high light has been observed in different plant species, with different studies using different

light regimes and focussing on different acclimation responses (Sims and Pearcy, 1993; Valladares et al., 1997; Balaguer et al., 2001; Leakey et al., 2003; Portes et al., 2008). However, research combining different light regimes and looking at the acclimation responses of different aspects of photosynthesis in different genotypes in one experiment is lacking. *Arabidopsis thaliana* (Arabidopsis) is the model species for plant genetic research, a choice that was motivated partly because of the considerable variation found in this species for many traits. The number and variety of natural genotypes of Arabidopsis make it increasingly valuable as physiological model (Alonso-Blanco et al., 2009). The variability of photosynthetic acclimation in naturally occurring genotypes of Arabidopsis has been investigated for light-use efficiency in one growth environment (El-Lithy et al., 2005), for NPQ responses to high light (Jung and Niyogi, 2009), for photosynthetic capacity in response to high light (Athanasiou et al., 2010), and for the response to short-term light flecks (Alter et al., 2012). To explore the phenotypic plasticity and genetic variation within *Arabidopsis thaliana* we have investigated the variability of the acclimation of multiple photosynthesis parameters to four constant growth irradiances and to a step-wise increase in the growth irradiance among 12 genotypically diverse accessions. To assess what part of the variability is due to genetic variation, we have calculated trait heritabilities, which are a measure of the extent of trait variation that is due to genetic variation. The possible genetic basis for trait variation can be determined using genome-wide association study (GWAS), in which genetic loci associated with a trait are identified by correlating genetic variation with trait variation (Atwell et al., 2010). To perform GWAS, there must be a description of genetic variation and the trait must be variable and heritable. It requires a large number of genotypes, so we used a population of 344 diverse Arabidopsis accessions which all had been genotyped for ~215 000 single nucleotide polymorphisms (SNPs) (Kim et al., 2007; Li et al., 2010). Importantly, because the genotypic description is restricted to the nuclear genome, any phenotypic variation arising from variation in cytoplasmic genomes cannot be associated with those genomes and will be a source of noise in the analysis. A GWAS for Φ_{PSII} measured one hour after a step-wise change in irradiance was used to identify genomic regions that are associated with the response of photosynthesis to step-wise increase in irradiance. These results highlight the genetic variation and physiological adaptability (or lack of it) of photosynthesis in Arabidopsis. The presence or absence of variability is of particular importance in relation to both the evolution of the photosynthetic properties of Arabidopsis and the future identification of those genetic factors that give rise to the photosynthetic phenotype.

MATERIALS AND METHODS

Plant material and growth conditions

The measurements described here can be divided into genome-wide association study (GWAS) and non-GWAS measurements. As the non-GWAS measurements were used as a pilot for the GWAS, many of the methods and genotypes used are common to both the non-GWAS and GWAS measurements.

The non-GWAS measurements were made on twelve genotypically diverse accessions of Arabidopsis which were used throughout the experiments in this study (Table I), grown in 3 replications. All these accessions are part of a core set of 360 natural accessions, which represents the global genetic diversity in Arabidopsis (http://www.naturalvariation.org/hapmap (Li et al., 2010)). For the GWAS, we used 344 accessions of the set of 360 accessions; included in the set of 344 accessions were all of the accessions used in the non-GWAS study. The 16 accessions that were not used were lines CS28051, CS28108, CS28808, CS28631, CS76086, CS76104, CS76110, CS76112, CS76118, CS76121, CS76138, CS76196, CS76212, CS76254, CS76257, and CS76302.

Table I. Origin of the twelve accessions of Arabidopsis used in this study

Accession	Full name	Latitude	Longitude	Origin
Bor-4	Borky	49.4	16.2	Czech Republic
Bur-0	Burren	53	-9	Ireland
C24	C24	41.2	-8.4	Portugal
Can-0	Canary Islands	29.2	-13.5	Spain
Col-0	Columbia	-	-	unknown
Cvi-0	Cape Verde Islands	15.1	-23.6	Cape Verde
Est-1	Estonia	58.3	25.3	Estonia
Ler-1	Landsberg *erecta*	52.7	15.2	Poland
NFA-8	NFA	51.4	-0.6	United Kingdom
Sha	Shahdara	38.3	68.5	Tajikistan
Tsu-0	Tsushima	34.4	136.3	Japan
Van-0	Vancouver	49.3	-123	Canada

For both GWAS and non-GWAS experiments seeds were pre-sown on filter paper in petri dishes wetted with filled with 0.5 mL demineralised water, and placed in the dark at 4°C for 4 days to stratify. Once stratified, the seeds were planted in a hydroponic cultivation system based on rockwool blocks (Grodan Rockwool Group, 40 X 40 X 40 mm in size). The blocks were positioned and secured using a frame (Fig. 1) of consisting of a baseplate made from a sheet of perforated stainless steel, a second PVC frame that was held 15 mm above the stainless steel base and into which the blocks were placed, and a black non-reflective foamed PVC cover-sheet drilled with countersunk holes 60 mm apart and 3 mm diameter that were positioned over the centres of the blocks. The seeds were placed on the rockwool surface exposed in these holes and the plants then grew up through the holes with the leaves spreading across the surface of the upper, black PVC sheet. The three layers of the growing system were secured by stainless steel screws and spacers and placed in a basin to which nutrient solution could be added. The baseplate was supported 5 mm above the floor of the basin, allowing nutrient solution to pass freely and uniformly under the growing frame and circulate through the frame via the holes in the perforated metal baseplate and the 10 mm spaces between the blocks. The black plastic upper plate prevented the growth of algae on the rockwool blocks and offered a good background for imaging of the plants.

For the smaller scale non-GWAS experiments the growing frame was 180 X 180 mm in size (Fig. 1) and could hold 9 individual rockwool blocks in a 3 x 3 array. Three seeds were sown per accession and the total of 36 seeds were randomized over four growing systems, with the limitation that two seeds of the same accession were never planted in the same growing system. For the GWAS experiment the growing frame was 390 x 85 cm and could hold 720 rockwool blocks in a 60 x 12 array. Two of these 60 x 12 growing systems, each in a separate basin, were combined to potentially grow a total of 1440 (allowing for four replicates of 360 genotypes) plants for the GWAS. Each growing frame was notionally sub-divided in two blocks, giving a total of four growing blocks. Four seeds were sown per accession in the GWAS experiment, and each set of 344 seeds was randomized over each of the four blocks.

For both GWAS and non-GWAS experiments plants were grown hydroponically using a nutrient solution developed for Arabidopsis (pH 7; EC 1.4 mS/cm) consisting of 1.7 mmol NH_4^+, 4.5 mmol K^+, 0.4 mmol Na^+, 2.3 mmol Ca^{2+}, 1.5 mmol Mg^{2+}, 4.4 NO_3^-, 0.2 mmol Cl^-, 3.5 mmol SO_4^{2-}, 0.6 mmol HCO_3^-, 1.12 mmol PO_4^{3-}, 0.23 mmol SiO_3^{2-}, 21 µmol Fe^{2+} (chelated using 3% diethylene triaminopentaacetic acid), 3.4 µmol Mn^{2+}, 4.7 µmol Zn^{2+},

14 µmol BO_3^{3-}, 6.9 µmol Cu^{2+}, and <0.1 MoO_4^{4-}, which was added to the basins containing the growing frames for 5 minutes 3 times a week.

For the non-GWAS experiments plants were grown at either constant irradiances of 100, 200, 400 or 600 µmol m^{-2} s^{-1} (Philips fluorescent tubes, MASTER TL5 HO, 80W), or the irradiance was increased from 100 µmol m^{-2} s^{-1} to 600 µmol m^{-2} s^{-1} at noon, 24 days after sowing on rockwool. In all cases the photoperiod was 10h/14h day/night cycle, temperature was 20/18°C (day/night), relative humidity was 70% and CO_2 levels were ambient. Following the step increase in irradiance the photosynthetic acclimation response was measured over five days, by measuring light response curves once a day in the morning 30 minutes after light onset. Other conditions were kept similar, although an increase of leaf temperature due to energy absorbed by the black cover needed for imaging could not be prevented. The highest irradiance we used in this study was well within the adaptive range of the accessions used so even the highest irradiance used was non-stressful insofar that it provoked no significant sign of light stress (eg a decrease in the dark-adapted F_v/F_m or anthocyanin formation). At the end of the acclimation period to increased growth irradiance in this second experiment, when Φ_{PSII} had stabilized, light response curves were compared to curves of plants grown at either a constant low (100 µmol m^{-2} s^{-1}) or high (600 µmol m^{-2} s^{-1}) growth irradiance. Plants were measured using chlorophyll fluorescence imaging for the first time at 30 minutes after light onset on the 24th day after sowing on rockwool. Depending on the experiment, this imaging was continued daily at the same time until plants began to overlap.

For the GWAS experiments plants were grown at constant irradiance of 100 µmol m^{-2} s^{-1} (Philips fluorescent tubes, MASTER TL5 HO, 80W). The irradiance was increased to 550 µmol m^{-2} s^{-1} on day 25 after sowing, at the onset of irradiance. In all cases the photoperiod was 10h/14h day/night cycle, temperature was 20/18°C (day/night), relative humidity was 70% and CO_2 levels were ambient. The plants were imaged one hour after light onset on day 24 ('measurement before the increase in irradiance'), as well as one hour after light onset on day 25 ('measurement after the increase in irradiance').
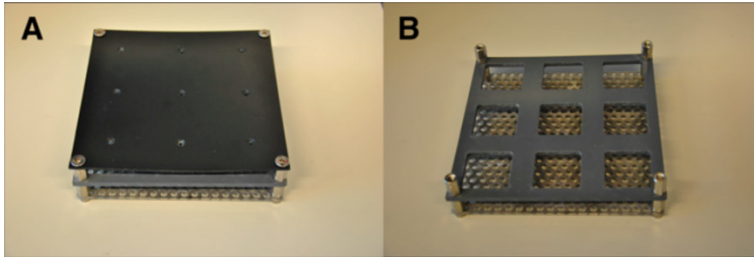
Figure 1. Growing system for Arabidopsis used in this study;

(A) top view showing non-reflective cover with small holes covering rock wool blocks on which Arabidopsis is germinated and grown; (B) when the non-reflective cover is removed, the rock wool block can be placed in 4 x 4 cm square holes, on a stainless steel grid, which is supported by short pins allowing nutrient solution to spread evenly underneath the rock wool blocks.

Chlorophyll a fluorescence imaging and analysis

For the non-GWAS experiments chlorophyll *a* fluorescence was measured using an imaging fluorimeter (Open FluorCam, P.S.I., Brno, Czech Republic, http://www.psi.cz), driven by the Fluorcam software package (FluorCam7). Fluorescence was detected by a camera of which the electronic shutter time and sensitivity were adapted to the irradiance being used. Measurements of the dark-adapted F_o and F_m were measured after 20 minutes of dark-adaptation. Images of the dark-adapted F_o were measured using non-actinic measuring flashes provided by light emitting diodes (LEDs). Next, a 1-s duration pulse of saturating light (6500 µmol m^{-2} s^{-1}) generated by the same and other LED-panels was given produce the maximum fluorescence level in the dark, F_m. An image of F_v/F_m was then calculated. To measure the irradiance response of parameters describing the operation and regulation of PSII the plants were illuminated with a series of increasing actinic irradiances (100, 225, 450, 700, and 1150 µmol m^{-2} s^{-1}). Each irradiance was applied for 15 minutes after which the F_t (steady-state fluorescence yield) and F_m' yield were measured. Pilot experiments showed that using these irradiances 15 minutes was sufficient time to allow F_t and F_m' to stabilise after each irradiance increase. The F_m' fluorescence yield was measured during a 1-s duration pulse of saturating light (6500 µmol m^{-2} s^{-1}). Values for F_o, F_m, F_t and F_m' in the images were averaged over all pixels per plant; derived values for Φ_{PSII}, F_v/F_m, NPQ, q_P, rETR, F_o', and F_v'/F_m' were calculated using these averages of F_o, F_m and F_m' (Oxborough and Baker, 1997; Baker, 2008).

For the imaging of the 344 accessions used for GWAS, we used a laboratory built high-throughput chlorophyll fluorescence imager. This system imaged plants in groups of 12 (a

3 X 4 array). Chlorophyll fluorescence was measured at 730 nm and excited using radiation from Phlatlight leds (Luminus, Billerica, Massachusetts, USA) (peak emission wavelength 624 nm). Φ_{PSII} was imaged at growth-room irradiance, and the irradiances supplied by the growth room (produced by fluorescent tubes) and the imager (produced by LEDs) were matched by comparing Φ_{PSII} (measured using a chlorophyll fluorimeter (MiniPam, Walz, Effeltrich, Germany)) in leaves under the growth room irradiance and the imager irradiance. The matching of the irradiances provided by the growth-room lights and the actinic irradiance of the imager meant that there was only minor disturbance of photosynthesis as a result of positioning the camera over the plants; a 30 s recovery time was found to be enough to allow the disappearance of any disturbance before the imaging procedure for Φ_{PSII} was begun.

Genetic variation

To estimate the genetic variation for a parameter, we calculated its heritability. Heritability, in this case broad sense heritability (H^2), is a term used in quantitative genetics that describes the portion of the total phenotypic variance in a population that is contributed by genetic variance (Visscher et al., 2008).

Genetic variance and the total phenotypic variance within an experiment were calculated with an ANOVA using type III sums of squares in a general linear model, in the IBM statistical software program SPSS. The genetic variance was estimated as the proportion of variance explained by differences between genotypes based on measurement of three plants per genotype. Standard errors for heritability were calculated using the heritabilities of three repeated experiments. Heritability for a response was calculated by first calculating the response values for a trait between two time points or two light steps. These response values were always calculated relative to the initial value of the first measurement of the two. When a relation between different parameters in different environments needed to be parameterized, we estimated the curve of the relation using regression statistics and parameterized it using the statistical model that fitted closest to the curve, with the IBM statistical software program SPSS. We then used the parameterized value for each individual to calculate the variances in the population.

Genome wide association analysis

The analysis was performed using the publicly available web application for genome-wide association mapping in Arabidopsis (GWAPP; gwas.gmi.oeaw.ac.at), using the accelerated mixed model option (Seren et al., 2012). GWAS was performed for Φ_{PSII}

measured one hour after a step-wise increase in irradiance from 100 to 550 µmol m^{-2} s^{-1}, by providing a list with average values of three biological replicates per accession. The website already 'knows' the 215 000 SNPs used for mapping, and will output a list with association scores for all these SNPs. For our analysis, we classified the SNPs with an association score > 4 as 'associated SNPs'. A core set of candidate genes was selected by cataloguing the genes which contained the associated SNPs in their coding region. The same web application was used to calculate the level of linkage disequilibrium (LD) for a SNP, and to catalogue the genes in these LD-regions (Seren et al., 2012); these genes were added to the core set of genes to form the complete list of candidate genes. A description for all candidate genes was obtained from TAIR (www. arabidopsis.org).

Gene ontology enrichment analysis

All gene ontology (GO) annotations were downloaded from TAIR (www.arabidopsis.org). The gene ontology enrichment analysis was performed for three categories: cellular component, molecular function, and biological process (Ashburner et al., 2000). Per category, the fraction of genes annotated to a certain ontology class for the list of candidate genes from GWAS was compared to the fraction of genes annotated to the same ontology class in a control group consisting of all the genes in the genome of Arabidopsis.

RESULTS

Phenotypic and genotypic variation in light response curves of various PSII parameters among 12 Arabidopsis accessions grown at 100 µmol m^{-2} s^{-1}

To assess genotypic variation for the irradiance response of photosynthesis in 12 genotypically diverse Arabidopsis accessions grown under constant growth irradiance of 100 µmol m^{-2} s^{-1}, the operating light use efficiency of photosystem II (Φ_{PSII}) was measured under a range of steady-state actinic irradiances. Φ_{PSII} measures the proportion of the light absorbed by PSII that is used in photochemistry, it is widely used as a proxy for the quantum yield of linear electron transport and for photosynthesis in general (Maxwell and Johnson, 2000). Figure 2A shows the light response curves of Φ_{PSII} for the 12 accessions used in this study, and figure 2B shows the light response curves of the values for the relative linear electron transport rate (rETR; the product of Φ_{PSII} and irradiance) derived from the Φ_{PSII} values in Figure 2A. The ETR is considered relative because we do not account for leaf light absorptance or the distribution of excitation energy between the two photosystems, nor apply any correction to the apparent quantum yield of PSII photochemistry provided by chlorophyll fluorescence measurements to give actual quantum yields for PSII electron transport. We will use the rETR at light saturation as a proxy for the maximum photosynthetic capacity (Pmax) in vivo (Genty et al., 1989). Figure 2B shows that when grown at 100 µmol m^{-2} s^{-1}, light saturation of photosynthesis occurs between 550 - 650 µmol m^{-2} s^{-1} for all 12 accessions. While the amount of phenotypic variance among the 12 accessions increases with the increase of the actinic irradiance level so does the genetic variance, resulting in similar heritabilities (Inset, Fig. 2B).

Φ_{PSII} is the product of the quantum efficiency of the open PSII reaction centres (F$_v$'/F$_m$') and the PSII efficiency factor (q$_p$) (Genty et al., 1989). The loss of Φ_{PSII} can therefore be accounted for by decreases in one or both of these parameters. For plants grown at a growth irradiance of 100 µmol m^{-2} s^{-1}, F$_v$'/F$_m$' remains constant at about 0.8 for actinic irradiances of 225 µmol m^{-2} s^{-1} or less, but decreases when the actinic irradiance is increased above this (Fig. 2C). Heritability for the response of F$_v$'/F$_m$' to increases in irradiance increases with increasing actinic irradiance (Fig. 2C). Similar to F$_v$'/F$_m$', q$_P$ also decreases with increasing actinic irradiance for plants grown at 100 µmol m^{-2} s^{-1} growth irradiance (Fig. 2D). However, unlike F$_v$'/F$_m$', q$_P$ shows decreases in response to actinic irradiances of less than 225 µmol m^{-2} s^{-1}. In contrast to the heritability for the irradiance

response of F_v'/F_m', the heritability for the irradiance response of q_P decreases with increasing actinic irradiance (Fig. 2D).

The values of non-photochemical quenching calculated according to the Stern-Volmer model (NPQ; F_m/F_m' - 1), q_P, and F_v'/F_m' measured at an actinic irradiance of 700 µmol m^{-2} s^{-1} (ie at light saturation), are shown plotted against the value of Φ_{PSII} measured at 700 µmol m^{-2} s^{-1} (Fig. 2E, 2F, and 2G), and the correlation between NPQ and F_v'/F_m' is shown in Fig. 2H. NPQ, q_P and F_v'/F_m' are linearly related to Φ_{PSII} with the correlation being negative in the case of NPQ and positive for q_P and F_v'/F_m'. The parameters F_v'/F_m' and q_P are more strongly correlated to Φ_{PSII} than is NPQ (Fig. 2E, 2F, 2G).

Figure 2 (on next page). Light response curves of various PSII parameters among 12 Arabidopsis accessions grown at 100 µmol m^{-2} s^{-1} and the correlation between parameters

(A) PSII operating light use efficiency (Φ_{PSII}) of 12 Arabidopsis accessions. Error bars indicate the standard error of the mean, N=3. Φ_{PSII} was measured on plants that were grown in 100 µmol m^{-2} s^{-1} for 24 days, after reaching steady state photosynthesis in five different actinic irradiances: 100, 225, 450, 700, and 1150 µmol m^{-2} s^{-1} (B) relative electron transport rates (rETR) in the presence of different actinic irradiances of 12 accessions of Arabidopsis, calculated from PSII operating light use efficiencies.; the inset shows the average heritabilities over three independent experiments for the individual measurement points and for the response of these values to actinic irradiance level; (C) light use efficiency of the open PSII reaction centres in the presence of different actinic irradiances (F_v'/F_m') of 12 accessions of Arabidopsis; (D) PSII efficiency factor (q_P) in the presence of different actinic irradiances of 12 accession of Arabidopsis; (E) correlation of Φ_{PSII} and NPQ of 12 accessions each with three replicates grown in 100 µmol m^{-2} s^{-1} and measured at light saturation (700 µmol m^{-2} s^{-1}); (F) correlation of Φ_{PSII} and q_P of 12 accessions each with three replicates grown in 100 µmol m^{-2} s^{-1} and measured at light saturation (700 µmol m^{-2} s^{-1}); (G) correlation of Φ_{PSII} and F_v'/F_m' of 12 accessions each with three replicates grown in 100 µmol m^{-2} s^{-1} [1] and measured at light saturation (700 µmol m^{-2} s^{-1}) ; (H) correlation of NPQ and F_v'/F_m' of 12 accessions each with three replicates grown in 100 µmol m^{-2} s^{-1} [1] and measured at light saturation (700 µmol m^{-2} s^{-1})

Panel A: Φ_{PSII} vs actinic irradiance ($\mu mol\ m^{-2}\ s^{-1}$)

Legend: bor-4, bur-0, c24, can-0, col-0, cvi-0, est-1, ler-1, nfa-8, sha, tsu-0, van-0

Panel B: rETR vs actinic irradiance ($\mu mol\ m^{-2}\ s^{-1}$)

Actinic irradiance ($\mu mol\ m^{-2}\ s^{-1}$)	Heritability ± SE, n=3
100	0.59 ± 0.06
225	0.52 ± 0.08
450	0.53 ± 0.07
700	0.56 ± 0.05

Response	Heritability
100 - 225	0.38 ± 0.19
225 - 450	0.51 ± 0.09
450 - 700	0.18 ± 0.01

Panel C: F_v'/F_m' vs actinic irradiance ($\mu mol\ m^{-2}\ s^{-1}$)

Actinic irradiance ($\mu mol\ m^{-2}\ s^{-1}$)	Heritability ± SE, n=3
100	0.09 ± 0.05
225	0.20 ± 0.10
450	0.24 ± 0.12
700	0.26 ± 0.07

Response	Heritability
100 - 225	0.14 ± 0.02
225 - 450	0.19 ± 0.07
450 - 700	0.30 ± 0.03

Panel D: q_P vs actinic irradiance ($\mu mol\ m^{-2}\ s^{-1}$)

Actinic irradiance ($\mu mol\ m^{-2}\ s^{-1}$)	Heritability ± SE, n=3
100	0.32 ± 0.12
225	0.42 ± 0.12
450	0.30 ± 0.18
700	0.47 ± 0.12

Response	Heritability
100 - 225	0.60 ± 0.03
225 - 450	0.35 ± 0.02
450 - 700	0.33 ± 0.11

Panel E: $\Phi_{PSII\ (700)}$ vs NPQ (700), $R^2 = 0.5102$

Panel F: $\Phi_{PSII\ (700)}$ vs q_P (700), $R^2 = 0.9502$

Panel G: $\Phi_{PSII\ (700)}$ vs F_v'/F_m' (700), $R^2 = 0.8089$
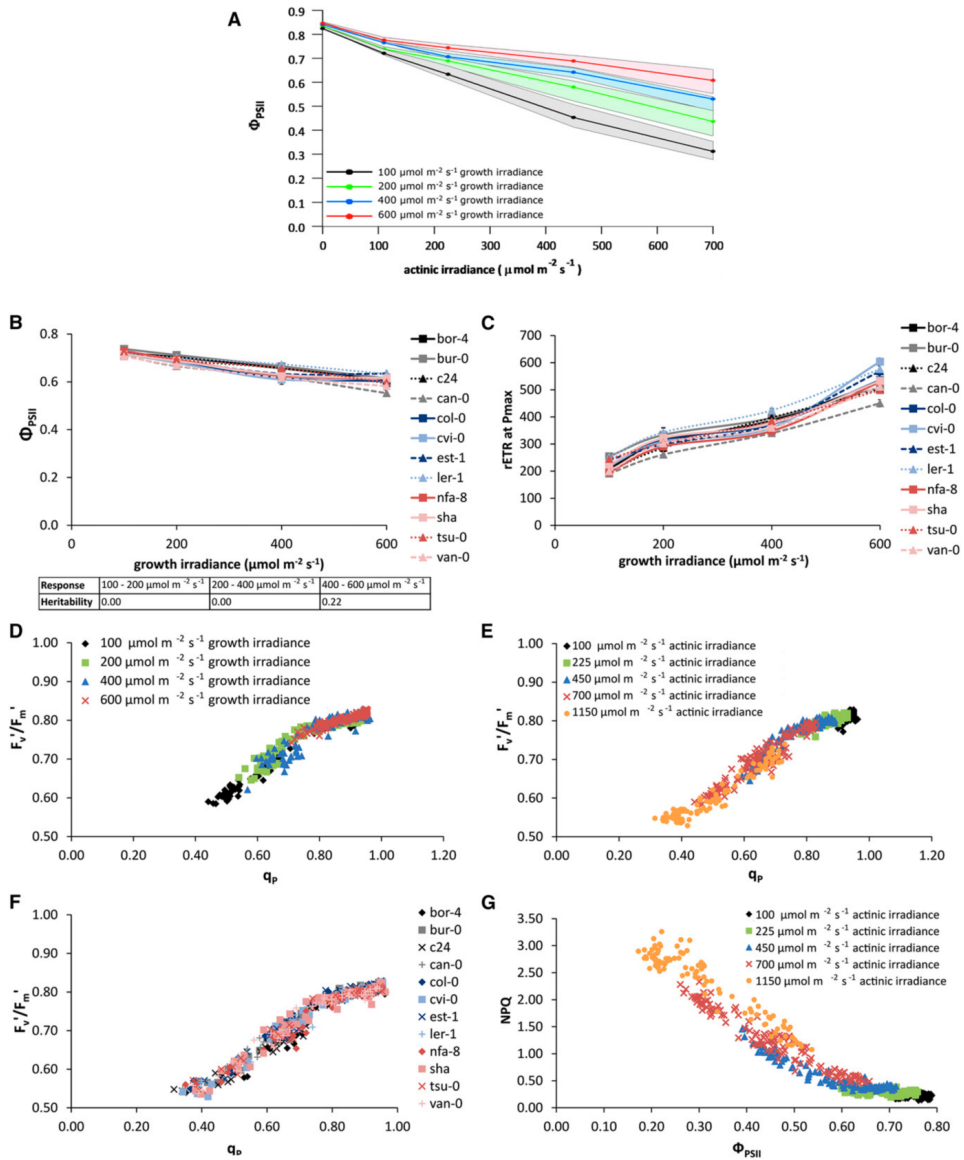
Panel H: NPQ (700) vs F_v'/F_m' (700), $R^2 = 0.6055$

Light use efficiency responses to different, constant growth irradiances

At an actinic irradiance of 600 µmol m^{-2} s^{-1} plants grown at 100 µmol m^{-2} s^{-1} have an average Φ_{PSII} of 0.35, while for plants grown at 200 µmol m^{-2} s^{-1} the average Φ_{PSII} is 0.48, for plants grown at 400 µmol m^{-2} s^{-1} it is 0.58 and for plants grown at 600 µmol m^{-2} s^{-1} it is 0.65 (Fig. 3A). This shows there is long-term photosynthetic acclimation to growth irradiance for Arabidopsis. Genetic variation for this acclimation is present. For example for some accessions the irradiance response of Φ_{PSII} for plants grown at 600 µmol m^{-2} s^{-1} is the same as that for those grown at 400 µmol m^{-2} s^{-1}, whereas for other accessions the irradiance response of Φ_{PSII} for plants grown at a 600 µmol m^{-2} s^{-1} differs to that of plants grown at 400 µmol m^{-2} s^{-1} while the response of plants grown at 200 and 400 µmol m^{-2} s^{-1} is similar (Supplementary Fig. S1).

The value of Φ_{PSII} measured at an actinic irradiance equal to growth irradiance shows, overall, an apparently linear decrease with increasing irradiance (Fig. 3B). In detail, however, at growth irradiances above 400 µmol m^{-2} s^{-1} this decline ceases for some accessions (Fig. 3B). This leads to a heritability of 0.20 for the difference in this parameter when comparing the data obtained from plants grown at an irradiance of 600 µmol m^{-2} s^{-1} to those grown at 400 µmol m^{-2} s^{-1} (inset Fig. 3B).

Figure 3 (on next page). Light response of PSII light use efficiency (Φ_{PSII}) of 12 Arabidopsis accessions , grown in different constant growth irradiances: 100, 200, 400 or 600 µmol m^{-2} s^{-1} (A) Φ_{PSII} light response curves measured on 24-days-old plants after reaching steady state photosynthesis in four different actinic irradiances: 100, 225, 450, and 700 µmol m^{-2} s^{-1}. The lines represent the average of all accessions, the area around the line represents the extent of deviation among the accessions (highest value minus lowest value in population); (B) variation in Φ_{PSII} among 12 Arabidopsis accessions, when grown at four different constant growth irradiances (100, 200, 400, and 600 µmol m^{-2} s^{-1}) for 24 days and measured at actinic irradiance identical to the growth irradiance. Error bars indicate the standard error of the mean, N=3; the inset shows the heritabilities of the response of these values to growth irradiance level (C) variation in maximum relative electron transport rates (rETR) measured at saturating actinic irradiance (Pmax) among 12 accessions, grown at four different growth irradiances (100, 200, 400, and 600 µmol m^{-2} s^{-1}) for 24 days. When grown at 100 µmol m^{-2} s^{-1}, the saturating actinic irradiance level used was 600 µmol m^{-2} s^{-1}, at 200 µmol m^{-2} s^{-1} this was 700 µmol m^{-2} s^{-1}, at 400 µmol m^{-2} s^{-1} it was 800 µmol m^{-2} s^{-1}, and at 600 µmol m^{-2} s^{-1} it was 1150 µmol m^{-2} s^{-1}. Error bars indicate the standard error of the mean, N=3; (D) Correlation of F_v'/F_m' and q_p for different growth irradiances (100, 200, 400, and 600 µmol m^{-2} s^{-1}); (E) Correlation of F_v'/F_m' and q_p for different actinic irradiances (100, 225, 450, 700, and 1150 µmol m^{-2} s^{-1}); (F) Correlation of F_v'/F_m' and q_p for the 12 different accessions of Arabidopsis; (G) Correlation of NPQ and Φ_{PSII} for different actinic irradiances (100, 225, 450, 700, and 1150 µmol m^{-2} s^{-1})*

34

Response	100 - 200 µmol m^{-2} s^{-1}	200 - 400 µmol m^{-2} s^{-1}	400 - 600 µmol m^{-2} s^{-1}
Heritability	0.00	0.00	0.22

The correlation between the maximum rETR and growth irradiance shows genotypic variation (Fig. 3C). For some accessions this relationship is triphasic (Supplementary Fig. S2), with a sharp increase over the lower irradiance range (100-200 µmol m^{-2} s^{-1}), a much lower increase between 200 and 400 µmol m^{-2} s^{-1} growth irradiance, and a second sharp increase between 400 and 600 µmol m^{-2} s^{-1}. For other accessions this relationship is biphasic (Supplementary Fig. S2), while for others it is linear (Supplementary Fig. S2). Curve estimation of this relation using a cubic statistical model resulted in different fitted values for all 12 accessions (Supplementary Fig. S3). The heritability for this relation is 0.52.

The partitioning of the decrease in Φ_{PSII} into decreases in F_v'/F_m' and q_p is shown for different growth irradiance levels (Fig. 3D), actinic irradiance levels (Fig. 3E), and genotypes (Fig. 3F). While there is some variation in the partitioning of the loss of Φ_{PSII} between losses in F_v'/F_m' and q_p, this variation seems to be independent of genotype or growth irradiance. A negative correlation between NPQ and Φ_{PSII} (Fig. 2E) has already been noted, but in addition Fig. 3G also shows that considering all the data from all 12 genotypes, the correlation between Φ_{PSII} and NPQ is curvilinear, with NPQ decreasing more strongly with Φ_{PSII} at lower values of Φ_{PSII}. Overall, the correlation between Φ_{PSII} and NPQ does not show much genotypic variation or dependency on growth irradiance.

Long-term acclimation of light use efficiency to a step-wise increase in growth irradiance

During acclimation to a step-wise increase in growth irradiance from 100 µmol m^{-2} s^{-1} to 600 µmol m^{-2} s^{-1}, F_o stays constant (Fig. 4A), whereas F_m decreases on the first day after the increase to high light (HL) and then recovers to its baseline value within 3-4 days (Fig. 4B), resulting in a decrease in F_v/F_m on day 1 after the increase to HL (Fig. 4C). This decrease in F_v/F_m is correlated significantly to the levels of Φ_{PSII} and q_P before the increase in growth irradiance (Supplementary Table S1), as well as to the levels of Φ_{PSII} and q_P on each day of the subsequent acclimation period. NPQ started to decline within the first 24 hours after the irradiance increase and continued to decline until day 3 (Fig. 4E). The level of NPQ on day 1 after the increase to HL is significantly correlated to the decrease in F_v/F_m on that same day, but this correlation disappears after the start of the acclimation of NPQ (Table S1). The decline of NPQ in the subsequent days of the acclimation period is accompanied by an increase in Φ_{PSII} (Fig. 4E; 4F). Both NPQ and Φ_{PSII} stabilize after three days of long-term acclimation.
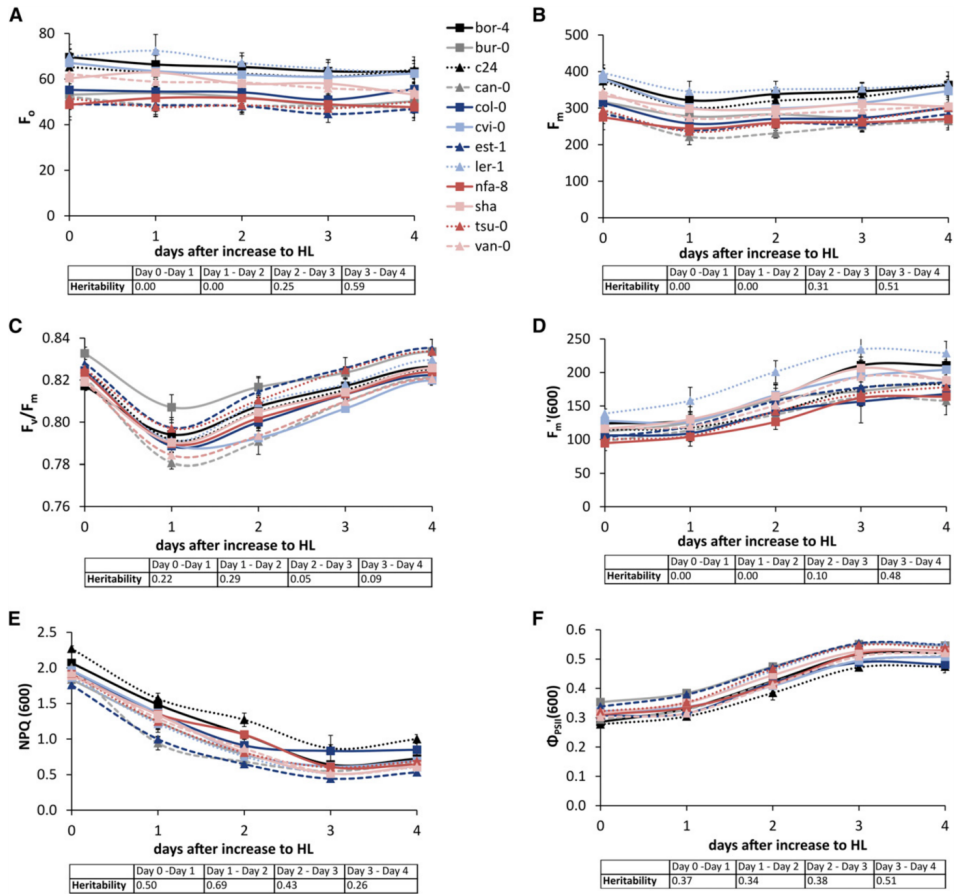
Figure 4. Variation in long term acclimation response of 12 Arabidopsis accessions to increased growth irradiance after 24 days of growth, from 100 μmol m^{-2} s^{-1} to 600 μmol m^{-2} s^{-1} (high light, HL).

(A) F_o, (B) F_m, (C) F_v/F_m, (D) F_m' measured with an actinic irradiance level of 600 μmol m^{-2} s^{-1}, (E) NPQ measured with an actinic irradiance level of 600 μmol m^{-2} s^{-1}, and (F) Φ_{PSII} measured with an actinic irradiance level of 600 μmol m^{-2} s^{-1}. Day 0 represents the baseline measurement taken on day 24 after sowing the plants on rockwool. All measurements were taken in the morning, 30 minutes after light onset. Error bars indicate the standard error of the mean, N=3. The insets show the heritabilities of the daily responses relative to the day before for the corresponding values (F_o, F_m, F_v/F_m, $F_m'(600)$, NPQ (600), or $\Phi_{PSII}(600)$).

Genotypic variation was observed for both the decline of NPQ and the increase in Φ_{PSII} during acclimation to increased growth irradiance (heritabilities insets in Figures 4E and 4F). Furthermore, there is some genotypic variation for the decrease in F_v/F_m on day 1 after the increase to HL as well as its recovery on day 2 (heritabilities in inset Fig. 4C). After three days, all the measured photosynthetic parameters had stabilized; some genotypic variation is also noted for the kinetics of this stabilization process, as shown by the heritabilities (insets, Fig. 4).

While some accessions acclimate fully (Fig. 5A and 5C) to an increase in growth irradiance (ie after acclimation to the increased irradiance their $\Phi_{PSI\ I}$-irradiance response becomes identical to that they have when grown continuously at this higher irradiance), others do not (Fig. 5B and 5D). Among the twelve accessions used in this study we could distinguish only these two kinds of responses; the responses for the accessions not shown in Figure 5 are in supplementary Figure S4.
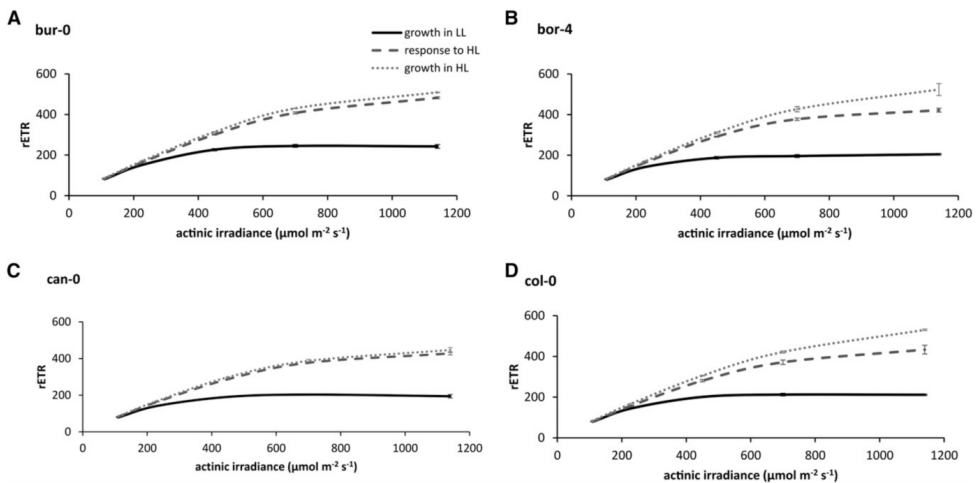

Figure 5. Variation in light response curves of relative electron transport rate (rETR) of four Arabidopsis accessions grown at a low growth irradiance (growth in LL), grown in LL for 24 days followed by a high growth irradiance (HL) for 4 days (response to HL), and grown in HL for 24 days (growth in HL).

The low growth irradiance level is 100 μmol m^{-2} s^{-1}; high growth irradiance level is 600 μmol m^{-2} s^{-1}. Error bars indicate the standard error of the mean, N=3.

Genome-wide association analysis

Φ_{PSII} was measured on 344 accessions of Arabidopsis one day before and one hour after an increase in growth irradiance from 100 µmol m^{-2} s^{-1} to 550 µmol m^{-2} s^{-1}; Φ_{PSII} measurements before and after the increase were correlated significantly, with a Pearson correlation coefficient of 0.436. At both time points the measurements were normally distributed (Supplementary figure S5), but the phenotypic distribution, and consequently also the trait heritability, was larger one hour after the increase in irradiance compared to before the increase in irradiance (H^2=0.26 vs H^2=0.09). A genome-wide association study (GWAS) was performed for the measurements taken one hour after a step-wise increase in growth irradiance to identify potential candidate genes associated with the short-term high light response of photosynthesis (Fig. 6). All of these genes are nuclear because the cytoplasmic genomes cannot be included in the analysis because neither the mitochondrial nor the chloroplast genomes have been genotyped for the Arabidopsis population we used (nor for any other large Arabidopsis population) so there are no SNPs (or any other genetic markers) available for these genomes. Any phenotypic variation arising from the variation in the cytoplasmic genetic factors will therefore not be accounted for.
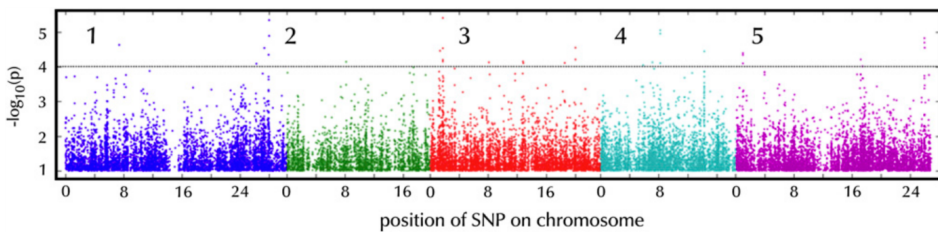

Figure 6. Genome-wide association analysis of Φ_{PSII} one hour after an increase in growth irradiance from 100 µmol m^{-2} s^{-1} to 550 µmol m^{-2} s^{-1}.

Based on the analysis of 344 diverse Arabidopsis accessions. Every point indicates the –log$_{10}$(p) value for all SNPs that have been tested. Different colours distinguish the SNPs mapped to one of the five chromosomes of Arabidopsis. The dotted line represents the arbitrary threshold for significance of –log$_{10}$(p) = 4.

The strongest association between a SNP and the phenotype we found had a $-\log_{10}(p)$ value of 5.31, where 'p' is the probability of obtaining the association by chance. This strength of association was found twice, at position 27981096 on chromosome 1, and for position 12784017 on chromosome 3. Using an arbitrary threshold of significance for $-\log_{10}(p)$ of 4, we defined the SNPs with $-\log_{10}(p)$ values above this threshold as 'associated SNPs'. This yielded 30 associated SNPs, corresponding to 25 candidate genes (some genes contain more than one SNP), which increases to 63 candidate genes when all genes in linkage disequilibrium (LD) with these SNPs are included (Table II). Besides information on the genes localized (either directly or in LD) to the associated SNPs, Table II shows extra information about the population genetics of the associated SNPs, such as minor allele frequency in the population, the effect size on the trait, and the percentage of variation it explains. The functions, if known, of those genes directly associated with the SNPs is also described in Table II; the functions of the genes in the LD regions with the associated SNPs are described in Supplementary Table S2. No genes previously reported to be involved in photosynthesis were found among the 63 candidate genes., The candidate gene list is, however, enriched for genes encoding proteins that are targetted to the chloroplast, cytosol, and nucleus (Fig. 7A). When examined for protein function, there is enrichment for kinase activity, protein binding, transferase activity, and transporter activity (Fig. 7B), while the processes DNA/RNA metabolism, response to abiotic or biotic stimulus, response to stress, and transport are most represented (Fig. 7C). Of the 63 candidates, 13 (nuclear encoded) proteins are targetted to the chloroplast (Table III).

Table II. List of candidate genes localized to SNPs

Candidate genes are those genes containing the SNP and those genes in linkage disequilibrium (LD) with the SNP associated with a –log10(p) >4 for Φ_{PSII} measured one hour after a step-wise increase in irradiance from 100 to 550 $\mu mol\ m^{-2}\ s^{-1}$, selected upon a genome wide association study on 344 Arabidopsis accessions. Chr., chromosome; gene, the gene to which the associated SNP localizes, if two genes are indicated, the SNP is mapped in between two genes; SNP pos., the chromosome position(s) of the SNP(s); MAF, minor allele frequency, the letter in parenthesis indicates whether it represents the Col-0 allele (C) or the non-Col-0 allele (NC); -log10(p), the significance level of the associated SNP expressed as –log10(p); effect size, the contribution of the Col-0 allele of the SNP on Φ_{PSII}; perc.of.genetic.var, the percentage of genetic variation explained by the SNP; description, the annotation of the gene function as indicated in TAIR (www.arabidopsis.org); LD, the genes found to be in linkage disequilibrium (r> 0.45) with the indicated SNP.

Chr.	Gene	SNP Pos.	MAF	-log10(p)	Effect size	Perc.of. genetic. var	Description	LD
1	AT1G21080/ AT1G21090	7384441	0.146 (C)	4.6	0.018	9	DNAJ heat shock N-terminal domain-containing protein / Cupredoxin superfamily protein	AT1G21060 to AT1G21140
1	AT1G69770	26249116	0.254 (NC)	4.3	-0.014	8.1	Chromomethylase 3; involved in methylating cytosine residues at non-CG sites.	-
1	AT1G72560	27329236	0.246 (NC)	4.6	0.014	8.1	PAUSED, a karyopherin	-
1	AT1G74180	27899243	0.351 (C)	4.4	0.013	8.6	Receptor-like protein 14, located in chloroplast	AT1G74190
1	AT1G74440	27979318; 27981096	0.447 (C); 0.365 (NC)	5.0; 5.3	0.013; 0.013	9.0; 9.8	Unknown protein	-
2	AT2G26280	11189311	0.196 (NC)	4.3	-0.018	8.3	CID7, CTC-interacting domain7, functions in DNA binding and mismatch repair, located in chloroplast.	AT2G26290
3	AT3G04910	1353894	0.155 (NC)	4.3	-0.016	8.3	WNK1, With No Lysine Kinase1, serine/threonine protein kinase, whose transcription is regulated by circadian rhythm.	AT3G04880 to AT3G04910
3	AT3G05860	1750265; 1750573; 1750946; 1751042	0.175; 0.167; 0.167; 0.211 (C)	4.2; 4.5; 4.2; 5.4	0.016; 0.017; 0.016; 0.016	8.3; 9.1; 8.3; 9.8	MADS-box transcription factor family protein	AT3G05790 to AT3G05890
3	AT3G22910	8120853	0.307 (NC)	4.1	0.015	7.9	ATPase E1-E2 type family protein / haloacid dehalogenase-like hydrolase family protein	-

Chr.	Gene	SNP Pos.	MAF	-log10(p)	Effect size	Perc.of. genetic. var	Description	LD
3	AT3G31410	12784017	0.377 (C)	5.3	-0.015	8.7	Transposable element	-
3	AT3G44230	15932189	0.184 (NC)	4.1	-0.016	6.6	Unknown protein	-
3	AT3G54010	20000766	0.289 (NC)	4.7	-0.014	9.6	Immunophilin-like protein	AT3G54000
4	AT4G11300	6872903	0.480 (C)	4.2	0.014	7.6	Unknown protein	-
4	AT4G14250	8209018; 8209226	0164; 0.187 (C)	4.9; 5.1	0.017; 0.016	9.3; 9.1	Pseudogene	-
4	AT4G21760	11561583	0.053 (NC)	4.2	0.023	6.3	Beta-glucosidase 47, involved in carbohydrate metabolic process	AT4G21750 to AT4G21770
5	AT5G03760	987180; 987216; 988003	0.216 (C); 0.272; 0.240	4.9; 4.3; 4.4	0.014; 0.014; 0.014	7.7; 8.5; 8.3	Cellulose Synthase Like A9	AT5G03750
5	AT5G42870	17186178	0.345 (C)	4.3	-0.012	8	PAH2, a phosphatidate phosphohydrolase	-
5	AT5G43390	17424158	0.450 (C)	4.0	-0.012	8.5	Uncharacterised conserved protein, located in chloroplast	-
5	AT5G64960	25956134	0.465 (C)	4.3	-0.013	9.9	CDKC2, expression of CDKC2 modifies the location of spliceosomal components	AT5G64910-AT5G65030
5	AT5G64980	25963073	0.465 (C)	4.5	-0.013	9.9	Unknown protein	
5	AT5G65000/AT5G65005	25967700	0.354 (NC)	4.9	0.013	9.4	Nucleotide-sugar transporter family protein / Polynucleotidyl transferase	
5	AT5G65010	25968943	0.284 (NC)	4.2	0.014	10.1	ASN2, Asparagine Synthetase 2	
5	AT5G65030	25975808	0.480 (C)	4.4	-0.013	10.4	Unknown protein	
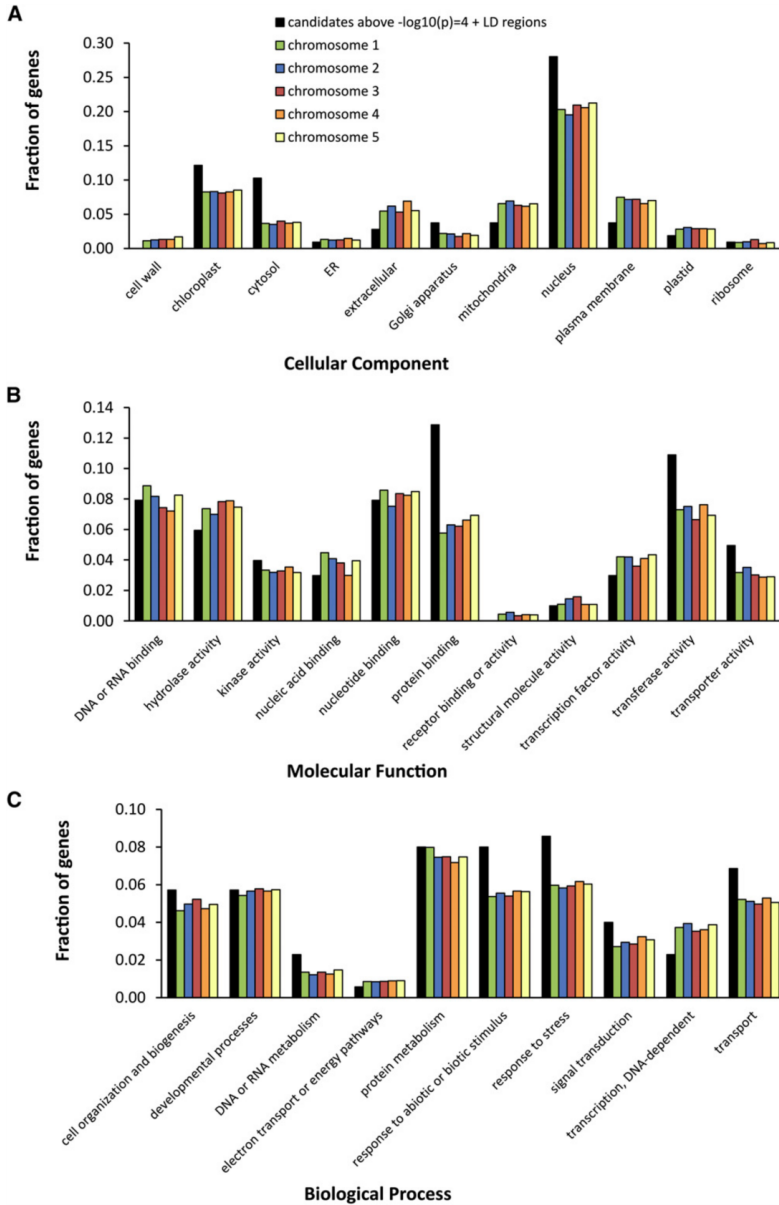
Figure 7. Gene ontology enrichment analysis

(A) Cellular Component, (B) Molecular Function, and (C) Biological Process. The graphic depicts the fraction of genes from a list (gene candidate list directly localized to, and in LD regions of, the SNPs associated in GWAS above –log10(p) = 4; list of all genes on chromosome 1; on chromosome 2; on chromosome 3; on chromosome 4; and on chromosome 5) annotated to different gene ontology categories.

Table III. List of candidate genes that encode proteins predicted to localize at the chloroplast.
Selected from 63 genes found to be directly localized, or be in linkage disequilibrium with the associated SNPs identified in the GWAS.

Gene	SNP	Description
AT1G21060	in LD with 7384441	Unknown protein
AT1G21065	in LD with 7384441	Unknown protein
AT1G74180	directly localized to 27899243	Receptor-like protein 14, located in chloroplast
AT1G74440	27979318; 27981096	Unknown protein
AT2G26280	directly localized to 11189311	CID7, CTC-interacting domain 7, functions in DNA binding and mismatch repair
AT3G05790	in LD with 1750265; 1750573; 1750946; 1751042	Lon-protease 4, for degradation of abnormal, damaged, and unstable protein
AT3G05810	in LD with 1750265; 1750573; 1750946; 1751042	Chromatin assembly/disassembly protein
AT4G21770	in LD with 11561583	Pseudouridine synthase, involved in RNA modification
AT5G43390	directly localized to 17424158	Uncharacterised conserved protein
AT5G64930	in LD with 25956134; 25963073; 25967700; 25968943; 25975808	Regulator of expression of pathogenesis-related genes. Participates in signal transduction pathways involved in plant defence.
AT5G64940	in LD with 25956134; 25963073; 25967700; 25968943; 25975808	Oxidative stress-related ABC1-like protein (ATP-binding cassette)
AT5G65000	directly localized to 25967700	Nucleotide-sugar transporter family protein / Polynucleotidyl transferase
AT5G65020	in LD with 25956134; 25963073; 25967700; 25968943; 25975808	Annexin 2, calcium binding protein

DISCUSSION

Short-term response of plants to increased irradiances

In 12 genotypically diverse Arabidopsis accessions grown at 100 µmol m^{-2} s^{-1} there is variability in the responses of Φ_{PSII} to short-term (minutes time scale) changes in irradiance (Fig. 2A, Fig. 2B). There is more phenotypic variance for electron transport rate the closer the actinic irradiance level is to light saturation (Fig. 2B), which would be expected given that increasing irradiances move the leaf from light-limitation to light-saturation (Björkman, 1981; Evans and Poorter, 2001). In a light-limited leaf, Φ_{PSII} is close to a maximum value (c. 0.80 – 0.83) that is similar across many groups of plants (Björkman and Demmig, 1987). The value for Φ_{PSII} at steady state is due to the balance between supply side processes, that give rise to the formation of excited states of chlorophyll a (chl*) in PSII following light absorption by photosystem II, and demand side processes that dissipate these chl* photochemically (Genty et al., 1989). If supply exceeds demand then the light-use efficiency for photosynthesis must decrease. For plants grown at 100 µmol m^{-2} s^{-1} such a decrease has already occurred at an actinic irradiances equal to the growth irradiance (Fig. 2A), which implies that even at low growth irradiances acclimation did not maximise light-use efficiency. In a light-saturated leaf, Φ_{PSII} is limited by electron transport or metabolic factors that generally can differ greatly between species (Seemann, 1989; Murchie and Horton, 1997; Valladares et al., 1997) and within species (Balaguer et al., 2001; Walters et al., 2003; Ptushenko et al., 2013).

Values for heritability generally range from zero to one (Visscher et al., 2008), where a value of one means that all of the observed phenotypic variance is solely due to genetic variation. The heritability for Φ_{PSII} ranges around 0.50, independent of the actinic irradiance at which it is measured (inset Fig. 2B), from which we conclude the amount of genetic variation for short-term responses of Φ_{PSII} to increased irradiance is independent of the level of the irradiance. To further dissect the variation for photosynthetic light use efficiency, Φ_{PSII} can be broken down into its F_v'/F_m' and q_p components (Genty et al., 1989). Overall, F_v'/F_m' and q_p decrease as Φ_{PSII} decreases, but not in parallel (Harbinson et al., 1989). In the absence of photodamage or slowly reversible down-regulation of PSII (Demmig-Adams and Adams, 2006), decreases in F_v'/F_m' are due to the activation of a non-photochemical dissipation mechanism that gives rise to the q_E component of NPQ (Demmig et al., 1987). Decreases in q_p are due to the reduction of Q_A, though the relationship between Q_A redox state and q_p is non-linear (Kramer et al., 2004). In response to a moderate increase in irradiance (from 100 to 200 µmol m^{-2} s^{-1}), the

decrease in Φ_{PSII} is due only to decreases in q_P (Fig. 2C and 2D). The loss of q_P at low irradiances, which is due to an over-excitation of PSII compared to PSI and not to a limitation of electron transport (Genty and Harbinson, 1996), is still correlated with a loss of light-use efficiency for carbon dioxide fixation (Hogewoning et al., 2012). The lack of any decrease in F_v'/F_m' at the lowest measurement irradiances is paralleled by the pattern of heritability for the irradiance responses of q_p and F_v'/F_m' (insets, Fig. 2C and 2D)

The parameters F_v'/F_m' and NPQ quantify the effect of inducible (ie not present in the dark-adapted state) non-photochemical dissipation in PSII on the efficiency of open PSII traps (F_v'/F_m') and the quenching of F_m (NPQ). Even if F_m' changes, the F_v'/F_m' calculated using a measured value of F_o' should be unaffected by state transitions, in contrast to the NPQ parameter. In our case F_o' was calculated from F_v, F_m and F_m' (Oxborough and Baker, 1997) and while this allows a good estimate of F_o', it cannot estimate the impact of q_T quenching which is where the impact of using a calculated F_o' in place of a measured F_o' will be greatest. Q_T quenching is due to state transitions (Horton and Hague, 1988; Quick and Stitt, 1989) on F_o'. Q_T quenching (and state transitions) is limited to low irradiances (Walters and Horton, 1991; Rintamäki et al., 1997). An F_v'/F_m' based on a calculated F_o' is therefore likely to be better correlated with NPQ than would be an F_v'/F_m' based on a measured F_o', especially at low irradiances. Figure 2E, 2F, and 2G show a high correlation of NPQ, q_P, and F_v'/F_m' with Φ_{PSII} measured at light saturation (actinic light of 700 µmol m^{-2} s^{-1}). F_v'/F_m' and q_P are more strongly correlated with Φ_{PSII} than is NPQ (Fig. 2E, 2F, 2G), which is to be expected as Φ_{PSII} is the product of q_P and F_v'/F_m'. The correlation between NPQ and F_v'/F_m' (Fig. 2H) is also expected given that under the experimental conditions used both these parameters will be predominantly affected by the energy-dependent quenching mechanism that gives rise to q_E. These results suggest that there is little variability in the extent to which the loss of Φ_{PSII} can be absorbed via the thermal dissipation processes that give rise to NPQ and produce the decrease in F_v'/F_m'.

Φ_{PSII} in plants grown at different constant growth irradiances

In response to increasing growth irradiances, all accessions of Arabidopsis showed a smaller loss of Φ_{PSII} with increasing actinic irradiance (Fig. 3A). As a result, Φ_{PSII} measured at an actinic irradiance identical to the growth irradiance decreases only slightly with growth irradiance (maximally 25%, Fig. 3B). This response shows that Arabidopsis has considerable flexibility in its photosynthetic apparatus and responds strongly to high irradiances, a trait not found in all species (Murchie and Horton, 1997). Genotypic variation for this trait is minor amongst the 12 genotypes used in this study

(Fig. 3B). More genotypic variation can be found in the relationship between the rETR at light saturation and growth irradiance (Fig. 3C). For some accessions this relation is linear, for some it is bi-phasic, and for some tri-phasic, confirming the presence of separate low and high light responses in Arabidopsis (Bailey et al., 2001).

The pattern of partitioning of losses in Φ_{PSII} between F_v'/F_m' and q_p is independent of both growth irradiance (Fig. 3D) and actinic irradiance (Fig. 3E), and genotype (Fig. 3F). These results imply that non-photochemical dissipation in PSII is highly and consistently regulated across diverse genotypes grown under a range of growth irradiances. Another implication is that when evaluating and comparing the development and extent of the inducible non-photochemical dissipation processes that give rise to decreases in F_v'/F_m' and to increases in NPQ, the underlying change in PSII efficiency should be taken into account (Fig. 3G).

Long-term responses to a step-wise increase in growth irradiance

The decrease in F_v/F_m (0.02 - 0.04) one day after a step-increase in growth irradiance from 100 to 600 µmol m^{-2} s^{-1} is due to a decrease in F_m, which is followed by a recovery in F_v/F_m, an increase in Φ_{PSII} and a decrease in NPQ (Fig. 4A, B, C). The decrease in F_v/F_m was correlated to the values for Φ_{PSII} and q_P before the increase in irradiance, as well as to the values for Φ_{PSII}, q_P, and NPQ on the first day after the increase in irradiance (Supplementary Table S1). Slowly reversible decreases in F_v/F_m are an indicator of photodamage or of slowly reversible down-regulation of PSII (Walters and Horton, 1991; Demmig-Adams and Adams, 1992; Niyogi, 1999; Demmig-Adams and Adams, 2006). We were not able to distinguish between these two mechanisms in our experiments, but overall the phenomenon of slowly reversible loss of F_v/F_m seems to occur if the short-term protection mechanisms that give rise to NPQ are insufficient to protect PSII from damage.

The kinetics of NPQ decay and Φ_{PSII} recovery after a step-increase in irradiance show genotypic variation (Fig. 4E and 4F), implying there is variation in the regulation of photosynthetic recovery after an irradiance increase, whereas the ultimate extent of acclimation after four days shows no genotypic variation. The extents of the changes in Φ_{PSII} in response to a step-increase in irradiance found by use are similar to those found by Yin et al. (2012), but their Φ_{PSII} values decreased for two days following the increase in irradiance before recovering on day three, whereas our data showed a recovery of Φ_{PSII} beginning on the first day after the increase in irradiance. This difference could be caused by the relatively greater irradiance increase they used (from 120 µmol m^{-2} s^{-1} to 950 µmol m^{-2} s^{-1} versus from 100 µmol m^{-2} s^{-1} to 600 µmol m^{-2} s^{-1} in our case), causing more

extensive slowly reversible loss of F_v/F_m. Yin et al identified two potential regulatory mechanisms that are variable among three Arabidopsis accessions in response to increased irradiance; one is the abundance of kinases that facilitate state transitions and the other is a mechanism to facilitate lateral protein traffic in the membrane by diluting chlorophyll-protein complexes with additional lipids and carotenoids (Yin et al., 2012). The variation we found for the kinetics of NPQ decay and Φ_{PSII} recovery is likely to reflect these different mechanisms found by Yin et al (2012), and in addition possible other regulatory mechanisms yet undefined.

After full acclimation to a step-wise increase in irradiance from 100 to 600 µmol m^{-2} s^{-1}, all accessions had a photosynthetic capacity higher than that achieved under a constant growth irradiance of 100 µmol m^{-2} s^{-1} (Fig. 5, Supplementary Figure S4). In contrast to our results, a similar study performed by Athanasiou et al. (2010) revealed significant variation in the ability of different accessions to acclimate to an increased irradiance. While Athanasiou et al. increased irradiance after 8 weeks of growth at 100 µmol m^{-2} s^{-1}, we increased it after 3.5 weeks of growth. Plant age or size therefore might have an effect on the capacity of photosynthesis to respond to the increase in irradiance. We also grew the plants hydroponically while Athanasiou et al. used soil-based cultivation, and differences in plant nutritional state might have contributed to the different responses of photosynthesis. Whatever the explanation, the fact that there are these differences implies that there are extra dimensions to the irradiance responses of photosynthesis in Arabidopsis that need to be understood. There is genotypic variation for the ability of leaves grown at 100 µmol m^{-2} s^{-1} before a step-increase in irradiance to 600 µmol m^{-2} s^{-1} to acclimate their photosynthetic capacity to that found in leaves grown at a constant irradiance 600 µmol m^{-2} s^{-1} (Fig. 5). A possible role for leaf anatomy in limiting the response of photosynthetic capacity in leaves subjected to an increase in irradiance has been reported (Oguchi et al., 2003) and there is variation in leaf architecture in Arabidopsis (Pérez-Pérez et al., 2002).

Natural genetic variation and GWAS

The fact that there is genetic variation for photosynthesis could mean that natural selection has favoured different optima depending on the local environment, especially since it is hard to imagine that genetic drift will be the sole cause of variation for such an important trait (Alonso-Blanco et al., 2009; Trontin et al., 2011). To investigate this it is crucial to identify the genes involved and the effect of alleles of those genes on the photosynthesis phenotype. Identifying causal allelic variation is easier when there is

substantial genetic variation for a trait, as quantified by the heritability values (Barton and Keightley, 2002) and the effect size of the QTL (Falke and Frisch, 2011). It is hard to predict how much heritability is required before a trait will be amenable to genetic analysis, as this depends on the number of loci that contribute to the heritability (i.e. the genetic complexity of the trait) and on the population used in the study (Visscher et al., 2008; Brachi et al., 2011). In this study of 12 Arabidopsis accessions it is clear that there are some photosynthetic traits for which heritability values look more promising for further genetic analysis than others

The heritability calculated for Φ_{PSII} in the 344 accessions used for the GWAS (H^2=0.09 before, and H^2=0.26 one hour after, the increase in growth irradiance (Figure S5) is different from the heritability calculated for the population of 12 accessions (H^2=0.59 before, and H^2=0.53 after the increase in growth irradiance; Figure 2B). Different heritabilities for the same trait in different populations can be explained by different allele frequencies (Visscher et al., 2008); in this case it looks like the small set of 12 diverse accessions already captured most of the genetic variation for Φ_{PSII} also found in the larger set of 344 accessions. Even though alleles get more heterogeneous when studying a bigger natural population (Brachi et al., 2011; Gibson, 2012), if the larger heterogeneity found in the set of 344 accessions does not contribute to larger phenotypic variation than in the set of 12 accessions, but merely a dilution of the phenotypic effect of extreme genotypes, the result will be a reduction in heritability.

Successful GWAS studies have identified an over-representation in a-priori candidate genes (Atwell et al., 2010), or identified only a small number of genes that were associated above the Bonferroni threshold of $-\log_{10}(p)$ = 6.50 (Chao et al., 2012; Meijón et al., 2014). The Bonferroni threshold is a very stringent statistical test correcting for multiple testing (Holm, 1979). In our study, no genetic associations are detected with a $-\log_{10}(p)$ above the Bonferroni threshold. As the change in photosynthesis efficiency in response to an increase in irradiance is a highly polygenic trait, we expect that the effects of the individual underlying genes will be small. Such genes are likely to remain hidden in associations that do not exceed the Bonferroni threshold because of epistatic and interactive effects (Gibson, 2010; Korte and Farlow, 2013). By lowering the $-\log_{10}(p)$ threshold to 4, some of these hidden associations were be revealed (Fig. 6), allowing us to select 63 candidate genes which either contained an associated SNP or were in linkage disequilibrium (LD) with the SNP (Table II). No genes previously reported to be involved in photosynthesis were found among these candidate genes. To provide validation for our approach, a gene ontology (GO) enrichment analysis was performed

from which we could extract the ontology classes that are relevant for the natural variation of our trait (Fig. 7) (Huang et al., 2009). There was enrichment for regulation of protein abundance (enriched ontology classes: golgi apparatus, kinase activity, transferase activity, protein binding, protein metabolism, response to (a)biotic stimulus or to stress), as well as to responses limited to the nucleus (enriched ontology class: nucleus) and the chloroplast (enriched ontology classes: chloroplast, cytosol, transporter activity). Out of the 63 candidate genes, 13 of the (nuclear-) encoded proteins localized to the chloroplast (Table III). Close analysis of the function of these 13 genes validates the enrichment for abiotic stress responses, as some genes are involved with the sensing of a stress (receptor; oxidative stress protein; calcium binding protein), others with regulating a stress response (chromatin assembly/disassembly; RNA modification; regulator of expression of defence genes), and others are involved with the act of responding to (photosynthetic) stress (DNA mismatch repair; protease for degrading abnormal and damaged proteins; carbohydrate transport) (Table III). Only four genes have no known function.

Conclusion

In conclusion, we have demonstrated that for Arabidopsis accessions there is genotypic variation for the short-term response of photosynthetic light use efficiency to a step-wise increase in growth irradiance as well as its long-term acclimation. The data also show that over the range of growth irradiances employed, the light use efficiency of photosynthesis (measured by Φ_{PSII}) acclimates strongly to the level of growth irradiance so that the Φ_{PSII}, measured at an actinic irradiance identical to the growth irradiance, only decreases slightly with higher levels of growth irradiance. A broader phenotypic distribution is found by measuring Φ_{PSII} at light saturation (Fig. 2B, 3A, 5, and supplementary Fig. S5). In relation to productivity and yield, the ability of photosynthesis to acclimate has been shown to increase plant fitness of Arabidopsis in a greenhouse environment where natural fluctuations in irradiance and other environmental factors would have occurred (Athanasiou et al., 2010). If there was a desire to breed Arabidopsis for improved photosynthetic properties leading to increased yield, more might be gained by focussing on the dynamic regulatory acclimation response of photosynthesis to different light environments instead of investigating acclimation to stable environments (Leister, 2012). The response described here will be useful when selecting light environments for optimal, uniform growth of Arabidopsis, and also serves as a reminder that while often grown at low irradiances (100-200 μmol m^{-2} s^{-1}), Arabidopsis has photosynthetic responses that are more typical of a high-light adapted plant, in accordance with its natural habitat which

is disturbed sites, possibly with light shade (Pigliucci, 1998; Mitchell-Olds and Schmitt, 2006). In addition, we have shown that for those traits for which there is considerable heritability, it is possible to use GWAS to identify novel candidates for genetic components of the plant photosynthetic response to light.

ACKNOWLEDGEMENTS

SUPPLEMENTARY TABLES AND FIGURES

Table S1. Correlation between the relative decrease of Fv/Fm on the first day after increasing the growth irradiance from 100 μmol m^{-2} s^{-1} to 600 μmol m^{-2} s^{-1} and other photosynthetic parameters during the acclimation period to increased growth irradiance.

*Dark grey cells indicated with ** represent significant correlations at P=0.05; light grey cells indicated with * represent significant correlations at P=0.10.*

DAY0		$F_\sqrt{}/F_m$	F_v'/F_m'(600)	NPQ(600)	$_qP$(600)	Φ_{PSII}(600)
Decrease in $F_\sqrt{}/F_m$ on day 1 relative to day 0	Pearson Correlation	0.088	0.031	0.025	.395**	0.296*
	Sig. (2-tailed)	0.616	0.862	0.886	0.019	0.085

DAY1 (after HL increase)		$F_\sqrt{}/F_m$	F_v'/F_m'(600)	NPQ(600)	$_qP$(600)	Φ_{PSII}(600)
Decrease in $F_\sqrt{}/F_m$ on day 1 relative to day 0	Pearson Correlation	.792**	.077	.364**	.525**	.393**
	Sig. (2-tailed)	.000	.659	.032	.001	.019

DAY2 (after HL increase)		$F_\sqrt{}/F_m$	F_v'/F_m'(600)	NPQ(600)	$_qP$(600)	Φ_{PSII}(600)
Decrease in $F_\sqrt{}/F_m$ on day 1 relative to day 0	Pearson Correlation	.636**	.109	.255	.394**	0.286*
	Sig. (2-tailed)	.000	.533	.139	.019	.096

DAY3 (after HL increase)		$F_\sqrt{}/F_m$	F_v'/F_m'(600)	NPQ(600)	$_qP$(600)	Φ_{PSII}(600)
Decrease in $F_\sqrt{}/F_m$ on day 1 relative to day 0	Pearson Correlation	.617**	0.311*	-.040	.387**	.396**
	Sig. (2-tailed)	.000	.069	.819	.022	.018

DAY4 (after HL increase)		$F_\sqrt{}/F_m$	F_v'/F_m'(600)	NPQ(600)	$_qP$(600)	Φ_{PSII}(600)
Decrease in $F_\sqrt{}/F_m$ on day 1 relative to day 0	Pearson Correlation	.505**	0.306*	-.084	.382**	.365**
	Sig. (2-tailed)	.002	.074	.631	.024	.031

Table S2. Annotations of the gene function as indicated in TAIR (www.arabidopsis.org) of all the genes found to be in linkage disequilibrium (r> 0.45) with the SNPS associated with a – log10(p) >4 for ΦPSII measured one hour after a step-wise increase in irradiance from 100 to 550 µmol m-2 s-1.

| Gene	Description
AT1G21060	Unknown protein
AT1G21065	Unknown protein
AT1G21070	Nucleotide-sugar transporter family protein
AT1G21100	IGMT1, indole glucosinolate O-methyltransferase 1
AT1G21110	IGMT3, indole glucosinolate O-methyltransferase 3
AT1G21120	IGMT2, indole glucosinolate O-methyltransferase 2
AT1G21130	IGMT4, indole glucosinolate O-methyltransferase 4
AT1G21140	Nodulin-like1, transcript abundance repressed under conditions of Fe-deficient growth
AT1G74190	Receptor-like protein 15, located in endomembrane system
AT2G26290	Root-specific kinase1
AT3G04880	Encodes a novel protein involved in DNA repair from UV damage
AT3G04890	Unknown protein
AT3G04900	Heavy metal transport/ detoxification superfamily protein
AT3G04903	Encodes a defensin-like family protein
AT3G05790	Lon-protease 4, for degradation of abnormal, damaged, and unstable protein
AT3G05800	AIF1 (activation-tagged BRI1 suppressor 1)-interacting factor 1, involved in MAPK cascade, major regulator
AT3G05810	Chromatin assembly/disassembly protein
AT3G05820	Encodes a putative plastid-targeted alkaline/neutral invertase
AT3G05830	Encodes an intermediate filament-liek protein, function unknown
AT3G05835	tRNA-Ile
AT3G05840	Encodes a kinase involved in meristem organization
AT3G05850	Encodes a member of a domesticated transposable element gene family
AT3G05858	Unknown protein
AT3G05870	Subunit of the anaphase promoting complex in cell division
AT3G05880	Encodes a small, highly hydrophobic protein induced by low temperatures, dehydration and salt stress (A)
AT3G05890	Encodes a small, highly hydrophobic protein induced by low temperatures, dehydration and salt stress (B)
AT3G54000	Unknown protein
AT4G21750	MERISTEM LAYER 1, a homeobox protein similar to GL2; expressed in both the apical and basal daughter cells of the zygote.
AT4G21770	Pseudouridine synthase, involved in RNA modification
AT5G03750	Unknown protein
AT5G64910	Unknown protein
AT5G64920	Encodes a RING-H2 protein, involved in ubiquitination
AT5G64930	Regulator of expression of pathogenesis-related genes. Participates in signal transduction pathways involved in plant defence.
AT5G64940	Oxidative stress-related ABC1-like protein (ATP-binding cassette)
AT5G64950	Mitochondrial transcription termination factor family protein
AT5G64970	Mitochondrial substrate carrier family protein
AT5G64990	RAB GTPase homolog, GTPase activity, located in mitochondrion
AT5G65020	Annexin 2, calcium binding protein
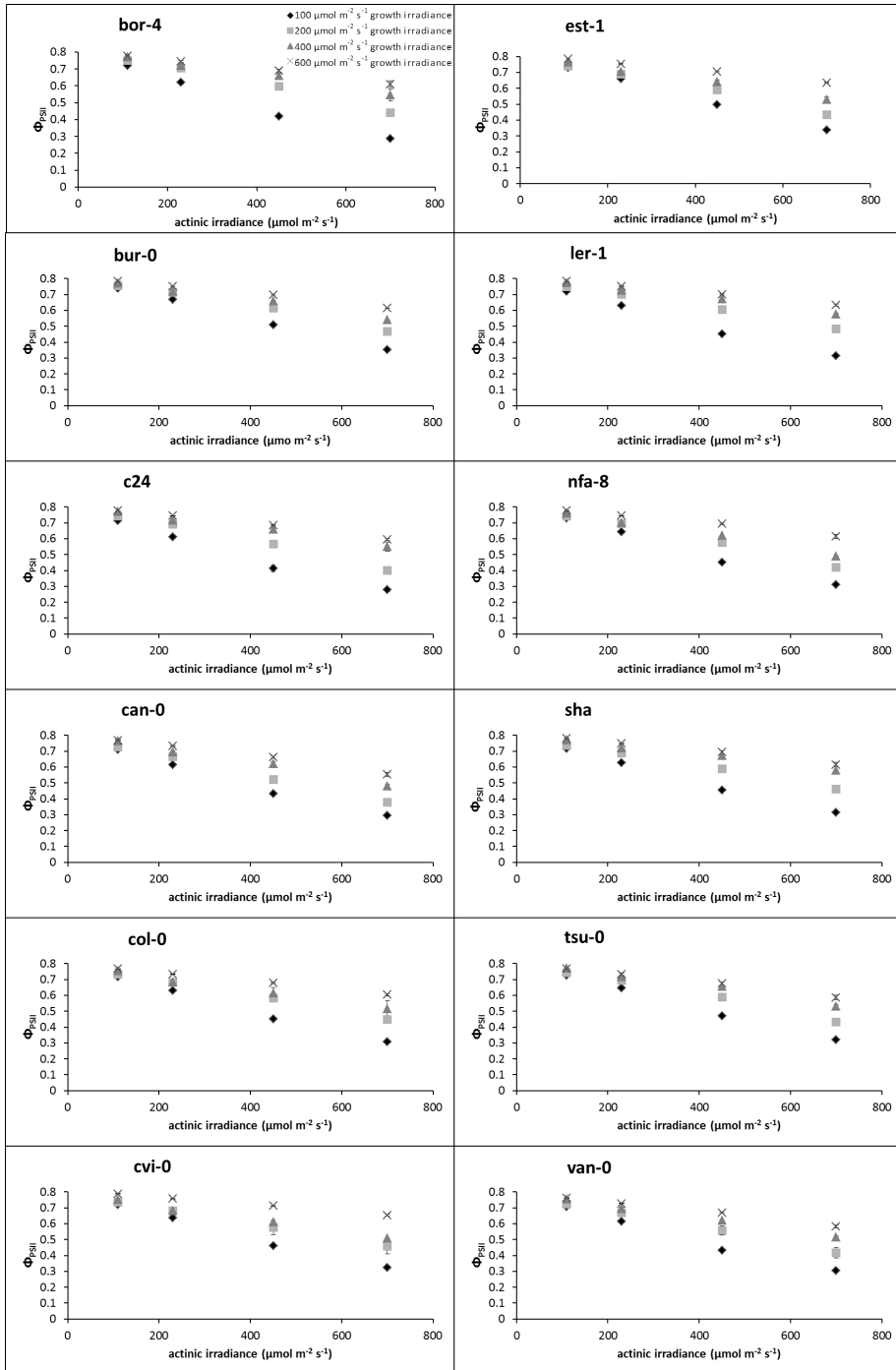
Figure S1. Light response curves per accession in different constant growth irradiances.

Error bars indicate the standard error of the mean, N=3.
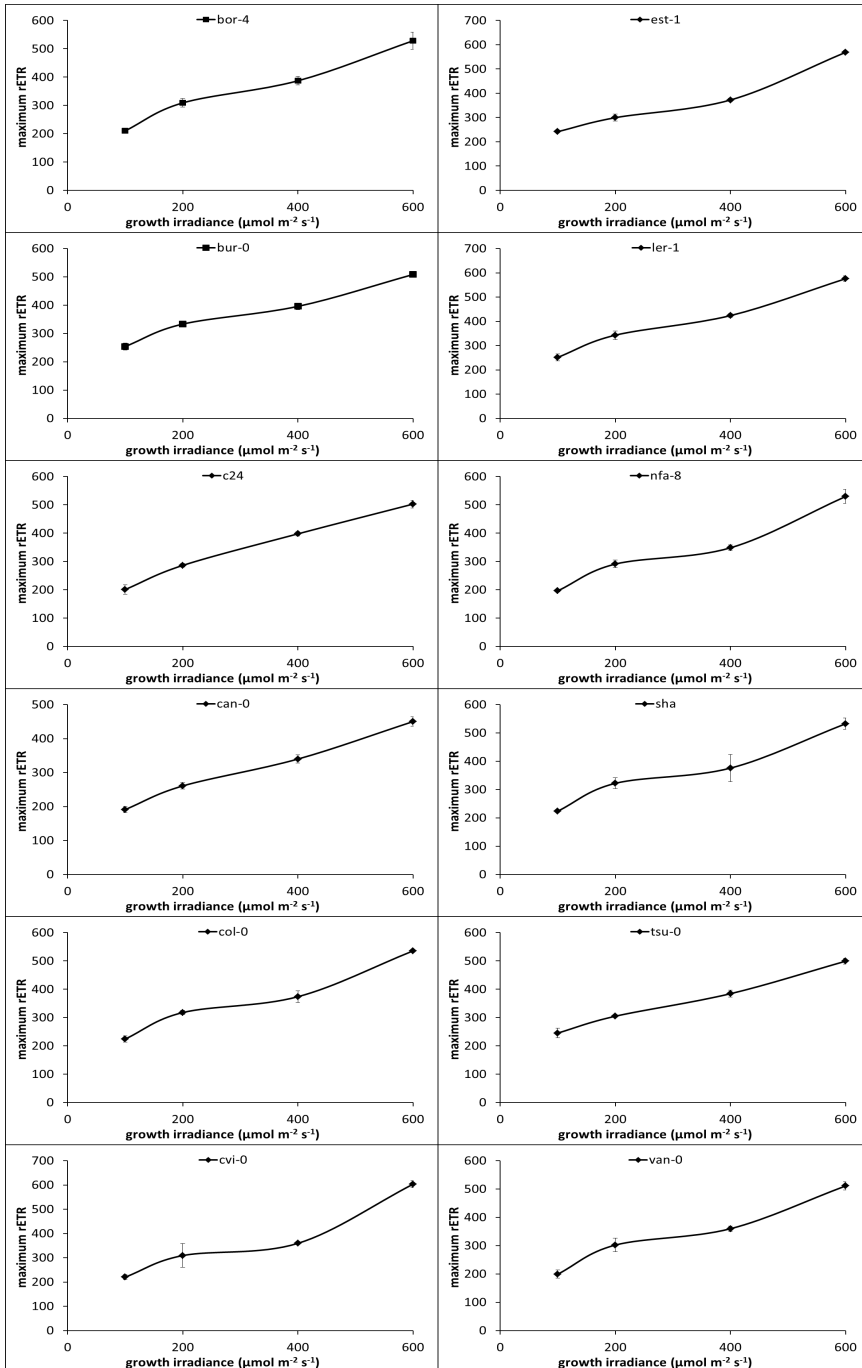
Figure S2. Maximum relative electron transport rates (rETR) measured at saturating actinic irradiance per accession in different constant growth irradiances.

Error bars indicate the standard error of the mean, N=3.

A Descriptives					Tukey's HSD test		
		Mean parameter-ized value	Std. Deviation	Std. Error	Subset for alpha = 0.05		
	N				1	2	3
tsu-0	3	1.1117	.58950	.34035	1.1117		
c24	3	1.3907	.56734	.32755	1.3907	1.3907	
est-1	3	1.4367	.37650	.21737	1.4367	1.4367	
cvi-0	3	1.5407	.36650	.21160	1.5407	1.5407	1.5407
can-0	3	1.6290	.27900	.16108	1.6290	1.6290	1.6290
sha	3	2.1377	.12150	.07015	2.1377	2.1377	2.1377
bur-0	3	2.1720	.19300	.11143	2.1720	2.1720	2.1720
bor-4	3	2.3607	.98273	.56738	2.3607	2.3607	2.3607
col-0	3	2.5650	.63877	.36879	2.5650	2.5650	2.5650
ler-1	3	2.6727	.58750	.33919	2.6727	2.6727	2.6727
nfa-8	3	2.9483	.75612	.43655		2.9483	2.9483
van-0	3	3.1210	.52400	.30253			3.1210
Sig.					.067	.068	.061
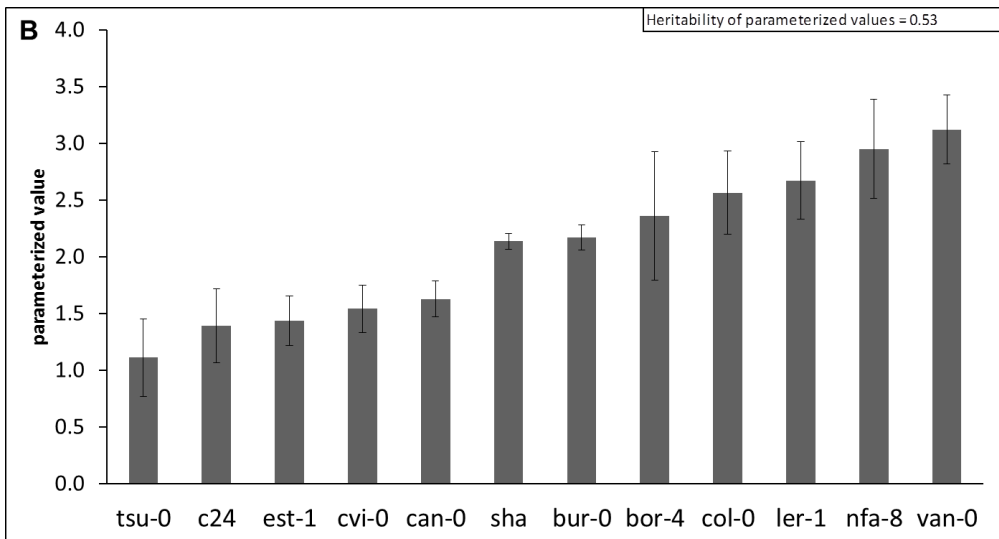
Figure S3. Variation in parameterized value of the relation of maximum rETR with growth irradiance level

(A) Descriptive ANOVA table including a Tukey's HSD test revealing three significantly different groups for the parameterized value at p=0.05; (B) Variation in parameterized value for the relation between photosynthetic capacity and growth irradiance, Error bars indicate the standard error of the mean, N=3. The top right inset shows the heritability calculated for this trait.
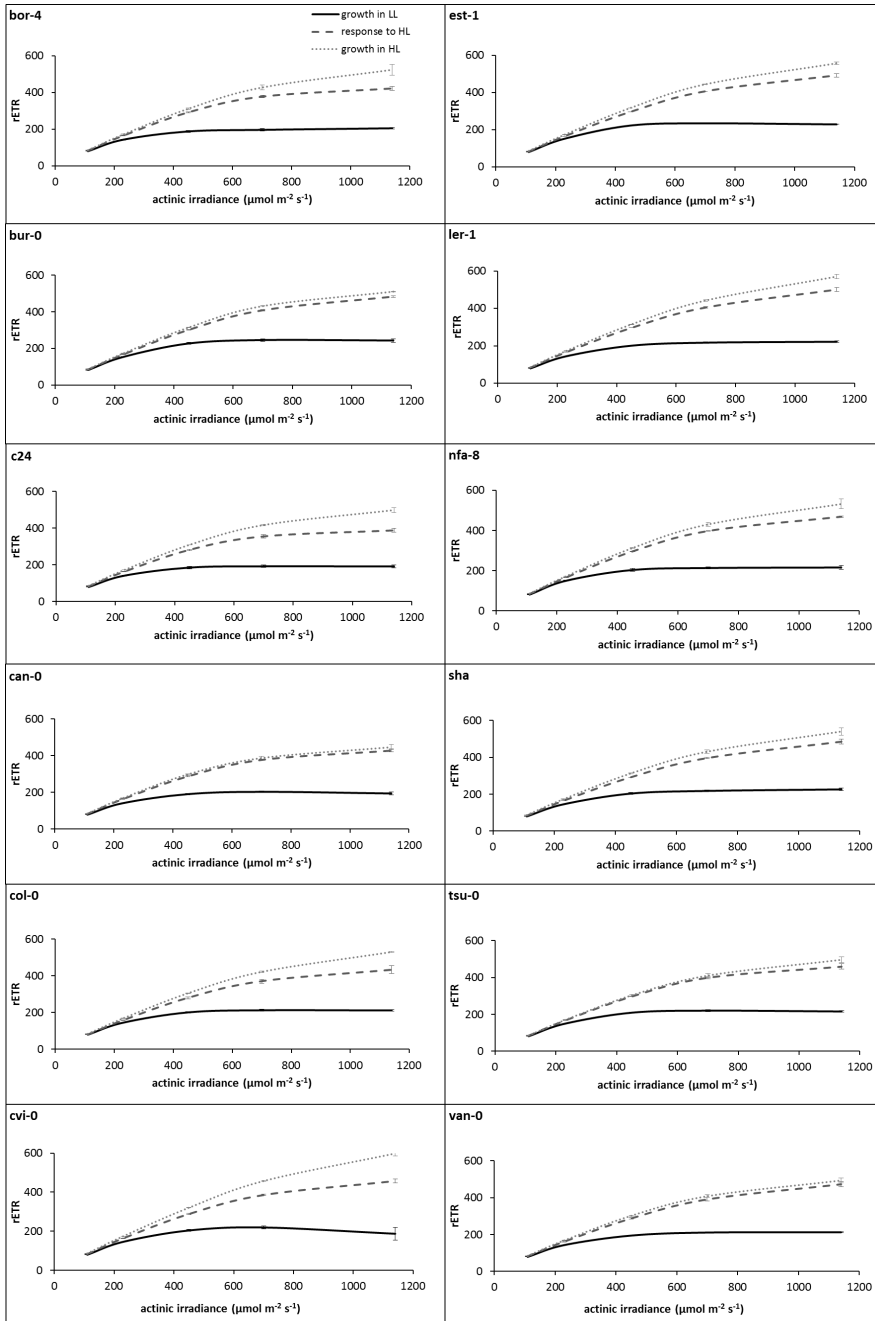
Figure S4. Complete variation in light response curves of rETR of all 12 accessions grown in low growth irradiance level (LL), response to high growth irradiance level (HL), or grown in HL
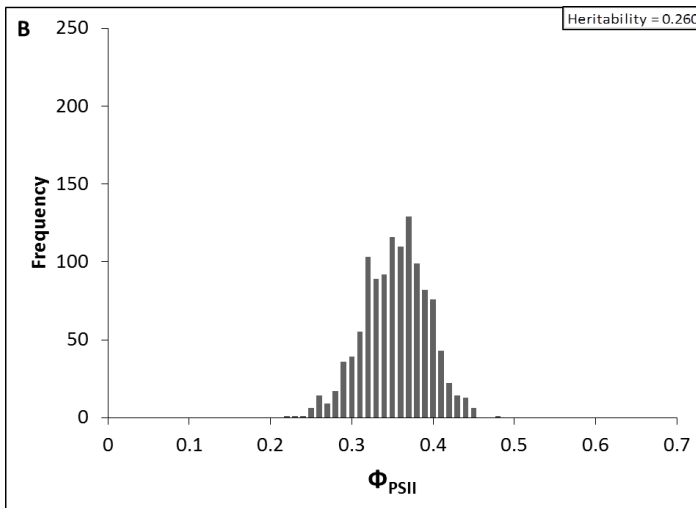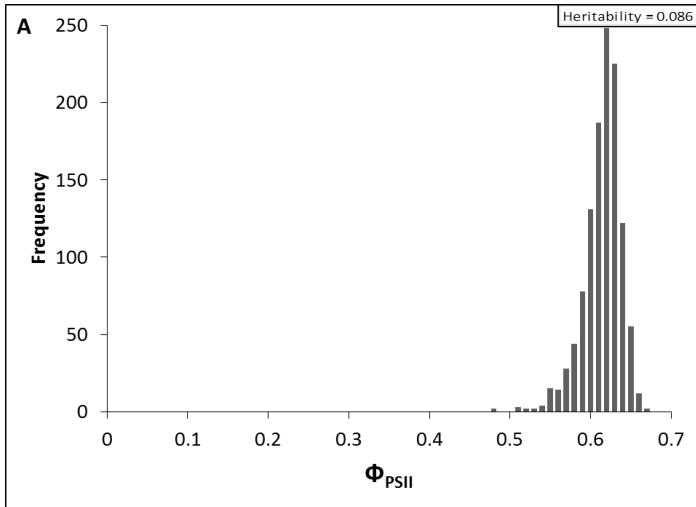
Figure S5. Phenotypic distribution of Φ_{PSII} **one day before (A) and one hour after (B) an increase in growth irradiance from 100 μmol m^{-2} s^{-1} to 550 μmol m^{-2} s^{-1} for the 344 accessions used for the GWAS.**

Chapter 3

A regulator in anterograde signalling underlies natural variation for plant photosynthesis

Roxanne van Rooijen[1,2], Jeremy Harbinson[2], Mark G.M Aarts[1]

[1]Laboratory of Genetics & [2]Horticulture and Product Physiology, Wageningen University, Droevendaalsesteeg 1, 6708 PB Wageningen, The Netherlands

ABSTRACT

Increases in irradiance levels damage the photosynthesis machinery, but plants can protect themselves from this damage and adapt to acclimate (Demmig-Adams and Adams, 1992; Walters, 2005). Natural genetic variation for this acclimation should be exploited to identify the genes involved (Van Rooijen et al., 2015). Here we show it is feasible to dissect natural genetic variation in photosynthesis efficiency down to the genomic DNA level, by confirming that allelic sequence variation at the *YELLOW SEEDLING1* (*YS1)* gene explains natural variation in *Arabidopsis thaliana* photosynthesis acclimation. *YS1* encodes a Pentatrico-Peptide-Repeat (PPR) protein involved in RNA editing of plastid encoded genes (anterograde signalling), (Zhou et al., 2009). A genome-wide association (GWA) study was performed in a time-course manner to genetically dissect the photosynthetic acclimation response of *Arabidopsis thaliana*. Candidate genes were prioritized according to recurrence of association over time, in combination with relevant functional clues regarding gene ontology, expression and function. Reverse genetics supported the involvement of four gene candidates. Quantitative complementation and gene expression analysis confirmed that polymorphisms in the GT-1 binding site of the light responsive element in the promoter of *YS1* are the cause of the variation in photosynthetic acclimation.

INTRODUCTION

Light, as the driving force for photosynthesis, is a conspicuously important determinant of photosynthetic activity. Genetic variation exists in plants for what constitutes a high light leaf or a low light leaf, for the range of irradiances to which the leaf is capable of responding, and for the actual photosynthetic properties that emerge from any environmental treatment. A sudden increase in growth irradiance beyond light saturation causes light stress in the photosynthetic apparatus, especially in photosystem II (PSII). Within a few seconds this provokes a protective regulatory response in the metabolism of the leaf (Demmig-Adams and Adams, 1992; Dietz, 2015). If the increased irradiance level is sustained it will induce a photosynthetic acclimation response via changes in the composition of mesophyll cells in terms of their proteins, pigments, and lipids, and other cofactors involved in electron transport and reactive-oxygen species metabolism (Bailey et al., 2004; Walters, 2005; Li et al., 2009). The regulation of photosynthetic acclimation starts with signals originating either from photoreceptors, or from the photosynthetic machinery itself, going to the nucleus and altering patterns of nuclear gene expression (retrograde signalling), (Li et al., 2009). By identifying the genomic regions that associate with phenotypic variation before or after the increase in irradiance, or both, we can distinguish those regions that are associated with photosynthetic light use efficiency in general from those genomic regions that are associated with photosynthetic acclimation to an increase in irradiance (Moore et al., 2013; Bac-Molenaar et al., 2015). Annotating the genes that give rise to the photosynthetic acclimation response will reveal at which regulatory level natural genetic variation for photosynthesis exists. Photosynthesis is a complex trait at both the physiological and genetic levels and as a result natural genetic variation in photosynthesis is an underused resource for identification of the genetic regulation of photosynthesis (Flood et al., 2011; Van Rooijen et al., 2015). The poor understanding of the genetic foundations of photosynthetic traits together with the complex relationship between photosynthesis and yield has resulted in photosynthesis being underused in plant breeding programmes (Flood et al., 2011; Driever et al., 2014). Nevertheless it does have great potential for crop improvement (Lawson et al., 2012; Long et al., 2015).

MATERIALS AND METHODS

Plant material and growth conditions

A set of 344 *Arabidopsis thaliana* (Arabidopsis) accessions was used for GWA, which are all part of a core set of 360 natural accessions that represent the global genetic diversity of the species (https://www.arabidopsis.org/servlets/TairObject?type=stock&id=4501958598)(Li et al., 2010). Sixteen accessions of the core set were not used: CS28051, CS28108, CS28808, CS28631, CS76086, CS76104, CS76110, CS76112, CS76118, CS76121, CS76138, CS76196, CS76212, CS76254, CS76257 and CS76302. An overview of all T-DNA lines that were studied can be found in Table S3.

Plants were grown as previously described(Van Rooijen et al., 2015). In short, this involved growing plants in a climate controlled growth chamber, on rockwool supplied with a nutrient solution, at a constant irradiance of 100 µmol m^{-2} s^{-1} (Philips 610 fluorescent tubes, MASTER TL5 HO, 80W). The photoperiod was set to 10h/14h day/night, temperature was set to 20/18°C (day/night), relative humidity was set at 70% and CO_2 levels were ambient. The irradiance was increased to 550 µmol m^{-2} s^{-1}, at the onset of the photoperiod, on day 25 after sowing.

Chlorophyll a fluorescence imaging and analysis

Chlorophyll a fluorescence was measured using a high-throughput phenotyping system developed for Arabidopsis, as described previously(Van Rooijen et al., 2015). In all experiments, the photoperiod lasted from 8.00h until 18.00h CET and imaging of light use efficiency of photosystem II (Φ_{PSII}) was performed daily at 9.00h, 11.30h, 14.30h and 16.30h.

Genome-wide association (GWA) analysis

Using a mixed model(Kruijer et al., 2015), GWA analyses were performed twice for each time point, once for the Φ_{PSII}-values averaged per accession (3-4 replicates were used to produce the average value), and once on the individual measurements (using 3-4 replicates). For each time point this was achieved by associating the Φ_{PSII}-values (either averaged per accession or the individual measurements) to 215,000 SNPs that were scored either similar to the Col-0 accession (C) or not similar to the Col-0 accession (NC)(Kim et al., 2007); a minor SNP frequency of 0.05 was used to remove rare SNPs.

For each of the 215,000 SNPs, the -$\log_{10}(p)$ value was calculated, where 'p' represents the p-value of a t-test between the C- and NC-group of each SNP.

For each time point, SNPs with -$\log_{10}(p)>4$ were classified as quantitative trait loci (QTLs); whenever two or more SNPs were in linkage disequilibrium (LD; LD ≥ 0.45) they were lumped together to form one QTL. LD was determined by calculating the correlation coefficients between SNP calling frequencies in the population of study. The genome was divided into 2-Kbp blocks and the -$\log_{10}(p)$ values of all SNPs with -$\log_{10}(p)>4$ within these blocks were first summed to form cumulative association scores. The scores of each 2-Kbp region were then averaged with four adjacent 2-Kbp regions, two upstream and two downstream to smooth the data. QTLs were numbered according to physical position, and identified according to time of appearance, i.e. only in low light, early in the response to high light, late in the response to high light, or at all time points.

All genes in LD with the associated SNPs for each QTL were identified by first listing all SNPs in LD (LD ≥ 0.45) with each SNP with a -$\log_{10}(p)>4$, and then cataloguing all genes in LD with these linked SNPs. The LD was calculated using whole genome re-sequence data for 173 accessions out of the population of 344 accessions used for the GWA, obtained from the 1001 genomes project (http://1001genomes.org/; Table S4).

Candidate gene prioritization

All candidate genes in LD with the associated SNPs were prioritized in an *in silico* analysis using publicly available databases for:

 (1) gene ontology terms (www.arabidopsis.org),
 (2) gene co-expression patterns(Hruz et al., 2008) (www.genevestigator.com),
 (3) gene expression in the vegetative rosette(Schmid et al., 2005)
       (http://bar.utoronto.ca/) ,
 (4) known to have a function related to photosynthesis based on literature,
 (5) presence of polymorphisms segregating between two groups of 15 accessions with
       the most extreme phenotypes (http://1001genomes.org/).

Whenever a candidate gene scored positive for three out of these five criteria, it was included in the priority candidate list (Table 1). When multiple candidate genes for one QTL listed in the priority candidate list, we selected the priority candidate with segregating polymorphisms in the extreme accessions for our reverse screening. For some QTLs we chose multiple priority candidate genes for reverse screening, because multiple genes

complied with the segregating polymorphism-criterion, or because neighbouring genes with homologous/redundant functions were listed in this QTL.

Haplotype analysis

Haplotypes, representing natural alleles, were assigned based on all SNPs in the promoter and coding regions of candidate genes using the re-sequence data of 173 accessions. Those haplotypes that occurred in >4% of the 173 accessions were then associated with photosynthetic phenotypes. Haplotypes that resulted in different photosynthetic response to increased irradiance (based on two-sided Student's t-test) were selected for quantitative complementation tests.

Quantitative complementation

Quantitative complementation to confirm involvement of allelic difference at one locus to contribute to the observed phenotypic variation (Long et al., 1996a), was performed by crossing two accessions with different alleles for the gene involved, thought to contribute to the most contrasting phenotypes, to a T-DNA insertion knock-out mutant for the gene, in accession Columbia (Col) background, as well as to the Col wild type (both used as maternal line). The phenotype of resulting F1 plants (N = 16 per cross) for their photosynthetic response to increased irradiance was determined as described above, two-way ANOVA was performed for testing significance. For quantitative complementation of *YS1*, we used the accession CS76172 representative for allele 3 accessions and the accession CS76133 representative for allele 4 accessions. The whole experiment for quantitative complementation was performed twice in the laboratory.

Quantitative reverse transcription PCR (qRT-PCR)

At time point 11.00 am CET (i.e. 3h after lights on) on days 24 (LL plants) and 25 (HL plants) after sowing, whole rosettes were collected and flash-frozen in liquid nitrogen. RNA was isolated according to Onate-Sánchez and Vicente-Carbajosa (2008). After normalization of RNA concentrations, cDNA was synthesized using the Iscript cDNA synthesis kit (Bio-RAD, www.bio-rad.com). qRT-PCR was performed with three technical replicates for each biological replicate using the SYBR-green master mix (Bio-RAD, www.bio-rad.com). Three biological replicates were used per accession; four accessions were analysed per haplotype. Two reference genes were used for normalization: *UBIQUITIN7* (*UBQ7;* At2g35635) and *CYTOCHROME B5 ISOFORM E* (*CB5E;* At5g53560); transcription levels of *UBQ7* were shown to be constant under excess light

by Jung et al. (2013), and the transcription levels of *CB5E* were shown to be constant under excess light by Wunder et al. (2013). The primers used for qRT-PCR are listed in Table S5. We chose the accessions CS76113, CS28193, CS28492, and CS76297 to represent allele 1; the accessions CS76305, CS28685, CS76218, and CS76153 to represent allele 3; and the accessions CS28787, CS76133, CS76129, and CS76128 to represent allele 4. One-way ANOVA was used for testing significance.

RESULTS AND DISCUSSION

Using chlorophyll fluorescence imaging, the light-use efficiency of PSII electron transport (Φ_{PSII}) was measured in 344 Arabidopsis accessions at four time-points during the day, before and after the plants were subjected to a sudden increase in growth irradiance (Fig. 1a). The phenotypic distribution for Φ_{PSII} was narrow under steady low growth irradiance (100 µmol m^{-2} s^{-1}), got broader upon high irradiance exposure (550 µmol m^{-2} s^{-1}), and narrowed again during photosynthetic acclimation (Fig. 1b), reflecting the pattern of acclimation in the leaves – first young, then old leaves (Fig. 1a). All Φ_{PSII} measurements were highly positively correlated per accession, indicating a coordinate regulation of photosynthesis in these irradiance environments (Fig. 1c).

Figure 1 (on next page) Photosynthesis efficiency of photosystem II (ΦPSII) in response to an increase in growth irradiance.

(a) Photosynthetic acclimation of Φ_{PSII} of Arabidopsis accession Col-0. Shown are the Φ_{PSII} values over time (±s.e.m.) and a chlorophyll fluorescent image of the same Col-0 plant measured one hour after onset of the photoperiod. (b) Frequency distribution of Φ_{PSII} measured for 344 accessions at consecutive time points in the acclimation response, three replicate plants are measured per accession. (c) Pearson's correlation analysis of Φ_{PSII} measured at consecutive time points in the acclimation response for all accessions. All correlations are significant at p≤0.001.
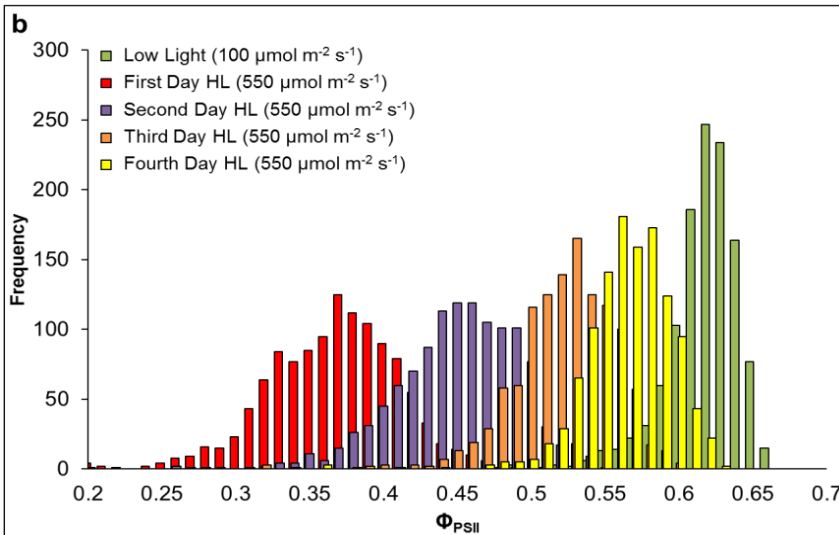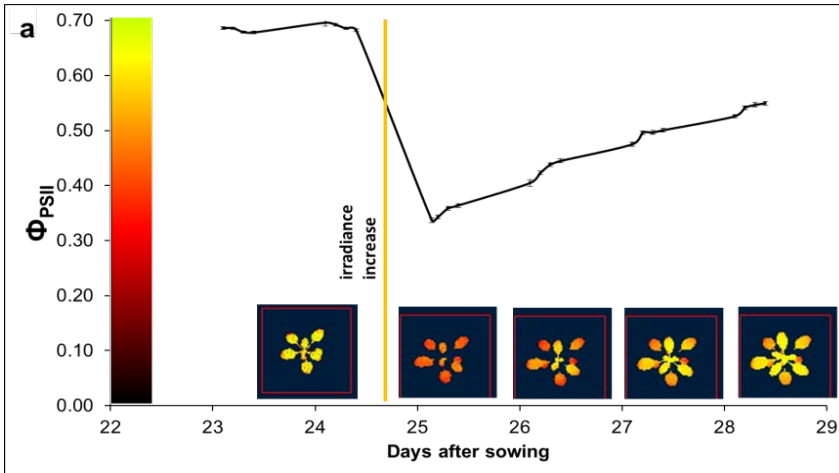
		First Day HL	Second Day HL	Third Day HL	Fourth Day HL
First Day HL	Pearson Correlation	0.427			
	Sig. (2-tailed)	5.640E-53			
Second Day HL	Pearson Correlation	0.298	0.867		
	Sig. (2-tailed)	2.077E-25	0.000E+00		
Third Day HL	Pearson Correlation	0.294	0.84	0.937	
	Sig. (2-tailed)	9.756E-25	0.000E+00	0.000E+00	
Fourth Day HL	Pearson Correlation	0.325	0.806	0.839	0.943
	Sig. (2-tailed)	2.820E-30	2.100E-268	0.000E+00	0.000E+00
		Low Light	**First Day HL**	**Second Day HL**	**Third Day HL**

Genome-wide association (GWA) analysis of Φ_{PSII} at each data point resulted in a non-linear time course of associations, which is represented in a heat map of the cumulative association scores (i.e. accumulation of $-\log_{10}(p)$ values) throughout the acclimation response (Fig. 2). Twenty-six quantitative trait loci (QTLs) were identified, which were classified according to the time and duration of their appearance: seven QTLs were specific for the low irradiance phase, thirteen appeared directly after the onset of the high light treatment, three occurred later in the response to high light, and three were present throughout the experiment, independent of the irradiance level. The power of GWA studies in plants to identify true associations has proven to be relatively low for complex polygenic traits, such as photosynthesis, because of small effect sizes of each of the individual genes that together cause the phenotype (Korte and Farlow, 2013). Lowering the threshold of significance in the association analysis, e.g. below the rather strict significance threshold following a Bonferroni correction, will highlight some associations that would otherwise be ignored (Van Rooijen et al., 2015), but is also likely to increase the number of false positives (Korte and Farlow, 2013). Selection of recurrent QTLs through time allows the distinction to be made between true associations and false positive associations, strengthening the mapping power in GWA studies (Fig. 2). In addition, it allows distinction between those non-specific QTLs that are present throughout the phenotyping phase and those that are time-specific (Bac-Molenaar et al., 2015).

To focus on the acclimation response of photosynthesis we conducted no further analysis on the seven QTLs specific for the low irradiance phase of the experiment. The three QTLs present throughout the experiment were included for further analysis as they were found to increase in cumulative association score after the irradiance increase (Fig. 2). We then determined the physical positions of those SNPs corresponding to the 19 QTLs associated specifically to photosynthetic acclimation (Fig. S1). Including all genes in linkage disequilibrium (LD) with these SNPs resulted in a list of 268 candidate genes for which allelic variation may have caused the association (Table S1). Of these genes, 33 scored positive for three out of five *in silico* selection criteria based on gene function that we used to prioritize the candidate genes: gene ontology, gene co-expression, gene expression in the vegetative rosette, and the presence of segregating polymorphisms in the coding sequence (Table S2). These 33 priority candidate genes corresponded to 15 of the 19 acclimation-specific QTLs. Reverse screening with T-DNA insertion lines was performed for 20 of the 33 priority candidate genes.
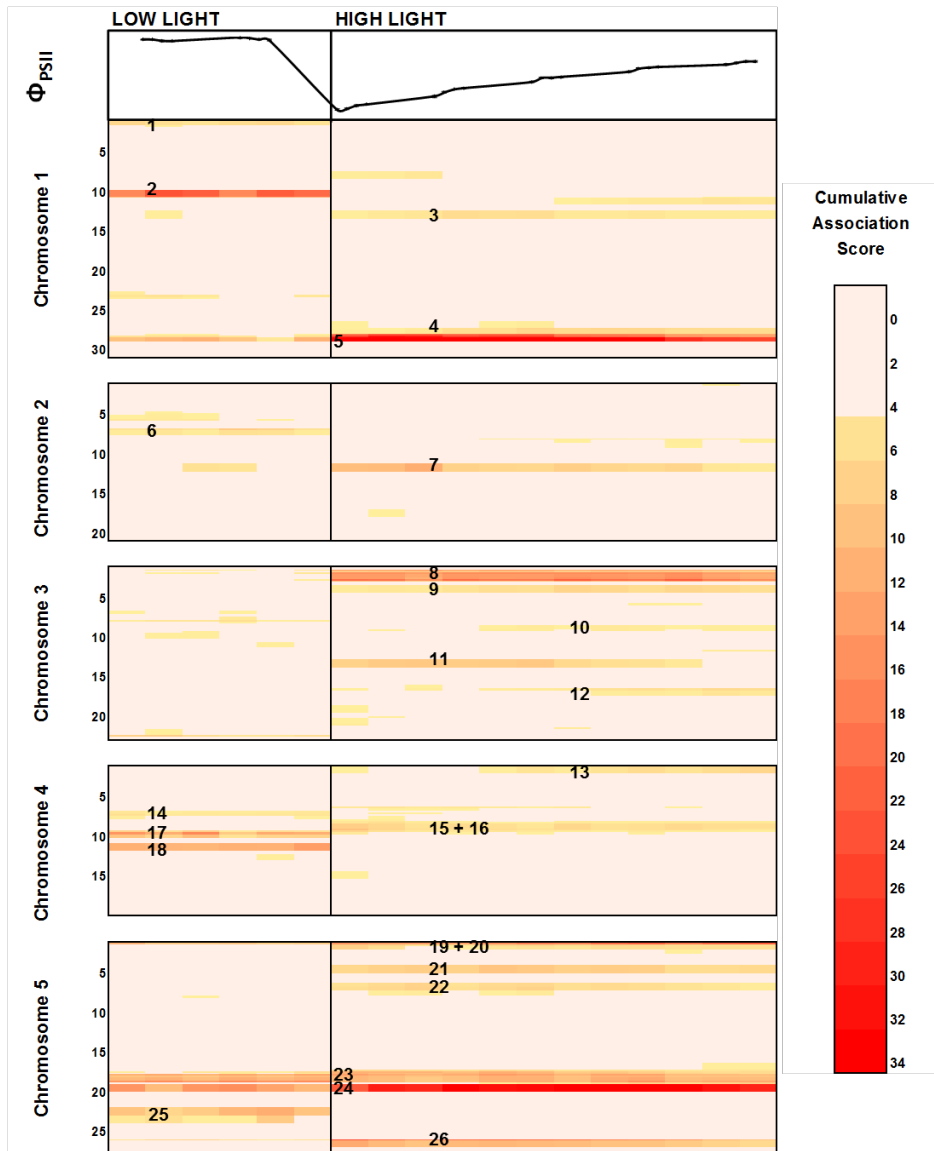
Figure 2 Heat map of cumulative association scores in a genome-wide association study of ΦPSII, before and after an increase in growth irradiance.

Plant Φ_{PSII} is measured three times per day, two days in low light (100 µmolm^{-2}s^{-1}) and four days in high light irradiance (550 µmolm^{-2}s^{-1}). Association scores of genomic regions of 0.2 megabasepairs (Mbp) per chromosome were summed and subsequently averaged within a 1-Mbp sliding window from the top to the bottom of each of the five A. thaliana chromosomes. The physical distance (Mb) in each chromosome is indicated. Each quantitative trait locus (QTL) is numbered, 1-26.

Four T-DNA insertion lines showed an aberrant phenotype for photosynthetic acclimation to increased irradiance (Fig. 3). These are insertion lines for *CTC-INTERACTING DOMAIN 7* (*CID7* (At2g26280), which encodes a protein involved in DNA binding and mismatch repair; corresponds to QTL7 of Fig. 2), *YELLOW SEEDLING 1* (*YS1* (At3g22690), which encodes a Pentatrico-Peptide-Repeat (PPR) protein involved in RNA editing of plastid encoded genes; corresponds to QTL10), *DGD1 SUPPRESSOR 1* (*DGS1* (At5g12290), which encodes a mitochondrial outer membrane protein involved in galactolipid biosynthesis; corresponds to QTL 21 of the heat map), and *ASPARAGINE SYNTHETASE 2* (*ASN2* (At5g65010), which encoding an asparagine synthetase; corresponds to QTL 26).
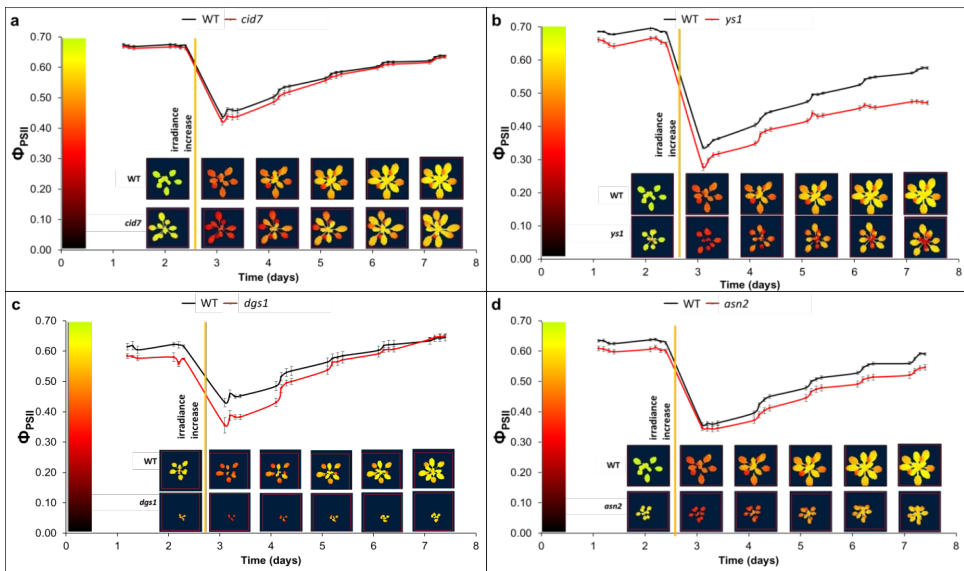
Figure 3. Photosynthesis efficiency response to increased irradiance for T-DNA insertion knock-out lines significantly different from the Col wild type (WT).

(a-d) Photosynthesis efficiency (Φ_{PSII}) response (±s.e.m.) over time and chlorophyll fluorescence images of plants carrying a T-DNA insertion in the (a) CTC-INTERACTING DOMAIN 7 (CID7); (b) YELLOW SEEDLING 1 (YS1); (c) DGD1 SUPPRESSOR 1 (DGS1); or (d) ASPARAGINE SYNTHETASE 2 (ASN2) gene. Day 1 of the measurements corresponds to day 22 after sowing. The chlorophyll fluorescence images are taken 1 hour after lights are switched on. The yellow bar indicates a shift in irradiance from 100 to 550 $\mu mol\ m^{-2}s^{-1}$.

Quantitative complementation was not performed for *CID7* (the insertion line was completely sterile; Fig. S2), and failed to identify *DGS1* and *ASN2* as causal for the identified QTLs (Fig. S3 and Fig. S4) but was successful for *YS1* (significant only on day 1 after irradiance increase; Fig. 4c). Within the available re-sequence data for the Arabidopsis accessions used for the GWA, five different *YS1* alleles were distinguished (Fig. 4a). Accessions carrying alleles 2, 4 and 5 displayed the highest photosynthesis efficiency in response to high light, and were significantly different from accessions with alleles 1 and 3, which displayed the lowest photosynthesis efficiency (Fig. 4b). No single polymorphisms in *YS-1* distinguished alleles 2,4 and 5 from alleles 1 and 3 (Fig. 4a), however we observed the average transcription of *YS1-4* alleles to be higher than *YS1-3* alleles (Fig. 4d). Since gene expression is regulated by its promoter, we *de novo*-sequenced the promoter region of the Col-0 *YS1-1* allele as well as those of five accessions with allele *YS1*-3 and five with allele *YS1*-4. We found three SNPs in the promoter region (Fig. S5): at positions 8 024 723; 8 025 056; and 8 025 189 bp. In addition, there was an 8-bp deletion in the promoter of allele *YS1-3*, between positions 8 024 863 and 8 024 871 bp, that was not present in the public re-sequence data (Fig. S5). Upon combining the gene expression analysis with the allelic polymorphisms, we conclude that the combination of $InDel^{8024863-8024871}$ and $SNP^{8025056}$ causes low *YS1* expression in low light conditions (Fig. 4e), while the combination of $SNP^{8024723}$ and $SNP^{8025189}$ causes increased *YS1* expression in high light when compared to low light conditions (Fig. 4e). Since allele 1 and allele 3 lead to low photosynthesis efficiency in response to high light (Fig. 4b), we conclude that only when the 8-bp deletion is absent and $SNP^{8025056}$ = T, $SNP^{8024723}$ = A, and $SNP^{8025189}$ = G (i.e. allele 4), gene expression is highest, leading to the highest photosynthesis efficiency in response to high light (Fig. 4e). $InDel^{8024863-8024871}$ overlaps with a binding site for the nuclear transcription factor GT-1, while $SNP^{8025189}$ locates in the core of another GT-1 binding site (Fig. S5), (Green et al., 1988; Gilmartin and Chua, 1990). No obvious transcription factor binding sites were found around $SNP^{8024723}$ or $SNP^{8025056}$. Mutations in GT-1 binding sites are known to affect a promoter's responsiveness to light (Gilmartin et al., 1990; Ouwerkerk et al., 1999), which is consistent with the correlations we found between the differences in expression of *YS1* alleles and the differences in photosynthesis acclimation responses (Fig. 4).
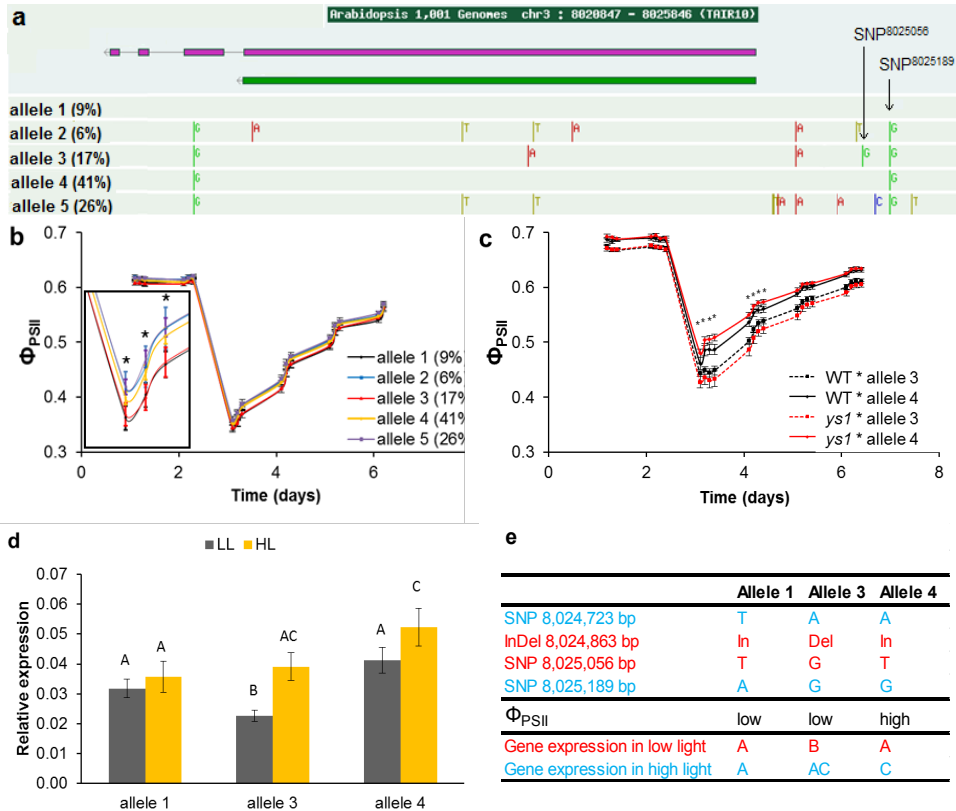
Figure 4. Characterization of natural alleles of YS1.

(a) Five most abundant haplotype alleles and frequency (%) for the YS1 gene (www.arabidopsis.org). Gene orientation is 3' to 5'; two splice variants are indicated[4]. SNPs differing from the Col-0 reference genome sequence (allele 1) are marked; two SNPs of significance for this study are indicated by arrows. (b) Average photosynthesis efficiencies (Φ_{PSII}) (±s.e.m.) of the five haplotype alleles before (LL) and after an increase in radiance (HL), the inset shows small but significant differences between allelic groups based on T-test series. (c) Φ_{PSII} of F1 plants of crosses between wild type (WT) or ys1 mutants with accessions carrying either YS1-3 or YS1-4 alleles confirming the QTL and the mutation in the YS1 locus are allelic, asterisks indicate significant difference in effect of allele 3 and allele 4 on the difference between Φ_{PSII} of the F1 with WT compared to the F1 with ys1 based on two-way ANOVA. (d) Relative transcription (±s.e.m.) of YS1 alleles. Letters indicate significant different groups independent of LL or HL. (e) Summary of genetic polymorphisms, Φ_{PSII} and transcription of three YS1 alleles. Blue and red distinguish co-segregating traits/polymorphisms.SNP[8025056] and SNP[8025189] are also indicated in panel (a) of this figure, whereas SNP[8024723] and InDel[802486] were not present in the re-sequence data but were found by de novo sequencing as presented in Extended Data Figure 5.

Previously, a *ys1* knock-out mutation of *YS1* was found to lead to disturbed chloroplast development in young seedlings (Zhou et al., 2009). We found that young leaves of the *ys1* mutant cannot acclimate after the irradiance increase (Fig. 3b), from which we conclude that similar developmental constraints occur in young leaves during photosynthetic acclimation to increased irradiance as in leaves of young seedlings. Differences in *YS1* expression have been found to lead to differences in the extent of sequence editing of *rpoB* transcipts, encoding for the β-subunit of the Plastid-Encoded Polymerase (PEP), (Okuda et al., 2009; Zhou et al., 2009). PEP is mainly involved in transcription of photosynthesis genes encoding photosystem I (PSI) and PSII components that are active in leaf chloroplasts (Hajdukiewicz et al., 1997). We conclude that disturbed PEP function in the *ys1* mutant leads to dysfunctional leaf maturation via aberrant transcription of genes encoding PSI and PSII components in the leaf chloroplasts.

ACKNOWLEDGEMENTS

SUPPLEMENTARY TABLES AND FIGURES

Table S1. List of candidate genes co-localized with SNPs repetitively associated with Φ_{PSII} upon an increase in growth irradiance.

These are genes containing the SNP, and those genes in linkage disequilibrium (LD) with the SNP, repetitively associated (-log10(p) ≥ 4) at different time points with Φ_{PSII} measured after an increase in growth irradiance from 100 to 550 µmol m^{-2} s^{-1} on day 25 after sowing. The SNPs were identified in genome-wide association (GWA) studies (once using average phenotypic values and once using individual measurement values) of 344 Arabidopsis accessions.

QTL, the QTL number shown in Fig 2; Chr., chromosome; Cond., condition in which the QTL is identified; SNP.Pos.on.Chr., the chromosome position(s) of the SNP(s); in black: significant only in GWA using average values, in orange: significant only in GWA using individual measurement values, in green: significant in both GWA studies; MAF, minor allele frequency, with indication whether it represents the Col-0 allele (C) or the non-Col-0 allele (NC); effect size, the contribution of the Col-0 SNP allele on Φ_{PSII}; Perc.of.gen.var., the percentage of genetic variation explained by the SNP; genes in LD region, all genes in the LD region of the indicated SNP(s), genes in red are genes associated with photosynthesis or with the chloroplast; location of gene, physical position of the gene on the indicated chromosome; description, the annotation of the gene function as indicated in TAIR (www.arabidopsis.org).

QTL	Chr.	Cond.	SNP. Pos. on Chr.	MAF	Effect size	Per c.of. gen. var	Genes in LD region	Location of gene	Description
3	1	Early HL	10596936	0.21NC	-0.01	8	AT1G30135	10596492-10597239	jasmonate-zim-domain protein 8 (JAZ8); CONTAINS InterPro DOMAIN/s: Tify (InterPro:IPR010399), CCT domain-like (InterPro:IPR018467);
			12275289	0.46C	0.01		AT1G30140	10598627-10599696	unknown protein
			12348136	0.10C	-0.01		AT1G30150	10602178-10605159	CACTA-like transposase family (Tnp1/En/Spm)
							AT1G33813	12273243-12274646	transposable element gene; copia-like retrotransposon family
							AT1G33817	12274982-12276763	transposable element gene; copia-like retrotransposon family
							AT1G33820	12278438-12279451	unknown protein
							AT1G33830	12279947-12281406	P-loop containing nucleoside triphosphate hydrolases superfamily protein; FUNCTIONS IN: GTP binding; INVOLVED IN: response to bacterium; LOCATED IN: cellular_component unknown; EXPRESSED IN: egg cellBLink).
							AT1G33835	12281847-12282297	transposable element gene; copia-like retrotransposon family
							AT1G33840	12283862-12285306	Protein of unknown function (DUF567)
							AT1G33850	12287913-12288210	Ribosomal protein S19 family protein; FUNCTIONS IN: structural constituent of ribosome; INVOLVED IN: translation; LOCATED IN: cytosolic small ribosomal subunit, ribosome; EXPRESSED IN: synergid0; Metazoa - 255; Fungi - 145; Plants - 198; Viruses - 0; Other Eukaryotes - 99 (source: NCBI BLink).
							AT1G33855	12291258-12292501	transposable element gene; Mutator-like transposase family
							AT1G33860	12294394-12295305	unknown protein
							AT1G33870	12301325-12302467	P-loop containing nucleoside triphosphate hydrolases superfamily protein; FUNCTIONS IN: GTP binding; INVOLVED IN: response to bacterium; LOCATED IN: cellular_component unknown; EXPRESSED IN: stem, root, seed; EXPRESSED DURING: F mature embryo stage

								AT1G33880	12303862-12304911	Avirulence induced gene (AIG1) family protein; FUNCTIONS IN: GTP binding; INVOLVED IN: N-terminal protein myristoylation, response to bacterium; LOCATED IN: cellular_component unknown; EXPRESSED IN: sperm cell
								AT1G33890	12308284-12309686	Avirulence induced gene (AIG1) family protein; FUNCTIONS IN: GTP binding; INVOLVED IN: response to bacterium; LOCATED IN: cellular_component unknown; EXPRESSED IN: pedicel; EXPRESSED DURING: 4 anthesis
								AT1G33900	12311518-12313518	P-loop containing nucleoside triphosphate hydrolases superfamily protein; FUNCTIONS IN: GTP binding; INVOLVED IN: response to bacterium
								AT1G33910	12314904-12316258	P-loop containing nucleoside triphosphate hydrolases superfamily protein; FUNCTIONS IN: GTP binding; INVOLVED IN: response to bacterium
								AT1G33920	12319905-12320870	phloem protein 2-A4 (PP2-A4)
								AT1G33930	12323888-12327084	P-loop containing nucleoside triphosphate hydrolases superfamily protein; FUNCTIONS IN: GTP binding; INVOLVED IN: response to bacterium; EXPRESSED IN: leaf lamina base, pedicel, petiole, leaf; EXPRESSED DURING: LP.04 four leaves visible, 4 anthesis
								AT1G33940	12330576-12332785	BEST Arabidopsis thaliana protein match is: Protein kinase family protein with ARM repeat domain (TAIR:AT5G18700.1);
								AT1G33950	12333046-12339182	Avirulence induced gene (AIG1) family protein; FUNCTIONS IN: GTP binding; INVOLVED IN: response to bacterium
								AT1G33960	12346232-12348513	AIG1; identified as a gene that is induced by avirulence gene avrRpt2 and RPS2 after infection with Pseudomonas syringae pv maculicola strain ES4326 carrying avrRpt2
								AT1G33970	12349463-12351203	P-loop containing nucleoside triphosphate hydrolases superfamily protein; FUNCTIONS IN: GTP binding; INVOLVED IN: response to bacterium; LOCATED IN: cellular_component unknown; EXPRESSED IN: 22 plant structures; EXPRESSED DURING: 13 growth stages
								AT1G33980	12351593-12355023	UPF3; Involved in mRNA surveillance, detects exported mRNAs with truncated open reading frames and initiates nonsense-mediated mRNA decay (NMD)
								AT1G33990	12355568-12358031	MES14; Encodes a protein predicted to act as a carboxylesterase. It has similarity to the SABP2 methyl salicylate esterase from tobacco. This protein does not act on methyl IAA, methyl JA, MeSA, MeGA4, or MEGA9 in vitro.
								AT1G34000	12357910-12358966	OHP2; ncodes a novel member of the Lhc family from Arabidopsis with one predicted transmembrane alpha-helix closely related to helix I of Lhc protein from PSI (Lhca4). Gene expression is triggered by light stress and both transcript and protein accumulate in a light intensity-dependent manner. Ohp2 is associated with PSI under low- or high-light conditions.
								AT1G34010	12359536-12361189	unknown protein
								AT1G34020	12366854-12369178	Nucleotide-sugar transporter family protein; LOCATED IN: plasma membrane, membrane; EXPRESSED IN: 22 plant structures; EXPRESSED DURING: 13 growth stages
								AT1G34030	12370065-12371553	Ribosomal protein S13/S18 family; FUNCTIONS IN: structural constituent of ribosome, protein binding; INVOLVED IN: translation; LOCATED IN: in 6 components; EXPRESSED IN: 23 plant structures; EXPRESSED DURING: 13 growth stages

							AT1G34040	12374433-12376179	Pyridoxal phosphate (PLP)-dependent transferases superfamily protein; FUNCTIONS IN: pyridoxal phosphate binding, carbon-sulfur lyase activity, catalytic activity; INVOLVED IN: biological_process unknown; LOCATED IN: endomembrane system
4	1	early HL	27891662	0.019NC	-0.01	10	AT1G74150	27880528-27883626	Galactose oxidase/kelch repeat superfamily protein
			27894888	0.16NC	0.01		AT1G74160	27886426-27891431	unknown protein
			27896712	0.44C	0.01		AT1G74170	27891494-27896355	receptor like protein 13 (RLP13)
			27897142	0.14NC	0.01		AT1G74180	27897197-27900908	receptor like protein 14 (RLP14); INVOLVED IN: signal transduction; LOCATED IN: chloroplast; EXPRESSED IN: 19 plant structures; EXPRESSED DURING: 13 growth stages
			27899243	0.35C	0.01		AT1G74190	27902590-27906158	receptor like protein 15 (RLP15); INVOLVED IN: signal transduction; LOCATED IN: endomembrane system
			27903238	0.24C	-0.01		AT1G74200	27906909-27909358	receptor like protein 16 (RLP16)
			27904597	0.39C	-0.01		AT1G74210	27910314-27912941	Encodes a member of the glycerophosphodiester phosphodiesterase (GDPD) family.
			27904633	0.40C	-0.01		AT1G74220	27913099-27914134	unknown protein; FUNCTIONS IN: molecular_function unknown; INVOLVED IN: biological_process unknown; LOCATED IN: chloroplast; EXPRESSED IN: male gametophyte, flower, pollen tube; EXPRESSED DURING: L mature pollen stage, M germinated pollen stage, 4 anthesis
			27904871	0.43C	-0.01		AT1G74230	27914699-27917083	encodes a glycine-rich RNA binding protein.
			27905270	0.43NC	0.01		AT1G74240	27917396-27920139	Mitochondrial substrate carrier family protein; FUNCTIONS IN: binding; INVOLVED IN: transport, mitochondrial transport, transmembrane transport; LOCATED IN: mitochondrial inner membrane, membrane; EXPRESSED IN: 11 plant structures; EXPRESSED DURING: 6 growth stages
			27905627	0.19NC	0.01		AT1G74250	27920328-27922414	DNAJ heat shock N-terminal domain-containing protein; FUNCTIONS IN: heat shock protein binding, zinc ion binding, nucleic acid binding; INVOLVED IN: protein folding; LOCATED IN: intracellular; EXPRESSED IN: 22 plant structures; EXPRESSED DURING: 13 growth stages
			27905987	0.44NC	0.01		AT1G74260	27922833-27927904	Encodes formylglycinamidine ribonucleotide synthase an enzyme involved in de novo purine biosynthesis. PUR4 is localizes to the chloroplast and mitochondria. Loss of PUR4 function affects male but not female gametophyte development.
							AT1G74270	27928171-27929497	Ribosomal protein L35Ae family protein; FUNCTIONS IN: structural constituent of ribosome; INVOLVED IN: translation, ribosome biogenesis; LOCATED IN: ribosome, cytosolic large ribosomal subunit; EXPRESSED IN: 22 plant structures; EXPRESSED DURING: 13 growth stages
							AT1G74280	27929662-27931364	alpha/beta-Hydrolases superfamily protein
							AT1G74290	27931836-27934268	alpha/beta-Hydrolases superfamily protein
5	1	early HL	27979318	0.45C	0.01	9	AT1G74440	27976502-27980404	Protein of unknown function (DUF962)
			27981096	0.37NC	0.01				
7	2	early HL	11189311	0.19NC	-0.02	9	AT2G26280	11187733-11191337	CID7, CTC-interacting domain7, functions in DNA binding and mismatch repair, located in chloroplast. smr (Small MutS Related) domain-containing protein mRNA, complete cds.
			11189443	0.18NC	-0.02		AT2G26290	11192137-11194259	root-specific kinase 1 (ARSK1);
8	3	early HL	1350656	0.45NC	-0.01	9	AT3G04820	1321228-1325953	Pseudouridine synthase family protein; FUNCTIONS IN: pseudouridine synthase activity; INVOLVED IN: pseudouridine synthesis, RNA modification; EXPRESSED IN: 21 plant structures; EXPRESSED DURING: 13 growth stages

			1353218	0.19NC	-0.01		AT3G04830	1326227-1329364	Protein prenylyltransferase superfamily protein; FUNCTIONS IN: binding; INVOLVED IN: biological_process unknown; LOCATED IN: cellular_component unknown; EXPRESSED IN: 23 plant structures; EXPRESSED DURING: 13 growth stages
			1353894	0.16NC	-0.01		AT3G04840	1329665-1331617	Ribosomal protein S3Ae; FUNCTIONS IN: structural constituent of ribosome; INVOLVED IN: translation; LOCATED IN: cytosolic small ribosomal subunit, cytosolic ribosome, plasma membrane, chloroplast; EXPRESSED IN: 27 plant structures; EXPRESSED DURING: 16 growth stages
							AT3G04850	1331946-1335993	Tesmin/TSO1-like CXC domain-containing protein
							AT3G04860	1339104-1340623	Plant protein of unknown function (DUF868)
							AT3G04870	1342718-1346387	Zeta-carotene desaturase (ZDS); involved in the biosynthesis of carotenes and xanthophylls, reduces zeta-carotene to lycopene.
							AT3G04880	1346273-1347377	DNA-damage-repair/toleration2 (DRT102); encodes a novel protein involved in DNA repair from UV damage. Isolated by functional complementation of E. coli UV-sensitive mutants (UVR genes).
							AT3G04890	1347646-1349202	Uncharacterized conserved protein (DUF2358); FUNCTIONS IN: molecular_function unknown; INVOLVED IN: biological_process unknown; LOCATED IN: chloroplast; EXPRESSED IN: 22 plant structures; EXPRESSED DURING: 13 growth stages
							AT3G04900	1349302-1349928	Heavy metal transport/detoxification superfamily protein ; FUNCTIONS IN: metal ion binding; INVOLVED IN: metal ion transport; LOCATED IN: cellular_component unknown
							AT3G04903	1350510-1350989	Encodes a defensin-like (DEFL) family protein.
							AT3G04910	1354635-1358211	With No Lysine (K) Kinase 1 (WNK1); serine/threonine protein kinase, whose transcription is regulated by circadian rhythm.
							AT3G04920	1360882-1362295	Ribosomal protein S24e family protein; FUNCTIONS IN: structural constituent of ribosome, nucleotide binding; INVOLVED IN: translation, ribosome biogenesis; LOCATED IN: in 7 components; EXPRESSED IN: 26 plant structures; EXPRESSED DURING: 13 growth stages
							AT3G04930	1362905-1364799	DNA-binding storekeeper protein-related transcriptional regulator
							AT3G04940	1365165-1367759	Encodes cysteine synthase CysD1.
							AT3G04943	1368248-1368678	Encodes a member of a family of small,secreted, cysteine rich protein with sequence similarity to the PCP (pollen coat protein) gene family.
							AT3G04945	1369114-1369532	Encodes a member of a family of small,secreted, cysteine rich protein with sequence similarity to the PCP (pollen coat protein) gene family.
							AT3G04950	1371705-1373477	unknown protein
							AT3G04960	1373688-1375850	Molecular chaperone, heat shock protein, Hsp40, DnaJ
							AT3G04970	1376175-1378500	DHHC-type zinc finger family protein; FUNCTIONS IN: zinc ion binding; INVOLVED IN: biological_process unknown; LOCATED IN: endomembrane system; EXPRESSED IN: 21 plant structures; EXPRESSED DURING: 13 growth stages
							AT3G04980	1378684-1382181	DNAJ heat shock N-terminal domain-containing protein; FUNCTIONS IN: unfolded protein binding, heat shock protein binding; INVOLVED IN: protein folding; LOCATED IN: cellular_component unknown; EXPRESSED IN: 12 plant structures; EXPRESSED DURING: 6 growth stages
							AT3G04990	1383996-1384679	Frigida-like protein (TAIR:AT5G27220.1)

9	3	early HL	1750265	0.17NC	0.02	8	AT3G05810	1730976-1732384	unknown protein; FUNCTIONS IN: molecular_function unknown; INVOLVED IN: biological_process unknown; LOCATED IN: mitochondrion; EXPRESSED IN: 22 plant structures; EXPRESSED DURING: 13 growth stages
			1750573	0.17NC	0.02		AT3G05820	1732991-1735757	Encodes a putative plastid-targeted alkaline/neutral invertase.
			1750946	0.17NC	0.02		AT3G05830	1736677-1738664	Encodes alpha-helical IF (intermediate filament)-like protein.
			1751042	0.21NC	0.02		AT3G05835	1738791-1738864	pre-tRNA; tRNA-Ile (anticodon: TAT)
			1755712	0.21NC	-0.01		AT3G05840	1740020-1743163	encodes a SHAGGY-like kinase involved in meristem organization.
							AT3G05850	1743413-1746785	transposable element gene; Mutator-like transposase family
							AT3G05860	1751406-1752355	MADS-box transcription factor family protein; FUNCTIONS IN: DNA binding, sequence-specific DNA binding transcription factor activity; INVOLVED IN: regulation of transcription, DNA-dependent; LOCATED IN: nucleus; EXPRESSED IN: embryo, endosperm
							AT3G05870	1753467-1755631	APC11; subunit of the anaphase promoting complex, a ubiquitin ligase complex that regulates progression through the cell cycle.
							AT3G05880	1755497-1756540	Induced by low temperatures, dehydration and salt stress and ABA. Encodes a small (54 amino acids), highly hydrophobic protein that bears two potential transmembrane domains.
10	3	Late HL	7992656	0.11(NC)	-0.02	7	AT3G22550	7991646-7993454	Protein of unknown function (DUF581)
			8120853	0.30(NC)	0.01		AT3G22555	7995486-7996636	pseudogene, putative DNA methyltransferase
							AT3G22560	7998857-7999533	Acyl-CoA N-acyltransferases (NAT) superfamily protein; FUNCTIONS IN: N-acetyltransferase activity; INVOLVED IN: metabolic process; LOCATED IN: membrane; EXPRESSED IN: leaf
							AT3G22570	8000515-8001238	Bifunctional inhibitor/lipid-transfer protein/seed storage 2S albumin superfamily protein; FUNCTIONS IN: lipid binding; INVOLVED IN: lipid transport; LOCATED IN: endomembrane system; EXPRESSED IN: root, pollen tube
							AT3G22580	8002762-8003145	Bifunctional inhibitor/lipid-transfer protein/seed storage 2S albumin superfamily protein; FUNCTIONS IN: lipid binding; INVOLVED IN: lipid transport; LOCATED IN: endomembrane system
							AT3G22590	8003934-8005579	Encodes PLANT HOMOLOGOUS TO PARAFIBROMIN (PHP), a homolog of human Paf1 Complex (Paf1C) subunit Parafibromin. Human Parafibromin assists in mediating output from the Wnt signaling pathway, and dysfunction of the encoding gene HRPT2 conditions specific cancer-related disease phenotypes. PHP resides in a ~670-kDa protein complex in nuclear extracts, and physically interacts with other known Paf1C-related proteins in vivo. Loss of PHP specifically conditioned accelerated phase transition from vegetative growth to flowering and resulted in misregulation of a very limited subset of genes that included the flowering repressor FLOWERING LOCUS C.
							AT3G22600	8006508-8007471	Bifunctional inhibitor/lipid-transfer protein/seed storage 2S albumin superfamily protein; FUNCTIONS IN: lipid binding; INVOLVED IN: lipid transport; LOCATED IN: anchored to membrane; EXPRESSED IN: 14 plant structures; EXPRESSED DURING: 10 growth stages
							AT3G22620	8008534-8009590	Bifunctional inhibitor/lipid-transfer protein/seed storage 2S albumin superfamily protein; FUNCTIONS IN: lipid binding; INVOLVED IN: lipid transport; LOCATED IN: chloroplast envelope; EXPRESSED DURING: 4 anthesis, C globular stage, petal differentiation and expansion stage

							AT3G22630	8009540-8010844	Encodes 20S proteasome beta subunit PBD1 (PBD1).
							AT3G22640	8011724-8013902	PAP85; FUNCTIONS IN: nutrient reservoir activity; INVOLVED IN: biological_process unknown; LOCATED IN: plant-type cell wall; EXPRESSED IN: stem, seed; EXPRESSED DURING: seedling growth, seed development stages
							AT3G22650	8014809-8015960	CEGENDUO (CEG); CONTAINS InterPro DOMAIN/s: F-box domain, cyclin-like, F-box domain, Skp2-like, F-box associated domain, type 1, F-box associated interaction domain
							AT3G22660	8016051-8017508	rRNA processing protein-related
							AT3G22670	8017771-8019459	Pentatricopeptide repeat (PPR) superfamily protein; INVOLVED IN: biological_process unknown; LOCATED IN: mitochondrion; EXPRESSED IN: 21 plant structures; EXPRESSED DURING: 10 growth stages
							AT3G22680	8019708-8020508	Encodes RNA-DIRECTED DNA METHYLATION 1 (RDM1), forming a complex with DMS3 (AT3G49250) and DRD1 (AT2G16390). This complex is termed DDR. The DDR complex is required for polymerase V transcripts and RNA-directed DNA methylation.
							AT3G22690	8021229-8024534	YS1; INVOLVED IN: photosystem II assembly, regulation of chlorophyll biosynthetic process, photosystem I assembly, thylakoid membrane organization, RNA modification; LOCATED IN: chloroplast; EXPRESSED IN: 13 plant structures; EXPRESSED DURING: LP.04 four leaves visible, 4 anthesis, petal differentiation and expansion stage, E expanded cotyledon stage, D bilateral stage
							AT3G22700	8024798-8025814	F-box and associated interaction domains-containing protein
							AT3G22710	8026202-8027274	F-box family protein
							AT3G22720	8028961-8030097	F-box and associated interaction domains-containing protein
							AT3G22730	8031341-8032459	F-box and associated interaction domains-containing protein
							AT3G22740	8032959-8035809	homocysteine S-methyltransferase (HMT3)
							AT3G22750	8037216-8039903	Protein kinase superfamily protein; FUNCTIONS IN: protein serine/threonine kinase activity, protein kinase activity, kinase activity, ATP binding; INVOLVED IN: protein amino acid phosphorylation; LOCATED IN: plasma membrane; EXPRESSED IN: 13 plant structures; EXPRESSED DURING: L mature pollen stage, M germinated pollen stage, LP.04 four leaves visible, 4 anthesis, petal differentiation and expansion stage
							AT3G22760	8044455-8047530	CXC domain containing TSO1-like protein 1. The gene is expressed in stamens, pollen mother cells, and immature ovules.
							AT3G22770	8048802-8052260	F-box associated ubiquitination effector family protein
							AT3G22780	8047684-8048667	putative DNA binding protein (tso1) mRNA, tso1-3 allele,
							AT3G22790	8052318-8058764	Encodes a member of the NET superfamily of proteins that potentially couples different membranes to the actin cytoskeleton in plant cells. It binds filamentous actin and is localized to the plasma membrane and plasmodesmata.
							AT3G22800	8062888-8064556	Leucine-rich repeat (LRR) family protein; FUNCTIONS IN: structural constituent of cell wall; LOCATED IN: endomembrane system; EXPRESSED IN: 8 plant structures; EXPRESSED DURING: petal differentiation and expansion stage
							AT3G22810	8068516-8071559	FUNCTIONS IN: phosphoinositide binding; INVOLVED IN: signal transduction; LOCATED IN: cellular_component unknown; EXPRESSED IN: 10 plant structures; EXPRESSED DURING: 4 anthesis, F mature embryo stage, petal differentiation and expansion stage, E expanded cotyledon stage, D bilateral stage

							Gene	Position	Description
							AT3G22820	8073271-8074138	allergen-related; FUNCTIONS IN: molecular_function unknown; INVOLVED IN: biological_process unknown; LOCATED IN: endomembrane system
							AT3G22830	8078820-8081051	member of Heat Stress Transcription Factor (Hsf) family
							AT3G22840	8084447-8085560	Encodes an early light-inducible protein.
							AT3G22845	8087307-8088747	emp24/gp25L/p24 family/GOLD family protein; INVOLVED IN: transport; LOCATED IN: vacuole; EXPRESSED IN: 24 plant structures; EXPRESSED DURING: 15 growth stages
							AT3G22850	8089003-8090470	Aluminium induced protein with YGL and LRDR motifs; FUNCTIONS IN: molecular_function unknown; INVOLVED IN: biological_process unknown; LOCATED IN: cytosol, nucleus, plasma membrane; EXPRESSED IN: 24 plant structures; EXPRESSED DURING: 15 growth stages
							AT3G22860	8090654-8093248	member of eIF3c - eukaryotic initiation factor 3c
							AT3G22870	8096230-8097471	F-box and associated interaction domains-containing protein
							AT3G22880	8097687-8100820	Expression of the AtDMC1 is restricted to pollen mother cells in anthers and to megaspore mother cells in ovules. Similar to meiosis-specific yeast DMC gene.
							AT3G22886	8108021-8108622	Encodes a microRNA that targets ARF family members ARF6 and ARF8. Essential for fertility of both ovules and anthers
							AT3G22890	8112723-8114992	encodes ATP sulfurylase, the first enzyme in the sulfate assimilation pathway of Arabidopsis. It may also participate in selenium metabolism.
							AT3G22900	8115177-8116253	Non-catalytic subunit specific to DNA-directed RNA polymerase IV; homologous to budding yeast RPB7
							AT3G22910	8116335-8119388	ATPase E1-E2 type family protein / haloacid dehalogenase-like hydrolase family protein; FUNCTIONS IN: calcium-transporting ATPase activity, calmodulin binding; INVOLVED IN: cation transport, calcium ion transport, metabolic process, ATP biosynthetic process; LOCATED IN: membrane; EXPRESSED IN: 12 plant structures; EXPRESSED DURING: LP.04 four leaves visible, 4 anthesis, C globular stage, petal differentiation and expansion stage
11	3	early HL	12784017	0.37 (C)	-0.01	11	AT3G31367	12735171-12737948	transposable element gene; gypsy-like retrotransposon family
							AT3G31370	12739412-12740362	transposable element gene
							AT3G31373	12742861-12745393	transposable element gene; pseudogene, putative replication protein
							AT3G31374	12745879-12747374	transposable element gene; gypsy-like retrotransposon family
							AT3G31375	12748365-12752403	transposable element gene; gypsy-like retrotransposon family
							AT3G31377	12753386-12754761	transposable element gene; pseudogene, putative replication protein
							AT3G31380	12758024-12758958	transposable element gene; copia-like retrotransposon family
							AT3G31390	12760805-12762223	transposable element gene; gypsy-like retrotransposon family
							AT3G31395	12762661-12766244	transposable element gene; non-LTR retrotransposon family
							AT3G31400	12768984-12769481	unknown protein;
							AT3G31403	12776573-12778649	transposable element gene; Mutator-like transposase family
							AT3G31406	12779538-12780473	transposable element gene
							AT3G31410	12780479-12783581	transposable element gene

12	3	late HL	15932189	0.18NC	-0.01	8	AT3G44770	16316080-16319458	Protein of unknown function (DUF626); FUNCTIONS IN: molecular_function unknown; INVOLVED IN: biological_process unknown; LOCATED IN: mitochondrion; EXPRESSED IN: 7 plant structures; EXPRESSED DURING: 4 anthesis, petal differentiation and expansion stage, E expanded cotyledon stage, D bilateral stage
			16316203	0.35C	-0.01				
			16318079	0.22C	-0.01				
			16318704	0.27C	-0.01				
13	4	Late HL	818905	0.53C	0.009	7	AT4G01860	801345-808060	Transducin family protein / WD-40 repeat family protein
			987887	0.89NC	-0.008		AT4G01865	808270-808342	tRNA-Phe (anticodon: GAA)
							AT4G01870	808376-810446	tolB protein-related
							AT4G01880	810699-812925	methyltransferases
							AT4G01883	813068-815170	Polyketide cyclase / dehydrase and lipid transport protein
							AT4G01890	816210-818428	Pectin lyase-like superfamily protein
							AT4G01895	819957-820379	systemic acquired resistance (SAR) regulator protein NIMIN-1-related
							AT4G01897	820336-821505	unknown protein
							AT4G01900	821685-823523	encodes a PII protein that may function as part of a signal transduction network involved in perceiving the status of carbon and organic nitrogen.
							AT4G01910	824568-826685	Cysteine/Histidine-rich C1 domain family protein
							AT4G01915	827237-828607	unknown protein
							AT4G01920	828890-831200	Cysteine/Histidine-rich C1 domain family protein
							AT4G01925	833173-834340	Cysteine/Histidine-rich C1 domain family protein
							AT4G01930	838802-840760	Cysteine/Histidine-rich C1 domain family protein
							AT4G01935	841057-842364	unknown protein
							AT4G01940	841989-843459	Encodes a protein containing the NFU domain that may be involved in iron-sulfur cluster assembly. Part of a five member gene family, more closely related to NFU2 and 3 than to NFU4 and 5. Targeted to the chloroplast.
							AT4G01950	844409-846787	putative sn-glycerol-3-phosphate 2-O-acyltransferase
							AT4G01960	851210-853165	unknown protein
							AT4G01970	853922-857008	Encodes a putative stachyose synthetase or raffinose synthase.
							AT4G01975	858636-862475	pseudogene
							AT4G01980	863351-864259	similar to myb family protein
							AT4G01985	866236-868126	unknown protein
							AT4G01990	871145-872913	Tetratricopeptide repeat (TPR)-like superfamily protein
							AT4G01995	873054-874772	unknown protein
							AT4G02000	874880-875903	unknown protein
							AT4G02010	881090-885399	Protein kinase superfamily protein
							AT4G02020	886600-891955	Encodes a polycomb group protein
							AT4G02030	892176-897318	Vps51/Vps67 family (components of vesicular transport) protein
							AT4G02040	897547-898370	unknown protein
							AT4G02050	898307-900870	sugar transporter protein 7 (STP7)
							AT4G02055	901176-901247	tRNA-His (anticodon: GTG)
							AT4G02060	901388-905590	Member of the minichromosome maintenance complex, involved in DNA replication initiation.
							AT4G02070	906079-912930	encodes a DNA mismatch repair homolog of human MutS gene, MSH6.
							AT4G02075	913419-916476	pitchoun 1 (PIT1); FUNCTIONS IN: zinc ion binding
							AT4G02080	921454-922777	A member of ARF-like GTPase family. A thaliana has 21 members, in two subfamilies, ARF and ARF-like (ARL) GTPases.

						AT4G02090	923100-923916	unknown protein
						AT4G02100	930065-932330	Heat shock protein DnaJ with tetratricopeptide repeat
						AT4G02110	935086-940191	transcription coactivators
						AT4G02120	940778-944291	CTP synthase family protein
						AT4G02130	944367-947085	Encodes a protein with putative galacturonosyltransferase activity.
						AT4G02140	949460-951063	unknown protein
						AT4G02150	950611-953690	Encodes IMPORTIN ALPHA 3. Mutant plants act as suppressors of snc1 response and salicylic acid accumulation. Located in the nucleus. Involved in protein import.
						AT4G02160	955101-955652	unknown protein
						AT4G02170	958049-958641	unknown protein
						AT4G02180	959964-963517	DC1 domain-containing protein
						AT4G02190	967372-969351	Cysteine/Histidine-rich C1 domain family protein
						AT4G02195	970007-972307	Encodes a member of SYP4 Gene Family that is a plant ortholog of the Tlg2/syntaxin16 Qa-SNARE.
						AT4G02200	972707-974692	Drought-responsive family protein
						AT4G02210	973924-976129	unknown protein
						AT4G02220	976278-979163	zinc finger (MYND type) family protein / programmed cell death 2 C-terminal domain-containing protein
						AT4G02230	979170-980670	Ribosomal protein L19e family protein
						AT4G02235	980955-981711	AGAMOUS-like 51 (AGL51)
						AT4G02250	983970-984523	Plant invertase/pectin methylesterase inhibitor superfamily protein
						AT4G02260	985232-991494	RELA/SPOT homolog 1 (RSH1)
						AT4G02270	992175-993038	root hair specific 13 (RHS13)
						AT4G02280	994927-998967	Encodes a protein with sucrose synthase activity (SUS3).
15	4	early HL	7346546	0.16NC	0.02	11	AT4G12400	7338659-7341361	HOP3; encodes one of the 36 carboxylate clamp (CC)-tetratricopeptide repeat (TPR) proteins (Prasad 2010, Pubmed ID: 20856808) with potential to interact with Hsp90/Hsp70 as co-chaperones.
			7810132	0.46NC	-0.01		AT4G12410	7342956-7343590	SAUR-like auxin-responsive protein family
			7810598	0.40NC	0.01		AT4G12420	7349662-7353074	Encodes a protein of unknown function involved in directed root tip growth. It is a member of 19-member gene family and is distantly related structurally to the multiple-copper oxidases ascorbate oxidase and laccase, though it lacks the copper-binding domains. The protein is glycosylated and GPI-anchored. It is localized to the plasma membrane and the cell wall. The gene is expressed most strongly in expanding tissues.
16	4	early HL	8209018	0.16C	0.02	10	AT4G14250	8208748-8213237	structural constituent of ribosome; FUNCTIONS IN: structural constituent of ribosome; INVOLVED IN: translation; LOCATED IN: ribosome, intracellular
			8209226	0.19C	0.02				
19	5	early HL	267918	0.31NC	0.01	10	AT5G01715	267185-269354	pseudogene, antisense mRNA to gene At5g01720
			272241	0.30C	0.01		AT5G01720	266723-270483	RNI-like superfamily protein; FUNCTIONS IN: ubiquitin-protein ligase activity; INVOLVED IN: ubiquitin-dependent protein catabolic process; LOCATED IN: endomembrane system; EXPRESSED IN: 17 plant structures; EXPRESSED DURING: 8 growth stages
			273701	0.28C	0.01		AT5G01730	272832-277561	Encodes a member of the SCAR family.These proteins are part of a complex (WAVE) complex.The SCAR subunit activates the ARP2/3 complex which in turn act as a nucleator for actin filaments.
			295648	0.17NC	0.01		AT5G01740	280722-281445	Nuclear transport factor 2 (NTF2) family protein; CONTAINS InterPro DOMAIN: Wound-induced protein, Wun1

			296004	0.33NC	-0.01		AT5G01747	287586-287734	Encodes a microRNA that targets several genes containing NAC domains including NAC1. Overexpression leads to decreased NAC1 mRNA and reduced lateral roots. Loss of function mutants have increased NAC1 and increased number of lateral roots. Also targets ORE1 to negatively regulate the timing of leaf senescence
			298229	0.17NC	0.01		AT5G01750	289765-291326	Protein of unknown function (DUF567); FUNCTIONS IN: molecular_function unknown; INVOLVED IN: biological_process unknown; LOCATED IN: chloroplast; EXPRESSED IN: 23 plant structures; EXPRESSED DURING: 13 growth stages
			299476	0.14NC	0.01		AT5G01760	291712-294304	ENTH/VHS/GAT family protein; FUNCTIONS IN: protein transporter activity; INVOLVED IN: intracellular protein transport, intra-Golgi vesicle-mediated transport; LOCATED IN: Golgi stack, intracellular
			302045	0.19NC	0.01		AT5G01770	294313-301984	Encodes one of two Arabidopsis RAPTOR/KOG1 homologs. RAPTOR proteins are binding partners of the target of rapamycin kinase that is present in all eukaryotes and play a central role in the stimulation of cell growth and metabolism in response to nutrients. Mutations in this gene have no visible effects on embryo or plant development.
			304375	0.42NC	-0.01		AT5G01780	302267-304188	2-oxoglutarate-dependent dioxygenase family protein; LOCATED IN: cellular_component unknown; EXPRESSED IN: 21 plant structures; EXPRESSED DURING: 11 growth stages
			305676	0.42C	0.01		AT5G01790	304897-305696	unknown protein; FUNCTIONS IN: molecular_function unknown; INVOLVED IN: biological_process unknown; LOCATED IN: chloroplast; EXPRESSED IN: 19 plant structures; EXPRESSED DURING: 13 growth stages
			308976	0.50C	0.01		AT5G01800	306968-308908	saposin B domain-containing protein; FUNCTIONS IN: molecular_function unknown; INVOLVED IN: N-terminal protein myristoylation, lipid metabolic process; LOCATED IN: endomembrane system; EXPRESSED IN: 23 plant structures; EXPRESSED DURING: 15 growth stages
			309253	0.39NC	0.01				
20	5	early HL	987180	0.22C	0.01	10	AT5G03750	984796-985497	unknown protein; BEST Arabidopsis thaliana protein match is: Transducin/WD40 repeat-like superfamily protein (TAIR:AT5G03450.1)
			987216	0.27C	0.01		AT5G03760	985675-990549	encodes a beta-mannan synthase that is required for agrobacterium-mediated plant genetic transformation involves a complex interaction between the bacterium and the host plant. 3' UTR is involved in transcriptional regulation and the gene is expressed in the elongation zone of the root.
			988003	0.24C	0.01				
21	5	early HL	3975495	0.27NC	-0.02	11	AT5G12290	3974171-3978160	DGS1, encodes a mitochondrial outer membrane protein, involved in galactoglycerolipid biosynthesis. The dgd1 mutant phenotype is suppressed in the dgs1 mutant background.
			3980151	0.10NC	-0.02		AT5G12300	3978313-3979795	Calcium-dependent lipid-binding (CaLB domain) family protein
							AT5G12310	3980226-3982442	RING/U-box superfamily protein; FUNCTIONS IN: zinc ion binding
							AT5G12320	3982684-3984078	ankyrin repeat family protein

22	5	early HL	6034111	0.19NC	0.01	10	AT5G18160	6002770-6003909	F-box and associated interaction domains-containing protein
			6180615	0.43C	-0.01		AT5G18170	6006039-6008472	GDH1; encodes the 43 kDa alpha-subunit of the glutamate dehydrogenase with a putative mitochondrial transit polypeptide and NAD(H)- and alpha-ketoglutarate-binding domains. Mitochondrial localization confirmed by subcellular fractionation. Combines in several ratios with GDH2 protein (GDH-beta) to form seven isoenzymes. Catalyzes the cleavage of glycine residues. May be involved in ammonia assimilation under conditions of inorganic nitrogen excess. The enzyme is almost exclusively found in the mitochondria of stem and leaf companion cells.
			6797296	0.45NC	0.01		AT5G18180	6008561-6009605	H/ACA ribonucleoprotein complex, subunit Gar1/Naf1 protein; FUNCTIONS IN: snoRNA binding, pseudouridine synthase activity, RNA binding; LOCATED IN: chloroplast thylakoid membrane, membrane; EXPRESSED IN: 14 plant structures; EXPRESSED DURING: LP.06 six leaves visible, 4 anthesis, F mature embryo stage, petal differentiation and expansion stage, E expanded cotyledon stage
			6797770	0.48C	0.01		AT5G18190	6009967-6014689	Protein kinase family protein; FUNCTIONS IN: protein serine/threonine kinase activity, protein kinase activity, kinase activity, ATP binding; INVOLVED IN: protein amino acid phosphorylation; LOCATED IN: cellular_component unknown; EXPRESSED IN: 24 plant structures; EXPRESSED DURING: 15 growth stages
							AT5G18200	6015225-6016782	encodes an adenylyltransferase
							AT5G18210	6017865-6019993	NAD(P)-binding Rossmann-fold superfamily protein; FUNCTIONS IN: oxidoreductase activity, binding, catalytic activity; INVOLVED IN: oxidation reduction, metabolic process; EXPRESSED IN: 22 plant structures; EXPRESSED DURING: 13 growth stages
							AT5G18220	6018914-6020453	O-Glycosyl hydrolases family 17 protein; FUNCTIONS IN: cation binding, hydrolase activity, hydrolyzing O-glycosyl compounds, catalytic activity; INVOLVED IN: carbohydrate metabolic process; LOCATED IN: anchored to membrane
							AT5G18230	6021444-6027249	transcription regulator NOT2/NOT3/NOT5 family protein; FUNCTIONS IN: transcription regulator activity; INVOLVED IN: negative regulation of transcription, regulation of transcription; LOCATED IN: nucleus; EXPRESSED IN: 24 plant structures; EXPRESSED DURING: 15 growth stages
							AT5G18240	6028285-6030802	Encodes MYR1 (MYR1).
							AT5G18250	6033702-6035380	unknown protein; FUNCTIONS IN: molecular_function unknown; INVOLVED IN: biological_process unknown; LOCATED IN: mitochondrion; EXPRESSED IN: 23 plant structures; EXPRESSED DURING: 13 growth stages
							AT5G18260	6036202-6038106	RING/U-box superfamily protein; FUNCTIONS IN: zinc ion binding
							AT5G18270	6040919-6042938	Arabidopsis NAC domain containing protein 87 (ANAC087); FUNCTIONS IN: sequence-specific DNA binding transcription factor activity; INVOLVED IN: multicellular organismal development, regulation of transcription; LOCATED IN: cellular_component unknown; EXPRESSED IN: 12 plant structures; EXPRESSED DURING: LP.06 six leaves visible, LP.04 four leaves visible, 4 anthesis, C globular stage, petal differentiation and expansion stage

							AT5G18470	6127797-6129285	Curculin-like (mannose-binding) lectin family protein; FUNCTIONS IN: sugar binding; INVOLVED IN: response to karrikin; LOCATED IN: plant-type cell wall; EXPRESSED IN: 22 plant structures; EXPRESSED DURING: 12 growth stages
							AT5G18475	6129237-6131015	Pentatricopeptide repeat (PPR) superfamily protein; FUNCTIONS IN: molecular_function unknown; INVOLVED IN: biological_process unknown; LOCATED IN: chloroplast; EXPRESSED IN: 22 plant structures; EXPRESSED DURING: 13 growth stages
							AT5G18480	6131203-6133906	plant glycogenin-like starch initiation protein 6 (PGSIP6); FUNCTIONS IN: transferase activity, transferring hexosyl groups, transferase activity, transferring glycosyl groups; INVOLVED IN: carbohydrate biosynthetic process, biosynthetic process; LOCATED IN: membrane; EXPRESSED IN: guard cell, leaf
							AT5G18490	6134152-6136765	Plant protein of unknown function (DUF946)
							AT5G18500	6138489-6141630	Protein kinase superfamily protein; FUNCTIONS IN: protein serine/threonine kinase activity, protein kinase activity, kinase activity, ATP binding; INVOLVED IN: protein amino acid phosphorylation; LOCATED IN: plasma membrane; EXPRESSED IN: 22 plant structures; EXPRESSED DURING: 13 growth stages
							AT5G18510	6141778-6143886	Aminotransferase-like, plant mobile domain family protein
							AT5G18520	6144963-6146570	Encodes a candidate G-protein Coupled Receptor that is involved in the regulation of root growth by bacterial N-acyl-homoserine lactones (AHLs) and plays a role in mediating interactions between plants and microbes.
							AT5G18525	6146743-6153742	protein serine/threonine kinases;protein tyrosine kinases;ATP binding;protein kinases; FUNCTIONS IN: protein serine/threonine kinase activity, protein tyrosine kinase activity, protein kinase activity, ATP binding; INVOLVED IN: protein amino acid phosphorylation; LOCATED IN: CUL4 RING ubiquitin ligase complex; EXPRESSED IN: 22 plant structures; EXPRESSED DURING: 13 growth stages
							AT5G18540	6153869-6156166	unknown protein
							AT5G18550	6160178-6163130	Zinc finger C-x8-C-x5-C-x3-H type family protein; FUNCTIONS IN: zinc ion binding, nucleic acid binding; INVOLVED IN: biological_process unknown; LOCATED IN: cellular_component unknown; EXPRESSED IN: 17 plant structures; EXPRESSED DURING: 8 growth stages
							AT5G18560	6164587-6165991	Encodes PUCHI, a member of the ERF (ethylene response factor) subfamily of B-1 of ERF/AP2 transcription factor family. The protein contains one AP2 domain. There are 15 members in this subfamily including ATERF-3, ATERF-4, ATERF-7, and leafy petiole. PUCHI is required for morphogenesis in the early lateral root primordium of Arabidopsis. Expressed in early floral meristem (stage 1 to 2). Required for early floral meristem growth and for bract suppression.
							AT5G18570	6171661-6174833	Encodes AtObgC, a plant ortholog of bacterial Obg. AtObgC is a chloroplast-targeting GTPase essential for early embryogenesis. Mutations in this locus result in embryo lethality. The protein is dually localized in the stroma and the inner envelope membrane and is involved in thylakoid membrane biogenesis and functions primarily in plastid ribosome biogenesis during chloroplast development.

							AT5G18580	6174996-6178401	FASS1; fass mutants have aberrant cell shapes due to defects in arrangement of cortical microtubules. Encodes a protein highly conserved in higher plants and similar in its C-terminal part to B' regulatory subunits of type 2A protein phosphatases. Interacts with an Arabidopsis type A subunit of PP2A in the yeast two-hybrid system.
							AT5G18590	6178354-6182761	Galactose oxidase/kelch repeat superfamily protein
							AT5G18600	6183258-6183954	Thioredoxin superfamily protein; FUNCTIONS IN: electron carrier activity, arsenate reductase (glutaredoxin) activity, protein disulfide oxidoreductase activity; INVOLVED IN: cell redox homeostasis; LOCATED IN: cellular_component unknown; EXPRESSED IN: 18 plant structures; EXPRESSED DURING: 10 growth stages
							AT5G20110	6791487-6793346	Dynein light chain type 1 family protein; FUNCTIONS IN: microtubule motor activity; INVOLVED IN: microtubule-based process; LOCATED IN: microtubule associated complex; EXPRESSED IN: 19 plant structures; EXPRESSED DURING: 11 growth stages
							AT5G20120	6795366-6797172	unknown protein
							AT5G20130	6797440-6798899	unknown protein
							AT5G20140	6798923-6800977	SOUL heme-binding family protein
23	5	early HL	17186178	0.35C	-0.01	8	AT5G42870	17185463-17189681	PAH2; the PAH2 gene encodes a phosphatidate phosphohydrolase. Mutant analysis revealed that it involvement in galactolipid synthesis pathway, and the membrane lipid remodeling
			17187071	0.35C	-0.01		AT5G42880	17191577-17194131	Plant protein of unknown function (DUF827)
			17187390	0.35C	-0.01				
24	5	early HL	18812710	0.39C	-0.01	8	AT5G46360	18806821-18808224	Encodes AtKCO3, a member of the Arabidopsis thaliana K+ channel family of AtTPK/KCO proteins. AtKCO3 is targeted to the vacuolar membrane. Forms homomeric ion channels in vivo.
			18872155	0.42C	-0.01		AT5G46370	18809576-18811772	Encodes AtTPK2 (KCO2), a member of the Arabidopsis thaliana K+ channel family of AtTPK/KCO proteins. AtTPK2 is targeted to the vacuolar membrane. May form homomeric ion channels in vivo.
			18872623	0.34C	-0.01		AT5G46380	18813088-18815974	Kinase-related protein of unknown function (DUF1296)
			18872638	0.34C	-0.01		AT5G46390	18816585-18819348	Peptidase S41 family protein; FUNCTIONS IN: serine-type peptidase activity; INVOLVED IN: proteolysis, intracellular signaling pathway; LOCATED IN: chloroplast thylakoid lumen
			18873842	0.34C	-0.01		AT5G46400	18820032-18824650	PRP39-2; INVOLVED IN: RNA processing; LOCATED IN: intracellular; EXPRESSED IN: 21 plant structures; EXPRESSED DURING: 13 growth stages
			18874929	0.49C	-0.01		AT5G46410	18825103-18829221	Encodes a SCP1-like small phosphatase (SSP). Three SSPs form a unique group with long N-terminal extensions: AT5G46410 (SSP4), AT5G11860 (SSP5), AT4G18140 (SSP4b). SSP4 and SSP4b were localized exclusively in the nuclei, whereas SSP5 accumulated in both nuclei and cytoplasm. All three SSPs encodes active CTD phosphatases like animal SCP1 family proteins, with distinct substrate specificities: SSP4 and SSP4b could dephosphorylate both Ser2-PO(4) and Ser5-PO(4) of CTD, whereas SSP5 dephosphorylated only Ser5-PO(4).
			18875337	0.32C	-0.01		AT5G46420	18829955-18832953	16S rRNA processing protein RimM family; FUNCTIONS IN: ribosome binding, nucleotidyltransferase activity; INVOLVED IN: metabolic process, rRNA processing, ribosome biogenesis; LOCATED IN: chloroplast; EXPRESSED IN: 22 plant structures.

			18875477	0.34C	-0.01		AT5G46430	18833267-18834564	Ribosomal protein L32e; FUNCTIONS IN: structural constituent of ribosome; INVOLVED IN: translation, ribosome biogenesis; LOCATED IN: ribosome, cytosolic large ribosomal subunit

#	#	#	#	#	#	#	Gene	Range	Description
			18875477	0.34C	-0.01		AT5G46430	18833267-18834564	Ribosomal protein L32e; FUNCTIONS IN: structural constituent of ribosome; INVOLVED IN: translation, ribosome biogenesis; LOCATED IN: ribosome, cytosolic large ribosomal subunit
							AT5G46440	18834643-18835153	FUNCTIONS IN: molecular_function unknown; INVOLVED IN: biological_process unknown; LOCATED IN: endomembrane system
							AT5G46450	18835618-18839546	Disease resistance protein (TIR-NBS-LRR class) family; FUNCTIONS IN: transmembrane receptor activity, nucleoside-triphosphatase activity, nucleotide binding, ATP binding; INVOLVED IN: signal transduction, defense response, apoptosis, innate immune response; LOCATED IN: intrinsic to membrane; EXPRESSED IN: 18 plant structures; EXPRESSED DURING: 11 growth stages
							AT5G46460	18840305-18842398	Pentatricopeptide repeat (PPR) superfamily protein; INVOLVED IN: biological_process unknown; LOCATED IN: mitochondrion; EXPRESSED IN: 20 plant structures; EXPRESSED DURING: 11 growth stages
							AT5G46470	18842701-18849741	Encodes RPS6 (RESISTANT TO P. SYRINGAE 6), a member of the TIR-NBS-LRR class resistance protein.
							AT5G46490	18850776-18853843	Disease resistance protein (TIR-NBS-LRR class) family; FUNCTIONS IN: transmembrane receptor activity, nucleoside-triphosphatase activity, nucleotide binding, ATP binding; INVOLVED IN: signal transduction, apoptosis, defense response, innate immune response; LOCATED IN: intrinsic to membrane
							AT5G46500	18856454-18857787	unknown protein; BEST Arabidopsis thaliana protein match is: disease resistance protein (TIR-NBS-LRR class) family (TAIR:AT5G46260.1)
							AT5G46510	18860451-18867013	Disease resistance protein (TIR-NBS-LRR class) family; FUNCTIONS IN: transmembrane receptor activity, nucleoside-triphosphatase activity, nucleotide binding, ATP binding; INVOLVED IN: signal transduction, defense response, apoptosis, innate immune response; LOCATED IN: intrinsic to membrane; EXPRESSED IN: 21 plant structures; EXPRESSED DURING: 12 growth stages
							AT5G46520	18867767-18872415	Disease resistance protein (TIR-NBS-LRR class) family; FUNCTIONS IN: transmembrane receptor activity, nucleoside-triphosphatase activity, nucleotide binding, ATP binding; INVOLVED IN: signal transduction, defense response, apoptosis, innate immune response; LOCATED IN: intrinsic to membrane
							AT5G46530	18875525-18876898	AWPM-19-like family protein; FUNCTIONS IN: molecular_function unknown; INVOLVED IN: biological_process unknown; LOCATED IN: endomembrane system, membrane
26	5	early HL	25956134	0.46C	-0.01	13	AT5G64910	25940711-25944114	unknown protein
			25963073	0.46C	-0.01		AT5G64930	25945712-25948341	Regulator of expression of pathogenesis-related (PR) genes. Participates in signal transduction pathways involved in plant defense (systemic acquired resistance -SAR).
			25967700	0.36NC	0.01		AT5G64940	25948973-25953822	Encodes a member of ATH subfamily of ATP-binding cassette (ABC) proteins.
			25968943	0.28NC	0.01		AT5G64960	25955381-25958995	Encodes CDKC;2, part of a CDKC kinase complex that is targeted by Cauliflower mosaic virus (CaMV) for transcriptional activation of viral genes. Also regulates plant growth and development. Co-localizes with spliceosomal components in a manner dependent on the transcriptional status of the cells and on CDKC2-kinase activity. Expression of CDKC2 modifies the location of spliceosomal components.

			25975808	0.48C	-0.01		AT5G64980	25960775-25963235	unknown protein
			25976943	0.32C	-0.01		AT5G65000	25964960-25967393	Nucleotide-sugar transporter family protein; FUNCTIONS IN: nucleotide-sugar transmembrane transporter activity, sugar:hydrogen symporter activity; INVOLVED IN: carbohydrate transport, nucleotide-sugar transport; LOCATED IN: integral to membrane, Golgi membrane
							AT5G65005	25967824-25968638	Polynucleotidyl transferase, ribonuclease H-like superfamily protein; FUNCTIONS IN: nucleic acid binding; INVOLVED IN: biological_process unknown; LOCATED IN: cellular_component unknown
							AT5G65010	25969190-25972575	Encodes asparagine synthetase (ASN2).
							AT5G65020	25973815-25975726	Annexin2; annexins are calcium binding proteins that are localized in the cytoplasm. When cytosolic Ca2+ increases, they relocate to the plasma membrane. They may be involved in the Golgi-mediated secretion of polysaccharides.
							AT5G65030	25975697-25976305	unknown protein

Table S2. Shortlist of 33 prioritized candidate genes potentially underlying quantitative trait loci (QTLs) for photosynthesis acclimation in Arabidopsis

These are the QTLs indicated in Fig. 2. These genes pass three out of the five selection criteria summarized in columns 2 to 6: gene ontology (genes in red have ontology terms 'chloroplast', 'photosynthesis', or 'light stress'); gene co-expression (values in red have a correlation value (r^2) that exceeds 0.800 when considering expression of light response genes from light intensity-associated microarray experiments; a dash means the gene is not represented on the microarray chip used for gene expression analysis); gene expression in the vegetative rosette; gene function; and presence of segregating polymorphisms in the gene coding sequence. The last column indicates for which genes T-DNA insertion mutants were screened; AT1G74190, AT5G64960, AT5G64980, AT5G65000, and AT5G65030 were included in T-DNA screening because of extreme high LD in these two QTLS (LD>0.9).

QTL	gene	r^2	rosette expression	known role in photosynthesis	polymorphisms in extreme accessions	T-DNA line screened
3	AT1G34000	0.951	yes	yes	no	yes
4	AT1G74180	0.669	yes	no	yes	yes
4	AT1G74190	0.337	no	no	yes	yes
4	AT1G74210	0.924	yes	no	yes	no
7	AT2G26280	0.467	yes	no	yes	yes
8	AT3G04840	0.847	yes	no	yes	no
8	AT3G04870	0.937	yes	yes	no	yes
8	AT3G04880	0.818	yes	no	yes	yes
8	AT3G04890	0.899	no	no	yes	no
8	AT3G04920	0.858	yes	no	yes	no
9	AT3G05810	0.884	yes	no	yes	no
10	AT3G22570	0.896	no	yes	no	no
10	AT3G22690	-	-	yes	yes	yes
13	AT4G01900	0.820	yes	yes	no	no
15	AT4G12400	0.952	no	yes	yes	yes
19	AT5G01750	0.746	no	yes	yes	no
20	AT5G03760	0.810	no	yes	no	yes
21	AT5G12290	0.940	yes	yes	no	yes
22	AT5G18170	0.840	no	yes	no	no
22	AT5G18570	0.958	yes	yes	no	no
22	AT5G20130	0.917	yes	no	no	no
22	AT5G20140	0.967	yes	yes	no	yes
23	AT5G42870	0.822	no	yes	yes	yes
24	AT5G46390	0.952	yes	no	yes	no
24	AT5G46420	0.958	yes	no	no	no
24	AT5G46530	-	-	no	yes	yes
26	AT5G64940	0.938	yes	no	no	yes
26	AT5G64960	0.612	yes	no	yes	yes
26	AT5G64980	0.841	no	no	yes	yes
26	AT5G65000	0.656	no	no	yes	yes
26	AT5G65010	0.903	yes	yes	yes	yes
26	AT5G65020	0.923	yes	no	no	yes
26	AT5G65030	-	-	no	yes	yes

Table S3. T-DNA lines screened for photosynthetic acclimation response to increased irradiance.

gene	NASC ID	name	insertion location in gene
AT1G34000	N406778	GK-071E10	first intron
AT1G74180	N65449	SAIL_513_A08	sixth (=last) exon
AT1G74190	N65450	SALK_041143	fifth (=last) exon
AT2G26280	N511487	SALK_011487	promoter
AT2G26280	N861393	SAIL_888_F10	intron 1700bp downstream of ATG-start
AT3G04870	N658302	SALK_079674	first exon
AT3G04880	N593180	SALK_093180	first exon
AT3G22690	N660581	SALK_123515	first exon
AT4G12400	N670406	SALK_023494	first exon
AT5G03760	N502194	SALK_002194	promoter
AT5G12290	N818029	SAIL_391_F04	third exon
AT5G20140	N829965	SAIL_683_H02	promoter
AT5G42870	N653185	SALK_047457	seventh intron
AT5G46530	N643165	SALK_143165	5'UTR
AT5G64940	N679867	SALK_080442	promoter
AT5G64960	N595246	SALK_095246	5'UTR
AT5G64980	N686875	SALK_138186	first exon
AT5G65000	N660110	SALK_112086	third intron
AT5G65010	N543167	SALK_043167	third intron
AT5G65020	N624483	SALK_124483	promoter
AT5G65030	N654708	SALK_069622	first exon

Table S4. The 173 re-sequenced accessions used for haplotype analysis.

Code	Accession	Code	Accession	Code	Accession	Code	Accession
cs22689	RRS-10	cs28759	Ting-1	cs76146	HSm	cs76232	Ste-3
cs28013	Alst-1	cs28779	Tscha-1	cs76147	In-0	cs76235	T1080
cs28014	Amel-1	cs28780	Tsu-0	cs76148	JEA	cs76236	T1110
cs28018	Ang-0	cs28786	Ty-0	cs76150	Kas-1	cs76237	T1130
cs28049	Ann-1	cs28787	Uk-1	cs76152	Kelsterbach-4	cs76239	T540
cs28053	Ba-1	cs28795	Utrecht	cs76153	Kin-0	cs76242	Ta-0
cs28054	Baa-1	cs28800	Ven-1	cs76154	Kno-18	cs76244	Tamm-2
cs28064	Benk-1	cs28804	Wa-1	cs76156	Kulturen-1	cs76245	TDr-1
cs28091	Boot-1	cs28822	Wl-0	cs76159	Lc-0	cs76246	TDr-17
cs28099	Bsch-0	cs76087	Ag-0	cs76164	Ler-1	cs76249	TDr-8
cs28128	Ca-0	cs76088	Alc-0	cs76166	Liarum	cs76250	Tomegap-2
cs28135	Chat-1	cs76091	An-1	cs76167	Lilloe-1	cs76251	Tottarp-2
cs28142	CIBC-5	cs76092	App1-16	cs76168	Lip-0	cs76268	Ts-1
cs28160	Cnt-1	cs76093	Baa1-2	cs76170	Lis-2	cs76293	Ull2-3
cs28193	Com-1	cs76094	Bay-0	cs76171	Lisse	cs76294	Ull2-5
cs28201	Da(1)-12	cs76096	Bg-2	cs76172	LL-0	cs76296	Uod-7
cs28210	Do-0	cs76097	Bla-1	cs76173	Lm-2	cs76297	Van-0
cs28241	Es-0	cs76098	Blh-1	cs76174	Lom1-1	cs76298	Vaar2-1
cs28279	Gel-1	cs76099	Bor-1	cs76175	Lov-5	cs76301	Wei-0
cs28280	Gie-0	cs76100	Bor-4	cs76176	Lp2-2	cs76302	Wil-1
cs28336	Ha-0	cs76101	Br-0	cs76177	Lp2-6	cs76303	Ws-0
cs28343	Hau-0	cs76102	Broet1-6	cs76178	Lund	cs76304	Wt-5
cs28344	Hey-1	cs76103	Bu-0	cs76191	Mrk-0	cs76305	Yo-0
cs28345	Hh-0	cs76105	Bur-0	cs76192	Mt-0		
cs28350	Hn-0	cs76106	C24	cs76193	Mz-0		
cs28364	Je-0	cs76109	Can-0	cs76194	N13		
cs28369	Jl-3	cs76111	CIBC-17	cs76195	Na-1		
cs28394	Kl-5	cs76113	Col-0	cs76196	NC-6		
cs28395	Kn-0	cs76114	Ct-1	cs76198	NFA-10		
cs28420	Kro-0	cs76116	Cvi-0	cs76199	NFA-8		
cs28490	Mc-0	cs76117	Dra3-1	cs76200	oemoe2-1		
cs28492	Mh-0	cs76118	Drall-1	cs76203	Oy-0		
cs28495	Mnz-0	cs76124	Duk	cs76210	Per-1		
cs28527	Nc-1	cs76125	Eden-2	cs76212	PHW-34		
cs28564	No-0	cs76126	Edi-0	cs76213	Pna-17		
cs28573	Nw-0	cs76127	Est-1	cs76214	Pro-0		
cs28578	Nz1	cs76128	FÃ¤b-4	cs76215	Pu2-23		
cs28583	Old-1	cs76129	Fei-0	cs76216	Ra-0		
cs28587	Or-0	cs76131	FjÃ¤1-2	cs76217	Rak-2		
cs28640	Pla-0	cs76132	FjÃ¤1-5	cs76218	Ren-1		
cs28650	Pog-0	cs76133	Ga-0	cs76219	Rev-2		
cs28685	Rhen-1	cs76135	Ge-0	cs76220	Rmx-A180		
cs28692	Rou-0	cs76136	Got-7	cs76222	Rsch-4		
cs28713	RRS-7	cs76137	Gr-1	cs76223	Sanna-2		
cs28725	Sav-0	cs76139	Gy-0	cs76224	Sap-0		
cs28729	Sei-0	cs76140	Hi-0	cs76226	Se-0		
cs28732	Sg-1	cs76141	Hod	cs76227	Shahdara		
cs28739	Si-0	cs76142	Hov4-1	cs76229	Sparta-1		
cs28743	Sp-0	cs76143	Hovdala-2	cs76230	Sq-8		
cs28758	Tha-1	cs76145	Hs-0	cs76231	St-0		

Table S5. Sequences (5'-3') of primers used for real-time quantitative Reverse Transcriptase-PCR of candidate and reference genes.

Gene	Forward Primer	Reverse Primer
YS1	GCCTCGCGTAACCACAAATC	TTTACGCCGAGTGTGGAGAG
DGS1	GAGTGGGAAGCAAGCAGTCA	GAGTTAGGAAGGCCACAGCA
CID7	GCTGTGCTCCTCAACACACT	CCAGTGGGTCAAGGAAACA
UBQ7	GCAGCGACACCATCGACAAT	AGGTCCGGCCATCTTCCAAT
CB5E	TGATCATCCTGGAGGCGATG	TTGCAGTGTCGCTGTGACCA

Chr.	SNP position	GWAS	L1.1	L1.2	L1.3	L2.1	L2.2	L2.3	H1.1	H1.2	H1.3	H2.1	H2.2	H2.3	H3.1	H3.2	H3.3	H4.1	H4.2	H4.3
1	548,483	AV	4.2	3	2.6	3.3	2.9	2.6	0.9	0.8	0.6	0.7	0.6	0.5	1	1	1	14	17	14
1	548,499	AV	4.1	3	2.6	3.7	3.8	2.7	1	0.8	0.7	0.8	0.8	1	12	15	15	17	2.2	19
1	552,796	AV+SM	2.9	2.1	2.7	2.5	4.1	2.8	0.3	0.3	0.3	0.3	0	0.1	0.1	0.3	0.3	0.1	0.7	0.6
1	703,755	AV	3.4	4.4	3.4	3.5	3.1	3.3	0.6	0.8	0.8	0.9	11	13	0.9	12	12	0.9	11	0.9
1	3,995,184	AV	0.6	0.6	1	1	16	13	11	12	0.9	13	19	2.7	2.3	3.3	3.6	2.6	3.6	4.1
1	7,384,441	AV+SM	12	14	0.9	11	0.5	12	4.6	4.8	5.3	4.1	3.8	3.4	3.7	2.9	2.6	3.3	2.5	2.4
1	9,765,217	AV	3.1	4.4	3.7	2.8	3.5	3.1	0.2	0.2	0.1	0.2	0.1	0	0.2	0	0.1	0.2	0	0.1
1	9,774,441	AV+SM	3.2	4.6	4.2	3	4	3.9	0.3	0.3	0.1	0.1	0	0.1	0	0.3	0.5	0.1	0.4	0.4
1	9,776,148	AV+SM	3.2	4.6	3.9	2.8	3.5	3.5	0.4	0.5	0.3	0.2	0.1	0	0.1	0.1	0.3	0	0.3	0.2
1	9,781,240	AV+SM	2.9	4.2	3.9	2.6	3.5	3.5	0.4	0.6	0.3	0.3	0.1	0	0.2	0.1	0.3	0	0.3	0.3
1	9,786,365	AV+SM	18	17	2.3	2.4	4	3	0.3	0.4	0.3	0.3	0.6	0.8	0.5	11	12	0.8	13	14
1	9,790,491	AV+SM	3.1	4.2	4.2	3.4	4	3.8	0.3	0.4	0.3	0.4	0.1	0.1	0	0	0.2	0.5	0.2	0.5
1	10,596,936	AV+SM	3.7	2.7	2.7	3.6	2.7	3.9	2.7	2.6	2.4	3.4	3.6	4.2	4.2	4.7	5.1	5.1	5.8	5.4
1	12,275,289	AV	1	0.6	0.3	0.4	0.5	0.2	2.9	3.4	3.2	4	3.9	3.9	3.4	2.9	3.1	3.1	2.8	2.5
1	12,348,136	AV	3.2	4	2.6	2.4	2.4	3.1	16	17	2.3	2.6	2.4	2.5	17	2.1	2.4	18	2	2.3
1	16,280,462	AV	4	2.6	3.6	2.4	2.7	15	0.5	0	0	0	0	0.1	0.1	0.1	0.1	0.1	0.2	0.3
1	22,409,810	AV	4.7	3.7	3.5	3.6	3.6	3.4	0.3	0.3	0.4	0.2	0.4	0.4	0.1	0.6	0.8	0.1	0.5	0.6
1	22,981,647	AV	3.6	3.8	3.4	2.3	2.4	4.1	0.8	0.7	0.5	0.7	0.6	0.5	0.6	0.6	0.8	0.5	0.7	0.7
1	22,982,345	AV	2.7	4.2	3.5	2.3	2	3	0.3	0.7	0.7	0.2	0.2	0.1	0.1	0.1	0.2	0.1	0.2	0.1
1	23,271,314	AV	2.7	2.9	2.3	2.1	4	18	0.3	0.6	0.7	0.3	0.2	0.3	0.1	0.1	0.1	0.1	0.1	0.2
1	23,441,407	AV	0.1	0	0.1	0.3	0.1	0.4	2	2	12	18	18	2.2	2.9	3.5	3.6	4	4.4	4.7
1	24,371,872	AV	4.1	2.4	2.9	3.3	3	3.2	0.3	0.3	0.3	0.3	0.5	0.5	0.1	0.2	0.2	0.1	0.2	0.3
1	26,249,116	AV	0	0.1	0.3	0.6	0	0.1	4.3	4.2	3.6	3.8	4.3	4.7	4.1	4.1	3.6	3.3	2.6	2.2
1	27,114,195	AV	0	0.1	0	0.5	0.1	0.3	0.9	0.8	0.8	16	19	2.6	2.5	3.6	3.8	3.3	4	4
1	27,114,604	AV	0.2	0.1	0	0.1	0.1	0.1	17	18	2.5	3.5	3.4	4.1	3.7	3.6	3.8	3.3	3.3	3.3
1	27,114,842	AV	0.3	0.2	0	0	0	0	18	19	2.8	3.5	3.3	4	3.7	3.6	3.7	3.6	3.4	3.3
1	27,329,236	AV+SM	18	11	12	14	0.9	0.7	4.6	4.1	4.2	4.3	3.8	3.6	3.7	3.2	3.3	2.4	2.7	2.7
1	27,891,662	AV	0	0.1	0.3	0.1	0	0.4	3.2	4.2	4	3.2	4	3.5	2.8	3	2.8	2.2	2	19
1	27,894,888	AV	0.8	0.9	1	11	0.4	1	2.1	4.2	3.9	2.7	3.4	3.2	2	2.2	2	14	14	11
1	27,896,712	AV	0	0.3	0.1	0.2	0.1	0.2	3.7	4.2	3.8	2.8	3.2	3.2	2.7	2.7	2.6	2.1	2	2
1	27,897,142	AV	0.8	0.7	0.9	0.9	0.4	13	2.6	4.4	4	2.4	3	3	2.1	2.2	2.1	14	17	16
1	27,899,243	AV	0.6	1	0.9	0.9	0.5	0.9	4.4	5.2	4.1	3.3	3.8	3.9	2.7	3.1	2.9	19	2	2.2
1	27,903,238	AV+SM	0.2	0.2	0.2	0.1	0	0.4	3.9	5	4.4	4.1	4	4	3.8	3.6	3.5	3.1	2.6	2.1
1	27,904,597	AV+SM	11	14	11	0.6	0.5	12	3.2	4.1	4.1	3.3	3.2	3.5	2.7	2.5	2.6	18	17	16
1	27,904,633	AV+SM	11	15	12	0.7	0.6	11	3.5	4.2	4.1	3.4	3.2	3.4	2.6	2.5	2.5	18	17	16
1	27,904,871	AV+SM	12	16	11	0.7	0.7	12	3.4	4.2	4	3.6	3.4	3.5	3	2.8	2.8	2	18	17
1	27,905,270	AV+SM	0.4	0.5	0.3	0.5	0	0.7	2.1	3.5	4	2.8	2.9	2.6	19	16	16	1	0.8	0.7
1	27,905,627	AV	0.5	0.7	0.7	0.9	0.3	0.9	3.1	4.4	3.9	3.2	3.6	3.4	2.3	2.7	2.6	16	17	18
1	27,905,987	AV+SM	0.5	0.4	0.3	0.3	0.2	0.8	2.9	4	3.9	3.2	3.5	3.3	2.9	2.5	2.4	17	14	13
1	27,979,318	AV+SM	0.5	0.5	13	0.5	0.3	0.4	4.9	4.2	5	5.4	5.2	5.2	4.5	4.2	4	3.6	3.4	3.2
1	27,981,096	AV	2.4	16	2.7	2	12	15	5.3	3.9	4.3	4.5	4.3	4.1	3.7	2.9	3	3	2.6	2.9
2	77,634	AV+SM	0	0	0.2	0.3	0.1	0.3	4	4.2	2.8	3.8	4.2	4.7	5	6	5.1	5.1	5.2	5
2	350,665	SM	2.7	18	2.7	2.4	2.6	2.4	2.4	2.4	18	2.1	2.2	2.6	2.9	3.3	3.5	3.6	4.3	4.2
2	3,537,208	AV	2.6	4.1	3.7	2.1	3.1	3.3	0.8	0.9	11	0.7	0.5	0.5	0.1	0.1	0.2	0	0.1	0.1
2	3,843,084	AV+SM	3.6	4.1	4	3.7	3.6	3.4	0.9	0.8	0.7	0.5	0.3	0.2	0.2	0	0.1	0.2	0.1	0
2	4,420,246	AV+SM	3.1	4.5	3.5	2.1	3.2	4.1	0.1	0.3	0.4	0.1	0.1	0.1	0.2	0.2	0.1	0.3	0.1	0.1
2	4,705,002	AV+SM	5.4	5	5.2	3.7	4.2	3.8	17	18	19	15	12	14	0.8	0.8	0.9	0.6	0.8	0.8
2	6,718,723	AV+SM	3	3.6	3.2	4	5	3.2	14	13	11	14	2	2.4	15	2.4	2.6	19	2.4	2.6
2	6,720,135	AV+SM	2.8	2.9	2.6	4.9	3.1	2.8	0.3	0.2	0.3	0.6	0.7	0.9	0.3	0.4	0.6	0.1	0.5	0.5
2	6,814,637	AV	3.7	4.2	3.5	3.1	3.5	3.3	0.2	0.2	0.1	0.1	0.1	0	0	0.1	0.1	0.1	0.2	0.2
2	7,404,313	AV	0.4	0.2	0.6	0.5	0.4	0.8	3.5	3.9	3.6	4.2	4.6	4.4	4.7	4.7	4.4	4.7	4.5	4.6
2	8,158,848	AV	0.4	0.5	0.9	0.9	0.8	0.7	4	2.9	2.4	3.4	3	2.6	3.9	3.1	3.5	4.2	3.5	4

Chr.	SNP position	GWAS	L1.1	L1.2	L1.3	L2.1	L2.2	L2.3	H1.1	H1.2	H1.3	H2.1	H2.2	H2.3	H3.1	H3.2	H3.3	H4.1	H4.2	H4.3
2	11,189,311	AV+SM	0.9	13	18	18	13	12	3.3	3.4	4.3	2.7	2.7	2.6	2.9	2.7	2.5	2.6	19	17
2	11,189,443	AV	1	13	18	19	11	12	3.2	3.3	4	2.5	2.3	2.3	2.6	2.2	2.1	2.3	16	14
2	11,189,829	SM	13	16	2.3	2.1	14	14	3.9	3.8	4	2.6	2.5	2.3	2.8	2.5	2.3	2.6	18	18
2	16,905,030	AV+SM	0.8	0.8	0.9	1	11	0.7	3.9	4.2	4	3	3.2	3.5	2.9	2.9	2.7	2.3	2.1	19
3	1,230,134	AV	0.9	11	11	11	0.9	0.8	3	3.5	4	2.9	3	2.3	16	15	17	12	1	13
3	1,350,656	SM	16	2	2.1	17	16	2	4.4	4	2.8	3	3.2	3.1	3	3.2	2.7	3	2.6	2.5
3	1,353,218	AV+SM	0.7	1	14	0.7	0.7	12	2.7	2.8	3.8	3.3	3.8	3.9	3.8	4.2	4.1	4.7	3.9	3.8
3	1,353,894	AV+SM	0.7	0.7	12	0.7	0.7	12	4.3	4.1	5	4.8	5	5	4.4	4.9	4.7	4.4	3.6	3.2
3	1,453,164	AV+SM	19	2.1	16	18	18	19	3.1	4.2	3.7	4.1	4.9	5.4	4.3	5.5	5.5	4.7	4.9	4.7
3	1,652,181	AV	0.8	0.7	0.3	0.5	0.6	1	3.5	2.9	2.5	3.2	3.6	3.6	4.4	5	4.7	4.8	4.6	4.6
3	1,714,987	AV	0.9	1	0.8	11	13	15	3.3	4.1	2.8	3	3.3	3	3.4	3.3	3	3.7	3.1	2.7
3	1,750,265	AV	0.3	0.4	0.4	0.2	0.2	0.5	4.1	3.7	2.9	4.3	3.3	3	3.3	2.6	2.4	2.7	2	15
3	1,750,573	AV	0.5	0.6	0.7	0.2	0.5	0.8	4.5	3.7	2.8	4.2	3.6	3.3	3.3	2.9	2.9	2.7	2.3	18
3	1,750,946	AV	0.5	0.5	0.6	0.2	0.5	0.7	4.2	3.4	2.5	3.9	3.2	3	3	2.6	2.6	2.4	2.1	16
3	1,751,042	AV	0.7	0.7	0.8	0.5	0.5	12	5.1	4.1	3.2	4.6	3.9	3.5	3.7	3.2	3.1	3.1	2.8	2.2
3	1,755,712	AV+SM	17	14	17	14	12	2	2.1	3.2	3.4	3.4	3.3	3.7	4	3.6	3.2	4.2	3.3	2.9
3	1,791,357	AV	0.2	0.2	0.2	0.1	0.2	0.5	19	2.2	2.1	2.7	2.9	3.3	3.8	3.8	3.8	4.6	3.9	3.9
3	1,791,485	AV	0.2	0.3	0.2	0.1	0.2	0.5	2.1	2.3	2.2	2.8	3	3.4	4	3.7	3.8	4.7	3.9	3.9
3	1,834,221	AV+SM	0.2	0.3	0.2	0.2	0.6	0.2	3.3	3.5	2.9	3.5	3.2	3.2	4.2	3.3	3.1	4.1	2.8	2.4
3	1,834,667	AV	0.1	0.1	0	0.1	0.3	0.1	3.5	3.7	3	3.4	3.3	3.4	4.3	3.8	3.9	4.6	3.7	3.3
3	1,835,145	AV	0	0.2	0	0	0.4	0.1	3.5	3.4	2.4	2.9	2.7	2.7	3.6	3.4	3.4	4.3	3.6	3.2
3	3,281,845	AV	0.1	0.4	0.4	0.1	0.2	0.1	18	18	15	14	2.2	2.4	3	3.7	3.6	3.8	4.2	3.9
3	3,382,240	AV+SM	0.3	0.4	0.6	0.5	0.3	0.3	3.1	3.4	3.6	4.4	4.1	3.7	4.6	3.4	2.9	3.5	2.8	2.3
3	4,496,216	AV	0.8	0.9	0.5	0.3	0.5	0.3	3.3	3.8	4.1	3.6	3.7	3.9	3.9	3.1	3.5	4.1	2.9	2.9
3	5,586,719	AV+SM	12	1	0.9	0.9	0.8	0.8	3.4	3.5	3.6	3.6	3.9	4.1	4.1	4.1	4.3	4.2	3.5	3.8
3	5,900,347	AV+SM	4.2	3.6	3.8	4.2	3.3	2.9	11	0.8	0.7	0.7	12	12	1	12	12	0.7	11	13
3	7,348,466	AV+SM	3	3.5	3	5	2.8	2.3	0.8	0.8	0.8	0.8	11	11	0.7	0.7	0.8	0.6	0.6	0.6
3	7,759,706	AV	2.9	3.3	4	3.9	2.8	3.6	13	12	13	11	13	12	0.9	1	11	0.9	0.7	0.8
3	7,760,604	AV	3.3	4.1	4	3.6	3.5	3.6	0.3	0.4	0.3	0.3	0.3	0.3	0.2	0.4	0.5	0.4	0.5	0.5
3	7,992,656	SM	0.9	0.7	13	0.6	0.8	0.9	18	19	2.2	3.9	4.5	5	4.5	5.1	4.9	4.6	4.7	4.2
3	8,120,853	AV+SM	15	16	17	19	19	2.4	4	4.6	3.3	3.8	4.6	4.7	4	5	4.8	3.9	4.5	4.3
3	8,226,290	AV	3.3	2.9	4.6	2.3	3.4	4.3	11	13	0.9	15	15	12	14	16	15	13	19	17
3	9,116,089	AV+SM	3.4	4.5	4.5	4	2.9	4.1	16	0.8	0.5	0.7	0.9	11	0.8	12	15	0.8	14	14
3	10,578,962	AV+SM	3.4	3.9	3.1	4.1	4.6	3	0.9	0.7	0.4	0.5	0.8	1	0.9	1	14	14	16	15
3	11,032,555	AV+SM	0	0.1	0.1	0.2	0.6	0.1	14	12	1	11	18	2.4	2.7	3.6	3.9	4.1	4.8	4.6
3	11,720,925	AV	0.2	0.7	0.8	0.6	0.6	0.7	3.1	4	4.2	3.9	2.7	2	2.3	15	13	15	0.8	0.7
3	12,765,053	AV	0.5	1	12	1	0.7	0.7	4	3.5	3.3	3.5	3.4	3.5	2.7	2.6	2.3	18	15	16
3	12,784,017	AV+SM	2.5	2.6	2.7	2.3	2.6	2.8	3.9	5.3	5.7	5	5.2	5.6	4.3	3.6	3.7	3.2	2.6	2.5
3	15,364,226	AV	11	0.8	11	0.9	0.8	0.8	2.6	2.9	4	3.3	2.6	2.6	2.4	18	19	19	13	15
3	15,932,189	AV+SM	0.4	0.1	0.1	0.2	0.1	0.1	3.7	4.3	4.8	3.9	3.6	3.6	4.4	3.6	3.8	4.3	3	3.1
3	16,316,203	AV+SM	2.7	3.4	3.9	2.7	3.8	4	12	11	14	13	15	13	1	12	1	12	16	11
3	16,318,079	SM	19	2.8	2.1	2.4	18	2.5	2.1	12	12	14	2	2.1	2.2	3.3	3.4	3	4.3	4
3	16,318,704	SM	1	12	11	1	0.7	16	19	16	18	16	2.4	2.7	2.7	3.9	4.4	3.4	5.2	4.9
3	16,698,957	AV+SM	2.2	2.4	2.7	4.6	3.1	3.3	14	14	12	13	12	14	16	17	19	2.1	2	19
3	16,844,909	AV	0.5	0.5	0.8	0.9	0.2	0.7	2.7	3.7	3.3	3.9	3.9	4.1	4.1	3.9	3.8	4.2	3.9	3.5
3	18,539,054	AV	0.5	0.4	0.6	0.5	0.2	0.6	4.3	3.4	2.6	2.5	2.9	3	2	2.6	2.6	19	2	2.3
3	19,985,321	AV	17	15	13	12	0.9	17	4	4.4	3.8	3.4	2.9	2.5	3	2.4	2.3	3.2	2.6	2.3
3	20,000,766	AV+SM	2.2	15	15	16	14	2.1	4.7	3.4	2.8	3.5	2.9	2.6	4.2	3.3	3.1	3.6	3.4	3.1
3	21,370,204	AV	0	0.5	0.6	0.1	0.7	0.4	3.6	3	2.9	3.9	3.8	3.9	4.8	3.4	3.3	4.1	3	2.5
3	21,528,062	AV	4.4	4.3	3.5	2.8	2.7	3.3	12	1	13	12	14	13	1	13	12	0.8	0.9	11
3	21,529,038	AV	3.8	4.2	3.1	2.6	2.6	3.3	0.7	0.6	0.8	0.7	1	0.9	0.5	0.8	0.7	0.4	0.5	0.7
4	818,905	AV	0.2	0.1	0.4	1	0.3	0.5	17	15	0.9	13	15	16	2.4	2.7	3.2	3.3	3.3	4

Chr.	SNP position	GWAS	L1.1	L1.2	L1.3	L2.1	L2.2	L2.3	H1.1	H1.2	H1.3	H2.1	H2.2	H2.3	H3.1	H3.2	H3.3	H4.1	H4.2	H4.3
4	987,887	AV	0.2	0.2	0.3	0.4	0.3	0.4	2.7	2.6	2.6	2.7	3	4	2.4	3.1	3.4	2.3	3.2	3.3
4	5,849,497	AV	0	0.1	0.1	0.6	0.3	0.3	4.1	3.1	2.5	3.9	3.2	2.8	3.7	3.5	2.9	3.3	2.9	2.9
4	6,016,113	SM	14	0.9	19	15	0.8	0.9	3.3	4.4	4.1	3.7	4	3.7	3.7	2.8	3	3	2.5	2.4
4	6,017,522	AV+SM	0.9	0.5	13	0.9	0.4	0.9	3.1	4	3.7	3.2	2.8	2.4	3	18	18	2.2	17	13
4	6,222,812	AV	3.9	4.1	3.6	3.3	3.7	3.1	12	13	16	13	14	16	11	13	15	12	13	13
4	6,320,947	AV+SM	3.1	3	4.2	2.9	3.2	3	0.6	0.4	0.8	11	0.8	0.7	0.8	0.7	0.8	0.4	0.5	0.5
4	6,644,701	AV	3.9	3.3	2.7	3.1	2.3	4.3	0.5	15	12	0.9	11	11	0.4	0.7	0.7	0.3	0.4	0.5
4	6,744,839	AV+SM	3.9	2.9	2.5	3.5	4.3	3.9	1	0.9	0.7	0.5	0.6	0.8	0.8	0.8	11	0.9	11	1
4	6,745,253	AV+SM	4.2	3.2	2.9	3.4	4.3	3.8	1	0.9	0.7	0.6	0.5	0.7	0.8	0.7	0.9	0.8	0.9	0.8
4	6,872,903	AV+SM	14	11	12	0.9	0.9	13	3.7	4.7	4.5	2.8	3.5	3.5	2.9	3.6	3.6	4	4	4.1
4	7,081,972	AV	4	3.1	3.2	3	2.3	2.3	11	0.7	0.4	0.1	0.5	0.4	0.3	0.8	0.6	0.6	1	11
4	7,149,183	AV	0.3	0	0.1	0.6	0.3	0.1	4	3	2.7	3	3.1	3.3	3.9	3.5	3.1	3.1	2.2	2.6
4	7,346,546	AV+SM	0.9	0.9	0.4	11	0.8	12	4	5.3	4.7	2.6	3.1	3.7	2.7	3.2	3.3	2.9	3.1	2.7
4	7,810,132	SM	0.6	0.6	0.8	1	0.6	0.8	3	3.2	19	3	2.6	2.4	3.7	3.5	3.6	3.8	4.4	4.5
4	7,810,598	AV	0	0.1	0.4	0.5	0.2	0.5	3.4	3.7	3.5	4.2	3	2.5	3.9	2.5	2.7	3.3	2.7	2.8
4	8,209,018	AV	0.3	0	0.1	0.3	0	0.3	4.9	3.4	2.6	2.9	3.1	2.8	3.3	2.7	2.8	3	2.6	2.4
4	8,209,226	AV+SM	0.6	0.3	0.2	0.7	0.2	0.1	5.1	4.3	3.6	3.5	3.5	3.3	3.7	3.3	3.3	3.7	3.2	2.9
4	9,122,369	AV	3.9	3.1	4.4	2.2	3.4	3.1	13	1	11	12	11	11	0.7	0.7	12	0.6	0.9	0.9
4	9,122,499	AV	3.9	3.1	4.4	2.2	3.4	3.1	13	1	11	12	11	11	0.7	0.7	12	0.6	0.9	0.9
4	9,122,802	AV	3.9	3.2	4.2	2	2.9	2.8	11	1	0.8	0.9	0.9	0.9	0.5	0.6	11	0.5	0.8	0.8
4	9,123,738	AV	3.7	3.1	4.2	2.4	3.2	3.2	13	12	1	1	11	11	0.5	0.6	11	0.5	0.8	0.8
4	9,755,226	AV	4	2.7	3.9	2.6	2.3	3.3	14	1	0.8	0.7	0.6	0.5	0.5	0.4	0.4	0.3	0.2	0.3
4	10,731,316	AV+SM	5	4.7	4.6	4.3	4.7	6.1	0.6	0.6	0.6	0.7	0.3	0.3	0.3	0.2	0.2	0.3	0.2	0.1
4	10,731,342	AV+SM	3.3	3.1	2.8	3.3	3.6	4.8	0.5	0.5	0.4	0.3	0.1	0.1	0.2	0.1	0.2	0.2	0.2	0.1
4	10,768,505	AV+SM	3.7	3.7	3.8	4.4	3.6	3.5	0.2	0.2	0	0.1	0	0.1	0.2	0	0	0.2	0.1	0
4	12,088,780	AV+SM	4.2	3.8	3.1	3.3	4.5	3.3	3	2.7	12	14	14	13	18	2.4	2.3	2.3	3.4	3.1
4	12,827,665	AV	0.9	12	11	0.6	0.4	0.5	3	4	3.8	2.7	2.5	2	2	1	0.9	1	0.4	0.5
4	14,264,880	AV	0.7	0.5	0.8	0.8	0.5	11	4.2	2.5	18	2.2	2.3	2.3	2.1	19	18	14	12	12
4	18,101,550	AV+SM	3.3	2.2	2.7	4	2.9	2.5	0.3	0.2	0.2	0.2	0.3	0.4	0.5	0.7	11	1	16	18
5	145,325	AV	3.3	19	13	4.1	3.1	2.6	13	1	0.9	0.5	11	13	0.6	1	0.8	0.6	0.8	0.7
5	267,918	AV+SM	5.3	4.3	3.9	4.1	3.2	4	3.1	2.9	2.5	3.1	3.8	4.1	3.2	4.4	4.7	3.3	4.6	4.5
5	268,505	AV+SM	5.1	4.2	3.7	4.1	2.7	4	15	14	12	17	19	2.2	19	2.4	2.8	17	2.5	2.6
5	272,241	AV+SM	3.2	2.9	3.2	2.5	2.4	2.6	2.1	2.2	2.2	3.1	3.1	3.2	3.9	4.3	4.6	3.5	4.2	4.3
5	273,701	SM	3.1	2.7	3.3	2.1	2.2	2.6	2.7	2.6	2.8	3.5	3.6	3.7	4.1	4.4	4.6	3.6	4.3	4.3
5	295,648	AV+SM	12	0.5	0.4	1	0.6	0.3	14	12	19	12	18	2.6	2.1	3.2	3.7	3	3.9	4.5
5	296,004	SM	1	0.8	0.4	0.7	0.6	0.6	2.6	2.5	2.5	2.7	3	3.5	3.3	3.8	3.9	3.5	3.8	4
5	298,229	AV+SM	12	0.5	0.4	1	0.6	0.3	14	12	19	12	18	2.6	2.1	3.2	3.7	3	3.9	4.5
5	299,476	AV+SM	11	0.4	0.4	1	0.5	0.2	17	13	2	13	15	2.3	2.5	3.1	3.6	3.4	3.6	4.2
5	302,045	AV+SM	2	1	0.9	17	11	0.7	19	16	19	14	19	2.7	2.4	3.4	3.9	3.5	4.3	4.9
5	304,375	AV+SM	12	15	13	11	12	14	2.6	2.8	3.3	2.5	2.4	2.9	2.9	3.3	3.6	3.7	4.4	4.4
5	305,676	AV+SM	14	1	11	0.8	0.8	0.9	2.4	2.9	3.5	2.7	2.4	3.2	3.6	3.8	4.3	4.7	4.7	4.9
5	308,976	SM	2.9	18	16	19	2	14	2.9	2.6	3.2	3.1	3.4	4	4.3	4	4.2	4.1	3.9	3.8
5	309,253	SM	2.5	12	15	12	14	13	3.3	3.4	4	2.9	3.1	3.6	3.8	3.8	4	4.2	4	4.2
5	513,637	AV+SM	0.4	0.7	0.7	0.6	0.7	1	3.4	4.6	4.9	4.7	5.4	5.3	5	4.5	4.2	3.9	3.4	3.5
5	987,180	AV	12	11	15	17	17	17	4.2	3.4	2	2.4	3.2	3.4	3.2	3.8	3.8	3.3	3.4	3.2
5	987,216	AV	1	12	17	13	14	17	4.5	3.8	2.4	2.6	3.3	3.4	2.6	3.5	3.5	2.6	3.1	3
5	988,003	AV+SM	11	0.9	13	12	12	12	4.5	3.1	18	18	2.7	2.8	2.2	3.1	2.9	2.4	2.8	2.9
5	1,486,024	AV+SM	0.8	0.4	0.5	0.6	0.6	0.8	3	2.1	19	2.1	19	2	2.9	2.8	2.9	4.2	3.4	3.5
5	3,975,495	AV	0.8	1	15	2.1	18	13	3.1	3	3	3.8	4.4	4	4.2	4.1	4.2	3.3	3.5	3.7
5	3,980,151	AV+SM	0.2	0.6	12	0.6	11	11	3.9	5	5.4	4.1	5.1	4.9	3.9	4.4	4.1	3.2	3.2	3.3
5	6,034,111	AV+SM	14	0.5	0.8	12	13	1	3.2	3	3.6	3.3	3.9	4.2	4.2	4.9	4.6	4	3.7	3.2
5	6,180,615	SM	0.9	15	13	0.9	12	15	2.7	3.7	4	2.6	2.9	3	18	2	18	17	16	16

Chr.	SNP position	GWAS	L1.1	L1.2	L1.3	L2.1	L2.2	L2.3	H1.1	H1.2	H1.3	H2.1	H2.2	H2.3	H3.1	H3.2	H3.3	H4.1	H4.2	H4.3
5	6,797,296	S M	0.7	0.5	0.9	0.2	0.7	0.4	3.7	3.9	4.3	3	3.8	4.4	3	3.3	3.3	2.9	2.9	2.5
5	6,797,770	S M	0.2	0	0.3	0.1	0.2	0.3	3.3	3.7	4.1	3.3	3.6	4.1	3.1	3.2	3.1	2.9	2.5	2.3
5	7,059,818	A V + S M	2.7	3.1	4.3	2.9	3.8	3.9	1	15	11	1	13	13	0.8	0.9	11	0.8	11	12
5	10,283,914	A V + S M	2.6	3.7	3.4	2.6	3.9	4.1	13	11	12	17	19	2.1	17	2.3	2.4	14	18	2.2
5	11,988,896	A V	4	3.1	2.7	2.2	3.4	2.6	0.4	0.5	0.6	0.4	0	0.1	0.3	0.1	0.2	0.1	0.2	0.2
5	13,518,211	A V	0.1	0	0.1	0.2	0.1	0	2.7	2.9	2.5	2.8	2.8	2.7	3.6	3.8	3.3	4.1	3.9	3.3
5	14,762,315	A V + S M	11	0.7	0.4	0.9	0.3	0.3	3	4.1	3	2	2.2	19	17	18	16	16	16	12
5	16,230,562	A V	2.2	13	2.2	0.9	13	13	2.2	2.2	15	19	18	18	2.5	2.9	3.5	3.7	4.6	4.6
5	17,186,178	A V	17	15	19	16	15	2.2	4.2	4	4.1	3.9	4.6	4	3.3	3.5	3.1	2.6	2.5	2.5
5	17,187,071	A V	15	13	17	17	15	2.2	3.8	3.9	3.9	3.3	4	3.6	2.7	2.9	2.6	2.1	2	2.1
5	17,187,390	A V	15	13	17	17	15	2.2	3.8	3.9	3.9	3.3	4	3.6	2.7	2.9	2.6	2.1	2	2.1
5	17,422,614	A V	18	16	14	2.4	13	2.3	3.7	3.6	2.9	3.2	3.9	4.2	2.7	3.3	2.9	2.4	2.9	2.6
5	17,423,798	A V	0.9	0.8	0.6	16	0.8	1	3.9	3.4	3.1	4.3	4.2	4.2	4	4.4	3.7	3.7	3.5	2.9
5	17,424,158	A V	0.6	0.8	0.5	11	0.9	12	4.5	3	2	3.6	3.2	2.7	3.3	3	2.3	2.6	2.3	17
5	17,427,025	A V	1	0.6	0.7	11	0.3	0.7	2.6	2.9	3.6	3.8	4.4	4.3	2.8	3.1	2.6	19	17	13
5	17,675,653	A V + S M	4.2	4.3	3.1	4.5	3.3	3.3	17	15	0.9	1	13	13	1	14	16	0.8	11	0.9
5	17,677,299	A V + S M	3.4	3.7	3.3	4.4	3.1	4.2	13	0.9	0.4	0.3	0.5	0.5	0.2	0.4	0.6	0.2	0.4	0.3
5	17,682,216	A V + S M	3	2.6	2.4	3.6	3.1	2.6	3.3	3.4	2.8	2.7	3.2	3	3	3.7	4.1	3.3	3.4	3.4
5	17,683,868	A V + S M	3.2	4.4	3.7	3.1	3.4	3.9	2.9	2.4	2.2	2.4	3.2	3.1	2.4	3	3.4	2.6	2.5	2.4
5	17,684,433	A V + S M	3.1	4	3.5	3.2	3.6	4.1	2.8	2.7	2.3	2.7	3.5	3.4	2.8	3.7	4.1	3.4	3.5	3.3
5	17,684,460	A V + S M	2.7	3.5	2.9	3.2	3.3	3.7	2.7	2.9	2.8	3.2	4.1	3.9	3.3	4.1	4.5	3.5	3.4	3.3
5	17,684,844	A V + S M	3.7	3.9	3.7	4.5	4.1	3.7	17	19	12	14	18	17	14	2	2.5	15	2	2
5	17,688,132	A V + S M	4.9	5.3	4.6	3.9	3.6	5	2.7	2.2	17	2.1	2.1	2	17	2.3	2.5	14	18	17
5	17,945,137	S M	14	14	14	17	19	2	2	2	16	16	2.4	2.7	3	3.5	4.1	3.9	4.1	4
5	17,946,540	A V + S M	0.8	0.6	0.7	2	17	0.9	17	18	17	15	2.2	3	2	3.1	3.7	2.8	3.4	4.1
5	18,807,935	A V + S M	0.8	0.6	0.9	0.6	11	0.9	2.9	2.8	3	4.5	4.1	3.8	4.6	4.7	4.3	4.4	4	3.5
5	18,812,710	S M	0.7	0.3	13	13	0.9	11	3	3.1	2.9	4.2	3.6	3.8	4.3	4.3	4.3	4.4	4.1	4.1
5	18,872,155	S M	11	11	14	14	1	0.8	2.5	3.5	4	4.4	3.4	3.5	3.9	3.3	3	3	2.3	2.3
5	18,872,623	S M	2.2	13	18	2.5	2	16	2.3	3.4	2.9	4	3.3	3.4	4	3.9	3.9	3.6	3.6	3.1
5	18,872,638	S M	2.6	16	2.1	2.5	2	15	2.9	3.7	3.2	4.3	3.5	3.6	4.5	4.4	4.4	4.3	4.1	3.9
5	18,873,842	A V + S M	2.8	19	2.3	2.4	2.1	18	19	3.2	3.5	4.3	3.5	3.5	4.4	4.1	3.9	4	3.8	3.1
5	18,874,929	S M	0.3	0.2	0.5	0.8	0.3	0.1	2.1	3.2	2.7	3.2	3.5	3.9	3.6	4.1	3.8	3.8	3.4	3.3
5	18,875,337	S M	2.6	18	2.6	2.4	2	16	2.3	3.3	3.5	4.3	3.4	3.5	4.4	4.1	4.1	3.8	3.6	3.5
5	18,875,477	S M	2.5	18	2.7	2.6	19	17	2.9	4.2	3.7	4.8	3.9	4.1	4.7	4.3	4.2	3.7	3.3	2.9
5	21,804,982	A V	2.2	2	2.3	4	3.4	3	11	14	0.8	0.9	19	15	13	2.1	18	16	2.5	2.3
5	21,946,280	A V	2.8	2.1	2.8	2.2	4.1	2.9	0.3	0	0.1	0	0.3	0.5	0.1	0.5	0.5	0.3	0.7	0.7
5	21,971,571	A V + S M	4.6	3.3	3.6	5	4.8	3.7	0.3	0.2	0.1	0	0	0.1	0.1	0.5	0.5	0.3	1	0.8
5	22,823,366	A V + S M	2.4	2.9	2.4	2.2	4.6	17	0.3	0.5	0.4	0.1	0	0.1	0.1	0.1	0.1	0.1	0.1	0
5	22,827,058	A V + S M	2.6	3.3	2.1	2.3	4.1	2	0.4	0.1	0.1	0.2	0.4	0.2	0.3	0.3	0.5	0.5	0.6	0.5
5	25,956,134	A V + S M	16	2.3	2.2	16	11	17	4.3	3.3	2.9	3.4	3.7	3.6	2.9	2.8	2.8	18	15	13
5	25,963,073	A V + S M	18	2.4	2.2	16	13	15	4.5	3.3	2.9	3.3	3.5	3.1	2.4	2.1	19	12	0.8	0.6
5	25,967,700	A V + S M	0.8	1	1	15	0.9	12	4.9	3.8	3.2	2.8	3.2	3.4	3.4	3.1	2.9	3	2.3	2
5	25,968,943	A V + S M	0.1	0	0.3	0.1	0.2	0.2	3.6	3.9	3.7	3.7	3.5	3.4	4	3.4	3.1	3.2	2.3	19
5	25,975,808	A V + S M	0.7	12	12	0.7	0.6	0.9	4.4	3.2	2.6	3.3	3.5	3.4	2.9	2.6	2.6	2.1	16	13
5	25,976,943	A V + S M	0.3	0.4	0.7	0.5	0.7	0.6	3.4	4	3.6	4.6	4.3	3.9	4.4	3.9	3.6	3.9	3	2.6
5	26,189,378	A V	0.6	0.4	0.4	0.7	0.7	0.5	0.7	0.5	0.3	0.7	0.7	1	14	18	2.4	2.5	3.8	4.1

Figure S2. Characterization of natural alleles of CID7

*(a) Overview of haplotype alleles and frequencies for the CID7 gene (AT2G26280), gene orientation is 3' to 5', SNPs differing from the Col-0 reference genome sequence (allele 1) are marked; (b) Average photosynthesis efficiencies (Φ_{PSII}) (±SE) of the seven haplotype alleles before and after an increase in radiance at the onset of day 3, alleles 1 and 2, 1 and 4, 2 and 7 and 4 and 7 are statistically significantly different; (c) relative mRNA expression (±SE) of CID7 in two T-DNA insertion lines (SALK_011487 and SAIL_888_F10) as determined by qRT-PCR. * indicates significant difference with the Col wild type.*
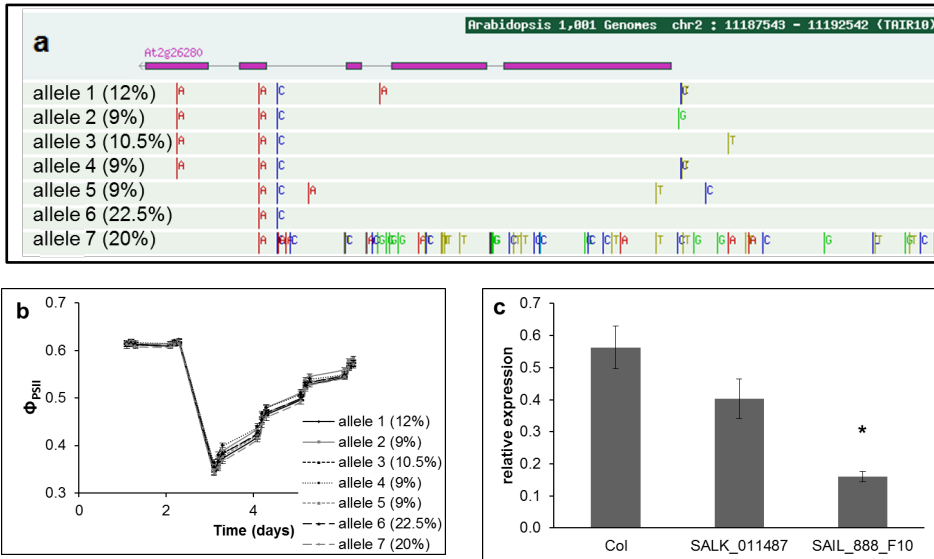
Figure S3. Characterization of natural alleles of DGS1

(a) Overview of haplotype alleles and frequencies for the DGS1 gene (AT5G12290), gene orientation is 3' to 5', SNPs differing from the Col-0 reference genome sequence (not indicated) are marked; **(b)** average photosynthesis efficiencies (Φ_{PSII}) (±SE) of the seven haplotype alleles before and after an increase in radiance at the onset of day 3, only allele 7 responds statistically significantly different from the other alleles; **(c)** In a quantitative complementation analysis, alleles 5 and 7 respond similarly regarding Φ_{PSII} in F1 plants upon crossing appropriate accessions with Col wild type or with T-DNA insertion mutant line SAIL_391_F04.
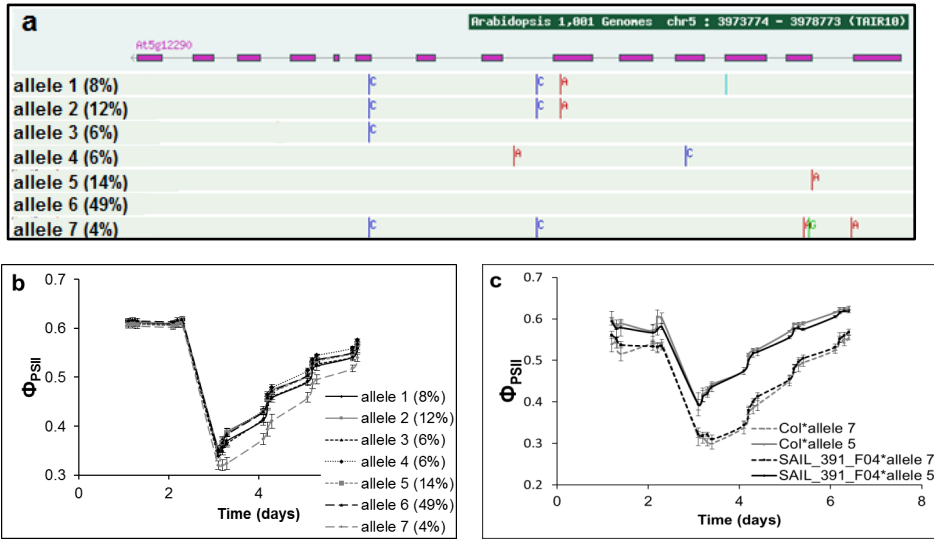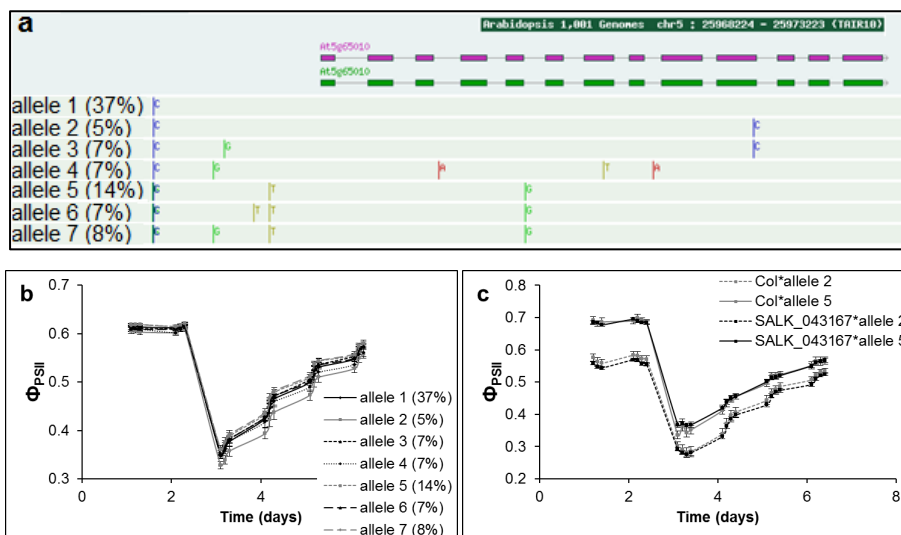
Figure S4. Characterization of natural alleles of ASN2

(a) Overview of haplotype alleles and frequencies for the ASN2 gene (AT5G65010), gene orientation is 5' to 3', SNPs differing from the Col-0 reference genome sequence (not indicated) are marked; (b) average photosynthesis efficiencies (Φ_{PSII}) (±SE) of the seven haplotype alleles before and after an increase in radiance at the onset of day 3, only allele 2 responds statistically significantly different from the other alleles; (c) In a quantitative complementation analysis, alleles 2 and 5 respond similarly regarding Φ_{PSII} in F1 plants upon crossing appropriate accessions with Col wild type or with T-DNA insertion mutant line SALK_043167.
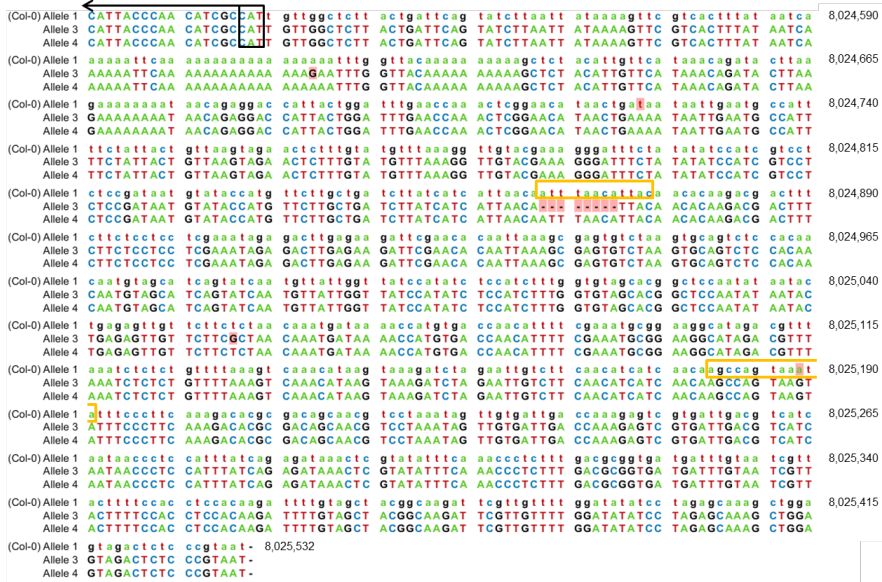
Figure S5. Genomic DNA sequence of the promoters of YS1 alleles 1, 3 and 4.

YS1 promoter sequence alignment (sequence is indicated 3' to 5', as YS1 is positioned in reverse orientation on chromosome 3 between 8021229 - 8024534 bp). The ATG-start codon is indicated with an arrowed box, with the arrow indicating the direction of translation. Polymorphisms are highlighted in pink. The yellow boxes indicated potential GT-1 binding sites (in opposite orientations relative to each other).

Chapter 4

Photosynthetic response to increased irradiance is mediated through heat shock response and lipid membrane remodelling

Roxanne van Rooijen[1,2], Jeremy Harbinson[2], Mark G.M Aarts[1]

[1]Laboratory of Genetics & [2]Horticulture and Product Physiology, Wageningen University, Droevendaalsesteeg 1, 6708 PB Wageningen, The Netherlands

ABSTRACT

Plants have evolved several mechanisms for sensing increased irradiance; they are known to sense it using several classes of photoreceptors (phototropins, phytochromes and cryptochromes), and to sense it through biochemical (reactive oxygen species, ROS) and metabolic signals. This results in the activation of heat shock genes and the activation of the transcription factor LONG HYPOCOTYL 5 (HY5, mediated by the cryptochrome photoreceptor 1, CRY1). Here we show the existence of another gene expression response pathway in Arabidopsis. This pathway starts with the SPX1-mediated activation of the transcription factor PHR1 and leads to the activation of several galactolipid biosynthesis genes. Gene expression analysis of accessions Ga-0 and Ts-1, with contrasting phenotypes for response to increased irradiance, showed stronger activation of heat responsive genes in Ga-0 and the opposite in Ts-1, when compared to Col-0, in line with the differences in the efficiency of photosynthesis. Furthermore, the SPX1/PHR1-mediated gene activation pathway acting on galactolipid biosynthesis genes was found to be active in Ga-0 as well as Col-0, but not in Ts-1, contributing to the difference between both accessions with contrasting increased irradiance response phenotypes.

INTRODUCTION

The light-use efficiency of photosynthesis depends on the molecular, structural and physiological state of the plant (Eberhard et al., 2008; Zhu et al., 2008; Foyer et al., 2012). The physiological state of the plant depends on many environmental factors, of which the level of irradiance has a direct relation with photosynthesis light-use efficiency as it is the driving force for photosynthesis. At low irradiances, photosynthesis is fully light-limited and photosynthetic light-use efficiency is maximal. At irradiances above the light-limiting level, light-use efficiency decreases with increasing irradiances, resulting in the overall phenomenon of light-saturation of photosynthesis at elevated irradiances (Long et al., 1994; Sinclair and Muchow, 1999). The decrease in light-use efficiency from its maximum under wholly light-limiting conditions implies that irradiance exceeds the capacity for photosynthetic metabolism (Long et al., 1994). A consequence of increased irradiance is an increase in the rate of damaging side reactions of photosynthesis that occurs as a result of the reactive nature of many intermediates formed (Vass, 2012). Reactive oxygen species (ROS), mainly singlet oxygen ($O^{\cdot}$), superoxide (O_2^-) and hydrogen peroxide (H_2O_2), are the most conspicuous damaging by-products of photosynthesis (Asada, 2006; Vass, 2012). The stress response of photosynthesis appears to reduce the formation of ROS, especially under high growth irradiances (Scheibe et al., 2005; Suzuki et al., 2012). The state of the photosynthesis apparatus – its composition, organisation and regulation – is thus under complex control that operates at the physiological and molecular levels. An increase in irradiance, leading to excess, will initially provoke a rapid physiological response, including q_E type quenching and increased CO_2 fixation activity (Demmig-Adams and Adams, 1992; Niyogi, 1999; Li et al., 2009). If persistent this increased irradiance will result in longer term acclimation of the photosynthetic apparatus, obvious on both transcript and protein level (Walters, 2005; Li et al., 2009). Different species and genotypes display different capacities to acclimate their photosynthetic apparatus to an irradiance increase so it is reasonable to infer that this is at least partly genetically determined (Van Rooijen et al., 2015).

An increase in irradiance brings about changes not only in photosynthesis, but also in leaf temperature and photoreceptor activity (Larcher, 2003). The transcriptome changes provoked by an increase in irradiance are therefore complex, part of them caused by the temperature increase rather than the irradiance increase (Swindell et al., 2007). Increased irradiance and increased temperature together induce a stress response by activation of heat shock proteins and the generation of ROS originating from the

chloroplast, the latter of which is required for the photosynthetic acclimation response to excess light (Rossel et al., 2002; Vanderauwera et al., 2005; Jung et al., 2013).

In addition to the increased temperature and the induced generation of ROS, plants detect increases in the irradiance level through their cryptochrome photoreceptors (Kleine et al., 2007). Of the two distinct plant cryptochromes in *Arabidopsis thaliana* (Arabidopsis) (CRY1 and CRY2), only CRY1 responds to increases in irradiance by initiating a transcriptional response mediated by the transcription factor LONG HYPOCOTYL 5 (HY5), (Kleine et al., 2007; Lee et al., 2007).

The gene expression response to increased irradiance initiated by the heat shock factors and the response initiated via the HY5 transcription factor are considered to be two distinct gene activation pathways, distinct both in function and in time (Yamamoto et al., 2004). The heat shock factors are thought to induce a direct response to cope with the ROS that are already formed; whereas the HY5-induced gene expression responds slower, and is thought to function in protecting the cells from newly formed ROS.

All transcriptome studies of Arabidopsis that analysed the response to increased irradiance so far, have used the Col-0 accession. This study includes additional, natural, accessions of Arabidopsis with contrasting photosynthesis responses to increased irradiance (Van Rooijen et al., 2015), to reveal which common and genotype-specific transcriptional responses are associated with differences in acclimation of photosynthesis efficiency. In addition, analysing different time-points within one study allows identification of transient expression patterns throughout the acclimation response.

MATERIALS AND METHODS

Plant material and growth conditions

Three Arabidopsis accessions, Columbia-0 (Col-0, CS76113), Gabelstein-0 (Ga-0, CS76133) and Tossa de Mar-1 (Ts-1, CS76268), were grown as previously described (Van Rooijen et al., 2015). In short, the plants were grown on rockwool in a 10h/14h day/night cycle, with the temperature set at 20/18°C (day/night), and relative humidity set at 70%. CO_2 levels were ambient. Under controlled conditions, plants in the light were kept at a constant irradiance of 100 µmol m^{-2} s^{-1} (Philips 610 fluorescent tubes, MASTER TL5 HO, 80W). In the increased irradiance treatment, the irradiance was increased to 550 µmol m^{-2} s^{-1} at the onset of the photoperiod on the 25th day after sowing. In the increased temperature treatment, the irradiance was kept at 100 µmol m^{-2} s^{-1}, but the temperature was increased from 20°C to 30 °C during the day. Photosynthesis efficiency was measured as previously described (Van Rooijen et al., 2015).

RNA sample preparation

On the 25th day after sowing, rosettes of plants were harvested 1 hour (1h) after the start of the photoperiod and flash-frozen in liquid nitrogen. Only for the Col-0 accession this was repeated at 3.5 hours (3.5h) after the start of the photoperiod, as well as one day later, at 1 hour after the start of the photoperiod, so 25 hours (25h) after increasing the irradiance to 550 µmol m^{-2} s^{-1}. Three rosettes for each accession-treatment combination were pooled as one sample for RNA isolation, in three replications.

Total RNA was extracted using the Direct-zol RNA mini prep kit from Zymo Research (www.zymoresearch.com). The RNA quality control, labelling, microarray hybridization and data extraction were performed at ServiceXS B.V. (part of GenomeScan B.V., Leiden, The Netherlands). The RNA concentration was measured using a DropSense96 spectrophotometer (Trinean N.V., Gentbrugge, Belgium). The RNA quality and integrity was determined using Lab-on-Chip analysis on the Agilent 2100 BioAnalyzer (Agilent TEchn9ologies, Inc., Santa Clara, CA, U.S.A.). Single-strand-cDNA (ss-cDNA) was prepared using the Ovation® PicoSL WTA System V2 (NuGEN Technologies, Inc., San Carlos, CA, U.S.A.) according to the manufacturer's specifications, with an input of 50 ng total RNA. Labelling and fragmentation of the ss-cDNA was performed with the Encore^{TM} Biotin Module (NuGEN Technologies, Inc., San Carlos, CA, U.S.A.).

Microarray hybridization, scanning and data analysis

Per sample, 2.5 µg of the labeled ss-cDNA was hybridized onto an AraGene 1.1ST Array plate (Affymetrix, Santa Clara, CA, U.S.A.). Hybridization and scanning was performed on a GeneTitan (Affymetrix, Santa Clara, CA, U.S.A.). Image analysis and extraction of raw expression data was performed with the Affymetrix Expression Console[TM] v1.2.1. with "Gene-level Default: RMA-Sketch" settings. Raw data were analysed using the Bioconductor packages in the statistical programming language R (http://www.r-project.org/)(Gentleman et al., 2004). The microarray oligonucleotide probe data were gene annotated using the TAIRT v19 cdf file (http://brainarray.mbni.med.umich.edu/Brainarray/Database/CustomCDF/19.0.0/tairt.asp) and gene expression was normalized using the Robust Multi-array Average (RMA) algorithm (Irizarry et al., 2003), after which a linear model was fitted for every gene. The empirical Bayes method was used to determine significant differences between the samples and the Benjamini and Hochberg method was used for adjustment of the P values for multiple testing (Benjamini and Hochberg, 1995; Efron and Tibshirani, 2002).

Quantitative Reverse Transcription PCR (qRT-PCR)

In a separate experiment, but with identical experimental set-up as used for the microarray experiment, rosettes were likewise harvested, on the 25th day after sowing, for all accession-treatment combinations at 1 and 3.5 h after the start of the photoperiod, and immediately frozen in liquid nitrogen. Three rosettes for each accession-treatment combination were pooled as one sample for RNA isolation, in three replications. RNA was extracted according to Onate-Sánchez and Vicente-Carbajosa (2008). After normalization of RNA concentrations, cDNA was synthesized using the Iscript cDNA synthesis kit from Bio-RAD (www.bio-rad.com). qRT-PCR was performed with three technical replicates for each biological replicate using the SYBR-green mastermix from Bio-RAD. Three reference genes were used for normalization: *UBIQUITIN7* (*UBQ7,* At2g35635), *CYTOCHROME B5 ISOFORM E* (*CB5E,* At5g53560), and *UBIQUITIN THIOESTERASE* (At1g28120), based on previous report. Expression levels of *UBQ7* and *CB5E* were previously found to be constant under excess light (Jung et al., 2013; Wunder et al., 2013), and expression levels of *UBIQUITIN THIOESTERASE* were previously found to be stable in several genome-wide expression studies involving irradiance changes (Genevestigator database (Hruz et al., 2011), https://genevestigator.com/gv/). The primers used for qRT-PCR are listed in Table S7.

RESULTS

Heat shock response and RNA binding protein genes are among the core group of genes responding to an increase in irradiance

Three Arabidopsis accessions, Col-0, Ga-0 and Ts-1, were grown for 25 days under 100 µmol m^{-2} s^{-1} growth irradiance (low light, LL), and then shifted to an increased irradiance (550 µmol m^{-2} s^{-1}, high light, HL), a condition which saturates photosynthesis (Van Rooijen et al., 2015). Upon exposure to increased irradiance, the accessions show different photosynthesis efficiencies, as determined by measuring ΦPSII (the light-use efficiency of photosystem II (PSII) electron transport, also known as Fq'/Fm') (Fig. 1A). A rosette transcriptome analysis was performed for these accessions to identify a core set of genes of which the response associates with increased photosynthesis efficiency. This analysis will also be used to identify accession-specific responses. In addition, a time-series transcriptome analysis was performed, for Col-0 only, to investigate the effect of diurnal rhythm on gene expression.

The effect of the genotype is larger than the time effect, although both can be distinguished from control experiments (Fig. 1B). Genes that were statistically significantly more than 1.4-fold up- or down-regulated after the increased irradiance treatment compared to the control treatment were identified (Fig. 2), which we will further refer to as 'responsive genes'.
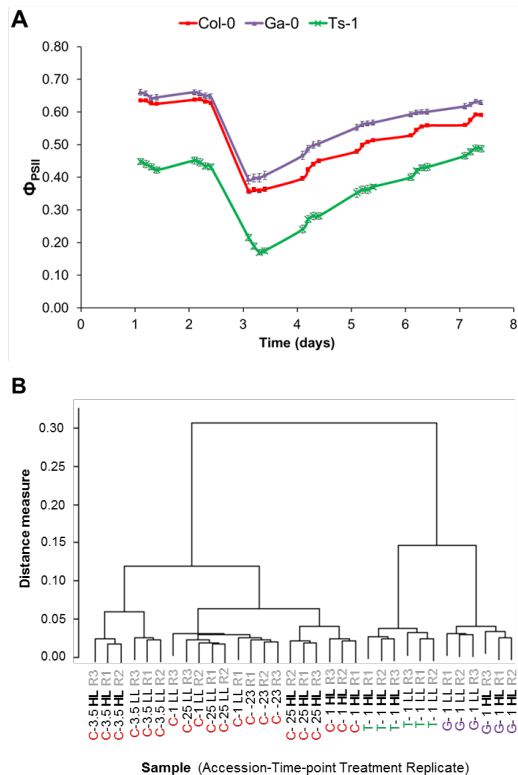
Figure 1. Genotypic effect on photosynthetic response to increased irradiance

(A) Representative photosynthetic (Φ_{PSII}) phenotypes for Arabidopsis accessions Col-0, Ts-1 and Ga-0, grown for 24 days in 100 µmol m^{-2} s^{-1} growth irradiance and subsequently 6 days in 550 µmol m^{-2} s^{-1} growth irradiance, measured from day 23 (first day of measurement) until day 31, at four time-points per day; (B) Dendrogram on Pearson distance measure between microarray-based transcriptome data representing gene expression in rosettes of Arabidopsis accessions Col-0, Ts-1 and Ga-0 exposed to low light (LL; 100 µmol m^{-2} s^{-1} growth irradiance) control conditions or increased irradiance (high light, HL; 550 µmol m^{-2} s^{-1} growth irradiance), sampled at 1h, 3.5h, and 25h after lights on (control, LL) or after the switch to increased irradiance (HL), in three experimental replicates (R1, R2 and R3).

A total of 752, resp. 440 genes was more than 1.4-fold up- or down-regulated, when compared to untreated plants, in at least one of the three accessions one hour after the irradiance increase from 100 to 550 µmol m^{-2} s^{-1} (Fig. 2A). Of these responsive genes, 161 up-regulated and 59 down-regulated genes were shared among all three accessions (Fig. 2A). A total of 1664, resp. 1356 genes was more than 1.4-fold up- or down-regulated, when compared to untreated Col-0 plants either at 1, 3 or 25 hours after the switch to increased irradiance (Fig. 2B). Of these responsive genes, 115 up-regulated genes and 120 down-regulated genes were responding at all time-points (Fig. 2B).
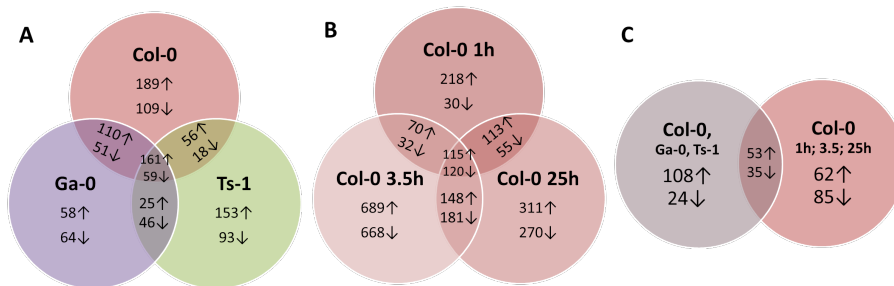108

Figure 2. Genotype- and time-specific gene expression response to increased irradiance

(A) Venn diagrams displaying the number of significantly (p=0.05) differentially (more than 1.4-fold up- or down-regulated) expressed genes when comparing rosettes of control plants (100 µmol m^{-2} s^{-1} growth irradiance) of three accessions (Col-0, Ga-0, or Ts-1) to those of plants one hour after exposure to increased irradiance (550 µmol m^{-2} s^{-1} growth irradiance); (B) Idem when comparing rosettes of control Col-0 plants (100 µmol m^{-2} s^{-1} growth irradiance) at 1 hour (h), 3.5 h or 25 h after lights on, to those of Col-0 plants at 1 h, 3.5 h or 25 h after exposure to increased irradiance (550 µmol m^{-2} s^{-1} growth irradiance); (C) Idem when comparing differentially expressed genes shared by all accessions (a) with those shared by all time-points in Col-0 (b).
Arrows indicate up- and down-regulation compared to controls.

In order to establish a core set of Arabidopsis genes constituting the general response to an increase in irradiance, the genes in common to both comparisons (i.e. accessions and time-points) were selected (Fig. 2C), meaning 53 up- and 35 down-regulated genes (Tables S1 and S2). Gene ontology analysis of this core set showed that heat shock response, photosynthesis and RNA binding were enriched processes among the up-regulated genes; while only modest enrichment for a genes involved in photosynthesis was found among the down-regulated genes (Fig. 3A). Figure 3B lists all genes classified in one of the enriched biological processes, and their expression difference when compared to control plants. Most prominent in terms of induced expression are the heat response genes, while most of the down-regulated genes show only modest down-regulation (Fig. 3B).

Comparing the fold changes of the core responsive genes between the three accessions (Ga-0, Ts-1, and Col-0) or between the three time-points (1, 3.5, and 25 hrs after exposure to irradiance increase) revealed differential responsiveness (e.g. 15-fold upregulated in Col-0, 1.8-fold in Ga-0, and 5-fold in Ts-1; where all are above 1.4-fold change, but 15-, 1.8- and 5-fold are significantly different from each other) between

accessions and/or time-points for some of the core genes (Tables S1 and S2). To distinguish if this differential responsiveness was high light specific or was common between the three accessions and/or three time-points, we selected the differentially responsive genes between accessions or between time-points that were not differentially expressed in control conditions and referred to those as high light specifically differentially responsive genes. Two, resp. 27, resp. 9 genes were found high light specifically differentially responsive between accessions, between time-points, or between both accessions and time-points (Tables S1 and S2). The two high light specifically responsive core genes up-regulated to different extent between accessions were *DEHYDRATION RESPONSIVE ELEMENT BINDING 2A (DREB2A)* and *SERINE-ARGININE RICH RNA BINDING PROTEIN 45a (SR45a)*, annotated to photosynthesis-related transcription factor activity and RNA alternative splicing, respectively (Fig. 3B and Table S1). The 27 high light specifically responsive core genes up-regulated to different extent between time-point or between both accessions and time-points were all heat shock response genes (Fig. 3B and Table S1). Given the annotations of these high light specific responsive core genes, we focussed on similar processes/functions when analysing the accession- and time-point-specific gene expression responses.

Figure 3 (on next page). Gene ontology and functional annotation of Arabidopsis rosette genes showing core transcriptional response upon exposure to increased irradiance.

(A) Gene ontology enrichment for biological process of Arabidopsis rosette genes differentially expressed at 1, 3.5 or 25 hrs after exposure to increased irradiance when compared to control plants, either when comparing accessions Ga-0, Ts1, and Col-0 or time-points (Col-0 only); (B) Heat map for fold changes in increased irradiance conditions versus control conditions of core genes with biological functions in photosynthesis (yellow highlighted), response to heat (grey highlighted), and RNA binding (green highlighted). Core genes are more than 1.4-fold up- or down regulated in all time-points and accessions. For the complete gene list see Supplementary Tables S1 and S2. G-1 = Ga-0 time-point 1h; T-1 = Ts-1 time-point 1h; C-1 = Col-0 time-point 1h; C-3.5 = Col-0 time-point 3.5h; C-25 = Col-0 time-point 25h.

A

up-regulated   down-regulated

Percentage

60 50 40 30 20 10 0

Biological process

carbohydrate metabolism · cell organization · DNA repair · electron transport · hypocotyl growth · leaf morphology · lipid transport · metal ion binding · microtubule motor activity · multicellular organism. dev. · oxidation-reduction process · photosynthesis · protein ubiquitination · phosphate biosynthesis · response to cadmium ion · response to drought · response to heat · RNA binding · trichome morphogenesis · vein patterning

B

Molecular function	Gene ID	Gene name	G1	T1	C1	C3.5	C25	Fold Change
chlorophyll binding/ flavon-oid biosynthesis	At3g22840	EARLY LIGHT-INDUCIBLE PROTEIN 1 (ELIP1)						HL vs LL
	At4g14690	EARLY LIGHT-INDUCIBLE PROTEIN 2 (ELIP2)						
H₂O₂	At1g07890	ASCORBATE PEROXIDASE 1 (APX1)						
	At4g31870	GLUTATHIONE PEROXIDASE 7 (GPX7)						
transcription factor activity	At2g20880	ERF/AP2 FAMILY, ETHYLENE RESPONSE FACTOR 53 (ERF53)						
	At4g28140	ERF/AP2, A6 FAMILY						
	At5g05410	ERF/AP2 FAMILY, DEHYDRATION RESPONSE ELEMENT BINDING 2A (DREB2A)						
	At5g07580	ERF/AP2, B3 FAMILY						
	At5g25190	ERF/AP2, B6 FAMILY						
	At5g44190	GOLDEN2-LIKE2 (GLK2)						
chaperones	At1g07400	HSP20-like chaperones superfamily protein						
	At1g53540	HSP20-like chaperones superfamily protein						
	At1g54050	HSP20-like chaperones superfamily protein						
	At1g59860	HSP20-like chaperones superfamily protein						
	At2g19310	HSP20-like chaperones superfamily protein						
	At2g29500	HSP20-like chaperones superfamily protein						
	At5g51440	HSP20-like chaperones superfamily protein						
	At2g46240	A member of Arabidopsis BAG (Bcl-2-associated athanogene)						
	At5g48570	Tetratricopeptide repeat (TPR) protein, interacts with Hsp90/Hsp70 as co-chaperones						
heat shock	At2g26150	HEAT SHOCK TRANSCRIPTION FACTOR A2 (HSFA2)						
	At4g36990	HEAT SHOCK FACTOR 4 (HSF4)						
heat shock	At1g74310	HEAT SHOCK PROTEIN 101 (HSP101)						
	At2g20560	DNAJ heat shock family protein						
	At2g25140	Casein lytic proteinase/heat shock protein 100 family.						
	At3g08970	J domain protein localized in ER lumen, shows similarity to HSP40 proteins						
	At3g12580	HEAT SHOCK PROTEIN 70 (HSP70)						
	At3g23990	HSP60; mitochondrial chaperonin HSP.						
	At3g46230	HEAT SHOCK PROTEIN 17.4 (HSP17.4)						
	At4g12400	Hop3, a tetratricopeptide repeat (TPR) protein, interacts with Hsp90/Hsp70						
	At4g25200	MITOCHONDR.-LOCALIZED SMALL HEAT SHOCK PROTEIN 23.6 (HSP23.6-MITO)						
	At5g09590	Heat shock protein 70 (Hsc70-5)						
	At5g12020	17.6 KDA CLASS II HEAT SHOCK PROTEIN (HSP17.6II)						
	At5g12030	HEAT SHOCK PROTEIN 17.6A (HSP17.6A)						
	At5g52640	HEAT SHOCK PROTEIN 90.1 (HSP90.1)						
unknown	At1g30070	unknown						
	At5g64510	TUNICAMYCIN INDUCED 1 (TIN1), a plant-specific ER stress-inducible protein						
alternative splicing	At1g07350	Serine-arginine rich RNA binding protein (SR45a) involved in alternative splicing						
	At1g09140	Serine-arginine rich RNA binding protein (SR30) involved in alternative splicing						
translation	At5g12110	Translation elongation factor EF1B/ribosomal protein S6						

Fold Change HL vs LL scale: 24, 22, 20, 18, 16, 14, 12, 10, 8, 6, 4, 2, 1, 0.9, 0.8, 0.7, 0.6, 0.5, 0.4, 0.3, 0.2, 0.1, 0

Differential expression in genes for heat shock response and lipid remodelling when comparing phenotypically contrasting accessions

 Accession-specific expression responses were characterized between three photosynthetically contrasting accessions to identify any associations between gene expression responses and photosynthesis efficiency responses to increased irradiance. A total of 752, resp. 440 genes was more than 1.4-fold up- or down-regulated, when compared to untreated plants, in at least one of the three accessions one hour after the irradiance increase from 100 to 550 $\mu mol \; m^{-2} \; s^{-1}$ (Fig. 2A). Of these 1192 responsive genes, 155 genes were identified as accession-specific responsive genes (Tables S3 and S4), meaning they were also differentially (P=0.05) responsive between two or three accessions when comparing Col-0, Ga-0 and Ts-1 (e.g. 15-fold upregulated in Col-0, 1.8-fold in Ga-0, and 5-fold in Ts-1). Of these 155 accession-specific responsive genes, 123 were found high light specifically differentially responsive between accessions (and not different between accessions independent of irradiance, Tables S3 and S4).
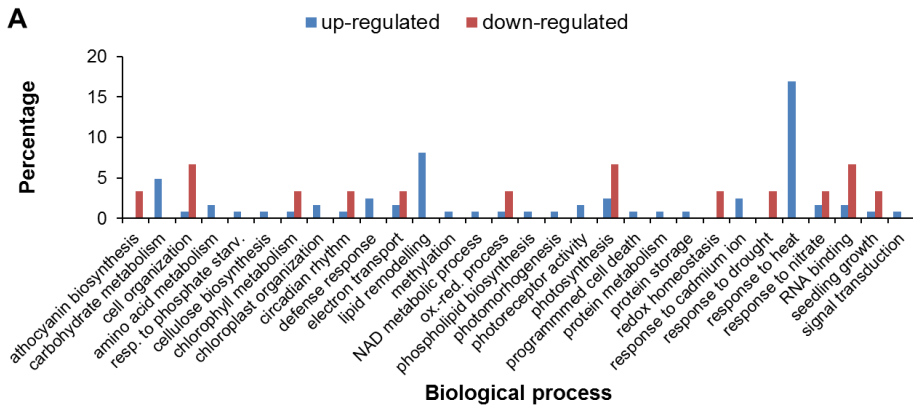
The up-regulated accession-specific responsive genes were enriched for the biological processes of heat shock response, lipid remodelling and photosynthesis (Fig. 4A). The down-regulated time-point-specific responsive genes were enriched for cell organization, photosynthesis response, and RNA binding (Fig. 4A). Figure 4B lists all genes classified in one of the enriched biological processes, and their expression difference when compared to control plants. Most prominent in terms of expression are the heat shock response genes (Fig. 4B).

Differential expression in genes for photosynthetic and heat shock response when comparing sequential time-points after increased irradiance in Col-0

Time-point-specific expression responses were characterized in Col-0 between three time-points after irradiance increase to identify transient expression patterns throughout the acclimation response and to study the effect of diurnal rhythms on gene expression response during long-term acclimation. A total of 1664, resp. 1356 genes was more than 1.4-fold up- or down-regulated, when compared to untreated Col-0 plants either at 1, 3 or 25 hours after the switch to increased irradiance (Fig. 2B). When comparing the fold changes of these 2785 responsive genes, 2280 genes were identified as time-specific responsive genes, meaning they were differentially (P=0.05) responsive between two or three time-points when comparing 1, 3.5, and 25 hours after irradiance increase (e.g. 15-fold upregulated at 1 hour and 1.8-fold at 3.5 hour after irradiance increase; at both time-

112

points classified above 1.4 but time-point-specifically). Increasing the threshold to 2.0 fold up- or down regulated to be more exlcusive resulted in 229, resp. 155 genes more than 2.0 fold up- or down-regulated (Supplementary Tables S5 and S6). Of these 384 time-specific responsive genes, 270 were found high light specifically differentially responsive between time-points (Tables S5 and S6).

The more than 2.0 fold up-regulated time-point-specific responsive genes were enriched for the biological processes of photosynthesis response, heat shock response, lipid remodelling, RNA binding and carbohydrate metabolism (Fig. 5A). The down-regulated time-point-specific responsive genes were enriched for cell organization, photosynthesis response, and lipid remodelling (Fig. 5A). Figure 5B lists all time-point-specific responsive genes classified in one of the enriched biological processes, and their expression difference when compared to control plants.

A

B

Molecular function	Gene ID	Gene name	G1	T1	C1
anthocyanin	At1g56650	PRODUCTION OF ANTHOCYANIN PIGMENT 1 (PAP1)			
photoprotection	At4g04020	Fibrillin precursor protein, involved in abscisic acid-mediated photoprotection			
NAD(H) kinase	At3g21070	NAD(H) kinase			
transcription	At2g20880	ERF/AP2 FAMILY, ETHYLENE RESPONSE FACTOR 53 (ERF53)			
	At4g25470	ERF/AP2 FAMILY, DREB subfamily A-1			
	At5g05410	ERF/AP2 FAMILY, DEHYDRATION RESPONSE ELEMENT BINDING 2A (DREB2A)			
	At5g61590	ERF/AP2, B3 FAMILY			
chaperones	At1g71000	Chaperone protein dnaJ-related			
	At2g46240	A member of Arabidopsis BAG (Bcl-2-associated athanogene) proteins			
	At3g13470	Subunit of chloroplasts chaperonins CHAPERONIN-60BETA2 (CPN60BETA2)			
	At5g43260	Chaperone protein dnaJ-related			
heat shock factor	At3g51910	HEAT SHOCK TRANSCRIPTION FACTOR A7 A (HSFA7A)			
heat shock protein	At1g53540	HSP20-like chaperones superfamily protein			
	At2g32120	Heat-shock protein 70T-2 (HSP70T-2)			
	At3g08970	J domain protein localized in ER lumen, shows similarity to HSP40 proteins			
	At3g46230	HEAT SHOCK PROTEIN 17.4 (HSP17.4)			
	At4g12400	Hop3, a tetratricopeptide repeat (TPR) protein, interacts with Hsp90/Hsp70			
	At4g25200	MITOCHONDRION-LOCALIZED SMALL HEAT SHOCK PROTEIN 23.6 (HSP23.6-MITO)			
	At5g09590	Heat shock protein 70 (Hsc70-5)			
	At5g37670	HSP20-like chaperones superfamily protein			
	At5g51440	HSP20-like chaperones superfamily protein			
	At5g56030	HEAT SHOCK PROTEIN 81-2 (HSP81-2)			
unknown	At1g03070	Apoptosis-promoting Bax inhibitor-1 family protein			
	At1g17870	ETHYLENE-DEPENDENT GRAVITROPISM-DEFICIENT AND YELLOW-GREEN-LIKE 3 (EGY3)			
	At1g66510	AAR2 protein family			
	At4g21320	heat-stress-associated 32-kD protein			
	At5g13200	GRAM domain family protein			
	At5g64510	TUNICAMYCIN INDUCED 1 (TIN1), a plant-speci-c ER stress-inducibl protein			
alternative splicing	At1g07350	Serine-arginine rich RNA binding protein (SR45a) involved in alternative splicing			
unknown	At2g18510	Embryo defective 2444 (emb2444)			
	At3g09160	RNA-binding (RRM/RBD/RNP motifs) family protein			
	At4g03110	unkown RNA binding protein			

Fold Change
HL vs LL

24
22
20
18
16
14
12
10
8
6
4
2
1
0.9
0.8
0.7
0.6
0.5
0.4
0.3
0.2
0.1
0

ascorbic acid synthesis	At1g67070	PHOSPHOMANNOSE ISOMERASE 2 (PMI2), also known as DARK INDUCED 9 (DIN9)			
mannose binding lectin protein	At1g78820	D-mannose binding lectin protein			
cell wall synthesis	At5g49360	a bifunctional {beta}-D-xylosidase/{alpha}-L-arabinofuranosidase			
sugar tansport	At5g57100	Nucleotide/sugar transporter family protein			
HY5 target, chloroplast	At5g23730	REPRESSOR OF UV-B PHOTOMORPHOGENESIS 2 (RUP2)			
	At5g52250	REPRESSOR OF UV-B PHOTOMORPHOGENESIS 1 (RUP1)			
lipid transfer	At2g38530	LIPID TRANSFER PROTEIN 2 (LTP2)			
MGDG	At2g11810	MONOGALACTOSYLDIACYLGLYCEROL SYNTHASE 3 (MGD3)			
	At5g20410	MONOGALACTOSYLDIACYLGLYCEROL SYNTHASE 2 (MGD2)			
phosphatase	At3g17790	PURPLE ACID PHOSPHATASE 17 (PAP17)			
phospholipid	At3g02040	GLYCEROPHOSPHODIESTER PHOSPHODIESTERASE 1 (GDPD1)			
SQDG synthesis	At4g33030	SULFOQUINOVOSYLDIACYLGLYCEROL 1			
	At5g01220	SULFOQUINOVOSYLDIACYLGLYCEROL 2			
transcription factor activity	At3g03790	Ankyrin repeat family protein / regulator of chromosome condensation			
unknown	At2g26660	SPX DOMAIN GENE 2 (SPX2)			
	At5g20150	SPX DOMAIN GENE 1 (SPX1)			
transcription	At4g00150	Belongs to one of the LOM (LOST MERISTEMS) genes			
transcription factor activity	At4g37180	Myb family transcription factor, contains Pfam domain			
unknown	At2g40610	Alpha-Expansin Gene Family. Inv. in the form. of nematode-induced syncytia in roots			

Figure 4. Gene ontology and functional annotation of Arabidopsis rosette genes showing accession-specific transcriptional response upon exposure to increased irradiance.

(A) Gene ontology enrichment for biological process of Arabidopsis rosette genes differentially (P=0.05) expressed at 1 hr after exposure to increased irradiance when comparing control plants with plants exposed to increased irradiance in minimal one accession and differentially (P=0.05) expressed between two or three accessions when comparing Ga-0, Ts1, and Col-0; (B) Heat map for fold changes in increased irradiance conditions versus control conditions of accession-specific responsive genes (P=0.05) with enriched biological functions photosynthesis (yellow highlight), response to heat (grey highlight), RNA binding (green highlight), carbohydrate metabolism (blue highlight), photoreceptor activity (pink highlight), lipid remodelling (light-green highlight), and cell organization (orange highlight). Accession-specific responsive genes are more than 1.4-fold up- or down regulated in minimal one accession measured 1h after irradiance increase and in addition are differentially (P=0.05) up- or down-regulated between two or three accession when comparing Ga-0, Ts1, and Col-0. Only enriched biological processes among these accession-specific responsive genes are presented, for complete list see Supplementary Tables S3 and S4. G-1 = Ga-0 time-point 1h; T-1 = Ts-1 time-point 1h; C-1 = Col-0 time-point 1h.

A

B
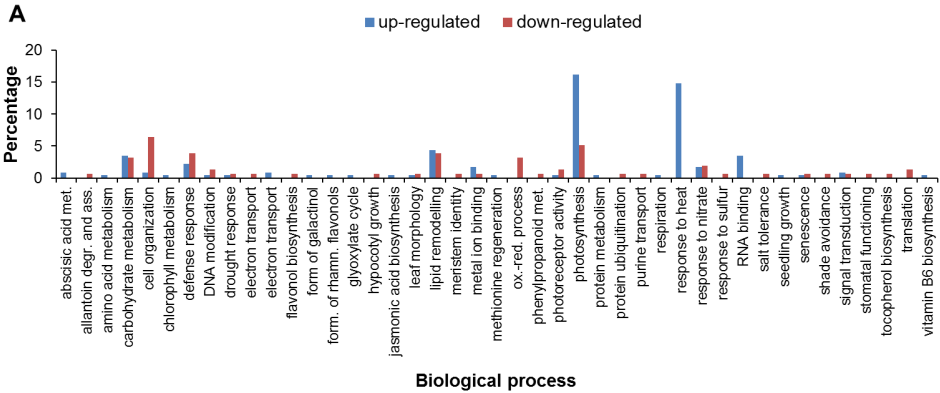
Molecular function	Gene ID	Gene name	C 1	C 3.5	C 2 5
chlorophyll binding	At3g22840	EARLY LIGHT-INDUCABLE PROTEIN (ELIP1)			
	At4g14690	EARLY LIGHT-INDUCIBLE PROTEIN 2 (ELIP2)			
chlorophyll biogenesis	At4g27440	light-dependent NADPH:protochlorophyllide oxidoreductase B			
chloroplast biogenesis	At1g69200	fructokinase-like protein			
	At3g54090	fructokinase-like protein			
chloroplast protein	At2g28900	involved in plastid import of protochlorophyllide oxidoreductase A			
	At3g13470	subunit of chloroplasts chaperonins			
chloroplast transcription/	At2g04530	protein with RNAse Z activity			
flavonoid biosynthesis	At2g23910	NAD(P)-binding Rossmann-fold superfamily protein			
	At2g24550	unknown protein			
	At3g29590	malonyl-CoA:anthocyanidin 5-O-glucoside-6"-O-malonyltransferase			
	At3g51240	flavanone 3-hydroxylase			
	At4g14090	anthocyanidin 5-O-glucosyltransferase			
	At4g22880	leucoanthocyanidin dioxygenase			
	At5g07990	Required for flavonoid 3' hydroxylase activity			
	At5g08640	FLAVONOL SYNTHASE 1 (FLS1)			
	At5g13930	chalcone synthase (CHS)			
	At5g17220	GLUTATHIONE S-TRANSFERASE PHI 12 (GSTF12)			
	At5g42800	dihydroflavonol reductase			
	At5g48880	peroxisomal 3-keto-acyl-CoA thiolase 2 precursor			
	At5g62210	Embryo-specific protein 3			
glucose:flavonoid glucosyl transferase	At5g54060	anthocyanin 3-O-glucoside			
H2O2 scavenging	At2g37770	NADPH-dependent aldo-keto reductase			
	At3g03630	protein that possesses S-sulfocysteine synthase activity			
	At4g31870	GLUTATHIONE PEROXIDASE 7 (GPX7)			
light harvesting	At2g34430	LIGHT-HARVESTING CHLOROPHYLL-PROTEIN COMPLEX II			
NAD metabolism	At5g14760	L-aspartate oxidase			
nutrient mobilization	At5g24770	VEGETATIVE STORAGE PROTEIN 2 (VSP2)			
	At5g24780	VEGETATIVE STORAGE PROTEIN 1 (VSP1)			
oxidation-reduction	At4g19170	similar to nine-cis-epoxycarotenoid dioxygenase			
photoprotection	At4g04020	Fibrillin precursor protein, involved in abscisic acid-mediated			
stomatal functioning	At5g22920	sequence similarity to RING, zinc finger proteins			
transcription factor	At1g27730	SALT TOLERANCE ZINC FINGER 10 (ZAT10)			
	At1g28370	ERF/AP2, B-1 family			
	At1g74930	ERF/AP2, DREB A-5 family			
	At2g20880	ERF/AP2, ERF53			
	At2g47460	MYB12			
	At4g17500	ERF/AP2, B-3 family			
	At5g05410	ERF/AP2 FAMILY, DEHYDRATION RESPONSE ELEMENT BINDING 2A (DREB2A)			
	At5g11590	ERF/AP2, DREB A-4 family			
	At5g25190	ERF/AP2, B-6 family			

Fold Change

HL vs LL

24
22
20
18
16
14
12
10
8
6
4
2
1
0.9
0.8
0.7
0.6
0.5
0.4
0.3
0.2
0.1
0

Category	Gene ID	Description
transferase activity	At5g44190	GOLDEN2-LIKE2 (GLK2)
	At5g59820	RESPONSIVE TO HIGH LIGHT 41 (RHL41)
	At1g54570	PHYTYL ESTER SYNTHASE 1 (PES1)
chaperone	At1g53540	HSP20-like chaperones superfamily protein
	At1g54050	HSP20-like chaperones superfamily protein
	At1g59860	HSP20-like chaperones superfamily protein
	At1g71000	Chaperone DnaJ-domain superfamily protein
	At2g46240	A member of Arabidopsis BAG (Bcl-2-associated athanogene) proteins
	At5g48570	tetratricopeptide repeat (TPR) proteins with potential to interact with Hsp90/Hsp70
	At5g56030	A member of heat shock protein 90 (HSP90) gene family
heat shock factor	At2g26150	HEAT SHOCK TRANSCRIPTION FACTOR A2 (HSFA2)
	At3g51910	HEAT SHOCK TRANSCRIPTION FACTOR A7A (HSFA7A)
	At4g36990	HEAT SHOCK FACTOR 4 (HSF4)
heat shock protein	At1g74310	belongs to the Casein lytic proteinase/heat shock protein 100
	At2g19310	HSP20-like chaperones superfamily protein
	At2g20560	DNAJ heat shock family protein
	At2g25140	belongs to the Casein lytic proteinase/heat shock protein 100 (Clp/Hsp100)
	At2g29500	HSP20-like chaperones superfamily protein
	At2g32120	heat-shock protein 70T-2 (HSP70T-2)
	At3g08970	J domain protein localized in ER lumen; similarity to HSP40 proteins
	At3g09350	Arabidopsis ortholog of the human Hsp70-binding protein 1 (HspBP-1)
	At3g25230	a high molecular weight member of the FK506 binding protein (FKBP) family
	At3g46230	HEAT SHOCK PROTEIN 17.4 (HSP17.4)
	At4g12400	Hop3, a tetratricopeptide repeat (TPR) protein, interacts with Hsp90/Hsp70
	At4g21320	heat-stress-associated 32-kD protein
	At4g25200	AtHSP23.6-mito mRNA
	At5g02490	Heat shock protein 70 (Hsp 70) family protein (Hsp70-2)
	At5g09590	heat shock protein 70 (Hsc70-5)
	At5g12030	HEAT SHOCK PROTEIN 17.6A (HSP17.6A)
	At5g37670	HSP20-like chaperones superfamily protein
	At5g51440	HSP20-like chaperones superfamily protein
	At5g52640	cytosolic heat shock protein AtHSP90.1
unknown	At1g30070	SGS domain-containing protein
	At1g66080	Unknown protein
	At5g13200	unknown
	At5g64510	TUNICAMYCIN INDUCED 1 (TIN1), a plant-speci-c ER stress-inducibl protein
alternative splicing	At1g07350	serine/arginine rich-like protein, SR45a
	At1g09140	serine/arginine rich-like protein, SR30
methyl transferase	At5g57280	Gene encodes a methyltransferase-like protein involved in pre-rRNA
organellar RNA editing	At3g22310	PUTATIVE MITOCHONDRIAL RNA HELICASE 1 (PMH1)
ribosome biogenesis	At1g15440	nucleolar protein that is a ribosome biogenesis co-factor
	At5g22100	RNA cyclase family protein
	At5g39850	Ribosomal protein S4
rRNA editing	At4g25630	encodes a fibrillarin directing 2'-O-ribose methylation of the rRNA
beta galactosidase	At5g63800	Involved in mucilage formation
beta-hexosaminidase	At1g65590	protein with beta-hexosaminidase activity
enzyme, pectin lyase	At1g48100	Pectin lyase-like superfamily protein
enzyme, alpha amylase	At1g76130	alpha-amylase, putative / 1,4-alpha-D-glucan glucanohydrolase
lectin family protein	At5g03350	Legume lectin family protein
nodulin family protein	At3g28007	SWEET4; a nodulin MtN3 family protein
starch degradation	At4g09020	isoamylase-like protein
	At4g15210	cytosolic beta-amylase
	At4g17090	beta-amylase targeted to the chloroplast
sucrose-proton symporter	At1g71880	Sucrose transporter
transporter	At5g13170	member of the SWEET sucrose efflux transporter family
transporter glucose6-phosphate	At1g61800	glucose6-Phosphate/phosphate transporter 2 (GPT2)
unknown	At4g23820	Pectin lyase-like superfamily protein
HY5 homologue	At3g17609	Encodes a homolog of HY5 (HYH). Involved in phyB signaling pathway.
phytochrome signalling	At5g04190	phytochrome kinase substrate 4

Function	Gene ID	Description
unknown	At1g18810	phytochrome kinase substrate-related
glycosyl transferase	At1g32900	GRANULE BOUND STARCH SYNTHASE 1 (GBSS1)
hydrolase activity	At1g58520	RXW8; functions in hydrolase activity, acting on ester bonds, lipase activity
lipid binding	At2g37870	Bifunctional inhibitor/lipid-transfer protein
	At2g42540	COLD-REGULATED 15A (COR15A)
	At2g45180	Bifunctional inhibitor/lipid-transfer protein
	At4g22490	Bifunctional inhibitor/lipid-transfer protein
	At5g48490	Bifunctional inhibitor/lipid-transfer protein
	At5g59320	LIPID TRANSFER PROTEIN 3 (LTP3)
lipid transport	At3g23080	Polyketide cyclase/dehydrate and lipid transport superfamily protein
MGDG synthesis	At5g20410	MONOGALACTOSYLDIACYLGLYCEROL SYNTHASE 2 (MGD2)
SQDG synthesis	At4g33030	SULFOQUINOVOSYLDIACYLGLYCEROL 1 (SQD1)
	At5g01220	SULFOQUINOVOSYLDIACYLGLYCEROL 2 (SQD2)
phospholipid catabolism	At3g02040	GLYCEROPHOSPHODIESTER PHOSPHODIESTERASE 1 (GDPD1)
transferase activity	At1g09390	GDSL-motif esterase/acyltransferase/lipase
	At3g16370	GDSL-motif esterase/acyltransferase/lipase
unknown	At5g20150	SPX DOMAIN GENE 1 (SPX1)
acetylesterase	At1g57590	Pectinacetylesterase family protein
alpha expansin	At1g69530	Alpha-Expansin Gene Family. Inv. in the form. of nematode-induced
	At2g40610	Alpha-Expansin Gene Family. Inv. in the form. of nematode-induced syncytia in roots
auxin transport	At2g01420	Encodes PIN-FORMED 4 (PIN4), a putative auxin efflux carrier
	At2g38120	Encodes an auxin influx transporter
cellulose synthase	At4g23990	encodes a protein similar to cellulose synthase
fatty acid biosynthetic	At1g01120	3-ketoacyl-CoA synthase 1 (KCS1), inv. in fatty acid elongation process
hydrolase activity	At4g32940	a vacuolar processing enzyme, cysteine proteinase associated with
microtubule	At4g16520	autophagy 8f (ATG8F)
	At4g20260	Encodes a Ca2+ and Cu2+ binding protein.
transcription factor	At4g00150	Belongs to one of the LOM (LOST MERISTEMS) genes
transferase activity	At4g03210	encodes a member of xyloglucan endotransglucosylase/hydrolases

Figure 5. Gene ontology and functional annotation of Arabidopsis Col-0 rosette genes showing time-point-specific transcriptional response upon exposure to increased irradiance.

(A) Gene ontology enrichment for biological process of Arabidopsis Col-0 rosette genes differentially (P=0.05) expressed after exposure to increased irradiance when comparing control plants with plants exposed to increased irradiance at minimal one time-point and differentially (P=0.05) expressed between two or three time-points when comparing 1, 3.5 and 25 hrs after exposure to increased irradiance; (B) Heat map for fold changes in transcription when comparing increased irradiance conditions versus control conditions of time-specific responsive genes (P=0.05) with enriched biological functions photosynthesis (yellow highlight), response to heat (grey highlight), RNA binding (green highlight), carbohydrate metabolism (blue highlight), photoreceptor activity (pink highlight), lipid remodelling (light-green highlight), and cell organization (orange highlight). Time-specific responsive genes are more than 2.0-fold up- or down regulated in minimal one time-point after irradiance increase in Col-0 increase and in addition are differentially (P=0.05) up- or down-regulated between two or three time-points when comparing 1, 3.5 and 25 hrs after exposure to increased irradiance. Only enriched biological processes among these time-specific responsive genes are presented, for complete list see Supplementary Tables S5 and S6. C-1 = Col-0 time-point 1h; C-3.5 = Col-0 time-point 3.5h; C-25 = Col-0 time-point 25h. The colour-scale is similar to figures 3 and 4.

Light response versus heat response

In order to distinguish between the direct effects of an increase in irradiance and the indirect effect caused by the increase in temperature due to the increased irradiance, the expression of nine genes, selected from the classes of differentially expressed genes with enriched biological functions (Fig. 3, 4 and 5), was determined using quantitative reverse transcriptase PCR (qRT-PCR). For this experiment, plants were grown at either increased irradiance or increased temperature but no increased irradiance, conditions, and compared to plants grown under control conditions (no increased irradiance, no increased temperature). Of the core genes we selected two genes involved in RNA binding (*SR45a* [At1g07350] and *SR30* [At1g09140]) to compare their expression under these conditions (Fig. 6). The up-regulation of *SR45a* and *SR30* in response to excess light was observed for Col-0 and Ga-0 at 1 h after lights on, but not in Ts-1 and not after 3.5 h after lights on in either accession. Both genes were also induced by increased temperature, not significantly different from the induction by increased irradiance.

Another core responsive gene encodes for the transcription factor GLK2 (At5g44190), which was down-regulated upon increased irradiance (Fig 3.). Both Col-0 and Ga-0 showed a down-regulation of *GLK2*, at 1h after the irradiance increase, but not after the temperature increase (Fig. 6C). After 3.5 hours *GLK2* was found to be up-regulated in Col-0 in response to an irradiance increase, but not to a temperature increase. Expression of *GLK2* in Ts-1 was unaltered when comparing treatments.

Figure 6 (on next page). Expression of genes selected for their response to increased irradiance to distinguish response to increase irradiance and response to increased temperature

Expression differences measured as fold changes (average ± SE) upon qRT-PCR analysis, of genes selected for their specific response based on the microarray analysis, determined at 1 h (1H; orange) and 3.5 h (3.5H; red) after an irradiance increase from 100 to 550 $\mu mol\ m^{-2}\ s^{-1}$ (HL), as well as 1 h (light blue) and 3.5 h (dark blue) after a temperature increase from 20 to 30°C (HT), compared to control conditions, 1 h after lights on; (A) SR45a [At1g07350]; (B) SR30 [At1g09140]; (C) GLK2 [At5g44190]; (D) HSFA2 [At2g26150]; (E) HOP3 [At4g12400]; (F) CPN60beta2 [At3g13470]; (G) SPX1 [At5g12150]; (H) GDPD1 [At3g02040]; (I) DREB2A [At5g05410]. Letters indicate statistically significant differences as determined by analysis of variance (P<0.05).
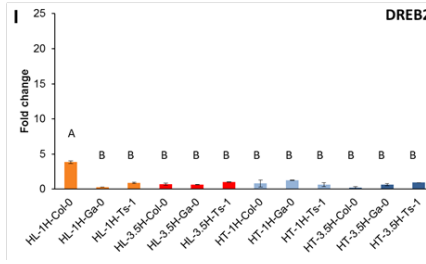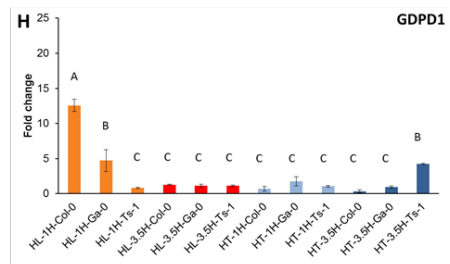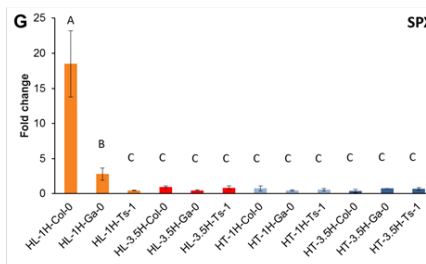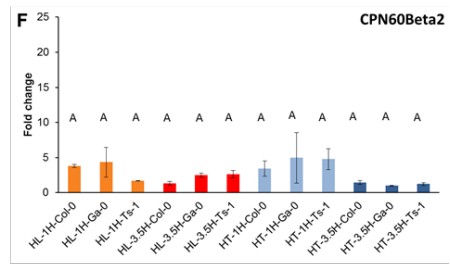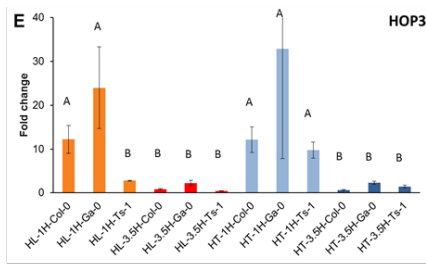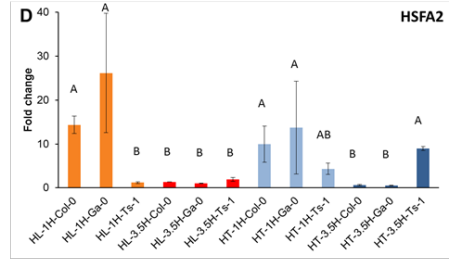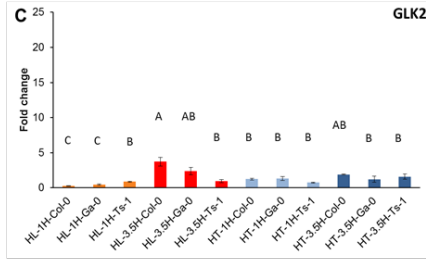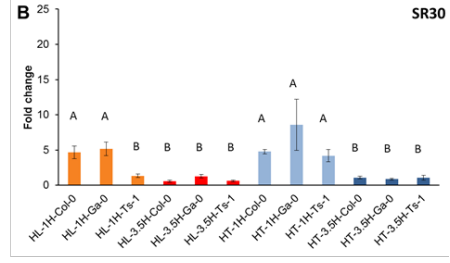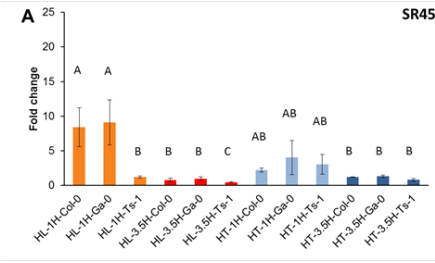
The largest group among both the core as well as accession-specific responsive genes were heat shock response genes (Fig. 3A). Three of these genes were selected for further analysis, *HSFA2* [At2g26150]), up-regulated in all accessions; *HOP3* [At4g12400]), most upregulated in Col-0; and *CPN60BETA2* [At3g13470], up-regulated only in Col-0 and Ga-0. *HSFA2* was confirmed to be induced 1 h after both the irradiance increase and the temperature increase in both Col-0 and Ga-0, but only after 3.5 h after temperature increase in Ts-1 (Fig. 6D). Expression of *HOP3* was confirmed by qRT-PCR to be increased one hour after the irradiance increase as well as after temperature increase for Col-0 and for Ga-0, though after temperature increase the expression of *HOP3* was induced in Ts-1 similarly as in Col- 0 and Ga-0 (Fig. 6E). In all accessions the activation of *HOP3* had significantly reduced by 3.5 hours after the induction of any stress treatment. Expression of *CPN60Beta2* was not confirmed by qRT-PCR to be up-regulated in response to irradiance increase (Fig. 6F).

Another biological process enriched among the accession-specific responsive genes is classified as lipid remodelling (Fig. 4A and 5A). Two genes (*SPX1* [At5g12150] and *GDPD1* [At3g02040]) were selected for further analysis. qRT-PCR showed that expression of *SPX1* was strongly activated in Col-0 and to lesser extent in Ga-0 during the first hour after the irradiance increase (Fig. 6G). Similar results were found for *GDPD1*, except for an increase in *GDPD1* expression for Ts-1 after 3.5 hours of exposure to high temperature (Fig. 6H).

The transcription factor DREB2A [At5g05410] is well known for its response to drought, but is also known to be heat responsive (Sakuma et al., 2006). It was found among the accession-specific responsive genes (Fig. 4B), and was selected to further analyse its expression response to excess light and to a temperature increase without a light increase. qRT-PCR confirmed that expression was increased only in Col-0 in the first hour of the irradiance increase, but not after only temperature increase (Fig. 6I).

Of the nine genes selected for qRT-PCR confirmation of the microarray results, eight were confirmed to be responsive to increased irradiance (Fig. 6). Of these eight confirmed genes, four genes (*GLK2, SPX1, GDPD1,* and *DREB2*) were found to be irradiance increase specific and not to be responsive to temperature increase only (Fig. 6). All of these four genes were accession-specifically responsive, with an absent response in Ts-1 for all four genes. The four genes responsive to both irradiance and temperature increase (*SR30, SR45a, HSFA2*, and *HOP3*) were accessions-specific as well, with also for these genes an absent response in Ts-1. For *SR30, SR45a, HSFA2*,

and *HOP3,* the accession-specific effect was more pronounced after irradiance increase than after temperature increase (Fig. 6).

DISCUSSION

This study investigated whether association of increases in Φ_{PSII} with time following an increase in growth irradiance (Fig. 1A) with gene expression patterns (Fig. 2A) in natural accessions of Arabidopsis would reveal which gene responses are associated with high photosynthesis efficiency acclimation. In addition, analysing different time-points in Col-0 within one study (Fig. 2B) would allow identification of transient expression patterns throughout the acclimation response. A core set of Arabidopsis genes was established by selecting the core responsive genes in common to both comparisons (i.e. accessions and time-points, Fig. 2C), constituting the general response to an increase in irradiance.

Transient gene expression through time reveals photosynthetic acclimation

Plants have evolved three mechanisms for sensing increased irradiance. This can be through several classes of photoreceptors (phototropins, phytochromes and cryptochromes), responding to irradiance levels directly; but also through biochemical signals (reactive oxygen species, ROS); and metabolic signals (sugar levels or protein phosphorylation status), (Li et al., 2009). Our study reveals gene expression responses in all three sensing mechanisms (Fig. 7A). It confirms the photoreceptor response mediated through the CRY1/HY5 genetic regulators leading to induced expression of many flavonoid biosynthesis genes (Fig. 5B) (Vanderauwera et al., 2005; Kleine et al., 2007); it confirms the biochemical response mediated through heat shock factors leading to induced expression of ROS scavenging genes (Fig. 5B); and it confirms the metabolite response through the up-regulated ERF/AP2 transcription factor family (Fig. 5B), known to sense distorted metabolite levels in response to increased irradiance, leading to systemic induced acclimation (Rossel et al., 2007; Moore et al., 2014; Vogel et al., 2014). In addition, it identifies another increased irradiance response, sensing distorted internal phosphate metabolite levels leading to induced expression of membrane lipid remodelling genes (Fig. 7B).

Photosynthetic acclimation is known to occur in several phases. Around three hours after the irradiance increase the initial photoprotection response, provoking a rapid physiological response, including q_E type quenching and increased CO_2 fixation activity (Demmig-Adams and Adams, 1992; Niyogi, 1999; Li et al., 2009), will be replaced by the more long-term photoacclimation response, leading to a change in the composition of mesophyll cells in terms of their proteins, lipids, pigments, and other cofactors involved in electron transport and reactive-oxygen species metabolism (Bailey et al., 2004; Walters, 2005). This photosynthetic acclimation response involves alterations in photosynthetic

124

protein structures, and is thought to stay active over days (Walters, 2005). However, our study shows that gene expression levels the next day early morning (25 hours after increased irradiance) correlate better with gene expressions one hour after increased irradiance (considered to be within the photoprotection response) than with gene expressions at 3.5 hours after increased irradiance (considered to be after the switch to the photoacclimation response) (Fig. 1B). This suggests that the diurnal rhythm has more effect on plant gene expression than the effect of the increased irradiance. This effect of diurnal rhythms on photosynthetic gene expression can be explained by the importance of the interaction of the increased irradiance with the increased temperature. The light onset in the morning is followed by a temperature increase, causing the reappearance of differentially expressed heat responsive genes to re-occur on several mornings after the increased growth irradiance (Fig. 5B).
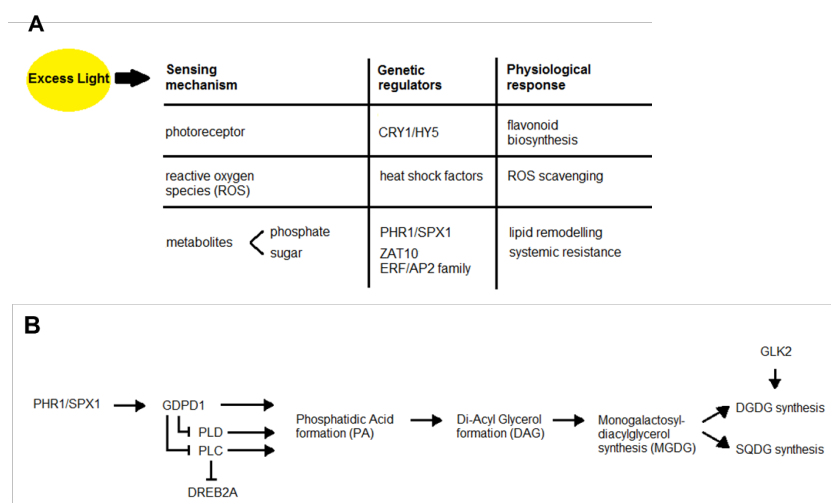
Figure 7. Model summarizing (A) the signal transduction pathways leading to transcriptional responses upon increased irradiance; and (B) the signal transduction pathway leading to phosphate deficiency dependent lipid remodelling, for which several genes were found to be up-regulated in response to increased irradiance.

CRY1 = CRYPTOCHROME 1; HY5 = LONG HYPOCOTYL 5; PHR1 = PHOSPHATE STARVATION RESPONSE 1; ZAT10 = SALT TOLERANCE ZINC FINGER 10; ERF/AP2 = ETHYLENE RESPONSE FACTOR/ APETALA2; SPX1 = SYG1, PHO81, AND XPR1 HOMOLOGUE 1; GDPD1 = GLYCEROPHOSPHO-DIESTER-PHOSPHO-DIESTERASE1; PLD = PHOSPHOLIPASE D; PLC = PHOSPHOLIPASE C; DREB2A = DEHYDRATION RESPONSE ELEMENT BINDING PROTEIN 2A; DGDG = DIGALACTOSYL DIACYLGLYCEROL; SQDG = SULFOQUINOVOSYL DIACYLGLYCEROL; GLK2 = GOLDEN-LIKE 2

From 3.5 h after the irradiance increase transcripts involved in RNA-binding are upregulated (Fig. 5), which will contribute to *de novo* protein synthesis, and is in line with the expression of new proteins as part of the acclimation response (Walters, 2005). Two genes regulating alternative splicing of many downstream RNAs are known to be up-regulated already within one hour after increased irradiance (*SERINE/ARGININE-RICH PROTEIN 45a* and *30 [SR45a* and *SR30]*) (Rossel et al., 2002; Tanabe et al., 2007). The observation that *SR45a* and *SR30* are up-regulated within one hour after increased irradiance suggests these genes are important regulators initiating a translational response of many genes that are induced in response to increase irradiance after 3.5 hours by alternatively splicing the mRNAs of these genes. In addition to the induced expression of many RNA-binding genes 3.5 h after the irradiance increase, these alternative splicing events contribute to the synthesis of new proteins, being part of the acclimation response (Walters, 2005). In our study, both *SR45a* and *SR30* are classified as core responsive genes, meaning they were responsive in all accessions and all time-points (Fig. 3B), although the subsequent qRT-PCR experiments showed there is some variation in the level of expression depending on accession and time-point (Fig. 4B, 5B, 6A, and 6B). *SR45a* was less up-regulated after a temperature increase compared to irradiance increase, the accession-specific effect was lost after temperature increase, and the increase in *SR45a* transcript was most obvious in the first hour after the irradiance increase (Fig. 6A and 6B), although both genes are up-regulated in increased irradiance conditions compared to control conditions also after 3.5 hours and after 25 hours (Fig. 5, 6A, and 6B). By regulating alternative splicing of many downstream genes, SR45a is an important regulator of the high light response. In an *sr45a* null mutant over 200 genes involved in signal transduction, regulation of transcription, protein turn-over and cell cycle regulation are altered in expression, with at least 10 of them through differences in alternative splicing (Yoshimura et al., 2011). SR30 has not been investigated in great detail yet, but the similarity in gene expression profile (Fig 6B) and the similarity in subcellular localization (Mori et al., 2012) suggests a similar biological function as for SR45a. Its early activation and its involvement in the regulation of expression of many transcriptional activators make it likely that SR45a (and possibly also SR30) initiates a gene responsive pathway activating photosynthetic acclimation in response to increased irradiance.

Photoreceptor response

Three types of photoreceptors are known to be involved in the response to increased irradiance: cryptochrome (CRY), phytochrome (PHY), and phototropin (PHOT), (Li et al.,

2009). The CRY1 photoreceptor is known to regulate a large number of genes in response to increased irradiance through the HY5 transcription factor (Kleine et al., 2007). *CRY, PHY*, or *PHOT* were not induced in any of the three accessions upon increased irradiance; nor did we see any induced transcription of *HY5*, suggesting regulation at the protein level. However, accession-specific increase in expression of two down-stream targets of HY5 was found (Fig. 4B), and a homologue of HY5 (*HY5 HOMOLOGUE [HYH]*) was found to be time-point-specific responsive (Fig. 5B). The function of HYH partially overlaps with that of HY5, and the accumulation of the HYH protein depends on the expression of HY5 (Holm et al., 2002) The increased expression of HYH together with two down-stream targets of HY5 confirms the involvement of the CRY1/HY5 response pathway. Two phytochrome signalling genes were down-regulated, one of which is *PHYTOCHROME KINASE SUBSTRATE 4 (PKS4),* a phytochrome signalling component involved in phototropism, phosphorylated in a PHOT1-dependent manner (Demarsy et al., 2012); the other a phytochrome kinase substrate-related protein with unknown molecular function (Fig. 5B). Together, these suggest a phytochrome-receptor response to increased irradiance mediating a phototropism response, not directly related to photosynthesis efficiency response.

Biochemical response

Two major biochemical signals are known to be responsive to increased irradiance, a pH-change within the chloroplast across the thylakoid membrane beginning within milliseconds after the induction of the irradiance increase (proton gradient dependent regulation) and and redox signals mediated via changes in the degree of thioredoxin reduction, the degree of plastoquinone reduction and increased formation of ROS (redox-dependent regulation). The redox changes are a result from combined irradiance- and temperature increases (Apel and Hirt, 2004). This combined irradiance and temperature effect causes activation of heat shock proteins and heat shock factors, initiating photosynthetic acclimation responses (Jung et al., 2013).

Using heat filters to block infrared light and thus reduce the heating effect that often accompanies and irradiance increase (Rossel et al., 2002), or by running parallel experiments with light and temperature increases and a temperature increase with no irradiance increase (as done in this study), it is possible to separate of the acclimation responses of an irradiance increase from those due to a temperature increase. We found most pronounced expression induction in response to increased irradiance of several genes encoding heat shock proteins and/or heat shock factors (Fig. 3), of which

some were accession-specifically (Fig. 4) and some time-point-specifically induced (Fig. 5). The expression of heat shock genes was least induced in Ts-1 (Fig. 4B), an observation that is in line with its observed low photosynthetic efficiency response to excess irradiance (Fig. 1A).

qRT-PCR confirmed the accession-specific expression response of *HSFA2* (Fig. 6D), a gene known to be associated with photosynthesis acclimation through the ascorbate peroxidase pathway (Jung et al., 2013) and the expression of *HOP3* (Fig. 6E). HOP3 is known to assist in undamaged import of photosynthetic pre-proteins synthesized outside the chloroplast by interacting with HSP70 and HSP90 (Fellerer et al., 2011). Both *HSFA2* and *HOP3* were induced in Ga-0 and Col-0, but not Ts-1, again in line with the differences found in photosynthesis efficiency measurements for these accessions (Fig. 1A).

Metabolite response

Response to changed metabolite levels resulting from increased irradiance levels are sensed and signalled by the ERF/AP2 transcription factor family (Moore et al., 2014; Vogel et al., 2014). Members of this family showed transcriptional response to increased irradiance (Fig. 3, 4, and 5). The ERF/AP2 transcription factors are induced by ZAT10, a transcription factor activated by a MAP kinase (Nguyen et al., 2012; Vogel et al., 2014). *ZAT10* was found to be transcriptionally up-regulated in this study (Fig. 5B). ZAT10 has been reported to initiate a systemic acclimation response to excess light (Rossel et al., 2007; Munekage et al., 2015).

One regulatory gene that was characterized before to be responsive to increased irradiance is *SPX1* (Rossel et al., 2002). SPX1, so-called because it shares a domain with the yeast proteins Syg1 and Pho81, and the human protein Xpr1, is a phosphate-dependent inhibitor of the transcription factor PHOSPHATE STARVATION RESPONSE 1 (PHR1), (Puga et al., 2014). The physical interaction between SPX1 and PHR1 is reduced in the absence of inorganic phosphate (Pi), leading to transcription of many Pi starvation induced genes by PHR1 (Bustos et al., 2010; Puga et al., 2014). Among these PHR1-induced genes is *SPX1*, but the SPX1 protein is unable to bind PHR1 until Pi becomes available again (Puga et al., 2014). In this study, *SPX1* was up-regulated in Col-0 and to a lesser extent in Ga-0 (but not Ts-1) one hour after the irradiance increase, (Fig. 6G). It was also found to be specifically responsive to irradiance increase and not to temperature increase (Fig. 6G). This agrees with Rossel et al (2002) who found that *SPX1* was specifically induced by one hour fHL (filtered for the heat-producing infrared).

128

Therefore, we conclude that SPX1, acting in concert with PHR1, rapidly initiates a pathway of increased irradiance responsive genes that is independent of heat shock, and is associated with natural variation in photosynthesis efficiency acclimation (Fig. 1A). Expression of *PHR1* was not responsive to increased irradiance; probably because *PHR1* transcription levels are kept stable by SPX1. Besides *SPX1*, the genes *GLK2, GDPD1* and *DREB2A* were found to be accession-specifically induced in response to increased irradiance independent of heat shock (Fig. 6). The next paragraph describes how these three genes connect to lipid remodelling, summarized in Fig. 7B.

Phosphate-deficiency-dependent lipid remodelling response

Several lipid remodelling genes are activated one hour after the irradiance increase, mainly in Col-0 (Fig. 4 and 5). Increased irradiance induces a condition where more phosphate is required for additional photosynthesis structures and where photosynthetically produced sugars are in excess. An interaction between phosphate and sugar metabolism is known to exist on the transcriptional level (Müller et al., 2007); several genes involved in galactolipid biosynthesis were up-regulated in response to combined phosphate starvation and sugar accumulation (Müller et al., 2007). The interaction between phosphate and sugar metabolism was hypothesized to be important for either (1) maintenance of the ratio of available Pi and carbon by reducing the cellular sucrose content via galactolipid synthesis; or (2) supply of galactolipids as components of the plasma membrane to support enhance growth under sucrose supplementation (Murakawa et al., 2014). Our study supports this hypothesis, as both phosphate-deficiency-initiated lipid remodelling genes as well as carbohydrate (sucrose) metabolism genes were found to be light-responsive (Fig. 4 and 5).

Compared to Ga-0 and Ts-1, there is enhanced expression in Col-0 of several genes involved in galactolipid biosynthesis (Fig. 4 and Table S3) and reduced expression of one particular gene (*GOLDEN2-LIKE2 [GLK2]*, Table S4). Golden2-like transcription factors (GLK) are required for chloroplast development by regulating genes involved in chlorophyll biosynthesis (Waters et al., 2009). GLK2 was shown to be a pivotal regulator of *DGD1*, which encodes for the key enzyme of di-galactosyl-diacyl-glycerol (DGDG) synthesis (Kobayashi et al., 2014). DGDG is a bilayer-forming galactolipid, important for the integrity of the chloroplast protein-import apparatus (Chen and Li, 1998). In addition, DGDG replaces phospholipids in several organelles and membranes in phosphate-limited conditions (Härtel et al., 2000). *GLK2* expression was repressed in Col-0 and Ga-0 (but not Ts-1) one hour after increased irradiance, and activated in Col-0 and Ga-0 (but not

Ts-1) 3.5 hours after increased irradiance (Fig. 6C). Additionally, it was found to be specifically responsive to light increase (and not to temperature increase; Fig. 6C). This expression pattern implies that GLK2-induced DGDG replacement of phospholipids is activated only after 3.5 hours of excess light.

Three metabolic pathways are known for the release of Pi from phospholipids during Pi deficiency (Ruelland et al., 2015), two of which – galactolipid formation through the generation of phosphatidic acid (PA) by phospholipase C (first route) or, alternatively, phospholipase D (second route) – are extensively studied (Gaude et al., 2008; Nakamura et al., 2009). *GLYCEROPHOSPHO-DIESTER-PHOSPHO-DIESTERASE1* (*GDPD1*) is another gene known to respond to phosphate limitation that was found up-regulated upon increased irradiance (Fig. 4B and 5B); GDPD1 is suggested to mediate the third route for the release of Pi from phospholipids during Pi starvation (Cheng et al., 2011). In our experiment, the GDPD1 pathway is the only of the three phosphate limitation activated pathways normally up-regulated in excess light, that is significantly higher induced in Col-0 compared to Ga-0 and Ts-1 (Fig. 6H). The promoters of the *GDPD* family were found to all include Pi response elements binding to the PHR1 transcription factor (Cheng et al., 2011). To release Pi from phospholipids, the phospholipids are catalyzed into glycerophophodiesters and then hydrolyzed into glycerol-3-phosphate (G-3-P) by GDPD. It is unknown how Pi is released from G-3-P in Pi starved plants, but is suggested to be released via the *de novo* pathway of DGDG and/or SQDG synthesis (Cheng et al., 2011). Through this pathway, G-3-P is first converted into phosphatidic acid (PA) and then Pi is released in the subsequent conversion of PA into di-acyl-glycerol (DAG) by phosphatidic acid phosphohydrolases (PAH), (Nakamura et al., 2009). DAG is the direct substrate for synthesis of either MGDG (by *MGD1, MGD2*, and *MGD3*), DGDG (by *DGD1* and *DGD2*), or SQDG (by *SQD1* and *SQD2*), where MGDG is the precursor of both end-products DGDG and SQDG. The *gdpd1* mutant did not affect DGDG content, but SQDG content was not measured (Cheng et al., 2011). In this study, *DGD1* and *DGD2* were not transcriptionally responsive to excess light, whereas *SQD1* and *SQD2* were both up-regulated, only in Col-0, comparable to *SPX1* and *GDPD1* (Fig. 4B and 5B). Therefore, this study supports the hypothesis of Cheng et al (2011) in the part of release of extra Pi needed in phosphate-limited conditions mediated through SQDG synthesis. We hypothesize that the preference of SQDG over DGDG for replacement of phospholipids for releasing extra Pi in response to excess light is explained by the fact that SQDG brings a charge balance to the photosynthetic membranes that is overcharged as a result of the excess light, as, in contrast to MGDG and DGDG, SQDG is negatively charged. We suggest this preference for SQDG is mediated by reduced DGDG synthesis as result

130

of decreased *GLK2* expression leading to reduced *DGD1* expression (Fig. 7B). When after ~ 3.5 hrs, the charge balance is recovered, *GLK2* transcription is induced (Fig. 6C), leading to activation of DGDG synthesis.

Besides the PHR transcription factor, we found expression of another transcription factor gene previously implicated to be responsive to increased irradiance, encoding the dehydration-responsive element binding protein DREB2A (Rossel et al., 2002). *DREB2A* is induced by hydrogen peroxide and is known as a key regulator of drought response, though it is known to be involved in response to heat stress (Sakuma et al., 2006). DREB2A belongs to the ERF/AP2-type transcription factor family, binding to drought responsive elements (DRE) in the promoters of transcriptional target genes. *DREB2A* is transcriptionally up-regulated one hour after irradiance increase, only in Col-0 (Fig. 6I), as are *SPX1* and *GDPD1*. It is known that the expression of *DREB2A* is repressed by the phosphoinositide dependent-phospholipase C (PI-PLC) pathway in basal conditions (Ruelland et al., 2013), one of the pathways for the release of Pi from phospholipids. We propose that the activation of the GDPD pathway, as a result of Pi limitation, outcompetes the PLC pathway, leading to reduced PLC-mediated repression of *DREB2A*, leading to activation of drought responsive genes, explaining the crosstalk (Fig. 7B).

Conclusion

Our gene expression analysis shows the existence of a gene activation pathway for photosynthetic acclimation to increased irradiance that starts with the SPX1-mediated activation of the transcription factor PHR1 and activates the physiological process of membrane lipid remodelling (Fig. 7B). The involvement of PHR1 for photosynthetic responses to high light has been demonstrated before (Nilsson et al., 2011); the current study adds insights into the physiological mechanism behind it. It is hypothesized to involve the replacement of phospholipids by SQDG (preferred of DGDG) for releasing extra Pi needed for photosynthetic structures and for creating a charge balance to the photosynthetic membranes that is overcharged as a result of the excess light.

In addition, we suggest a gene activation pathway that starts with the activation of the regulators SR45a and SR30, which mediate alternative splicing activities. However, the downstream targets of these regulators and their involvement with photosynthetic acclimation remain to be elucidated.

This study aimed to explain natural variation in photosynthetic acclimation to increased irradiance at the transcriptional level, for which we studied gene regulation in three

accessions. Based on the results of this study, stronger expression of heat responsive genes in the accession Ga-0 might explain its slightly higher photosynthesis efficiency compared to Col-0. The absence of induced expression of heat responsive genes in Ts-1 partly explains its lower photosynthetic efficiency. The importance of the combined light and heat shock responsive pathway to increased irradiance is well known for the scavenging of reactive oxygen species for the maintenance of proper functioning of the photosynthetic membrane. Furthermore, a new, increased irradiance responsive PHR-mediated gene activation pathway was found, acting on membrane remodelling. This pathway was active in both Ga-0 and Col-0, providing additional explanation for the higher photosynthesis efficiencies in these accessions compared to Ts-1, in which the activation of both the heat shock responsive pathway as well as the PHR-mediated pathway is absent.

ACKNOWLEDGEMENTS

SUPPLEMENTARY TABLES AND FIGURES

Table S1. Core genes responsive to irradiance increase; genes more than 1.4-fold up-regulated at all time points in Col-0 as well as in both Ga-0 and Ts-1 at 1 hour after light onset, when comparing plants exposed to increased irradiance to control plants.

Unlogged fold changes are shown, green shading indicates accession-specific difference in expression present in control conditions independent of irradiance increase, orange shading indicates high light specific accession- or time-point differences. Acc. spec. = Accession-specific difference in expression (P=0.05) when comparing Col-0, Ga-0 and Ts-1; Time spec. = Time-specific difference (P=0.05) when comparing 1, 3.5, and 25 hours; Acc. spec. in cont. = Accession-specific difference in expression present in control conditions, independent of irradiance increase; Time spec. in cont. = Time-specific difference in expression present in control conditions, independent of irradiance increase; HL spec. acc. = High light specific accession difference; HL spec. time = High light specific time-point difference

Gene ID	Gene name and description	C-1	C-3.5	C-25	G-1	T-1	GO Biological Process	GO Molecular Function	GO Cellular Component	Acc. spec.	Time spec.	Acc. spec. in cont.	Time spec. in cont.	HL spec. acc.	HL spec. time
At1g02460	Pectin lyase-like superfamily protein, FUNCTIONS IN: polygalacturonase activity, INVOLVED IN: carbohydrate metabolic process	1.60	1.91	1.43	1.58	1.47	carbohydrate metabolic process	hydrolase activity	extracellular	no	no	no	no		
At5g25450	Cytochrome bd ubiquinol oxidase, 14kDa subunit, FUNCTIONS IN: ubiquinol-cytochrome-c reductase activity; INVOLVED IN: mitochondrial electron transport, ubiquinol to cytochrome c	3.63	1.43	2.40	3.29	2.53	electron transport	ubiquinol-cytochrome-c reductase activity	mitochondria	no	yes	no	no		
At5g05365	Heavy metal transport/detoxification superfamily protein	1.79	1.97	1.76	1.46	1.51	metal ion transport	metal ion binding	cytoplasm	no	no	no	no		
At1g77450	NAC domain containing protein 32 (NAC032), FUNCTIONS IN: sequence-specific DNA binding transcription factor activity; INVOLVED IN: multicellular organismal development, regulation of transcription	1.59	1.90	1.52	1.69	1.49	multicellular organismal development	transcription factor activity	nucleus	no	no	no	yes		
At3g22840	EARLY LIGHT-INDUCABLE PROTEIN 1 (ELIP1)	2.97	9.66	5.03	2.03	2.28	photosynthesis	chlorophyll binding; flavonoid biosynthetic process	chloroplast	no	yes	no	yes		
At4g14690	EARLY LIGHT-INDUCIBLE PROTEIN 2 (ELIP2)	2.95	5.11	5.54	3.14	3.78	photosynthesis	chlorophyll binding; flavonoid biosynthetic process	chloroplast	no	yes	yes	yes		
At4g31870	Encodes glutathione peroxidase7 (GPX7)	1.98	3.55	2.51	2.06	2.81	photosynthesis	H2O2 scavenging	chloroplast	no	yes	no	yes		
At2g20880	Encodes ERF53, a drought-induced transcription factor. Belongs to the AP2/ERF superfamily, and has a highly conserved AP2 domain. Regulates drought-responsive gene expressions by binding to the GCC box and/or dehydration-responsive element (DRE) in the promoter of downstream genes.	2.84	1.62	1.93	2.50	1.68	photosynthesis; drought response	transcription factor activity	nucleus	yes	yes	no	no	yes	yes
At4g28140	Encodes a member of the DREB subfamily A-6 of ERF/AP2 transcription factor family. The protein contains one AP2 domain.	2.47	1.69	1.60	3.02	1.77	photosynthesis; drought response	transcription factor activity	nucleus	no	no	no	no		
At5g05410*	Encodes the transcription factor DREB2A that specifically binds to DRE/CRT cis elements (responsive to drought and low-temperature stress). Belongs to the DREB subfamily A-2 of ERF/AP2 transcription factor family (DREB2A). There are eight members in this subfamily including DREB2B. The protein contains one AP2 domain. Overexpression of transcriptional activation domain of DREB2A resulted in significant drought stress tolerance but only slight freezing tolerance in transgenic Arabidopsis plants.	3.64	1.42	1.46	2.24	3.86	photosynthesis; drought response; response to heat	transcription factor activity	nucleus	yes	yes	no	yes	yes	
At1g07890	Encodes a cytosolic ascorbate peroxidase APX1. Ascorbate peroxidases are enzymes that scavenge hydrogen peroxide in plant cells. Eight types of APX have been described for Arabidopsis; three cytosolic (APX1, APX2, APX6), two chloroplastic types (stromal sAPX, thylakoid tAPX), and three microsomal (APX3, APX4, APX5) isoforms. At least part of the induction of heat shock proteins during light stress in Arabidopsis is mediated by H2O2 that is scavenged by APX1. Expression of the gene is downregulated in the presence of paraquat, an inducer of photo-oxidative stress.	1.47	1.68	1.50	1.59	1.61	photosynthesis; response to heat	H2O2 scavenging	cytoplasm	no	no	no	no		
At3g16050*	Encodes a protein with pyridoxal phosphate synthase activity whose transcripts were detected mostly in roots and accumulate during senescence.	2.89	1.65	1.57	2.85	2.72	pyridoxal phosphate biosynthesis	protein binding	cytoplasm	no	yes	no	yes		

Gene ID	Gene name and description	C-1	C-3,5	C-25	G-1	T-1	GO Biological Process	GO Molecular Function	GO Cellular Component	Acc. spec.	Time spec.	Acc. spec. in cont.	Time spec. in cont.	HL spec. acc.	HL spec. time
At3g53230	ATPase, AAA-type, CDC48 protein; FUNCTIONS IN: hydrolase activity, nucleoside-triphosphatase activity, binding, nucleotide binding, ATP binding; INVOLVED IN: response to cadmium ion; LOCATED IN: cytosol, nucleus, plasma membrane;	3.05	1.81	2.57	2.89	1.99	response to cadmium ion	hydrolase activity	cytosol	no	yes	no	no		yes
At2g37180	A member of the plasma membrane intrinsic protein PIP2, functions as aquaporin and is involved in desiccation.	1.74	2.09	1.58	1.65	1.46	response to drought	transporter	plasma membrane	no	no	no	no		
At1g07400	HSP20-like chaperones superfamily protein	4.45	3.32	3.68	4.01	5.89	response to heat	chaperone	cytoplasm	no	no	no	yes		
At1g53540	HSP20-like chaperones superfamily protein	8.12	3.32	3.45	7.41	3.23	response to heat	chaperone	cytoplasm	yes	yes	no	no	yes	yes
At1g54050	HSP20-like chaperones superfamily protein	3.23	1.56	1.98	5.77	4.28	response to heat	chaperone	cytoplasm	no	yes	yes	no		
At1g59860	HSP20-like chaperones superfamily protein	4.55	1.42	2.54	4.61	4.52	response to heat	chaperone	cytoplasm	no	yes	no	no		yes
At2g19310	HSP20-like chaperones superfamily protein	2.02	1.63	1.45	1.99	1.65	response to heat	chaperone	cytoplasm	no	yes	no	no		yes
At2g29500	HSP20-like chaperones superfamily protein	14.12	9.75	6.82	17.19	9.83	response to heat	chaperone	cytoplasm	no	yes	no	no		yes
At2g42240	A member of Arabidopsis BAG (Bcl-2-associated athanogene) proteins, plant homologs of mammalian regulators of apoptosis. Expression of BAG6 in leaves was strongly induced by heat stress	7.26	1.60	3.05	9.31	4.27	response to heat	chaperone	nucleus	yes	yes	no	no	yes	yes
At5g12030	HEAT SHOCK PROTEIN 17.6A (HSP17.6A)	20.49	5.26	12.83	23.43	19.53	response to heat	chaperone	cytoplasm	no	yes	no	no		yes
At5g49570	Encodes one of the 36 carboxylate clamp (CC)-tetratricopeptide repeat (TPR) proteins with potential to interact with Hsp90/Hsp70 as co-chaperones.	9.47	3.27	4.30	9.68	9.34	response to heat	chaperone	nucleus	no	yes	yes	yes		
At4g36990	Encodes HEAT SHOCK FACTOR 4 (HSF4)	2.60	1.66	1.74	1.91	1.97	response to heat	hat shock factor	nucleus	no	yes	yes	yes		
At2g26150	Encodes HEAT SHOCK TRANSCRIPTION FACTOR A2 (HSFA2)	3.69	1.63	1.81	3.73	4.52	response to heat	heat shock factor	nucleus	no	yes	no	yes		
At1g74310	HEAT SHOCK PROTEIN 101 (HSP101)	5.50	2.14	2.55	5.35	5.59	response to heat	heat shock protein	chloroplast	no	yes	no	yes		
At2g20560	DNAJ heat shock family protein	4.46	1.66	2.40	3.91	3.64	response to heat	heat shock protein	cytoplasm	no	yes	no	yes		
At2g25140	Encodes ClpB4, which belongs to the Casein lytic proteinase/heat shock protein 100 (ClpHsp100) family.	3.13	1.58	2.12	3.25	2.27	response to heat	heat shock protein	chloroplast/mitochondria	no	yes	no	no		yes
At3g08970	J domain protein localized in ER lumen, shows similarity to HSP40 proteins and is induced by heat stress.	4.69	1.58	2.51	4.32	3.08	response to heat	heat shock protein	cytoplasm	yes	yes	no	no	yes	yes
At3g12580	HEAT SHOCK PROTEIN 70 (HSP70)	6.31	5.02	4.14	4.60	5.22	response to heat	heat shock protein	cytoplasm	no	no	yes	no		
At3g23990	HSP60, mitochondrial chaperonin HSP.	1.94	1.83	1.83	1.88	1.51	response to heat	heat shock protein	mitochondria	no	no	no	no		
At3g46230	HEAT SHOCK PROTEIN 17.4 (HSP17.4)	10.13	4.69	4.98	7.49	4.88	response to heat	heat shock protein	cytoplasm	yes	yes	no	no	yes	yes
At4g12400	Hop3, one of the 36 carboxylate clamp (CC)-tetratricopeptide repeat (TPR) proteins with potential to interact with Hsp90/Hsp70 as co-chaperones.	9.12	3.43	3.77	5.02	4.13	response to heat	heat shock protein	cytoplasm	yes	yes	yes	yes	yes	yes
At4g25200	MITOCHONDRION-LOCALIZED SMALL HEAT SHOCK PROTEIN 23.6 (HSP23.6-MITO)	5.64	2.83	3.04	8.13	3.93	response to heat	heat shock protein	mitochondrion	yes	yes	no	no	yes	yes
At5g09590	Heat shock protein 70 (Hsc70-5)	2.90	1.96	1.78	2.66	1.86	response to heat	heat shock protein	cytoplasm	yes	yes	no	no	yes	yes
At5g12020	17.6 KDA CLASS II HEAT SHOCK PROTEIN (HSP17.6II)	13.56	9.31	9.09	19.88	18.40	response to heat	heat shock protein	cytoplasm	no	no	yes	no		
At5g51440	HSP20-like chaperones superfamily protein	7.07	4.39	4.07	6.57	3.97	response to heat	heat shock protein	cytoplasm	yes	yes	no	no	yes	yes
At5g52640	HEAT SHOCK PROTEIN 90.1 (HSP90.1)	7.76	2.68	3.41	8.27	5.64	response to heat	heat shock protein	cytoplasm	no	yes	no	yes		
At1g30070	SGS domain-containing protein	3.56	1.46	2.31	3.07	2.62	response to heat	unknown	nucleus	no	yes	no	no		yes
At5g64510	TUNICAMYCIN INDUCED 1 (TIN1), a plant-speci-c ER stress-inducible protein. TIN1 mutation affects pollen surface morphology	4.90	2.36	2.22	3.32	2.94	response to heat	unknown	chloroplast	no	yes	no	no		yes
At1g07350	Encodes a serine/arginine rich-like protein, SR45a. Involved in the regulation of stress-responsive alternative splicing.	2.65	1.75	1.58	3.44	2.34	RNA binding	alternative splicing	unknown	yes	yes	no	yes	yes	
At1g09140	Encodes a serine-arginine rich RNA binding protein (SR30) involved in regulation of splicing (including splicing of itself). Exists as 3 alternative spliced forms that are differentially expressed.	2.36	2.30	1.67	2.04	1.71	RNA binding	alternative splicing	nucleus	no	yes	no	no		yes
At5g12110	Glutathione S-transferase, C-terminal-like; Translation elongation factor EF1B/ribosomal protein S6	3.66	3.17	3.52	3.89	3.58	RNA binding	translation elongation	plasma membrane	no	no	yes	no		

Gene ID	Gene name and description	C-1	C-3.5	C-25	G-1	T-1	GO Biological Process	GO Molecular Function	GO Cellular Component	Acc. spec.	Time spec.	Acc. spec. in cont.	Time spec. in cont.	HL spec. acc.	HL spec. time
At3g24500	One of three genes in A. thaliana encoding multiprotein bridging factor 1, a highly conserved transcriptional coactivator. May serve as a bridging factor between a bZIP factor and TBP. Its expression is specifically elevated in response to pathogen infection, salinity, drought, heat, hydrogen peroxide, and application of abscisic acid or salicylic acid. Constitutive expression enhances the tolerance of transgenic plants to various biotic and abiotic stresses.	2.55	1.94	1.72	2.46	2.73	unknown	transcription factor activity	nucleus	no	yes	no	yes		
At5g48840	Encodes bZIP protein; FUNCTIONS IN: DNA binding, sequence-specific DNA binding transcription factor activity; INVOLVED IN: regulation of transcription, DNA-dependent	2.44	1.52	1.56	2.39	2.13	unknown	transcription factor activity	nucleus	no	yes	no	no		yes
At5g09930	Encodes ATP-BINDING CASSETTE F2 (ABCF2); member of GCN subfamily	1.91	2.03	1.53	1.51	1.61	unknown	transporter	plasma membrane	no	no	yes	no		
At1g07500	Unknown protein	3.43	2.47	3.25	2.18	1.80	unknown	unknown	nucleus	yes	no	no	no		yes
At1g21550	Calcium-binding EF-hand family protein	5.07	1.57	2.02	2.87	2.78	unknown	unknown	cytoplasm	yes	yes	no	no	yes	yes
At3g24750	Unknown protein	1.84	2.68	4.22	1.74	1.90	unknown	unknown	nucleus	no	yes	yes	no		yes
At3g51238	Potential natural antisense gene, locus overlaps with AT3G51240	1.61	2.53	1.74	1.46	2.03	unknown	unknown	unknown	no	yes	no	yes		yes
At4g18422	Unknown protein	2.37	1.44	1.69	1.90	1.59	unknown	unknown	mitochondria	no	yes	no	no		
At4g35988	Upstream open reading frames (uORFs) are small open reading frames found in the 5' UTR of a mature mRNA, and can potentially mediate translational regulation of the largest, or major, ORF (mORF). CPuORF49 represents a conserved upstream opening reading frame relative to major ORF AT4G36990.1	2.60	1.66	1.74	1.91	1.97	unknown	unknown	mitochondria	no	yes	no	yes		
At5g03890	Unknown protein	1.44	1.57	1.76	2.38	1.58	unknown	unknown	nucleus	no	no	no	no		

Table S2 Core genes responsive to irradiance increase; genes more than 1.4-fold down-regulated in all time points in Col-0 as well as in both Ga-0 and Ts-1 at 1 hour after light onset, when comparing plants exposed to increased irradiance to control plants.

Unlogged fold changes are shown, green shading indicates accession-specific difference in expression present in control conditions independent of irradiance increase, orange shading indicates high light specific accession- or time-point differences. Acc. spec. = Accession-specific difference (P=0.05) when comparing Col-0, Ga-0 and Ts-1; Time spec. = Time-specific difference (P=0.05) when comparing 1, 3.5, and 25 hours; Acc. spec. in cont. = Accession-specific difference in expression present in control conditions, independent of irradiance increase; Time spec. in cont. = Time-specific difference in expression present in control conditions, independent of irradiance increase; HL spec. acc. = High light specific accession difference; HL spec. time = High light specific time-point difference.

Gene ID	Gene name and description	C-1	C-3.5	C-25	G-1	T-1	GO Biological Process	GO Molecular Function	GO Cellular Component	Acc. spec.	Time spec.	Acc. spec. in cont.	Time spec. in cont.	HL spec. acc.	HL spec. time
At3g27170	Encodes LONGIFOLIA2 (LNG2). Regulates leaf morphology by promoting cell expansion in the leaf-length direction. The LNG2 homologue LNG1 (At5g15580) has similar function.	0.62	0.47	0.60	0.50	0.56	cell organization and biogenesis	protein binding	nucleus	no	no	no	no		
At5g44680	DNA glycosylase superfamily protein; FUNCTIONS IN: DNA-3-methyladenine glycosylase I activity, catalytic activity; INVOLVED IN: DNA repair, base-excision repair	0.58	0.40	0.51	0.65	0.66	DNA repair	hydrolase activity	nucleus	no	yes	no	yes		
At5g17300	Myb-like transcription factor RVE1 (REVEILLE 1) that regulates hypocotyl growth by regulating free auxin levels in a time-of-day specific manner.	0.45	0.70	0.50	0.47	0.33	hypocotyl growth	transcription factor activity	nucleus	no	yes	no	yes		
At1g71030	Encodes a putative myb family transcription factor, MYB-LIKE 2 (MYBL2). In contrast to most other myb-like proteins its myb domain consists of a single repeat. A proline-rich region potentially involved in transactivation is found in the C-terminal part of the protein. Its transcript accumulates mainly in leaves.	0.62	0.27	0.62	0.31	0.36	leaf morphology	transcription factor activity	nucleus	yes	yes	yes	yes		
At5g94980	Bifunctional inhibitor/lipid-transfer protein/seed storage 2S albumin superfamily protein; FUNCTIONS IN: lipid binding; INVOLVED IN: lipid transport	0.38	0.17	0.23	0.43	0.40	lipid transport	lipid binding	extracellular	no	yes	no	no		yes
At5g20110	Dynein light chain type 1 family protein; FUNCTIONS IN: microtubule motor activity; INVOLVED IN: microtubule-based process	0.56	0.64	0.55	0.56	0.63	microtubule motor activity	hydrolase activity	cytoplasm	no	no	no	no		
At4g19170	Chloroplast-targeted member of a family of enzymes similar to nine-cis-epoxycarotenoid dioxygenase	0.43	0.29	0.18	0.56	0.45	oxidation-reduction process	protein binding	chloroplast	no	yes	yes	no		yes
At5g94190	Encodes GLK2, Golden2-like 2, one of a pair of partially redundant nuclear transcription factors that regulate chloroplast development in a cell-autonomous manner. GLK1, Golden2-like 1, is encoded by At2g20570. GLK1 and GLK2 regulate the expression of the photosynthetic apparatus.	0.54	0.60	0.36	0.58	0.53	photosynthesis	transcription factor activity	nucleus	no	yes	no	no		yes
At5g07580	Encodes a member of the ERF (ethylene response factor) subfamily B-3 of ERF/AP2 transcription factor family. The protein contains one AP2 domain. There are 18 members in this subfamily including ATERF-1, ATERF-2, AND ATERF-5.	0.67	0.56	0.60	0.55	0.58	photosynthesis; drought response	transcription factor activity	nucleus	no	no	no	no		
At5g25190	Encodes a member of the ERF (ethylene response factor) subfamily B-6 of ERF/AP2 transcription factor family. The protein contains one AP2 domain. There are 12 members in this subfamily including RAP2.11.	0.54	0.32	0.50	0.56	0.65	photosynthesis; drought response	transcription factor activity	nucleus	no	yes	no	no		yes
At1g67900	Phototropic-responsive NPH3 family protein; FUNCTIONS IN: signal transducer activity; INVOLVED IN: response to light stimulus	0.63	0.47	0.55	0.58	0.56	protein ubiquitination	signal transducer activity	plasma membrane	no	no	no	no		
At1g33240	Encodes GT-2-LIKE 1 (GTL1), a plant transcriptional activator that contains two separate, but similar, trihelix DNA-binding domains, similar to GT-2. Gene is expressed in all aerial parts of the plant, with higher level of expression in siliques. At-GTL2 was thought to be a duplicated copy of this gene but is likely to be a cloning artefact, the result of a chimeric clone.	0.46	0.47	0.42	0.48	0.60	trichome morphogenesis	transcription factor activity	nucleus	no	no	no	no		
At2g30424	In a tandem repeat with AT2g30432 (TCL1) and AT2g30420 (ETC2), it encodes a single-repeat R3 MYB transcription factor that is involved in the negative regulation of trichome formation.	0.44	0.52	0.47	0.64	0.68	trichome morphogenesis	transcription factor activity	nucleus	no	no	no	no		

Gene ID	Gene name and description	C-1	C-3.5	C-25	G-1	T-1	GO Biological Process	GO Molecular Function	GO Cellular Component	Acc. spec.	Time spec.	Acc. spec. in cont.	Time spec. in cont.	HL spec. acc.	HL spec. time
At3g03990	Alpha/beta-Hydrolases superfamily protein	0.56	0.57	0.60	0.63	0.60	unknown	hydrolase activity	cytoplasm	no	no	no	no		
At3g24420	Alpha/beta-Hydrolases superfamily protein; FUNCTIONS IN: hydrolase activity; INVOLVED IN: biological_process unknown; LOCATED IN: endomembrane system; EXPRESSED IN: guard cell	0.56	0.43	0.50	0.61	0.65	unknown	hydrolase activity	cytoplasm	no	no	no	no		
At2g02080	Indeterminate(ID)-domain 4 (IDD4); FUNCTIONS IN: sequence-specific DNA binding transcription factor activity; LOCATED IN: intracellular, chloroplast	0.50	0.56	0.42	0.56	0.55	unknown	transcription factor activity	nucleus	no	no	no	no		
At2g27050	Ethylene-insensitive3-like1 (EIL1)	0.57	0.45	0.62	0.68	0.67	unknown	transcription factor activity	nucleus	no	yes	no	no		yes
At3g57040	Response regulator ARR9. A two-component response regulator-like protein with a receiver domain with a conserved aspartate residue and a possible phosphorylation site and at the N-terminal half. Appears to interact with histidine kinase like genes ATHP3 and ATHP2	0.49	0.56	0.67	0.51	0.52	unknown	transcription factor activity	nucleus	no	no	no	no		
At4g01460	Basic helix-loop-helix (bHLH) DNA-binding superfamily protein	0.47	0.36	0.58	0.66	0.60	unknown	transcription factor activity	nucleus	no	yes	no	no		yes
At4g36540	BR enhanced expression 2 (BEE2); FUNCTIONS IN: DNA binding, sequence-specific DNA binding transcription factor activity	0.52	0.55	0.62	0.66	0.67	unknown	transcription factor activity	nucleus	no	no	no	no		
At5g54630	Zinc finger protein-related; FUNCTIONS IN: sequence-specific DNA binding transcription factor activity	0.55	0.45	0.59	0.60	0.60	unknown	transcription factor activity	nucleus	no	no	no	no		
At1g23390	Kelch repeat-containing F-box family protein	0.67	0.20	0.64	0.43	0.48	unknown	unknown	nucleus	no	yes	no	yes		
At1g30250	Unknown protein	0.46	0.29	0.35	0.62	0.62	unknown	unknown	mitochondria	no	yes	no	no		yes
At1g69160	Unknown protein	0.58	0.39	0.41	0.62	0.58	unknown	unknown	mitochondria	no	yes	no	no		yes
At1g71970	Unknown protein	0.63	0.46	0.62	0.59	0.69	unknown	unknown	nucleus	no	yes	no	no		yes
At3g06070	Unknown protein	0.66	0.33	0.50	0.62	0.57	unknown	unknown	unknown	no	yes	no	no		yes
At3g23880	F-box and associated interaction domain-containing protein	0.58	0.51	0.56	0.51	0.59	unknown	unknown	nucleus	no	no	no	no		
At3g59940	Galactose oxidase/kelch repeat superfamily protein	0.57	0.37	0.69	0.55	0.49	unknown	unknown	cytoplasm	no	yes	no	yes		
At5g19030	unknown protein	0.46	0.23	0.48	0.50	0.52	unknown	unknown	nucleus	no	yes	no	no		yes
At5g18030	SAUR-like auxin-responsive protein family	0.40	0.34	0.45	0.57	0.68	unknown	unknown	mitochondria	no	no	no	no		
At5g19190	Unknown protein	0.43	0.19	0.43	0.34	0.38	unknown	unknown	nucleus	no	yes	no	yes		
At5g54585	Unknown protein	0.53	0.41	0.30	0.55	0.65	unknown	unknown	unknown	no	yes	no	no		yes
At5g57760	Unknown protein	0.62	0.17	0.28	0.64	0.69	unknown	unknown	mitochondria	no	yes	no	no		yes
At5g65080	Unknown protein	0.64	0.31	0.54	0.66	0.71	unknown	unknown	nucleus	no	yes	no	yes		
At2g32010	Encodes an inositol polyphosphate 5'-phosphatase (5PTase). Mediating phosphoinositide signaling. Involved in establishment of foliar vein patterns.	0.58	0.50	0.56	0.63	0.62	vein patterning	hydrolase activity	cytoplasm	no	no	no	no		

Table S3. Accession specific genes responsive to irradiance increase; genes more than 1.4-fold up-regulated at 1 hour after light onset when comparing plants exposed to increased irradiance to control plants. in one, two or three accessions of Col-0, Ga-0 and Ts-1 and differentially (P=0.05) up-regulated between two or three accessions when comparing Col-0, Ga-0 and Ts-1.

Unlogged fold changes are shown, grey shaded values are >1.4 fold up-regulated, green shading indicates accession-specific difference in expression present in control conditions independent of irradiance increase. Acc. spec. in cont. = Accession-specific difference in expression present in control conditions, independent of irradiance increase

Gene ID	Gene name and description	C-1	G-1	T-1	GO Biological Process	GO Molecular Function	GO Cellular Component	Acc. spec. in cont.
At1g67070	Encodes PHOSPHOMANNOSE ISOMERASE 2 (PMI2), also known as DARK INDUCED 9 (DIN9) a protein with phosphomannose isomerase activity that is involved in synthesis of ascorbic acid. Expression is induced after 24 hours of dark treatment, in senescing leaves and treatment with exogenous photosynthesis inhibitor. Induction of gene expression was suppressed in excised leaves supplied with sugar. The authors suggest that the gene's expression pattern is responding to the level of sugar in the cell.	1.37	1.16	2.01	carbohydrate metabolism	mannose-6-phosphate isomerase activity	cytoplasm	no
At5g49360	Encodes a bifunctional (beta)-D-xylosidase/(alpha)-L-arabinofuranosidase required for pectic arabinan modification. Located in the extracellular matrix. Gene is expressed specifically in tissues undergoing secondary wall thickening. This is a member of glycosyl hydrolase family 3 and has six other closely related members.	1.05	1.07	1.72	carbohydrate metabolism	pectic arabinan modification	extracellular	yes
At1g78820	D-mannose binding lectin protein with Apple-like carbohydrate-binding domain; FUNCTIONS IN: sugar binding	0.92	0.92	1.44	carbohydrate metabolism	sugar binding	plasma membrane	no
At1g56650	Encodes PRODUCTION OF ANTHOCYANIN PIGMENT 1 (PAP1), a putative MYB domain containing transcription factor involved in anthocyanin metabolism and radical scavenging. Essential for the sucrose-mediated expression of the dihydroflavonol reductase gene. Auxin and ethylene responsiveness of PAP1 transcription is lost in myb12 mutants.	3.12	1.12	0.77	carbohydrate metabolism	transcription factor	nucleus	yes
At2g17270	Citrate synthase-related; FUNCTIONS IN: transferase activity, transferring acyl groups, acyl groups converted into alkyl on transfer.; INVOLVED IN: cellular carbohydrate metabolic process	1.44	0.88	1.03	carbohydrate metabolism	transferase activity	mitochondria	yes
At5g57100	Nucleotide/sugar transporter family protein	1.46	1.58	0.97	carbohydrate metabolism	transport	membrane	no
At4g37180	Myb family transcription factor, contains Pfam domain, PF00249: Myb-like DNA-binding domain I; also isolated as a putative cytoskeletal protein in a yeast screen	1.52	1.50	0.99	cell organization and biogenesis	transcription factor activity	nucleus	no
At1g65840	Encodes a peroxisomal polyamine oxidase PAO4, involved in the back-conversion polyamine degradation pathway.	1.08	1.08	1.60	cellular amino acid metabolism	polyamine degradation	nucleus	no
At5g53970	Encodes tyrosine aminotransferase which is strongly induced upon aging and coronatine treatment	1.22	1.03	1.69	cellular amino acid metabolism	transferase activity	cytoplasm	no
At2g03240	EXS (ERD1/XPR1/SYG1) family protein	0.96	1.24	1.48	cellular response to phosphate starvation	unknown	plasma membrane	no
At4g24010	Encodes a protein similar to cellulose synthase	1.46	0.80	0.91	cellulose biosynthesis	cellulose synthase	plasma membrane	yes
At4g26150	Encodes a member of the GATA factor family of zinc finger transcription factors. Modulate chlorophyll biosynthesis and glutamate synthase (GLU1/Fd-GOGAT) expression.	0.77	1.23	1.42	chlorophyll biosynthesis	transcription factor activity	nucleus	yes
At1g04770	Tetratricopeptide repeat (TPR)-like superfamily protein	0.74	0.77	1.45	chloroplast organization	unknown	nucleus	yes
At5g59220	Highly ABA-induced PP2C gene 1 (HAI1); FUNCTIONS IN: protein serine/threonine phosphatase activity, catalytic activity; INVOLVED IN: response to water deprivation, response to abscisic acid stimulus; LOCATED IN: chloroplast	3.53	2.42	1.37	chloroplast organization; stomatal movement	phosphatase activity	cytoplasm	yes

Gene ID	Gene name and description	C-1	G-1	T-1	GO Biological Process	GO Molecular Function	GO Cellular Component	Acc. spec. in cont.
At2g21130	Cyclophilin-like peptidyl-prolyl cis-trans isomerase family protein	1.75	1.40	1.07	circadian rhythm	protein binding	cytoplasm	yes
At1g61090	Disease resistance protein (TIR-NBS class); FUNCTIONS IN: transmembrane receptor activity, nucleoside-triphosphatase activity, nucleotide binding, ATP binding	2.37	1.21	0.95	defense response	kinase activity	chloroplast	no
At4g23310	Encodes a cysteine-rich receptor-like protein kinase.	0.95	1.07	1.44	defense response	kinase activity	extracellular	no
At4g03960	Encodes an atypical dual-specificity phosphatase involved in the negative regulation of defense response to a bacterial pathogen, P. syringae pv. tomato.	2.27	1.36	1.60	defense response	MAP kinase activity	cytoplasm	no
At3g19270	CYP707A4. Encodes a cytochrome P450 protein with ABA 8'-hydroxylase activity, involved in ABA catabolism.	1.89	1.45	1.09	electron transport	ABA catabolism	extracellular	no
At3g14620	Putative cytochrome P450 (CYP72A8).	2.02	0.80	0.74	electron transport	unknown	unknown	no
At2g38530	LIPID TRANSFER PROTEIN 2 (LTP2); Involved in lipid transfer between membranes. Belongs to a family of Lipid transfer proteins.	2.05	0.79	0.47	lipid remodelling	lipid transfer	golgi; extracellular	no
At2g11810	MONOGALACTOSYLDIACYLGLYCEROL SYNTHASE 3 (MGD3); MGD3 is the major enzyme for galactolipid metabolism during phosphate starvation. Does not contribute to galactolipid synthesis under P1-sufficient conditions.	1.64	1.04	1.06	lipid remodelling	MGDG biosynthesis	chloroplast	no
At5g20410	MONOGALACTOSYLDIACYLGLYCEROL SYNTHASE 2 (MGD2); Encodes a type B monogalactosyldiacylglycerol (MGDG) synthase. Strongly induced by phosphate deprivation, and in non-photosynthetic tissues. Does not contribute to galactolipid synthesis under Pi-sufficient conditions but does under Pi starvation.	2.22	1.18	1.68	lipid remodelling	MGDG biosynthesis	chloroplast	no
At3g17790	PURPLE ACID PHOSPHATASE 17 (PAP17). Expression is upregulated in the shoot of cax1/cax3 mutant.	2.91	1.64	1.40	lipid remodelling	phosphatase activity	extracellular	no
At3g02040	Encodes a member of the glycerophosphodiester phosphodiesterase (GDPD) family. Has glycerophosphodiester phosphodiesterase activity. Functions in maintaining cellular phosphate homeostasis under phosphate starvation.	6.54	2.26	2.58	lipid remodelling	phospholipid catabolism	cytoplasm	yes
At4g33030	SQD1, involved in sulfolipid biosynthesis	2.31	1.41	1.63	lipid remodelling	SQDG biosynthesis	chloroplast	no
At5g01220	SQD2, involved in sulfolipid biosynthesis	2.32	1.14	1.45	lipid remodelling	SQDG biosynthesis	chloroplast	no
At2g26660	SPX domain gene 2 (SPX2)	1.85	1.18	1.47	lipid remodelling	unknown	nucleus	no
At3g03790	Ankyrin repeat family protein / regulator of chromosome condensation (RCC1) family protein	1.50	1.04	1.16	lipid remodelling	unknown	nucleus	no
At5g20150	SPX DOMAIN GENE 1 (SPX1); Expression is upregulated in the shoot of cax1/cax3 mutant.	4.30	1.29	1.97	lipid remodelling	unknown	nucleus	yes
At3g09390	METALLOTHIONEIN 2A (MT2A); binds to and detoxifies excess copper and other metals, limiting oxidative damage	1.39	1.00	0.92	metal ion binding	copper detoxification	unknown	no
At2g41040	S-adenosyl-L-methionine-dependent methyltransferases superfamily protein	1.57	1.40	2.48	methylation	methyltransferase activity	chloroplast	no
At3g21170	Encodes a protein with NAD(H) kinase activity.	1.48	1.17	1.71	NAD metabolic process	NAD+ kinase activity	cytoplasm	no
At4g20820	FAD-binding Berberine family protein; FUNCTIONS IN: electron carrier activity, oxidoreductase activity, FAD binding, catalytic activity, INVOLVED IN: oxidation reduction	0.86	0.74	1.46	oxidation-reduction process	electron transport	chloroplast	no
At2g22240	Myo-inositol-1-phosphate synthase isoform 2 (MIPS2). Expressed in leaf, root and silique. Immunolocalization experiments with an antibody recognizing MIPS1, MIPS2, and MIPS3 showed endosperm localization.	1.64	1.27	0.93	phospholipid biosynthesis	chlorophyll catabolic process	cytoplasm	no
At1g52830	INDOLE-3-ACETIC ACID 6 (IAA6), an extragenic dominant suppressor of the hy2 mutant phenotype. Also exhibits aspects of constitutive photomorphogenetic phenotype in the absence of hy2.	1.15	1.40	2.00	photomorphogenesis	transcription factor activity	nucleus	no
At5g23730	Encodes REPRESSOR OF UV-B PHOTOMORPHOGENESIS 2 (RUP2). Functions as a repressor of UV-B signaling.	1.04	1.12	1.57	photoreceptor activity	chloroplast organization	cytoplasm	no

Gene ID	Gene name and description	C-1	G-1	T-1	GO Biological Process	GO Molecular Function	GO Cellular Component	Acc. spec. in cont.
At5g52250	Encodes REPRESSOR OF UV-B PHOTOMORPHOGENESIS 1 (RUP1), a transducin protein whose gene expression is induced by UV-B. This induction is reduced in hy5 mutant and may be a target of HY5 during UV-B response. Functions as a repressor of UV-B signaling.	1.37	1.38	2.22	photoreceptor activity	chloroplast organization	chloroplast	no
At4g04020	Fibrillin precursor protein. The fibrillin preprotein, but not the mature protein interacts with ABI2. Regulated by abscisic acid response regulators. Involved in abscisic acid-mediated photoprotection.	2.26	2.94	0.95	photosynthesis	photoprotection	chloroplast	yes
At2g20880	Encodes ERF53, a drought-induced transcription factor. Belongs to the AP2/ERF superfamily, and has a highly conserved AP2 domain. Regulates drought-responsive gene expressions by binding to the GCC box and/or dehydration-responsive element (DRE) in the promoter of downstream genes.	2.84	2.50	1.68	photosynthesis; response to drought	transcription factor activity	nucleus	no
At5g05410	Encodes DREB2A, a transcription factor that specifically binds to DRE/CRT cis elements (responsive to drought and low-temperature stress.) Belongs to the DREB subfamily A-2 of ERF/AP2 transcription factor family (DREB2A).	3.64	2.24	3.86	photosynthesis; response to drought	transcription factor activity	nucleus	no
At1g16420	Encodes MC8, a metacaspase (cysteine-type endopeptidase) that is involved in promoting programmed cell death in response to hydrogen peroxide (H2O2), UV light, and methyl viologen (MV).	1.07	1.16	1.94	programmmed cell death	cysteine-type endopeptidase	unknown	no
At5g43190	Galactose oxidase/kelch repeat superfamily protein	1.05	0.98	1.45	protein catabolism	ubiquitin-protein transferase activity	nucleus	no
At1g62710	Encodes a vacuolar processing enzyme belonging to a novel group of cysteine proteases that is expressed specifically in seeds and is essential for the proper processing of storage proteins.	1.44	0.89	0.66	protein storage	hydrolase activity	unknown	no
At3g08590	Phosphoglycerate mutase, 2,3-bisphosphoglycerate-independent; FUNCTIONS IN: manganese ion binding, phosphoglycerate mutase activity, 2,3-bisphosphoglycerate-independent phosphoglycerate mutase activity, catalytic activity, metal ion binding	1.49	1.35	1.11	response to cadmium ion	glucose catabolic process	cytoplasm	no
At1g53680	Encodes glutathione transferase GSTU28 belonging to the tau class of GSTs.	2.87	2.69	4.76	response to cadmium ion	glutathione transferase	cytoplasm	no
At1g65980	Thioredoxin-dependent peroxidase 1 (TPX1)	1.45	0.74	0.98	response to cadmium ion	peroxidase	cytoplasm	no
At2g46240	A member of Arabidopsis BAG (Bcl-2-associated athanogene) proteins, plant homologs of mammalian regulators of apoptosis. Expression of BAG6 in leaves was strongly induced by heat stress	7.26	9.31	4.27	response to heat	chaperone	nucleus	no
At3g13470	Encodes a subunit of chloroplasts chaperonins CHAPERONIN-60BETA2 (CPN60BETA2) that are involved in mediating the folding of newly synthesized, translocated, or stress-denatured proteins.	2.02	2.20	1.40	response to heat	chaperone	chloroplast	no
At5g37670	HSP20-like chaperones superfamily protein	4.25	4.54	2.61	response to heat	chaperone	cytoplasm	no
At5g43260	Chaperone protein dnaJ-related	1.21	0.95	1.62	response to heat	chaperone	chloroplast	no
At5g51440	HSP20-like chaperones superfamily protein	7.07	6.57	3.97	response to heat	chaperone	mitochondria	no
At1g03070	Apoptosis-promoting Bax inhibitor-1 family protein	4.02	1.58	1.18	response to heat	glutamate binding	unknown	no
At1g53540	HSP20-like chaperones superfamily protein	8.12	7.41	3.23	response to heat	heat shock protein	cytoplasm	no
At1g71000	Chaperone DnaJ-domain superfamily protein; FUNCTIONS IN: heat shock protein binding	3.91	3.43	1.94	response to heat	heat shock protein	cytoplasm	no
At2g32120	Heat shock protein 70T-2 (HSP70T-2)	2.60	3.37	2.02	response to heat	heat shock protein	cytoplasm	no
At3g08970	J domain protein localized in ER lumen, shows similarity to HSP40 proteins and is induced by heat stress.	4.69	4.32	3.08	response to heat	heat shock protein	endoplasmatic reticulum	no
At3g46230	HEAT SHOCK PROTEIN 17.4 (HSP17.4)	10.13	7.49	4.88	response to heat	heat shock protein	cytoplasm	no
At4g12400	Hop3, one of the 36 carboxylate clamp (CC)-tetratricopeptide repeat (TPR) proteins with potential to interact with Hsp90/Hsp70 as co-chaperones.	9.12	5.02	4.13	response to heat	heat shock protein	unknown	yes

Gene ID	Gene name and description	C-1	G-1	T-1	GO Biological Process	GO Molecular Function	GO Cellular Component	Acc. spec. in cont.
A4g21320	Encodes heat-stress-associated 32-kD protein. Up-regulated by heat shock. Thermotolerance in a knockout mutant was compromised following a long recovery period (> 24 h) after acclimation heat shock treatment.	2.29	2.69	1.72	response to heat	heat shock protein	nucleus	no
A4g25200	MITOCHONDRION-LOCALIZED SMALL HEAT SHOCK PROTEIN 23.6 (HSP23.6-MITO)	5.64	8.13	3.93	response to heat	heat shock protein	mitochondria	no
A5g09590	Heat shock protein 70 (Hsc70-5)	2.90	2.66	1.86	response to heat	heat shock protein	mitochondria	no
A5g56030	HEAT SHOCK PROTEIN 81-2 (HSP81-2), a member of heat shock protein 90 (HSP90) gene family	2.05	1.25	2.27	response to heat	heat shock protein	cytoplasm	yes
A1g17870	Encodes ETHYLENE-DEPENDENT GRAVITROPISM-DEFICIENT AND YELLOW-GREEN-LIKE 3 (EGY3), a S2P-like putative metalloprotease. Homolog of EGY1 found in cyanobacteria.	4.49	4.09	2.14	response to heat	metallopeptidase activity	mitochondria	no
A3g51910	Member of Heat Stress Transcription Factor (Hsf) family, HSFA7A	6.21	5.31	3.29	response to heat	transcription factor	nucleus	no
A1g66510	AAR2 protein family	1.24	1.73	1.15	response to heat	unknown	chloroplast	no
A5g13200	GRAM domain family protein	2.27	1.63	1.13	response to heat	unknown	cytoplasm	no
A5g64510	TUNICAMYCIN INDUCED 1 (TIN1), a plant-spec-c ER stress-inducible protein. TIN1 mutation affects pollen surface morphology	4.90	3.32	2.94	response to heat	unknown	chloroplast	yes
A1g17860	Kunitz family trypsin and protease inhibitor protein	2.35	1.81	1.33	response to nitrate; nitrate transport	protease inhibitor	extracellular	no
A1g25550	myb-like transcription factor family protein	1.89	1.14	1.07	response to nitrate; nitrate transport	transcription factor	nucleus	no
A1g07350	Encodes a serine/arginine rich-like protein, SR45a. Involved in the regulation of stress-responsive alternative splicing.	2.65	3.44	2.34	RNA binding	alternative splicing	unknown	no
A2g18510	Embryo defective 2444 (emb2444); FUNCTIONS IN: RNA binding, nucleotide binding, nucleic acid binding	1.46	1.29	1.09	RNA binding	unknown	nucleus	no
A5g66880	Encodes a member of SNF1-related protein kinases (SnRK2) whose activity is activated by ionic (salt) and non-ionic (mannitol) osmotic stress. Enzyme involved in the ABA signaling during seed germination, dormancy and seedling growth.	2.01	1.25	0.97	seedling growth	kinase activity	cytoplasm	no
A3g14720	Member of MAP Kinase (MPK19).	1.49	1.15	0.97	signal transduction	MAP kinase activity	nucleus	no
A1g73480	Alpha/beta-Hydrolases superfamily protein	1.67	1.35	0.82	unknown	hydrolase activity	cytoplasm	no
A3g17130	Plant invertase/pectin methylesterase inhibitor superfamily protein	1.89	1.49	1.21	unknown	hydrolase activity	extracellular	no
A1g16260	Wall-associated kinase family protein; FUNCTIONS IN: kinase activity, INVOLVED IN: protein amino acid phosphorylation	0.85	0.93	1.74	unknown	kinase activity	extracellular	no
A5g55830	Concanavalin A-like lectin protein kinase family protein	1.65	2.20	1.36	unknown	kinase activity	plasma membrane	no
A1g56170	Encodes a protein "NUCLEAR FACTOR Y, SUBUNIT C2" (NF-YC2) with similarity to a subunit of the CCAAT promoter motif binding complex of yeast.One of two members of this class (HAP5B) and expressed in vegetative and reproductive tissues	2.36	2.38	1.40	unknown	transcription factor activity	nucleus	no
A1g68670	Myb-like transcription factor family protein	2.12	1.42	1.41	unknown	transcription factor activity	nucleus	no
A2g27580	A20/AN1-like zinc finger family protein	1.84	1.98	1.21	unknown	transcription factor activity	nucleus	no
A3g05800	AtBS1(activation-tagged BRI1 suppressor 1)-interacting factor 1 (AIF1)	0.90	1.25	1.67	unknown	transcription factor activity	nucleus	no
A3g29575	ABI five binding protein 3 (AFP3)	2.48	1.75	1.25	unknown	transcription factor activity	nucleus	yes

Gene ID	Gene name and description	C-1	G-1	T-1	GO Biological Process	GO Molecular Function	GO Cellular Component	Acc. spec. in cont.
At5g01300	PEBP (phosphatidylethanolamine-binding protein) family protein	1.30	1.02	1.59	unknown	transcription factor activity	cytoplasm	no
At5g49330	MYB DOMAIN PROTEIN 111 (MYB111), member of the R2R3 factor gene family.	1.03	1.25	1.70	unknown	transcription factor activity	nucleus	yes
At1g08650	Encodes a phosphoenolpyruvate carboxylase kinase, PPCK1, that is expressed at highest levels in leaves. Expression is induced by light.	2.13	1.33	1.82	unknown	transferase/kinase activity	nucleus	no
At1g75170	Sec14p-like phosphatidylinositol transfer family protein	1.56	1.21	1.02	unknown	transport	plasma membrane	no
At3g19970	Alpha/beta-Hydrolases superfamily protein	2.27	1.32	1.51	unknown	transport	unknown	no
At1g70980	SYNC3, FUNCTIONS IN: in 6 functions; INVOLVED IN: asparaginyl-tRNA aminoacylation, aspartyl-tRNA aminoacylation, translation, tRNA aminoacylation for protein translation	0.90	1.48	0.96	unknown	tRNA aminoacylation	cytoplasm	no
At3g56300	Cysteinyl-tRNA synthetase, class Ia family protein	1.02	1.16	1.62	unknown	tRNA aminoacylation	chloroplast	no
At1g06980	Unknown protein	1.00	1.09	1.76	unknown	unknown	unknown	no
At1g07500	Unknown protein	3.43	2.18	1.80	unknown	unknown	nucleus	no
At1g21550	Calcium-binding EF-hand family protein	5.07	2.87	2.78	unknown	unknown	cytoplasm	no
At1g23140	Expression is upregulated in the shoot of cax1/cax3 mutant.	1.97	0.95	1.28	unknown	unknown	extracellular	no
At1g52690	Late embryogenesis abundant protein (LEA7) family protein	1.19	1.50	0.76	unknown	unknown	unknown	no
At1g61340	Encodes a F-box protein induced by various biotic or abiotic stress.	3.50	2.62	1.43	unknown	unknown	nucleus	no
At1g67360	Rubber elongation factor protein (REF)	2.00	1.58	1.23	unknown	unknown	cytoplasm	no
At2g02410	Unknown protein	1.07	1.31	1.46	unknown	unknown	chloroplast	no
At2g38820	Protein of unknown function (DUF506)	1.37	1.60	0.86	unknown	unknown	nucleus	no
At2g40960	Single-stranded nucleic acid binding R3H protein	1.71	1.05	1.01	unknown	unknown	nucleus	no
At2g42530	Cold regulated 15b (COR15B)	1.16	0.90	2.03	unknown	unknown	chloroplast	no
At3g05932	Potential natural antisense gene, locus overlaps with AT3G05930	0.90	0.82	1.46	unknown	unknown	unknown	no
At3g07150	Unknown protein	1.85	1.77	1.25	unknown	unknown	unknown	no
At3g10020	Unknown protein	3.21	3.75	1.71	unknown	unknown	nucleus	no
At3g21660	Unknown protein	1.66	1.23	0.98	unknown	unknown	nucleus	no
At3g24460	Ser/nc-domain containing serine and sphingolipid biosynthesis protein	0.79	0.69	1.24	unknown	unknown	plasma membrane	no
At3g25233	Unknown protein	0.98	0.98	1.63	unknown	unknown	unknown	no
At4g09750	NAD(P)-binding Rossmann-fold superfamily protein	1.73	1.08	1.50	unknown	unknown	unknown	yes

Gene ID	Gene name and description	C-1	G-1	T-1	GO Biological Process	GO Molecular Function	GO Cellular Component	Acc. spec. in cont.
At4g13800	Unknown protein	1.46	0.88	1.56	unknown	unknown	plasma membrane	no
At4g15420	Unknown protein	1.72	1.72	1.09	unknown	unknown	nucleus	no
At4g15765	FAD/NAD(P)-binding oxidoreductase family protein	0.94	1.08	1.55	unknown	unknown	unknown	no
At4g31875	Unknown protein	1.51	1.12	2.18	unknown	unknown	mitochondria	no
At4g34550	Unknown protein	1.27	1.02	1.87	unknown	unknown	unknown	no
At4g35750	SEC14 cytosolic factor family protein / phosphoglyceride transfer family protein	1.94	1.05	1.37	unknown	unknown	cytoplasm	no
At5g03210	Encodes a small polypeptide DBP-INTERACTING PROTEIN 2 (DIP2) contributing to resistance to potyvirus.	4.74	2.19	1.28	unknown	unknown	nucleus	yes
At5g08710	Regulator of chromosome condensation (RCC1) family protein	1.11	1.25	1.55	unknown	unknown	unknown	no
At5g09225	Unknown protein	1.58	1.14	1.67	unknown	unknown	mitochondria	no
At5g13210	Unknown protein	1.41	1.04	0.90	unknown	unknown	chloroplast	no
At5g20790	Unknown protein	2.86	1.01	1.28	unknown	unknown	extracellular	yes
At5g40790	Unknown protein	1.43	1.07	0.67	unknown	unknown	nucleus	no
At5g41740	Disease resistance protein (TIR-NBS-LRR class) family, FUNCTIONS IN: transmembrane receptor activity, nucleoside-triphosphatase activity, nucleotide binding, ATP binding	2.04	1.02	1.16	unknown	unknown	nucleus	no
At5g41750	Disease resistance protein (TIR-NBS-LRR class) family, FUNCTIONS IN: transmembrane receptor activity, nucleoside-triphosphatase activity, nucleotide binding, ATP binding	1.65	0.96	1.06	unknown	unknown	nucleus	no
At5g52420	Unknown protein	1.21	1.08	1.91	unknown	unknown	endoplasmic reticulum	no
At5g53048	Potential natural antisense gene, locus overlaps with AT5G53050	1.76	1.37	1.17	unknown	unknown	unknown	no
At5g64870	SPFH/Band 7/PHB domain-containing membrane-associated protein family	1.61	1.02	1.30	unknown	unknown	plasma membrane	no

Table S4. Accession specific genes responsive to irradiance increase; genes more than 1.4-fold down-regulated at 1 hour after light onset when comparing plants exposed to increased irradiance to control plants. Irradiance in one, two or three accessions of Col-0, Ga-0 and Ts-1 and differentially (P=0.05) down-regulated between two or three accessions when comparing Col-0, Ga-0 and Ts-1.

Unlogged fold changes are shown, grey shaded values are <1.4 fold down-regulated, green shading indicates accession-specific difference in expression present in control conditions independent of irradiance increase. Acc. spec. in cont. = Accession-specific difference in expression present in control conditions, independent of irradiance increase

Gene ID	Gene name and description	C-1	G-1	T-1	GO Biological Process	GO Molecular Function	GO Cellular Component	Acc. spec. in cont.
At1g71030	Encodes a putative myb family transcription factor, MYBL2. In contrast to most other myb-like proteins its myb domain consists of a single repeat. A proline-rich region potentially involved in transactivation is found in the C-terminal part of the protein. Its transcript accumulates mainly in leaves.	0.62	0.31	0.36	anthocyanin biosynthesis	transcription factor activity	nucleus	yes
At4g00150	Belongs to one of the LOM (LOST MERISTEMS) genes, AT2G45160 (LOM1), AT3G60630 (LOM2) and AT4G00150 (LOM3). LOM1 and LOM2 promote cell differentiation at the periphery of shoot meristems and help to maintain their polar organization.	0.49	0.62	0.78	cell organization and biogenesis	transcription factor activity	nucleus	no
At2g40610	Member of Alpha-Expansin Gene Family. Involved in the formation of nematode-induced syncytia in roots of Arabidopsis thaliana.	0.48	0.53	0.85	cell organization and biogenesis	unknown	extracellular	no
At2g19810	Encodes Oxidation-related Zinc Finger 1 (OZF1), a plasma membrane protein involved in oxidative stress.	1.16	0.77	0.61	chlorophyll catabolic processes	transcription factor activity	nucleus	no
At3g26740	Transcripts are differentially regulated at the level of mRNA stability at different times of day controlled by the circadian clock. mRNAs are targets of the mRNA degradation pathway mediated by the downstream (DST) instability determinant.	0.82	0.54	0.44	circadian rhythm	unknown	chloroplast	yes
At5g49740	Encodes a chloroplast ferric chelate reductase, FRO7. Shows differential splicing and has three different mRNA products. Expressed in the shoot, flower and cotyledon.	0.52	0.89	0.49	electron transport	ferric chelate reductase	chloroplast	yes
At3g03470	Member of CYP89A	0.70	0.66	1.40	oxidation-reduction process	unknown	unknown	yes
At4g25470	Encodes a member of the DREB subfamily A-1 of ERF/AP2 transcription factor family (CBF2). The protein contains one AP2 domain. There are six members in this subfamily including CBF1, CBF2, and CBF3. This gene is involved in response to low temperature, abscisic acid, and circadian rhythm.	1.36	0.66	0.82	photosynthesis, drought response	transcription factor activity	nucleus	no
At5g61590	encodes a member of the ERF (ethylene response factor) subfamily B-3 of ERF/AP2 transcription factor family. The protein contains one AP2 domain. There are 18 members in this subfamily including ATERF-1, ATERF-2, AND ATERF-5.	0.93	0.64	0.65	photosynthesis, drought response	transcription factor activity	nucleus	no
At4g15660	Thioredoxin superfamily protein; FUNCTIONS IN: electron carrier activity, arsenate reductase (glutaredoxin) activity, protein disulfide oxidoreductase activity; INVOLVED IN: cell redox homeostasis	0.68	1.22	1.37	redox homeostasis	arsenate reductase	cytoplasm	yes
At2g18050	Encodes HISTONE H1-3 (HIS1-3); a structurally divergent linker histone whose gene expression is induced by dehydration and ABA.	1.17	0.72	0.49	response to drought	transcription factor activity	nucleus	yes
At5g14120	Major facilitator superfamily protein	0.68	0.89	1.24	response to nitrate	unknown	vacuole	no
At4g03110	Encodes a putative RNA-binding protein that is located in the cytoplasm and is involved in the hypersensitive response and positively regulates salicylic acid-mediated immunity.	0.68	1.00	1.01	RNA binding	RNA binding	cytoplasm	no
At3g09160	RNA-binding (RRM/RBD/RNP motifs) family protein	0.64	0.70	0.98	RNA binding	transcription factor activity	nucleus	yes
At5g65310	Encodes a class I HDZip (homeodomain-leucine zipper) protein that is a positive regulator of ABA-responsiveness, mediating the inhibitory effect of ABA on growth during seedling establishment.	0.75	0.64	0.51	seedling growth	transcription factor activity	nucleus	no
At1g62290	Encodes a member of the proline-rich extensin-like receptor kinase (PERK) family. This family consists of 15 predicted receptor kinases (PMID: 15653807).	0.69	0.83	1.03	unknown	kinase activity	plasma membrane	no
At2g40970	MYBC1	1.14	0.67	0.73	unknown	transcription factor activity	nucleus	no
At3g56970	Encodes a member of the basic helix-loop-helix transcription factor family protein.	0.99	0.69	0.40	unknown	transcription factor activity	nucleus	yes
At5g15310	Member of the R2R3 factor gene family, MYB16.	0.68	0.93	1.09	unknown	transcription factor activity	nucleus	no

Gene ID	Gene name and description	C-1	G-1	T-1	GO Biological Process	GO Molecular Function	GO Cellular Component	Acc. spec. in cont.
At5g53200	TRIPTYCHON (TRY)	0.60	0.82	1.06	unknown	transcription factor activity	nucleus	no
At1g22160	Unknown protein.	1.44	0.81	0.66	unknown	unknown	mitochondria	no
At1g72430	SAUR-like auxin-responsive protein family	0.58	0.93	1.13	unknown	unknown	nucleus	yes
At2g17230	EXORDIUM like 5 (EXL5)	0.64	0.88	0.96	unknown	unknown	extracellular	no
At3g06145	Unknown protein	0.54	0.57	0.97	unknown	unknown	mitochondria	yes
At3g45970	Member of EXPANSIN-LIKE.	0.59	0.84	1.11	unknown	unknown	extracellular	no
At4g17245	RING/U-box superfamily protein	0.54	0.65	0.83	unknown	unknown	unknown	no
At5g10150	Unknown protein	0.48	0.58	0.74	unknown	unknown	nucleus	no
At5g18020	SAUR-like auxin-responsive protein family	0.47	0.73	0.98	unknown	unknown	mitochondria	yes
At5g28919	Unknown protein	0.67	1.04	1.12	unknown	unknown	mitochondria	yes
At5g40800	Unknown protein	1.39	1.02	0.58	unknown	unknown	unknown	yes

Table S5. Time specific genes responsive to irradiance increase; genes more than 2.0-fold up-regulated in Col-0 when comparing plants exposed to increased irradiance to control plants. at 1, 3.5 or 25 hours after the irradiance increase and differentially (P=0.05) up-regulated between two or three time-points when comparing 1, 3.5, and 25 hours. Unlogged fold changes are shown, grey shaded values are >2.0 fold up-regulated, green shading indicates accession-specific difference in expression present in control conditions independent of irradiance increase. Time spec. in cont. = Time-specific difference in expression present in control conditions, independent of irradiance increase

Gene ID	Gene name and description	C-1	C-3.5	C-25	GO Biological Process	GO Molecular Function	GO Cellular Component	Time spec. in cont.
At3g14440	Encodes 9-cis-epoxycarotenoid dioxygenase, a key enzyme in the biosynthesis of abscisic acid. Regulated in response to drought and salinity. Expressed in roots, flowers and seeds. Localized to the chloroplast stroma and thylakoid membrane.	2.56	1.19	2.10	abscisic acid biosynthesis	oxidation-reduction process	chloroplast	no
At2g29090	Encodes a protein with ABA 8'-hydroxylase activity, involved in ABA catabolism. Member of the CYP707A gene family.	1.05	2.10	1.17	abscisic acid catabolism	oxidoreductase activity	chloroplast	no
At4g39950	Belongs to cytochrome P450 and is involved in tryptophan metabolism. Converts Trp to indo-3-acetaldoxime (IAOx), a precursor to IAA and indole glucosinolates.	1.03	2.20	1.15	amino acid metabolism	cell organization and biogenesis	chloroplast	no
At1g76130	alpha-amylase, putative / 1,4-alpha-D-glucan glucanohydrolase	0.91	2.03	0.95	carbohydrate metabolism	enzyme, alpha amylase	extracellular region	yes
At1g48100	Pectin lyase-like superfamily protein	1.62	2.22	1.84	carbohydrate metabolism	enzyme, pectin lyase	extracellular region	yes
At3g28007	SWEET4, a nodulin MtN3 family protein	0.86	2.13	0.88	carbohydrate metabolism	nodulin family protein	plasma membrane	no
At4g09020	Encodes an isoamylase-like protein. Mutant studies show that the gene is strongly involved in starch breakdown. A GUS-protein fusion product was shown to localize to the surface of chloroplastic structures reminiscent of starch granules. In the mutants, the chloroplastic α-amylase AMY3 is upregulated.	1.20	2.10	1.86	carbohydrate metabolism	starch degradation	chloroplast	yes
At4g15210	cytosolic beta-amylase expressed in rosette leaves and inducible by sugar. RAM1 mutants have reduced beta amylase in leaves and stems.	1.62	7.15	5.40	carbohydrate metabolism	starch degradation	chloroplast	yes
At4g17090	Encodes a beta-amylase targeted to the chloroplast. Transgenic BMY8 RNAi lines fail to accumulate maltose during cold shock suggesting that maltose accumulation coincides with BMY8 expression. Apart from maltose, the sugar content of the RNAi lines were similar to wildtype (glucose and sucrose unaffected).	0.93	2.19	0.84	carbohydrate metabolism	starch degradation	chloroplast	yes
At5g13170	Encodes a member of the SWEET sucrose efflux transporter family proteins.	1.48	2.57	3.61	carbohydrate metabolism	transporter	plasma membrane	no
At1g61800	glucose6-Phosphate/phosphate transporter 2 (GPT2)	4.13	12.55	6.76	carbohydrate metabolism	transporter glucose6-phosphate	chloroplast	yes
At1g57590	Pectinacetylesterase family protein	1.19	2.44	1.28	cell organization	cell organization and biogenesis	extracellular region	yes
At4g23990	encodes a protein similar to cellulose synthase	1.27	2.16	1.47	cell organization	cell organization and biogenesis	plasma membrane	yes
At4g26150	Encodes a member of the GATA factor family of zinc finger transcription factors. Modulate chlorophyll biosynthesis and glutamate synthase (GLU1/Fd-GOGAT) expression.	0.77	2.72	0.48	chlorophyll biosynthesis	transcription factor activity	nucleus	yes
At1g66090	Disease resistance protein (TIR-NBS class)	2.37	0.84	1.77	defense response	defense response	chloroplast	no
At4g03960	Encodes an atypical dual-specificity phosphatase involved in the negative regulation of defense response to a bacterial pathogen, P. syringae pv. tomato.	2.27	1.17	1.46	defense response	hydrolase activity	cytoplasm	no
At4g08870	Encodes one of the two arginase in the genome. Gene expression is enhanced by methyl jasmonate treatment. It is involved in the defense response to B.cinerea.	1.02	2.27	1.37	defense response	hydrolase activity	chloroplast	no
At5g41740	Disease resistance protein (TIR-NBS-LRR class) family	2.04	0.91	1.32	defense response	signal transduction	nucleus	yes

Gene ID	Gene name and description	C-1	C-3.5	C-25	GO Biological Process	GO Molecular Function	GO Cellular Component	Time spec. in cont.
At2g38470	Member of the plant WRKY transcription factor family. Regulates the antagonistic relationship between defense pathways mediating responses to P. syringae and necrotrophic fungal pathogens. Located in nucleus. Involved in response to various abiotic stresses - especially salt stress.	2.47	0.78	1.81	defense response	transcription factor activity	nucleus	yes
At3g53830	Regulator of chromosome condensation (RCC1) family protein	2.07	1.10	1.64	DNA modification	chromatin binding	unknown	no
At4g27410	Encodes a NAC transcription factor induced in response to desiccation. It is localized to the nucleus and acts as a transcriptional activator in ABA-mediated dehydration response.	2.15	0.91	2.20	drought response	transcription factor activity	nucleus	no
At4g10040	Encodes cytochrome c. Promoter directs preferential expression in vascular tissues of cotyledons, leaves, roots, and hypocotyls, and in anthers.	1.42	2.05	1.35	electron transport	electron carrier activity	mitochondria	no
At5g25450	Cytochrome b/d ubiquinol oxidase, 14kDa subunit	3.63	1.43	2.40	electron transport	mitochondrial electron transport	mitochondria	no
At1g56600	GolS2, a galactinol synthase that catalyzes the formation of galactinol from UDP-galactose and myo-inositol. GolS2 transcript levels rise in response to methyl viologen, an oxidative damage-inducing agent. Plants over-expressing GolS2 have increased tolerance to salt, chilling, and high-light stress.	2.49	1.23	1.36	formation of galactinol	transferase activity	nucleus	yes
At1g06000	encodes a flavonol-7-O-rhamnosyltransferase involved in the formation of rhamnosylated flavonols	1.36	2.03	1.58	formation of rhamnosylated flavonols	transferase activity	nucleus	no
At3g16910	Encodes a peroxisomal protein with acetyl-CoA synthetase activity that is responsible for the activation of acetate for entry into the glyoxylate cycle.	1.13	2.25	1.09	glyoxylate cycle	nucleotide binding	peroxisome	yes
At3g25770	Encodes allene oxide cyclase. One of four genes in Arabidopsis that encode this enzyme, which catalyzes an essential step in jasmonic acid biosynthesis.	1.12	1.16	2.38	jasmonic acid biosynthesis	unknown	chloroplast	yes
At2g17040	Member of the NAC transcription factor family and more specifically, the ONAC022 subfamily. Involved in leaf and inflorescence stem morphogenesis.	2.29	0.75	1.98	leaf morphogenesis	transcription factor activity	nucleus	yes
At1g32900	Encodes GRANULE BOUND STARCH SYNTHASE 1 (GBSS1), a UDP-Glycosyltransferase superfamily protein	0.97	2.44	0.92	lipid remodelling	glycosyl transferase	chloroplast	yes
At1g58520	RXW8; FUNCTIONS IN: hydrolase activity, acting on ester bonds, lipase activity	1.23	2.42	1.13	lipid remodelling	hydrolase activity	chloroplast	yes
At2g37870	Bifunctional inhibitor/lipid-transfer protein/seed storage 2S albumin superfamily protein	1.25	2.22	1.16	lipid remodelling	lipid binding	extracellular region	no
At2g42540	Encodes COLD-REGULATED 15A (COR15A), a cold regulated gene whose product is targeted to the chloroplast. Cor15am protects stromal proteins from aggregation under various stress conditions.	1.88	2.36	1.27	lipid remodelling	lipid binding	chloroplast	yes
At5g59320	LIPID TRANSFER PROTEIN 3 (LTP3); predicted to encode a PR (pathogenesis-related) protein. Belongs the lipid transfer protein (PR-14) family.	2.11	4.65	1.85	lipid remodelling	lipid binding	extracellular region	yes
At5g20410	Encodes MONOGALACTOSYLDIACYLGLYCEROL SYNTHASE 2 (MGD2); a type B monogalactosyldiacylglycerol (MGDG) synthase. Strongly induced by phosphate deprivation, and in non-photosynthetic tissues. Does not contribute to galactolipid synthesis under Pi-sufficient conditions but does under Pi starvation.	2.22	0.83	1.08	lipid remodelling	MGDG synthesis	chloroplast	no
At4g33030	Encodes SULFOQUINOVOSYLDIACYLGLYCEROL 1 (SQD1); involved in sulfolipid biosynthesis	2.31	1.45	1.65	lipid remodelling	SQDG synthesis	chloroplast	no
At5g01220	Encodes SULFOQUINOVOSYLDIACYLGLYCEROL 2 (SQD2); a UDP-sulfoquinovose:DAG sulfoquinovosyltransferase that is involved in sulfolipid biosynthesis and whose expression is responsive to both phosphate (Pi) and phosphite (Phi) in both roots and shoots.	2.32	0.80	1.12	lipid remodelling	SQDG synthesis	chloroplast	no
At3g02040	Encodes SENESCENCE-RELATED GENE 3 (SRG3), a member of the glycerophosphodiester phosphodiesterase (GDPD) family.	6.54	0.97	1.85	lipid remodelling	transcription factor activity	chloroplast	yes
At5g20150	Encodes SPX DOMAIN GENE 1 (SPX1). Expression is upregulated in the shoot of cax1/cax3 mutant. Additionally, its expression is responsive to both phosphate (Pi) and phosphite (Phi) in both roots and shoots.	4.30	0.99	1.07	lipid remodelling	unknown	nucleus	yes
At1g17870	Encodes ETHYLENE-DEPENDENT GRAVITROPISM-DEFICIENT AND YELLOW-GREEN-LIKE 3 (EGY3); a S2P-like putative metalloprotease.	4.49	1.31	1.81	metal ion binding	metalloprotease	chloroplast	no
At3g49320	Metal-dependent protein hydrolase	1.08	2.39	1.61	metal ion binding	protein hydrolase	mitochondria	no
At5g17450	HEAVY METAL ASSOCIATED ISOPRENYLATED PLANT PROTEIN 21 (HIPP21); heavy metal transport/detoxification superfamily protein	1.07	2.35	1.26	metal ion binding	transporter	nucleus	no

Gene ID	Gene name and description	C-1	C-3.5	C-25	GO Biological Process	GO Molecular Function	GO Cellular Component	Time spec. in cont.
At5g52750	Heavy metal transport/detoxification superfamily protein	1.86	0.87	2.01	metal ion binding	transporter	nucleus	no
At3g03780	Encodes a cytosolic methionine synthase, involved in methionine regeneration via the activated methyl cycle (or SAM cycle)	1.44	2.01	1.57	methionine regeneration	transferase activity	chloroplast	yes
At3g17609	Encodes a homolog of HY5 (HYH). Involved in phyB signaling pathway.	1.24	2.16	0.92	photoreceptor response	HY5 homologue	nucleus	yes
At3g22840	Encodes EARLY LIGHT-INDUCABLE PROTEIN (ELIP1)	2.97	9.66	5.03	photosynthesis	chlorophyll binding	chloroplast	yes
At4g14690	Encodes EARLY LIGHT-INDUCIBLE PROTEIN 2 (ELIP2)	2.95	5.11	5.54	photosynthesis	chlorophyll binding	chloroplast	yes
At1g69200	Encodes a fructokinase-like protein (AT3G54090/FLN1, AT1G69200/FLN2; mutants display mutant chloroplast development, general plant growth and development defects and defects in PEP-dependent transcription.	0.92	1.42	2.27	photosynthesis	chloroplast biogenesis	chloroplast	no
At3g54090	Encodes a fructokinase-like protein (AT3G54090/FLN1, AT1G69200/FLN2), a member of the pfkB-carbohydrate kinase family. FLN1 and FLN2 are potential plastidial thioredoxin z (TRX z) targets. Mutants display mutant chloroplast development, general plant growth and development defects and defects in PEP-dependent transcription.	0.90	1.31	2.45	photosynthesis	chloroplast biogenesis	chloroplast	no
At2g28900	Encodes AtOEP16, a 16-KDa plastid outer membrane protein involved in plastid import of protochlorophyllide oxidoreductase A.	1.01	2.19	1.18	photosynthesis	chloroplast protein import	chloroplast	no
At3g13470	Encodes a subunit of chloroplasts chaperonins that are involved in mediating the folding of newly synthesized, translocated, or stress-denatured proteins.	2.02	1.60	2.42	photosynthesis	chloroplast protein import	chloroplast	no
At2g04530	Encodes a protein with RNAse Z activity suggesting a role in tRNA processing. Protein contains a signal sequence for import into the chloroplast.	0.91	1.58	2.23	photosynthesis	chloroplast transcription/translation	chloroplast	no
At2g23910	NAD(P)-binding Rossmann-fold superfamily protein	1.20	1.03	2.77	photosynthesis	flavonoid biosynthesis	unknown	no
At3g29590	A3g29590 (At5MAT) encodes a malonyl-CoA anthocyanidin 5-O-glucoside-6"-O-malonyltransferase that is coordinately expressed with a epistatic 5-O-anthocyanin glucosyltransferase (At4g14090). The enzyme is involved in the malonylation of anthocyanins in Arabidopsis.	1.17	1.28	2.66	photosynthesis	flavonoid biosynthesis	cytoplasm	no
At4g14090	The At4g14090 encodes a anthocyanidin 5-O-glucosyltransferase specifically glucosylating the 5-position of the flavonoid A-ring.	1.07	1.13	2.09	photosynthesis	flavonoid biosynthesis	chloroplast	no
At4g22880	encodes leucoanthocyanidin dioxygenase, which is involved in proanthocyanin biosynthesis. Mutant analysis suggests that this gene is also involved in vacuole formation.	1.97	1.35	7.59	photosynthesis	flavonoid biosynthesis	cytoplasm	yes
At5g07990	Required for flavonoid 3' hydroxylase activity. Enzyme abundance relative to CHS determines Quercetin/Kaempferol metabolite ratio.	1.21	1.72	4.03	photosynthesis	flavonoid biosynthesis	extracellular region	no
At5g08640	Encodes FLAVONOL SYNTHASE 1 (FLS1) that catalyzes formation of flavonols from dihydroflavonols. Co-expressed with CHI and CHS (qRT-PCR).	1.40	2.16	2.22	photosynthesis	flavonoid biosynthesis	cytoplasm	no
At5g13930	Encodes a chalcone synthase (CHS), a key enzyme involved in the biosynthesis of flavonoids. Required for the accumulation of purple anthocyanins in leaves and stems. Also involved in the regulation of auxin transport and the modulation of root gravitropism.	1.29	1.99	2.04	photosynthesis	flavonoid biosynthesis	cytoplasm	yes
At5g17220	Encodes GLUTATHIONE S-TRANSFERASE PHI 12 (GSTF12) belonging to the phi class of GSTs. Likely to function as a carrier to transport anthocyanin from the cytosol to tonoplasts.	1.91	1.29	6.66	photosynthesis	flavonoid biosynthesis	cytoplasm	yes
At5g42800	dihydroflavonol reductase. Catalyzes the conversion of dihydroquercetin to leucocyanidin in the biosynthesis of anthocyanins. Not expressed in roots (qRT-PCR).	1.56	1.39	6.68	photosynthesis	flavonoid biosynthesis	endoplasmic reticulum	yes
At5g48880	Encodes a peroxisomal 3-keto-acyl-CoA thiolase 2 precursor. EC2.3.1.16 thiolases. AT5G48880.1 is named PKT1 and AT5G48880.2 is named PKT2.	1.16	1.48	2.20	photosynthesis	flavonoid biosynthesis	peroxisome	yes
At5g62210	Embryo-specific protein 3, (ATS3)	1.80	1.89	4.23	photosynthesis	flavonoid biosynthesis	anchored component of membrane	no
At3g51240	Encodes flavanone 3-hydroxylase that is coordinately expressed with chalcone synthase and chalcone isomerases. Regulates flavonoid biosynthesis. Not responsive to auxin or ethylene stimulus (qRT-PCR).	1.64	2.43	1.75	photosynthesis	flavonoid biosynthesis	cytoplasm	yes
At5g54060	Encodes a anthocyanin 3-O-glucoside; 2"-O-xylosyl-transferase involved in anthocyanin modification that converts cyanidin 3-O-glucoside to cyanidin 3-O-xylosyl(1->2)glucoside. Its preferred sugar donor is UDP-xylose.	1.20	1.26	2.70	photosynthesis	glucose-flavonoid glucosyl transferase	chloroplast	no

Gene ID	Gene name and description	C-1	C-3,5	C-25	GO Biological Process	GO Molecular Function	GO Cellular Component	Time spec. in cont.
At2g37770	Encodes an NADPH-dependent aldo-keto reductase that can act on a wide variety of substrates in vitro including saturated and unsaturated aldehydes, steroids, and sugars. GFP-tagged AKR4C9 localizes to the chloroplast where it may play a role in detoxifying reactive carbonyl compounds that threaten to impair the photosynthetic process.	1.19	2.37	1.71	photosynthesis	H2O2 scavenging	chloroplast	no
At3g03630	Encodes a protein that possesses S-sulfocysteine synthase activity and lacks O-acetylserine(thiol)lyase activity.	0.87	1.02	2.10	photosynthesis	H2O2 scavenging	chloroplast	no
At4g31870	Encodes GLUTATHIONE PEROXIDASE 7 (GPX7)	1.98	3.55	2.51	photosynthesis	H2O2 scavenging	chloroplast	yes
At5g14760	At5g14760 encodes for L-aspartate oxidase involved in the early steps of NAD biosynthesis. In contrary to the E.C 1.4.3.16 (l-aspartate oxidase - deaminating) the enzyme catalyzes the reaction L-aspartate + O2 = iminoaspartate (alpha-iminosuccinate) + H2O2	0.91	2.08	0.75	photosynthesis	NAD metabolism	mitochondria	yes
At5g24770	VEGETATIVE STORAGE PROTEIN 2 (VSP2); has acid phosphatase activity dependent on the presence of divalent cations (Mg2+, Co2+, Zn2+, Mn2+) and anti-insect activity. Insects fed with the protein show a retarded development. Induced in response to abscisic acid, jasmonic acid, salt, water deficiency and wounding.	1.15	3.65	1.99	photosynthesis	nutrient mobilization	chloroplast	no
At5g24780	VEGETATIVE STORAGE PROTEIN 1 (VSP1); an acid phosphatase similar to soybean vegetative storage proteins. Gene expression is induced by wounding and jasmonic acid.	1.26	7.95	3.06	photosynthesis	nutrient mobilization	chloroplast	no
At4g04020	Fibrillin precursor protein. The fibrillin preprotein, but not the mature protein interacts with ABI2. Regulated by abscisic acid response regulators. Involved in abscisic acid-mediated photoprotection.	2.26	1.87	1.33	photosynthesis	photoprotection	chloroplast	yes
At1g27730	Encodes SALT TOLERANCE ZINC FINGER 10 (ZAT10); acts as a transcriptional repressor and is responsive to chitin oligomers. Also involved in response to photooxidative stress.	3.15	1.09	2.38	photosynthesis	photoprotection, transcription factor	nucleus	yes
At5g59820	RESPONSIVE TO HIGH LIGHT 41 (RHL41); encodes a zinc finger protein involved in high light and cold acclimation. Overexpression of this putative transcription factor increases the expression level of 9 cold-responsive genes and represses the expression level of 15 cold-responsive genes, including CBF genes. Also, lines overexpressing this gene exhibits a small but reproducible increase in freeze tolerance. Because of the repression of the CBF genes by the overexpression of this gene, the authors speculate that this gene may be involved in negative regulatory circuit of the CBF pathway	2.48	0.99	1.55	photosynthesis	transcription factor activity	nucleus	yes
At2g47460	"MYB12 belongs to subgroup 7 of the R2R3-MYB family. It strongly activates the promoters of chalcone synthase (CHS), flavanone 3-hydroxylase (F3H), flavonol synthase (FLS) and - to a lesser extent - chalcone flavanone isomerase (CHI), but cannot activate the promoters of flavonoid-3'hydroxylase (F3'H) and dihydroflavonol 4-reductase (DF).	1.82	1.17	3.04	photosynthesis	transcription factor activity, flavonoid biosynthesis	nucleus	no
At1g64570	Encodes PHYTYL ESTER SYNTHASE 1 (PES1); a protein with phytyl ester synthesis and diacylglycerol acyltransferase activities that is involved in the deposition of free phytol and free fatty acids in the form of phytyl esters in chloroplasts, a process involved in maintaining the integrity of the photosynthetic membrane during abiotic stress and senescence.	1.12	2.34	1.44	photosynthesis	photoprotection	chloroplast	no
At1g28370	encodes a member of the ERF (ethylene response factor) subfamily B-1 of ERF/AP2 transcription factor family.	2.68	1.22	2.13	photosynthesis; drought response	transcription factor activity	nucleus	yes
At1g74930	encodes a member of the DREB subfamily A-5 of ERF/AP2 transcription factor family.	3.85	0.85	3.55	photosynthesis; drought response	transcription factor activity	nucleus	no
At2g20880	Encodes ERF53, a drought-induced transcription factor. Belongs to the AP2/ERF superfamily.	2.84	1.62	1.93	photosynthesis; drought response	transcription factor activity	nucleus	no
At4g17500	Encodes a member of the ERF (ethylene response factor) subfamily B-3 of ERF/AP2 transcription factor family (ATERF-1). The protein contains one AP2 domain. There are 18 members in this subfamily including ATERF-1, ATERF-2, AND ATERF-5.	1.64	0.92	2.11	photosynthesis; drought response	transcription factor activity	nucleus	no
At5g05410	Encodes DRE-BINDING PROTEIN 2A (DREB2A); a transcription factor that specifically binds to DRE/CRT cis elements (responsive to drought and low-temperature stress). Belongs to the DREB subfamily A-2 of ERF/AP2 transcription factor family (DREB2A)	3.64	1.42	1.46	photosynthesis; drought response	transcription factor activity	nucleus	yes
At5g11590	encodes a member of the DREB subfamily A-4 of ERF/AP2 transcription factor family.	1.48	2.21	1.33	photosynthesis; drought response	transcription factor activity	nucleus	no

149

Gene ID	Gene name and description	C-1	C-3.5	C-25	GO Biological Process	GO Molecular Function	GO Cellular Component	Time spec. in cont.
At5g26860	Encodes a member of the Lon protease-like proteins (Lon1/At5g26860, Lon2/At5g47040, Lon3/At3g05780, Lon4/At3g05790). Lon is a multifunctional ATP-dependent protease which exists in bacteria, archaea and within organelles in eukaryotic cells. Lon proteases are responsible for the degradation of abnormal, damaged and unstable proteins.	1.10	2.40	1.55	protein metabolism	cell organization and biogenesis	mitochondria	no
At3g10020	Unknown protein	3.21	0.87	1.50	respiration	anaerobic respiration	nucleus	no
At1g53540	HSP20-like chaperones superfamily protein	8.12	3.32	3.45	response to heat	respiration	cytoplasm	no
At1g54050	HSP20-like chaperones superfamily protein	3.23	1.56	1.98	response to heat	chaperone	cytoplasm	yes
At1g71000	Chaperone DnaJ-domain superfamily protein	3.91	1.16	1.23	response to heat	chaperone	cytoplasm	no
At2g46240	A member of Arabidopsis BAG (Bcl-2-associated athanogene) proteins, plant homologs of mammalian regulators of apoptosis. Expression of BAG6 in leaves was strongly induced by heat stress.	7.26	1.60	3.05	response to heat	chaperone	nucleus	no
At5g48570	Encodes one of the 36 carboxylate clamp (CC)-tetratricopeptide repeat (TPR) proteins (Prasad 2010, PubMed ID: 20856808) with potential to interact with Hsp90/Hsp70 as co-chaperones.	9.47	3.27	4.30	response to heat	chaperone	cytoplasm	yes
At4g26780	Unknown protein	1.48	1.76	2.00	response to heat	chlorophyll biosynthesis	chloroplast	no
At2g26150	Encodes HEAT SHOCK TRANSCRIPTION FACTOR A2 (HSFA2); member of Heat Stress Transcription Factor (Hsf) family. Involved in response to misfolded protein accumulation in the cytosol.	3.69	1.63	1.81	response to heat	heat shock factor	chloroplast	yes
At3g51910	HEAT SHOCK TRANSCRIPTION FACTOR A7A (HSFA7A); member of Heat Stress Transcription Factor (Hsf) family	6.21	1.10	2.18	response to heat	heat shock factor	nucleus	yes
At4g36990	HEAT SHOCK FACTOR 4 (HSF4); encodes a protein whose sequence is similar to heat shock factors that regulate the expression of heat shock proteins. Transcript level is increased in response to heat shock. However, overexpression of this gene did not result in the increase of decrease of heat shock proteins.	2.60	1.66	1.74	response to heat	heat shock factor	nucleus	yes
At1g59860	HSP20-like chaperones superfamily protein	4.55	1.42	2.54	response to heat	heat shock protein	cytoplasm	no
At1g74310	Encodes ClpB1, which belongs to the Casein lytic proteinase/heat shock protein 100 (Clp/Hsp100) family.	5.50	2.14	2.55	response to heat	heat shock protein	chloroplast	yes
At2g19310	HSP20-like chaperones superfamily protein	2.02	1.63	1.45	response to heat	heat shock protein	cytoplasm	no
At2g20560	DNAJ heat shock family protein	4.46	1.66	2.40	response to heat	heat shock protein	cytoplasm	yes
At2g25140	Encodes ClpB4, which belongs to the Casein lytic proteinase/heat shock protein 100 (Clp/Hsp100) family.	3.13	1.58	2.12	response to heat	heat shock protein	chloroplast	no
At2g29500	HSP20-like chaperones superfamily protein	14.12	9.75	6.82	response to heat	heat shock protein	cytoplasm	no
At3g32120	heat shock protein 70T-2 (HSP70T-2)	2.60	1.36	2.00	response to heat	heat shock protein	cytoplasm	no
At3g08970	J domain protein localized in ER lumen; shows similarity to HSP40 proteins and is induced by heat stress.	4.69	1.58	2.51	response to heat	heat shock protein	endoplasmic reticulum	no
At3g09350	Encodes one of the Arabidopsis orthologs of the human Hsp70-binding protein 1 (HspBP-1)	4.70	1.31	1.50	response to heat	heat shock protein	cytoplasm	yes
At3g25230	Encodes a high molecular weight member of the FKBP binding protein (FKBP) family. It has three FKBP12-like domains, tetratricopeptide repeats, and a putative calmodulin binding domain. Modulates thermotolerance by interacting with HSP90.1 and affecting the accumulation of HsfA2-regulated sHSPs.	2.58	1.25	1.58	response to heat	heat shock protein	cytoplasm	no
At3g46230	HEAT SHOCK PROTEIN 17.4 (HSP17.4); member of the class I small heat-shock protein (sHSP) family, which accounts for the majority of sHSPs in maturing seeds	10.13	4.69	4.98	response to heat	heat shock protein	cytoplasm	no

Gene ID	Gene name and description	C-1	C-3,5	C-25	GO Biological Process	GO Molecular Function	GO Cellular Component	Time spec. in cont.
A14g12400	Encodes HOP3 (Hop3), one of the 36 carboxylate clamp (CC)-tetratricopeptide repeat (TPR) proteins (Prasad 2010, Pubmed ID: 20856808) with potential to interact with Hsp90/Hsp70 as co-chaperones.	9.12	3.43	3.77	response to heat	heat shock protein	nucleus	yes
A14g21320	Encodes heat-stress-associated 32-kD protein. Up-regulated by heat shock. Thermotolerance in a knockout mutant was compromised following a long recovery period (> 24 h) after acclimation heat shock treatment.	2.29	1.17	1.86	response to heat	heat shock protein	nucleus	no
A14g25200	AtHSP23.6-mito mRNA, nuclear gene encoding mitochondrial	5.64	2.83	3.04	response to heat	heat shock protein	mitochondria	no
A15g02490	Heat shock protein 70 (Hsp 70) family protein (Hsp70-2)	2.10	1.23	1.62	response to heat	heat shock protein	cytosol	no
A15g09590	heat shock protein 70 (Hsc70-5); nuclear	2.90	1.96	1.78	response to heat	heat shock protein	mitochondria	no
A15g12030	Encodes HEAT SHOCK PROTEIN 17.6A (HSP17.6A); a cytosolic small heat shock protein with chaperone activity that is induced by heat and osmotic stress and is also expressed late in seed development.	20.49	5.26	12.83	response to heat	heat shock protein	cytoplasm	no
A15g37670	HSP20-like chaperones superfamily protein	4.25	1.31	4.08	response to heat	heat shock protein	cytoplasm	no
A15g51440	HSP20-like chaperones superfamily protein	7.07	4.39	4.07	response to heat	heat shock protein	mitochondria	no
A15g52640	Encodes a cytosolic heat shock protein AtHSP90.1. AtHSP90.1 interacts with disease resistance signaling components SGT1b and RAR1 and is required for RPS2-mediated resistance.	7.76	2.68	3.41	response to heat	heat shock protein	cytosol	yes
A11g30070	SGS domain-containing protein	3.56	1.46	2.31	response to heat	heat shock protein	nucleus	no
A11g66080	Unknown protein	2.72	1.38	1.36	response to heat	unknown	cytoplasm	yes
A15g13200	Encodes a protein with unknown function that is involved in hormone mediated regulation of seed germination/dormancy.	2.27	1.12	1.65	response to heat	unknown	cytoplasm	no
A15g64510	Encodes Tunicamycin Induced 1(TIN1), a plant-speci-c ER stress-inducible protein. TIN1 mutation affects pollen surface morphology. Transcriptionally induced by treatment with the N-linked glycosylation inhibitor tunicamycin.	4.90	2.36	2.22	response to heat	unknown	chloroplast	yes
A15g56030	A member of heat shock protein 90 (HSP90) gene family. Expressed in all tissues and abundant in root apical meristem, pollen and tapetum. Expression is NOT heat-induced but induced by IAA and NaCl. Interacts with HsfA1d in the cytosol and the nucleus and negatively regulates HsfA1d. Did not bind to AtHsfA4c.	2.05	1.32	1.18	response to heat	chaperone	Golgi apparatus	yes
A15g13490	Encodes mitochondrial ADP/ATP carrier	1.08	2.25	1.44	response to nitrate	ammonium transporter	chloroplast	no
A11g64780	encodes an ammonium transporter protein believed to act as a high affinity transporter. It is expressed in the root, primarily in endodermal and cortical cells, and contributes to ammonium uptake in the root.	1.13	2.85	1.18	response to nitrate	ammonium transporter 1	plasma membrane	yes
A11g69870	Encodes a low affinity nitrate transporter NRT1.7. Expressed in phloem. Responsible for source-to-sink remobilization of nitrate.	1.28	2.57	1.63	response to nitrate	nitrate transporter	plasma membrane	no
A11g17860	Kunitz family trypsin and protease inhibitor protein	2.35	0.98	1.23	response to nitrate	protease inhibitor	cell wall	no
A11g07350	Encodes a serine/arginine rich-like protein, SR45a. Involved in the regulation of stress-responsive alternative splicing.	2.65	1.75	1.58	RNA binding	alternative splicing	spliceosomal complex	yes
A11g09140	Encodes a serine-arginine rich RNA binding protein SR30) involved in regulation of splicing (including splicing of itself).	2.36	2.30	1.67	RNA binding	alternative splicing	nucleus	no
A15g57280	Gene encodes a methyltransferase-like protein involved in pre-rRNA processing.	1.13	2.06	1.31	RNA binding	methyl transferase	nucleus	no
A13g22310	PUTATIVE MITOCHONDRIAL RNA HELICASE 1 (PMH1). Sequence similarity of DEAD-box RNA helicases. Binds RNA and DNA. Involved in drought, salt and cold stress responses.	0.91	2.01	1.16	RNA binding	organellar RNA editing	nucleus	no
A11g15440	Encodes a nucleolar protein that is a ribosome biogenesis co-factor. Mutants display aberrant RNA processing and female gametophyte development.	1.04	2.04	1.21	RNA binding	ribosome biogenesis	nucleus	no

Gene ID	Gene name and description	C-1	C-3,5	C-25	GO Biological Process	GO Molecular Function	GO Cellular Component	Time spec. in cont.
At5g22100	RNA cyclase family protein	1.07	2.05	1.28	RNA binding	ribosome biogenesis	nucleus	no
At5g39850	Ribosomal protein S4	1.23	2.00	1.36	RNA binding	ribosome biogenesis	cytosol	no
At4g25630	encodes a fibrillarin, a key nucleolar protein in eukaryotes which associates with box C/D small nucleolar RNAs (snoRNAs) directing 2'-O-ribose methylation of the rRNA.	1.02	2.02	1.56	RNA binding	rRNA editing	nucleus	yes
At5g66880	encodes a member of SNF1-related protein kinases (SnRK2) whose activity is activated by ionic (salt) and non-ionic (mannitol) osmotic stress. Enzyme involved in the ABA signaling during seed germination, dormancy and seedling growth.	2.01	0.89	1.32	seedling growth	kinase activity	cytoplasm	yes
At3g16050	Encodes a protein with pyridoxal phosphate synthase activity whose transcripts were detected mostly in roots and accumulate during senescence. The protein was found in very low abundance, which prevented a specific localisation.	2.89	1.65	1.57	senescence	protein binding	cytoplasm	yes
At1g19180	Encodes JASMONATE-ZIM-DOMAIN PROTEIN 1 (JAZ1), a nuclear-localized protein involved in jasmonate signaling	4.20	1.27	3.77	signal transduction	protein binding	nucleus	yes
At1g72520	PLAT/LH2 domain-containing lipoxygenase family protein	2.33	1.19	2.20	signal transduction	signal transduction	chloroplast	no
At1g03070	LIFEGUARD 4 (LFG4), a bax inhibitor-1 family protein	4.02	1.05	1.33	unknown	glutamate binding	integral component of membrane	no
At1g43910	P-loop containing nucleoside triphosphate hydrolases superfamily protein	1.22	1.26	2.03	unknown	hydrolase activity	Golgi apparatus	no
At2g23010	serine carboxypeptidase-like 9 (SCPL9)	1.25	2.03	2.48	unknown	hydrolase activity	extracellular region	yes
At2g27420	Cysteine proteinases superfamily protein	1.40	3.05	0.98	unknown	hydrolase activity	unknown	yes
At3g53230	ATPase, AAA-type, CDC48 protein	3.05	1.81	2.57	unknown	hydrolase activity	cytosol	no
At4g17470	alpha/beta-Hydrolases superfamily protein	0.99	2.70	1.45	unknown	hydrolase activity	chloroplast	no
At5g58310	Encodes a protein shown to have methyl IAA esterase activity in vitro. This protein does not act on methyl JA, MeSA, MeGA4, or MEGA9 in vitro.	1.01	1.45	2.18	unknown	hydrolase activity	cytoplasm	no
At1g19640	Encodes a S-adenosyl-L-methionine:jasmonic acid carboxyl methyltransferase (JMT) that catalyzes the formation of methyljasmonate from jasmonic acid.	0.92	2.39	1.17	unknown	jasmonic acid metabolic process	nucleus	no
At3g01820	P-loop containing nucleoside triphosphate hydrolases superfamily protein	1.41	2.47	1.11	unknown	kinase activity	mitochondria	no
At3g10530	Transducin/WD40 repeat-like superfamily protein	0.92	2.05	1.23	unknown	nucleotide binding	nucleus	no
At2g46650	member of Cytochromes b5	1.22	1.35	2.01	unknown	oxidation-reduction process	integral component of membrane	yes
At3g44970	Cytochrome P450 superfamily protein	1.07	0.96	2.22	unknown	oxidation-reduction process	unknown	no
At2g30830	encodes a protein whose sequence is similar to 2-oxoglutarate-dependent dioxygenase	1.19	2.50	1.18	unknown	oxidoreductase activity	cytoplasm	no
At4g12290	Copper amine oxidase family protein	1.10	2.13	1.16	unknown	oxidoreductase activity	Golgi apparatus	yes
At1g20510	OPC-8:0 CoA ligase1 (OPCL1); FUNCTIONS IN 4-coumarate-CoA ligase activity	1.92	1.08	2.08	unknown	phenylpropanoid metabolic process	peroxisome	yes
At2g18230	Encodes a protein that might have inorganic pyrophosphatase activity.	1.06	2.10	1.40	unknown	phosphate ion homeostasis	cytoplasm	no
At2g38170	Encodes a high affinity vacuolar calcium antiporter.	1.15	2.10	1.10	unknown	phosphate ion homeostasis	chloroplast	no

Gene ID	Gene name and description	C-1	C-3.5	C-25	GO Biological Process	GO Molecular Function	GO Cellular Component	Time spec. in cont.
At2g02010	glutamate decarboxylase 4 (GAD4)	1.19	2.49	1.28	unknown	protein binding	nucleus	no
At3g63060	EDL3 is an F-box protein involved that mediated the regulation of abscisic acid signaling.	1.59	2.11	1.48	unknown	protein binding	nucleus	no
At1g73325	Kunitz family trypsin and protease inhibitor protein	1.39	5.63	4.26	unknown	protein metabolism	extracellular region	yes
At1g19020	Unknown protein	1.99	0.78	2.17	unknown	response to oxidative stress	unknown	no
At3g10185	Encodes a Gibberellin-regulated GASA/GAST/Snakin family protein	1.21	3.67	2.21	unknown	signal transduction	extracellular region	no
At3g14720	member of MAP Kinase	1.49	2.16	1.51	unknown	signal transduction	nucleus	no
At4g34710	encodes a arginine decarboxylase (ADC), a rate-limiting enzyme that catalyzes the first step of polyamine (PA) biosynthesis via ADC pathway in Arabidopsis thaliana.	1.25	2.80	1.26	unknown	signal transduction	nucleus	no
At1g01210	DNA-directed RNA polymerase, subunit M, archaeal	1.12	2.05	1.02	unknown	transcription factor activity	nucleus	no
At1g06180	MYB13; member of MYB3R- and R2R3-type MYB- encoding genes	1.50	2.38	0.99	unknown	transcription factor activity	nucleus	yes
At1g56170	"NUCLEAR FACTOR Y, SUBUNIT C2" (NF-YC2)	2.36	1.34	2.30	unknown	transcription factor activity	nucleus	no
At1g68670	myb-like transcription factor family protein	2.12	0.99	1.51	unknown	transcription factor activity	nucleus	no
At1g80840	Pathogen-induced transcription factor.	2.59	1.03	2.32	unknown	transcription factor activity	nucleus	yes
At3g21150	Encodes a protein with a B-box domain predicted to act as a transcription factor. Expression of the BBX32 gene is affected by monochromatic red light.	1.17	2.42	0.77	unknown	transcription factor activity	nucleus	yes
At3g21890	B-box type zinc finger family protein	1.18	3.86	1.02	unknown	transcription factor activity	nucleus	yes
At3g24500	One of three genes in A. thaliana encoding multiprotein bridging factor 1, a highly conserved transcriptional coactivator. May serve as a bridging factor between a bZIP factor and TBP.	2.55	1.94	1.72	unknown	transcription factor activity	nucleus	yes
At3g62610	Member of the R2R3 factor gene family.	1.37	1.50	2.11	unknown	transcription factor activity	nucleus	no
At5g04840	bZIP protein; FUNCTIONS IN: DNA binding, sequence-specific DNA binding transcription factor activity	2.44	1.52	1.56	unknown	transcription factor activity	nucleus	no
At5g49330	Member of the R2R3 factor gene family.	1.03	2.26	0.91	unknown	transcription factor activity	nucleus	yes
At1g02930	Encodes GSTF6, a glutathione transferase belonging to the phi class of GSTs.	1.16	1.16	3.04	unknown	transferase activity	cytoplasm	no
At1g53680	Encodes glutathione transferase GSTU28; belonging to the tau class of GSTs.	2.87	1.14	1.36	unknown	transferase activity	cytoplasm	yes
At2g16890	UDP-Glycosyltransferase superfamily protein	1.12	2.12	1.37	unknown	transferase activity	chloroplast	yes
At3g03480	acetyl CoA:(Z)-3-hexen-1-ol acetyltransferase (CHAT)	0.94	2.16	1.12	unknown	transferase activity	cytoplasm	no
At4g15490	Encodes a protein that might have sinapic acid:UDP-glucose glucosyltransferase activity.	1.32	2.03	1.24	unknown	transferase activity	unknown	no
At4g16590	encodes a gene similar to cellulose synthase	1.06	6.69	3.85	unknown	transferase activity	Golgi apparatus	yes
At5g42760	Leucine carboxyl methyltransferase	1.17	2.27	0.93	unknown	transferase activity	nucleus	yes
At5g58770	Undecaprenyl pyrophosphate synthetase family protein	1.54	2.17	1.04	unknown	transferase activity	chloroplast	yes

Gene ID	Gene name and description	C-1	C-3,5	C-25	GO Biological Process	GO Molecular Function	GO Cellular Component	Time spec. in cont.
At5g63160	BTB and TAZ domain protein. Short-lived nuclear-cytoplasmic protein targeted for degradation by the 26S proteosome pathway. Acts redundantly with BT2 and BT3 during female gametophyte development.	1.03	3.62	0.85	unknown	transferase activity	cytoplasm	yes
At1g08650	Encodes a phosphoenolpyruvate carboxylase kinase (PPCK1) that is expressed at highest levels in leaves. Expression is induced by light.	2.13	0.78	0.73	unknown	transferase/kinase activity	nucleus	no
At3g15340	Encodes PP2 (proton pump interactor 2), a homologue of PPI1, a protein that interacts with the plasma membrane H+ ATPase AHA1.	2.14	1.12	1.75	unknown	transport	cytoplasm	no
At4g24570	Encodes one of the mitochondrial dicarboxylate carriers (DIC); DIC1 (AT2G22500), DIC2 (AT4G24570), DIC3 (AT5G09470).	2.22	0.66	1.61	unknown	transport	mitochondria	yes
At4g23493	Unknown protein	2.47	1.20	1.90	unknown	uknown	nucleus	no
At2g02820	Late embryogenesis abundant 3 (LEA3) family protein	0.90	3.26	0.69	unknown	unknown	chloroplast	yes
At1g06002	Potential natural antisense gene	1.37	2.28	1.76	unknown	unknown	unknown	no
At1g17100	SOUL heme-binding family protein	1.16	2.31	1.23	unknown	unknown	chloroplast	yes
At1g21550	Calcium-binding EF-hand family protein	5.07	1.57	2.02	unknown	unknown	cytoplasm	no
At1g29640	Unknown protein	1.55	2.02	1.28	unknown	unknown	nucleus	yes
At1g54575	Unknown protein	1.16	3.05	1.24	unknown	unknown	nucleus	no
At1g61340	Encodes a F-box protein induced by various biotic or abiotic stress.	3.50	1.94	2.64	unknown	unknown	nucleus	no
At2g07722	Unknown protein	1.43	2.04	2.58	unknown	unknown	mitochondria	no
At2g36885	Unknown protein	1.00	1.62	2.02	unknown	unknown	chloroplast	no
At3g02832	Unknown protein	1.00	2.01	1.13	unknown	unknown	unknown	no
At3g07090	PPPDE putative thiol peptidase family protein	2.57	1.08	1.58	unknown	unknown	cytoplasm	no
At3g14900	Unknown protein	0.99	1.88	2.24	unknown	unknown	chloroplast	no
At3g17800	mRNA level of the MEB5.2 gene (At3g17800) remains unchanged after cutting the inflorescence stem	1.33	2.06	0.90	unknown	unknown	nucleus	yes
At3g19970	alpha/beta-Hydrolases superfamily protein	2.27	1.04	1.35	unknown	unknown	unknown	no
At3g23170	Unknown protein	1.87	2.54	0.96	unknown	unknown	chloroplast	yes
At3g24460	Serine-domain containing serine and sphingolipid biosynthesis protein	0.79	2.26	1.23	unknown	unknown	membrane	yes
At3g24750	Unknown protein	1.84	2.68	4.22	unknown	unknown	nucleus	yes
At3g29000	Calcium-binding EF-hand family protein	2.34	0.96	2.22	unknown	unknown	plasma membrane	yes
At3g51238	Potential natural antisense gene, locus overlaps with AT3G51240	1.61	2.53	1.74	unknown	unknown	unknown	yes
At3g59820	LETM1-like protein	1.05	2.29	1.35	unknown	unknown	mitochondria	no
At3g61920	Unknown protein	1.19	2.57	1.50	unknown	unknown	nucleus	no

Gene ID	Gene name and description	C-1	C-3.5	C-25	GO Biological Process	GO Molecular Function	GO Cellular Component	Time spec. in cont.
At4g01080	Encodes a member of the TBL (TRICHOME BIREFRINGENCE-LIKE) gene family containing a plant-specific DUF231 (domain of unknown function) domain.	0.72	2.93	1.67	unknown	unknown	integral component of membrane	no
At4g02360	Unknown protein	1.51	3.25	1.26	unknown	unknown	extracellular region	no
At4g18280	glycine-rich cell wall protein-related	1.81	2.31	1.10	unknown	unknown	unknown	no
At4g18422	Unknown protein	2.37	1.44	1.69	unknown	unknown	mitochondria	no
At4g23680	Polyketide cyclase/dehydrase and lipid transport superfamily protein	1.35	2.02	1.26	unknown	unknown	unknown	no
At4g27652	Unknown protein	2.20	1.84	0.93	unknown	unknown	unknown	yes
At4g27657	Unknown protein	1.99	3.06	0.87	unknown	unknown	mitochondria	yes
At4g29780	Unknown protein	2.09	0.91	1.47	unknown	unknown	unknown	yes
At4g34550	Unknown protein	1.27	2.12	1.17	unknown	unknown	unknown	yes
At4g36010	Pathogenesis-related thaumatin superfamily protein	1.46	2.40	1.72	unknown	unknown	extracellular region	no
At4g36988	CONSERVED PEPTIDE UPSTREAM OPEN READING FRAME 49 (CPuORF49); upstream open reading frames (uORFs) are small open reading frames found in the 5' UTR of a mature mRNA.	2.60	1.66	1.74	unknown	unknown	mitochondria	yes
At4g39675	Unknown protein	2.10	1.30	0.91	unknown	unknown	unknown	no
At5g03285	other RNA	2.60	1.19	1.77	unknown	unknown	unknown	yes
At5g08760	Unknown protein	2.32	0.74	1.31	unknown	unknown	extracellular region	yes
At5g10695	Unknown protein	3.78	1.00	1.64	unknown	unknown	endoplasmic reticulum	no
At5g20790	Unknown protein	2.86	0.91	0.86	unknown	unknown	extracellular region	no
At5g35320	Unknown protein	3.28	1.33	1.45	unknown	unknown	nucleus	no
At5g48470	Unknown protein	0.89	1.57	2.43	unknown	unknown	chloroplast	no
At5g49480	AtCP1 encodes a novel Ca2+-binding protein, which shares sequence similarities with calmodulins. The expression of AtCP1 is induced by NaCl.	1.19	2.42	0.85	unknown	unknown	cytoplasm	yes
At5g54165	Unknown protein	3.62	1.39	2.72	unknown	unknown	chloroplast	no
At5g61820	Unknown protein	1.43	2.06	1.24	unknown	unknown	chloroplast	no
At5g63087	Encodes a Plant thionin family protein	1.39	2.26	1.58	unknown	unknown	extracellular region	yes
At5g64401	Unknown protein	4.63	1.63	1.28	unknown	unknown	mitochondria	yes
AtMg00170	Unknown protein	1.44	2.17	2.64	unknown	unknown	mitochondria	no
AtMg00620	Unknown protein	1.44	2.17	2.64	unknown	unknown	mitochondria	no
At1g24580	RING/U-box superfamily protein	1.48	2.48	1.48	unknown	zinc ion binding	nucleus	yes
At5g60540	PYRIDOXINE BIOSYNTHESIS 2 (PDX2); encodes a protein predicted to function in tandem with PDX1 to form glutamine amidotransferase complex with involved in vitamin B6 biosynthesis. PDX2 is predicted to function as glutaminase within the complex.	1.23	2.05	1.23	vitamin B6 biosynthesis	hydrolase activity	cytoplasm	no

Table S6. Time specific genes responsive to irradiance increase; genes more than 2.0-fold down-regulated in Col-0 when comparing plants exposed to increased irradiance to control plants. at 1, 3.5 or 25 hours after the irradiance increase and differentially (P=0.05) down-regulated between two or three time-points when comparing 1, 3.5, and 25 hours.
Unlogged fold changes are shown, grey shaded values are <2.0 fold down-regulated, green shading indicates accession-specific difference in expression present in control conditions independent of irradiance increase. Time spec. in cont. = Time-specific difference in expression present in control conditions, independent of irradiance increase

Gene ID	Gene name and description	C-1	C-3.5	C-25	GO Biological Process	GO Molecular Function	GO Cellular Component	Time spec. in cont.
At4g04955	Encodes an allantoinase which is involved in allantoin degradation and assimilation. Gene expression was induced when allantoin was added to the medium. The insertion mutant, ataln mt2-1, did not grow well on the MS medium where allantoin, instead of ammonium nitrate, was supplied.	0.97	0.32	0.71	allantoin degradation and assimilation	hydrolase activity	endoplasmic reticulum	no
At5g63800	Involved in mucilage formation. Mutants form columella and outer cell wall architecture of the mucilage cells resembles wild-type. However, mum2 seeds completely lack seed coat mucilage. This mutation appears to represent a later step in the development of this cell-type. Encodes a beta-galactosidase involved in seed coat mucilage biosynthesis. Member of Glycoside Hydrolase Family 35	0.80	0.40	0.64	carbohydrate metabolism	beta galactosidase	extracellular region	no
At1g65590	Encodes a protein with beta-hexosaminidase activity. Located on the plasma membrane.	0.72	0.46	0.73	carbohydrate metabolism	beta-hexosaminidase activity	plasma membrane	no
At5g03350	Legume lectin family protein; FUNCTIONS IN: carbohydrate binding, binding	0.87	0.48	0.86	carbohydrate metabolism	lectin family protein	chloroplast	yes
At1g71880	Sucrose transporter gene induced in response to nematodes; member of Sucrose-proton symporter family.	0.47	0.82	0.60	carbohydrate metabolism	sucrose-proton symporter	plasma membrane	no
At4g23820	Pectin lyase-like superfamily protein	0.91	0.42	0.65	carbohydrate metabolism	unknown	extracellular region	no
At1g69530	Member of Alpha-Expansin Gene Family. Naming convention from the Expansin Working Group (Kende et al, Plant Mol Bio). Involved in the formation of nematode-induced syncytia in roots of Arabidopsis thaliana.	0.64	0.67	0.44	cell organization	cell organization and biogenesis	extracellular region	no
At2g01420	Encodes PIN-FORMED 4 (PIN4), a putative auxin efflux carrier that is localized in developing and mature root meristems. It is involved in the maintenance of embryonic auxin gradients. A role for AtPIN4 in generating a sink for auxin below the quiescent center of the root meristem that is essential for auxin distribution and patterning is proposed. In the root, PIN4 is detected around the quiescent center and cells surrounding it, and localizes basally in provascular cells.	0.76	0.41	0.49	cell organization	cell organization and biogenesis	unknown	no
At2g38120	Encodes an auxin influx transporter. AUX1 resides at the apical plasma membrane of protophloem cells and at highly dynamic subpopulations of Golgi apparatus and endosomes in all cell types. AUX1 action in the lateral root cap and/or epidermal cells influences lateral root initiation and positioning. Shoot supplied ammonium targets AUX1 and inhibits lateral root emergence.	0.67	0.59	0.48	cell organization	cell organization and biogenesis	plasma membrane	no
At2g04610	member of Alpha-Expansin Gene Family. Naming convention from the Expansin Working Group (Kende et al, 2004. Plant Mol Bio). Involved in the formation of nematode-induced syncytia in roots of Arabidopsis thaliana.	0.48	0.16	0.31	cell organization	cell organization and biogenesis	extracellular region	no
At1g01120	Encodes a condensing enzyme KCS1 (3-ketoacyl-CoA synthase 1) which is involved in the critical fatty acid elongation process in wax biosynthesis.	0.89	0.59	0.44	cell organization	fatty acid biosynthetic process	endoplasmic reticulum	no
At4g32940	Encodes a vacuolar processing enzyme belonging to a novel group of cysteine proteinases that is expressed in vegetative organs and is upregulated in association with various types of cell death and under stressed conditions. They are essential in processing seed storage proteins and for mediating the susceptible response of toxin-induced cell death.	0.94	0.44	0.80	cell organization	hydrolase activity	extracellular region	no
At4g16520	autophagy 8f (ATG8F)	0.90	0.40	0.90	cell organization	microtubule cytoskeleton organization	unknown	no
At4g20260	Encodes a Ca2+ and Cu2+ binding protein. N-terminal myristylation on glycine 2 appears to enable it to associate tightly with the plasma membrane. Recombinant PCaP1 interacts strongly with phosphatidylinositol 3,5-bisphosphate (PtdIns(3,5)P2) and PtdIns (3,4,5)P3, and weakly with PtdIns(3,5)P2 and PtdIns(4,5). It also interacts with calmodulin (CaM) in a calcium-dependent manner. CaM does not interfere with PCaP1 membrane localization but does weaken interactions between it and the PtdInsPs. PCaP1 has an apparent Kd of 10 uM for Cu2+ and can bind six ions per protein. Transcript levels for PCaP1 first fall and then rise following exposure to CuCl2. Mannitol, sorbitol, and the fig22 oligopeptide also increase expression levels.	0.88	0.39	0.49	cell organization	microtubule cytoskeleton organization	chloroplast	no
At4g00150	Belongs to one of the LOM (LOST MERISTEMS) genes: AT2G45160 (LOM1), AT3G60630 (LOM2) and AT4G00150 (LOM3). LOM1 and LOM2 promote cell differentiation at the periphery of shoot meristems and help to maintain their polar organization.	0.49	0.97	0.57	cell organization	transcription factor activity	nucleus	no

Gene ID	Gene name and description	C-1	C-3.5	C-25	GO Biological Process	GO Molecular Function	GO Cellular Component	Time spec. in cont.
At4g03210	encodes a member of xyloglucan endotransglucosylase/hydrolases (XTHs) that catalyze the cleavage and molecular grafting of xyloglucan chains function in loosening and rearrangement of the cell wall. Gene is expressed in shoot apex region, flower buds, flower stalks and internodes bearing flowers.	0.88	0.48	0.81	cell organization	transferase activity	extracellular region	no
At2g23770	Encodes a LysM-containing receptor-like kinase LYK4. Shares overlapping function with LYK6 in mediating chitin-triggered immune responses.	0.76	0.43	0.72	defense response	kinase activity	chloroplast	no
At5g46330	Encodes a leucine-rich repeat serine/threonine protein kinase that is expressed ubiquitously. FLS2 is involved in MAP kinase signalling relay involved in innate immunity. Essential in the perception of flagellin, a potent elicitor of the defense response. FLS2 is directed for degradation by the bacterial ubiquitin ligase AvrPtoB.	0.78	0.47	0.56	defense response	protein binding	plasma membrane	yes
At2g40880	Encodes a protein with cysteine proteinase inhibitor activity. Overexpression increases tolerance to abiotic stressors (i.e. salt,osmotic, cold stress).	0.93	0.44	0.76	defense response	proteinase activity	extracellular region	no
At1g59870	ATP binding cassette transporter. Localized to the plasma membrane in uninfected cells. In infected leaves, the protein concentrated at infection sites. Contributes to nonhost resistance to inappropriate pathogens that enter by direct penetration in a salicylic acid ?dependent manner. Required for mlo resistance. Has Cd transporter activity (Cd2+ extrusion pump) and contributes to heavy metal resistance.	0.91	0.43	1.03	defense response	transporter	plasma membrane	no
At2g46220	Uncharacterized conserved protein	1.04	0.34	0.75	defense response	unknown	chloroplast	no
At3g04210	Disease resistance protein (TIR-NBS class)	0.86	0.37	0.71	defense response	unknown	cytoplasm	no
At1g21920	Histone H3 K4-specific methyltransferase SET7/9 family protein	0.67	0.44	0.62	DNA modification	kinase activity	chloroplast	no
At3g12610	Plays role in DNA-damage repair/toleration. Partially complements RecA- phenotypes.	0.76	0.45	0.71	DNA modification	DNA repair	chloroplast	no
At5g05860	Encodes a cytokinin N-glucosyltransferase that is involved in cytokinin homeostasis and cytokinin response in planta through cytokinin N-glucosylation. Expression is induced by ABA, mannitol and drought stress. Analysis of overexpressors and loss of function mutants indicate a role in response to osmotic and drought stress.	0.58	0.38	0.52	drought response	transferase activity	unknown	no
At3g21460	Glutaredoxin family protein	0.48	0.30	0.33	electron transport	electron carrier activity	cytoplasm	yes
At3g46130	Encodes a putative transcription factor (MYB48) that functions to regulate flavonol biosynthesis primarily in cotyledons.	0.44	1.04	0.70	flavonol biosynthesis	transcription factor activity	nucleus	no
At4g03400	Encodes a GH3-related gene involved in red light-specific hypocotyl elongation. Analysis of sense and antisense transgenic plants suggests that DFL2 is located downstream of red light signal transduction and determines the degree of hypocotyl elongation.	0.71	0.88	0.45	hypocotyl growth	signal transduction	cytoplasm	no
At4g39640	The gene encodes a gamma-glutamyltransferase (AKA gamma-glutamyl transpeptidase, EC 2.3.2.2) that is located in vascular tissues (predominantly phloem) of leaves and is involved in the degradation of glutathione. The encoded enzyme also mitigates oxidative stress by metabolizing GSSG (oxidized form of GSH - glutathione) in the apoplast.	0.87	0.46	0.85	leaf morphology	transferase activity	extracellular region	no
At5g45180	Bifunctional inhibitor/lipid-transfer protein/seed storage 2S albumin superfamily protein	0.90	0.41	0.68	lipid remodelling	lipid binding	chloroplast	no
At4g22490	Bifunctional inhibitor/lipid-transfer protein/seed storage 2S albumin superfamily protein	1.52	0.43	1.05	lipid remodelling	lipid binding	extracellular region	no
At5g48490	Bifunctional inhibitor/lipid-transfer protein/seed storage 2S albumin superfamily protein	0.38	0.17	0.23	lipid remodelling	lipid transport	extracellular region	yes
At3g23080	Polyketide cyclase/dehydrase and lipid transport superfamily protein	0.87	0.44	0.81	lipid remodelling	lipid transport	nucleus	no
At1g09390	GDSL-motif esterase/acyltransferase/lipase. Enzyme group with broad substrate specificity that may catalyze acyltransfer or hydrolase reactions with lipid and non-lipid substrates.	0.87	0.43	0.84	lipid remodelling	transferase activity	chloroplast	no
At3g16370	GDSL-motif esterase/acyltransferase/lipase. Enzyme group with broad substrate specificity that may catalyze acyltransfer or hydrolase reactions with lipid and non-lipid substrates.	0.96	0.50	0.59	lipid remodelling	transferase activity	extracellular region	no
At4g17460	Encodes a class II HD-ZIP protein that regulates meristematic activity in different tissues, and that it is necessary for the correct formation of the gynoecium.	0.78	0.50	0.69	meristem identity	transcription factor activity	nucleus	no
At5g49730	Encodes a plasma membrane-located ferric chelate reductase. Its mRNA is expressed in green aerial tissues (shoot, flower and cotyledon) in a light- and cell differentiation-specific manner.	0.79	0.27	0.55	metal ion binding	ferric chelate reductase	membrane	no
At5g35790	Encodes a plastidic glucose-6-phosphate dehydrogenase that is sensitive to reduction by DTT and whose mRNA is more prevalent in developing organs but absent in the root.	0.67	0.37	0.77	oxidation-reduction	dehydrogenase activity	chloroplast	no
At3g56060	Glucose-methanol-choline (GMC) oxidoreductase family protein	0.76	0.34	0.50	oxidation-reduction	unknown	unknown	no
At4g27710	member of CYP709B	0.89	0.41	0.90	oxidation-reduction	unknown	unknown	no
At5g06690	Encodes a thioredoxin (WCRKC1) localized in chloroplast stroma. Contains a WCRKC motif.	0.84	0.41	0.78	oxidation-reduction	unknown	chloroplast	no
At5g18600	Thioredoxin superfamily protein	0.75	0.30	0.68	oxidation-reduction	unknown	cytoplasm	no

Gene ID	Gene name and description	C-1	C-3.5	C-25	GO Biological Process	GO Molecular Function	GO Cellular Component	Time spec. in cont.
At2g22990	sinapoylglucose:malate sinapoyltransferase. Catalyzes the formation of sinapoylmalate from sinapoylglucose. Mutants accumulate excess sinapoylglucose.	0.86	0.36	0.67	phenylpropanoid metabolic process	transferase activity	extracellular region	no
At5g04190	Encodes phytochrome kinase substrate 4, a phytochrome signaling component involved in phototropism. It is phosphorylated in a phot1-dependent manner in vitro. Phosphorylation is transient and regulated by a type 2-protein phosphatase.	0.65	0.48	0.62	photoreceptor activity	phytochrome signalling	plasma membrane	no
At1g18810	phytochrome kinase substrate-related	0.66	0.43	0.42	photoreceptor activity	unknown	plasma membrane	no
At4g27440	light-dependent NADPH:protochlorophyllide oxidoreductase B	0.98	0.34	0.74	photosynthesis	chlorophyll biosynthesis	membrane chloroplast	no
At2g24550	unknown protein	0.89	0.36	0.73	photosynthesis	flavonoid biosynthesis	nucleus	no
At2g34430	Encodes LIGHT-HARVESTING CHLOROPHYLL-PROTEIN COMPLEX II SUBUNIT B1 (LHB1B1)	0.95	0.28	0.40	photosynthesis	light harvesting	chloroplast	no
At2g29290	NAD(P)-binding Rossmann-fold superfamily protein	0.84	0.44	0.58	photosynthesis	NAD binding	unknown	no
At3g09580	FAD/NAD(P)-binding oxidoreductase family protein	0.65	0.49	0.92	photosynthesis	NAD binding	chloroplast	no
At4g19170	chloroplast-targeted member of a family of enzymes similar to nine-cis-epoxycarotenoid dioxygenase	0.43	0.29	0.18	photosynthesis	oxidation-reduction process	chloroplast	yes
At5g44190	Encodes GLK2, Golden2-like 2, one of a pair of partially redundant nuclear transcription factors that regulate chloroplast development in a cell-autonomous manner. GLK1, Golden2-like 1, is encoded by At2g20570. GLK1 and GLK2 regulate the expression of the photosynthetic apparatus.	0.54	0.60	0.36	photosynthesis	transcription factor activity	nucleus	no
At5g25190	encodes a member of the ERF (ethylene response factor) subfamily B-6 of ERF/AP2 transcription factor family. The protein contains one AP2 domain. There are 12 members in this subfamily including RAP2.11.	0.54	0.32	0.50	photosynthesis, drought response	transcription factor activity	nucleus	no
At3g19850	Phototropic-responsive NPH3 family protein	0.67	0.28	0.57	protein ubiquitination	transport	plasma membrane	no
At1g19770	Member of a family of proteins related to PUP1, a purine transporter. May be involved in the transport of purine and purine derivatives such as cytokinins, across the plasma membrane.	0.78	0.48	0.68	Purine transport	transport	integral component of membrane	no
At1g77760	Encodes NITRATE REDUCTASE 1 (NIA1), the cytosolic minor isoform of nitrate reductase (NR). Involved in the first step of nitrate assimilation, it contributes about 15% of the nitrate reductase activity in shoots. Similar to molybdopterin oxidoreductases at the N-terminus, and to FAD/NAD-binding cytochrome reductases at the C-terminus. Cofactors: FAD, heme iron (cytochrome B-557), and molybdenum-pterin.	0.50	0.73	0.54	response to nitrate	nitrate assimilation	mitochondria	no
At1g68840	RaV2 is part of a complex that has been named 'regulator of the (H+)-ATPase of the vacuolar and endosomal membranes' (RAVE).	1.25	0.47	1.17	response to nitrate	regulator of the (H+)-ATPase transferase activity	nucleus	no
At2g43820	Induced by Salicylic acid, virus, fungus and bacteria. Involved in the tryptophan synthesis pathway. Independent of NPR1 for their induction by salicylic acid. UGT74F1 transfers UDP-glucose to salicylic acid (forming a glucose ester (SGE)) and a glucose ester (SGE)), benzoic acid, and abietalate in vitro. UGT74F2 shows a weak ability to catalyze the formation of the p-aminobenzoate-glucose ester in vitro. But, UGT74B1 appears to be the dominant tyrABA acylglucosyltransferase in vivo based on assays in leaves, flowers, and siliques. The true biological substrate(s) of UGT74F2 are not known, but mutant plants lacking UGT74F2 have a decreased level of SAG and SGE.	0.77	0.44	0.58	response to nitrate	transport	cytoplasm	no
At5g24655	RESPONSE TO LOW SULFUR 4 (LSU4)	0.78	0.99	0.49	response to sulfur	unknown	nucleus	yes
At2g41560	Encodes a calmodulin-regulated Ca(2+)-ATPase that improves salt tolerance in yeast. Localized to the vacuole. Lesion mimic phenotype when mutation in the gene is combined with a mutation in ACA11. Lesion mimic phenotype of double knockout can be suppressed by nutritional supplements that increase anion levels (e.g. 15 mM Nitrate, Chloride, or Phosphate).	0.75	0.31	0.54	salt tolerance	transport	vacuole	yes
At1g69490	Encodes a member of the NAC transcription factor gene family. It is expressed in floral primordia and upregulated by AP3 and PI. Its expression is associated with leaf senescence.	1.00	0.31	0.83	senescence	transcription factor activity	nucleus	no
At1g73830	Encodes the brassinosteroid signaling component BEE3 (BR-ENHANCED EXPRESSION 3). Positively modulates the shade avoidance syndrome in Arabidopsis seedlings.	0.82	0.39	0.77	shade avoidance	transcription factor activity	nucleus	no
At2g30520	light inducible root phototropism 2 encoding a signal transducer of the phototropic response in Arabidopsis	0.90	0.40	0.63	signal transduction	signal transduction	plasma membrane	no
At5g22920	Encodes a protein with sequence similarity to RING, zinc finger proteins. Loss of function mutations show reduced (15%) stomatal aperture under non stress conditions.	0.78	0.35	0.59	stomatal functioning	unknown	nucleus	no
At5g04490	Encodes a protein with phytol kinase activity involved in tocopherol biosynthesis.	0.77	0.39	0.73	tocopherol biosynthesis	kinase activity	chloroplast	no
At4g30690	Translation initiation factor 3 protein	0.84	0.37	0.84	translation	unknown	cytoplasm	no
At5g24490	30S ribosomal protein, putative	0.95	0.43	1.09	translation	unknown	ribosome	no
At1g04280	P-loop containing nucleoside triphosphate hydrolases superfamily protein	0.87	0.49	0.66	unknown	hydrolase activity	nucleus	no
At1g25230	Calcineurin-like metallo-phosphoesterase superfamily protein	0.81	0.43	0.65	unknown	hydrolase activity	extracellular region	no
At2g41250	Haloacid dehalogenase-like hydrolase (HAD) superfamily protein	0.52	0.22	0.45	unknown	hydrolase activity	unknown	no
At4g02330	Encodes a pectin methylesterase that is sensitive to chilling stress and brassinosteroid regulation.	0.77	0.49	0.73	unknown	hydrolase activity	extracellular region	yes

Gene ID	Gene name and description	C-1	C-3.5	C-.25	GO Biological Process	GO Molecular Function	GO Cellular Component	Time spec. in cont.
At5g18630	alpha/beta-Hydrolases superfamily protein	0.84	0.39	1.00	unknown	hydrolase activity	extracellular region	no
At5g44020	HAD superfamily, subfamily IIIB acid phosphatase	0.83	0.24	0.57	unknown	hydrolase activity	membrane	no
At5g44530	Subtilase family protein	0.75	0.42	0.57	unknown	hydrolase activity	extracellular region	no
At5g65730	xyloglucan endotransglucosylase/hydrolase 6 (XTH6)	0.91	0.42	0.62	unknown	hydrolase activity	extracellular region	no
At1g16110	WAK-like kinase	1.19	0.48	1.03	unknown	kinase activity	extracellular region	no
At1g29720	Leucine-rich repeat transmembrane protein kinase	0.71	0.45	0.64	unknown	kinase activity	integral component of membrane	yes
At2g44740	cyclin p4;1 (CYCP4;1)	0.69	0.44	0.69	unknown	kinase activity	unknown	no
At4g01330	Protein kinase superfamily protein	0.61	0.43	0.59	unknown	kinase activity	plasma membrane	no
At4g23300	Encodes a cysteine-rich receptor-like protein kinase.	0.70	0.46	0.75	unknown	kinase activity	extracellular region	yes
At3g03470	member of CYP89A	0.70	0.87	0.49	unknown	oxidation-reduction process	integral component of membrane	yes
At5g42250	Zinc-binding alcohol dehydrogenase family protein	0.93	0.52	0.48	unknown	oxidation-reduction process	cytoplasm	yes
At1g04040	HAD superfamily, subfamily IIIB acid phosphatase	0.95	0.34	0.80	unknown	phosphatase activity	cell wall	no
At2g05380	glycine-rich protein 3 short isoform (GRP3S) mRNA, complete	0.90	0.81	0.42	unknown	protein binding	extracellular region	yes
At4g27450	Aluminium induced protein with YGL and LRDR motifs	1.31	0.41	0.59	unknown	protein binding	plasma membrane	no
At5g02160	unknown protein	0.88	0.40	0.72	unknown	protein binding	chloroplast	no
At4g00970	Encodes a cysteine-rich receptor-like protein kinase.	0.89	0.47	0.84	unknown	protein metabolism	chloroplast	yes
At1g56220	Dormancy/auxin associated family protein	0.82	0.28	0.64	unknown	protein transport	nucleus	no
At5g53500	Transducin/WD40 repeat-like superfamily protein	0.64	0.81	0.48	unknown	signal transduction	cytoplasm	no
At2g27050	ethylene-insensitive3-like1 (EIL1)	0.57	0.45	0.62	unknown	transcription factor activity	nucleus	no
At3g48590	Encodes a protein with similarity to a subunit of the CCAAT promoter motif binding complex of yeast. One of two members of this class (HAP5A) and expressed in vegetative and reproductive tissues.	0.85	0.38	0.84	unknown	transcription factor activity	nucleus	no
At3g58120	Encodes a member of the BZIP family of transcription factors. Forms heterodimers with the related protein AtbZIP34. Binds to G-boxes in vitro and is localized to the nucleus in onion epidermal cells.	0.58	0.38	0.49	unknown	transcription factor activity	nucleus	no
At4g01460	basic helix-loop-helix (bHLH) DNA-binding superfamily protein	0.47	0.36	0.58	unknown	transcription factor activity	nucleus	no
At4g32340	Tetratricopeptide repeat (TPR)-like superfamily protein	0.72	0.36	0.60	unknown	transcription factor activity	unknown	no
At5g57660	CONSTANS-like 5 (COL5)	0.76	0.43	0.63	unknown	transcription factor activity	nucleus	no
At5g63470	"nuclear factor Y, subunit C4" (NF-YC4)	0.85	0.41	0.72	unknown	transcription factor activity	nucleus	no
At1g15125	S-adenosyl-L-methionine-dependent methyltransferases superfamily protein	1.16	0.43	0.99	unknown	transcription factor activity	nucleus	no
At1g15740	Leucine-rich repeat family protein	0.82	0.40	0.92	unknown	transferase activity	plasma membrane	no
At1g55450	S-adenosyl-L-methionine-dependent methyltransferases superfamily protein	1.28	0.49	1.18	unknown	transferase activity	cytoplasm	no
At1g63800	ubiquitin-conjugating enzyme 5 (UBC5)	0.78	0.40	0.94	unknown	transferase activity	cytoplasm	no
At3g16520	UDP-glucosyl transferase 88A1 (UGT88A1)	0.74	0.50	0.73	unknown	transferase activity	nucleus	no
At3g50270	HXXXD-type acyl-transferase family protein	0.69	0.46	0.91	unknown	transferase activity	chloroplast	no
At4g00750	S-adenosyl-L-methionine-dependent methyltransferases superfamily protein	0.70	0.50	0.63	unknown	transferase activity	Golgi apparatus	no
At5g28020	Encodes cysteine synthase CysO2.	0.82	0.41	0.74	unknown	transferase activity	mitochondria	no
At5g39080	HXXXD-type acyl-transferase family protein	0.54	0.38	0.52	unknown	transferase activity	unknown	no
At1g72150	novel cell-plate-associated protein that is related in sequence to proteins involved in membrane trafficking in other eukaryotes	0.87	0.26	0.36	unknown	transport	plasma membrane	no
At1g72820	Mitochondrial substrate carrier family protein	0.69	0.50	0.71	unknown	transport	mitochondria	no
At2g16380	Sec14p-like phosphatidylinositol transfer family protein	0.75	0.46	0.72	unknown	transport	Golgi apparatus	no

Gene ID	Gene name and description	C-1	C-3.5	C-25	GO Biological Process	GO Molecular Function	GO Cellular Component	Time spec. in cont.
At5g64410	oligopeptide transporter	0.78	0.47	0.56	unknown	transport	Int comp of membrane	no
At1g10682	other RNA	0.90	0.50	0.72	unknown	unknown	unknown	no
At1g18620	Unknown protein	0.77	0.47	0.61	unknown	unknown	nucleus	no
At1g20010	beta tubulin	0.85	0.47	0.83	unknown	unknown	chloroplast	no
At1g22690	Gibberellin-regulated family protein	0.81	0.44	0.87	unknown	unknown	Extracel.region	no
At1g25275	Unknown protein	0.90	0.47	1.15	unknown	unknown	Extracel.region	no
At1g27290	Unknown protein	0.71	0.37	0.63	unknown	unknown	mitochondria	no
At1g30250	Unknown protein	0.46	0.29	0.35	unknown	unknown	mitochondria	no
At1g33590	Leucine-rich repeat (LRR) family protein	0.82	0.37	1.08	unknown	unknown	plasma membrane	no
At1g55330	Encodes a putative arabinogalactan-protein (AGP21).	0.71	0.42	0.50	unknown	unknown	plasma membrane	no
At1g65845	Unknown protein	1.08	0.50	0.56	unknown	unknown	unknown	no
At1g69160	Unknown protein	0.58	0.39	0.41	unknown	unknown	mitochondria	no
At1g71970	Unknown protein	0.63	0.46	0.62	unknown	unknown	nucleus	no
At1g72430	SAUR-like auxin-responsive protein family	0.58	0.74	0.47	unknown	unknown	nucleus	yes
At1g74670	Gibberellin-regulated family protein	0.80	0.18	0.22	unknown	unknown	Extracel. region	no
At2g05540	Glycine-rich protein family	0.93	0.85	0.43	unknown	unknown	Extracel.region	no
At2g15960	unknown protein	0.86	0.46	0.56	unknown	unknown	unknown	no
At2g30230	unknown protein	0.98	0.38	0.86	unknown	unknown	unknown	no
At2g33815	Potential natural antisense gene, locus overlaps with AT2G33810	0.79	0.93	0.49	unknown	unknown	unknown	no
At3g06070	unknown protein	0.66	0.33	0.50	unknown	unknown	unknown	no
At3g12150	unknown protein	0.81	0.50	0.83	unknown	unknown	Extracel.region	no
At3g15450	Aluminium induced protein with YGL and LRDR motifs	0.86	0.49	0.68	unknown	unknown	chloroplast	no
At3g22121	Potential natural antisense gene, locus overlaps with AT3G22120	0.69	0.44	0.86	unknown	unknown	unknown	no
At3g55646	unknown protein	0.77	0.69	0.47	unknown	unknown	nucleus	no
At4g00950	maternal effect embryo arrest 47 (MEE47)	0.74	0.45	0.49	unknown	unknown	nucleus	no
At4g04040	maternal effect embryo arrest 51 (MEE51)	1.03	0.40	0.94	unknown	unknown	cytoplasm	no
At4g05070	Wound-responsive family protein	0.78	0.47	0.51	unknown	unknown	nucleus	no
At4g08950	EXORDIUM (EXO)	0.63	0.70	0.50	unknown	unknown	Extracel.region	no
At4g26290	unknown protein	0.63	0.47	0.79	unknown	unknown	nucleus	no
At4g27740	Yippee family putative zinc-binding protein	0.77	0.44	1.16	unknown	unknown	nucleus	no
At4g33666	unknown protein	0.81	0.37	0.75	unknown	unknown	unknown	no
At4g35430	unknown protein	0.75	0.50	0.84	unknown	unknown	mitochondria	no
At4g37240	unknown protein	0.74	0.43	0.65	unknown	unknown	unknown	no
At4g38550	Arabidopsis phospholipase-like protein (PEARLI 4) family	1.04	0.41	0.81	unknown	unknown	nucleus	no
At5g03230	Protein of unknown function	1.05	0.43	0.80	unknown	unknown	Extracel.region	no
At5g05250	unknown protein	0.83	0.76	0.42	unknown	unknown	nucleus	yes
At5g15350	early nodulin-like protein 17 (ENODL17)	0.64	0.47	0.57	unknown	unknown	Int comp of membrane	no
At5g16030	unknown protein	0.46	0.23	0.48	unknown	unknown	nucleus	no
At5g16400	Encodes an f-type thioredoxin (Trx-f2) localized in chloroplast stroma.	0.89	0.50	0.85	unknown	unknown	chloroplast	no
At5g19140	AILP1; response to auxin stimulus, response to aluminum ion	1.06	0.43	0.60	unknown	unknown	cytoplasm	no
At5g24570	unknown protein	0.70	0.51	0.42	unknown	unknown	unknown	yes
At5g44568	unknown protein	0.94	0.47	0.86	unknown	unknown	unknown	yes
At5g44585	unknown protein	0.53	0.41	0.30	unknown	unknown	unknown	no
At5g56100	glycine-rich protein / oleosin	0.79	0.28	0.79	unknown	unknown	nucleus	no
At5g57760	unknown protein	0.62	0.17	0.28	unknown	unknown	mitochondria	no
At4g11360	Encodes a putative RING-H2 finger protein RHA1b.	0.86	0.47	0.61	unknown	zinc ion binding	nucleus	no
At4g17245	RING/U-box superfamily protein	0.54	0.27	0.43	unknown	zinc ion binding	unknown	no

Table S7. Primers used for qRT-PCR

Name	Gene	Forward Primer	Reverse Primer
SR45a	At1g07350	GATGCAACGGTTAGCATCACC	TCCTGGACCCATGGACTAGA
SR30	At1g09140	CCGAAGTCGACACCCATCAA	AGATTCCACCGAGACCTCCT
GLK2	At5g44190	TTGCACGTATGGGGTCATCC	TGGATGACCTGGCCAAGATG
HSFA2	At2g26150	CAGCAAGGATCTGGGATGTCA	GCTACAAGCACACCATGATCC
HOP3	At4g12400	GTACTCCTGTTGCTCCAGCT	GCCTGCGATTGAGACTTTCC
CPN60BETA2	At3g13470	CTTGGTTCGTTGCTTGCTCC	ACTATGGCAGGACGGGATCT
SPX1	At5g20150	CTGCCTTGCGGGTTTTGAAG	GGCTTCTTGCTCCAACAATGG
GDPD1	At3g02040	TCACCTCCGAGACAATCCCT	TGTACCACGACACGAGAAGG
DREB2A	At5g05410	GGAGGACCAGAGAATAGCC	CCAAAGCCTGCTACCTCGAT
UBQ7	At2g35635	GCAGCGACACCATCGACAAT	AGGTCCGGCCATCTTCCAAT
CBE-5	At5g53560	TTGCAGTGTCGCTGTGACCA	TGATCATCCTGGAGGCGATG
UBQ.THIO	At1g28120	TGGTTGATCTTCCACTGATG	TGAAGGATGAAGCGGAAGTA

Chapter 5

Natural variation in photosynthetic response to increased irradiance explained by epistatic interaction between *PHOSPHATIDIC ACID PHOSPHOHYDROLASE 2* and *ASPARAGINE SYNTHETASE 2*

Roxanne van Rooijen[1,2], René Boesten[1], Ianis Mavraganis[3], Jitao Zou[3], Jeremy Harbinson[2], and Mark G.M. Aarts[1]

Laboratories of [1]Genetics and of [2]Horticulture and Product Physiology, Wageningen University, Droevendaalsesteeg 1, 6708 PB Wageningen, The Netherlands
[3]National Research Council Canada, Saskatoon, Saskatchewan S7N 0W9, Canada

ABSTRACT

Photosynthetic light use efficiency is inevitably connected with the incoming growth irradiance level. Specifically acclimation to increased irradiance is crucial, as increased incoming light levels lead to the production of reactive oxygen species (ROS) that are harmful to the integral cellular structures of the plant that could be lethal when persistent. The combination of genome wide association mapping (GWAS) and linkage mapping allowed the dissection of part of the genetic complexity and the underlying genetic variation explaining phenotypic variation in photosynthetic efficiency response to increased irradiance. It revealed an epistatic relation between two genes, *PHOSPHATIDIC ACID PHOSPHOHYDROLASE 2 (PAH2)* and *ASPARAGINE SYNTHETASE 2 (ASN2)*. PAH2 acts in membrane lipid remodelling in response to phosphate starvation, and ASN2 acts in detoxifying excess ammonium levels by transporting it via asparagine from source to sink organs. Three natural alleles could be found in the GWAS population for both genes. This study shows strong indications for the involvement of specific combinations of these *PAH2* and *ASN2* natural alleles in keeping high photosynthesis efficiencies in response to increased irradiance.

INTRODUCTION

A plant's capacity and efficiency to convert incoming light and CO_2 to biomass and O_2 through the process of photosynthesis is of major interest to present society with increasing population and rising CO_2 levels, as photosynthesis uses CO_2 (and light) to produce plant biomass (Long et al., 2015). Many possible targets have been identified to manipulate for increasing photosynthetic efficiency (Evans, 2013). These targets range from the canopy level to the thylakoid membrane level and from light capture to CO_2 conductance (Evans, 2013). Understanding genetic variation for photosynthesis and its response to fluctuating environments is crucial, as it will allow plant breeders to select for the photosynthetically best performing genotypes in an early stage, which might lead to faster growth and higher yields in later stages (Athanasiou et al., 2010). This study focusses on the process of light use efficiency, a trait that is inevitably connected with the incoming growth irradiance level (Van Rooijen et al., 2015). The ability of a plant to acclimate to fluctuations in irradiances is of major importance to maintain high photosynthetic rates over those conditions (Walters, 2005; Leister, 2012; Van Rooijen et al., 2015). Specifically acclimation to increased irradiance is crucial, as increased incoming light levels lead to the production of reactive oxygen species (ROS) that are harmful to the integral cellular structures of the plant, which could be lethal when persistent (Powles, 1984).

A sudden increase in growth irradiance provokes a regulatory response in the plant's metabolism within seconds, called photoprotection (Demmig-Adams and Adams, 1992). When the high irradiance level persists for longer time, photosynthetic acclimation will change the composition of mesophyll cells in terms of their proteins, lipids, pigments, and other cofactors involved in electron transport and reactive-oxygen species metabolism (Bailey et al., 2004; Walters, 2005). Increasingly more research is being performed to identify the genetic loci that are regulating these (sub-) processes in photosynthetic acclimation (Suorsa et al., 2012; Albrecht-Borth et al., 2013; Jin et al., 2014; Van Rooijen et al., 2015). The natural allelic variants of the genes underlying such loci can be applied for breeding for photosynthetic performance (Van Rooijen et al., 2015).

Natural allelic variants result from random mutations of the genomic DNA sequence. Phenotypic variation in a trait such as photosynthetic light use efficiency can be related to variation at the genome sequence level, which allows the identification of the associated genes (Alonso-Blanco et al., 2009; Flood et al., 2011; Alonso-Blanco and Méndez-Vigo, 2014). To do this, *Arabidopsis thaliana* is the model species of choice, because of its

well-described genetics, its wide availability of natural accessions, and the ability to exploit it in genome wide association studies (GWAS), (Atwell et al., 2010; Bergelson and Roux, 2010; Ogura and Busch, 2015). GWAS are performed in populations consisting of a large number of natural isogenic lines collected from nature, that have genetically adapted to different ecological conditions over thousands of years. In order to genetically map quantitative traits to the genome, GWAS take advantage of the recombination events that have accumulated over all those generations resulting in a high mapping resolution (Bergelson and Roux, 2010). An important aspect to consider when performing GWAS is Linkage Disequilibrium (LD), which is the non-random association of alleles at different loci, affecting the number of recombination events occurring through time (Kim et al., 2007). When LD is only over short lengths in the genome, it requires a very high density of genotyping to find causal loci for a phenotypic trait in GWAS. Also the interpretation of association peaks in GWAS is not straightforward as population structure can lead to the occurrence of false positive associations; and the presence of causal alleles with low allele frequency, the presence of multiple alleles having the same phenotype, or the presence of a genetic interaction between two loci can lead to hidden heritability (Korte and Farlow, 2013). Epistasis is an example of a genetic interaction between two loci, where the phenotypic effect of one allele one locus is obscured by the genotype at another locus (Bateson, 1909).

A more traditional method to link phenotypic variation to genetics is to do family mapping (Lander and Botstein, 1989). For this, two different accessions are crossed, the heterozygous plant that arises is self-fertilized, and the segregating offspring are phenotyped for the trait of interest, and genotyped for enough molecular markers to cover the genome. Less genetic complexity exists within family mapping compared to GWAS, as it deals with the presence of only two alleles per locus, coming from the two parents, increasing the mapping power. While family mapping provides the mapping power that is lacking in GWAS, it has a very low resolution because it depends upon the limited number of recombination events that have occurred in one (or a few) generation(s). The combination of GWAS and family mapping has proven to be a successful strategy in unravelling complex plant genetics (Keurentjes et al., 2011; Motte et al., 2014).

This study uses the combination of genome wide association mapping and family mapping to identify the underlying genetic variation of phenotypic variation in photosynthetic efficiency response to increased irradiance. A GWAS population and an experimental F2 population were phenotyped for photosynthesis efficiency response to increase irradiance. Both these populations revealed to be segregating for the trait of

interest and were used for genetic mapping. Genetic mapping revealed two epistatic quantitative trait loci (QTLs) on chromosome 5 were associated to photosynthesis efficiency levels after one hour of irradiance stress in both populations. Haplotype and expression analyses revealed the underlying genes were *PHOSPHATIDIC ACID PHOSPHOHYDROLASE 2 (PAH2)* and *ASPARAGINE SYNTHASE 2 (ASN2)*, acting in the conversion of membrane phospholipids to galactolipids and the removal of excess ammonia, respectively.

This study identifies genetic epistasis, a factor that is thought to be limiting the power in genetic mapping of complex traits with many underlying genes (Korte and Farlow, 2013). Additionally, it reveals three natural alleles for both PAH2 as well as three natural alleles for ASN2 are underlying natural variation in photosynthesis efficiency in response to increased irradiance.

MATERIALS AND METHODS

Plant material and growth conditions

A set of 344 accessions was used for GWAS, as described in Chapter 3 of this thesis. The accessions S96 and SLSP30 were crossed, and one F1 plant was self-fertilized to produce an F2 mapping population. Of this F2 population, 306 plants were grown, genotyped for 384 single nucleotide polymorphisms (SNPs), and phenotyped for photosynthesis response to excess irradiance.

With the aid of the re-sequence data of the 1001 genomes project as described in (http://1001genomes.org/), the accessions Baa-1, Ga-0, S96, Uk-1, and Got-7 were selected to represent the ASN2-PAH2-genotype '*ASN2-5,6,7-PAH2-1,2,3,5,6*'; the accessions Ra-0, Old-1, Yo-0, Faeb-4, and Broet1-6 to represent the genotype "*ASN2-5,6,7-PAH2-4*"; accessions Fei-0, Kin-0, Ren-1, and Chat-1 to represent the genotype "*ASN2-2,3-PAH2-1,2,3,5,6*"; and the accessions Ts-1, LL-0, Com-1, and SLSP30 to represent the genotype "*ASN2-2,3-PAH2-4*".

The T-DNA insertion knock-out line *asn2-1* (SALK_043167) was kindly donated by the laboratory of Dr. Akira Suzuki (INRA Centre de Versailles-Grignon, France). The double T-DNA insertion knock-out line *pah1pah2* (originated from SALK_042970 and SALK_047457) was kindly donated by the laboratory of Dr. Peter Eastmond (Department of Plant Biology and Crop Science, Rothamsted Research, United Kingdom).

All plants were grown and phenotyped as described in Chapter 3 of this thesis

Genetic analysis

Genome wide association analysis was performed for Φ_{PSII}-values averaged per accession (at least three replicates were used to determine the average value), combined with the 215,000 SNP database for 360 accessions (Kim et al., 2007), using a mixed model analysis software package, written within the R project environment for statistical computing (https://www.r-project.org/).

For analysis of the F2 population derived from the cross between S96 and SLSL30, all 306 F2 plants were genotyped for 384 SNPs using Illumina's GoldenGate Genotyping with VeraCode Technology. A genetic map was created using Joinmap 4 (Van Ooijen, 2006). Multiple QTL Mapping (MQM) was performed using MapQTL6 (Van Ooijen, 2009).

Haplotypes were generated based on all SNPs in the promoter and coding regions of the two candidate genes using the re-sequence data of 173 accessions, which are those out of the 344 GWAS accessions of which re-sequence data were available at the time of the analysis (http://1001genomes.org/). Those haplotypes that occurred in >4% of the 173 accessions were then associated with photosynthetic phenotypes. Haplotypes that resulted in significantly different photosynthetic response to increased irradiance (based on t-test) were further compared per SNP for association with the phenotype.

Gene expression analysis

Gene expression was determined using quantitative reverse transcriptase PCR (qRT-PCR) as described in Chapter 3 of this thesis. The primers used are listed in table S1.

Lipid profiling

Rosettes of Arabidopsis plants grown for 33 days in 600 µmol m^{-2} s^{-1} growth irradiance were harvested and flash-frozen in liquid nitrogen. Frozen rosettes were broken into pieces and immersed for 15 minutes in 2 ml isopropanol with 0.01% butylated hydroxytoluene (BHT), preheated to 80 °C. Subsequently, 1 ml chloroform and 0.4 ml water were added, mixed, and the solution was agitated for 1 hour at room temperature. Lipid extracts were transferred to glass tubes with Teflon-line screw-caps; 2 ml chloroform/methanol (2:1) with 0.01% BHT was added to the remaining leaf pieces, and the solution was agitated for 30 minutes at room temperature. The second lipid extract was added to the first extract and the extraction procedure was repeated until all leave pieces became white. Subsequently, 0.5 ml of 1M potassium chloride was added to the combined extract, mixed and centrifuged to separate the lipids from the proteins and carbohydrates. The upper phase was discarded, 0.5 ml water was added to the lower phase, mixed and centrifuged. The upper phase was discarded again, and the lower phase was dried with nitrogen stream.

The dried lipid extracts were analysed by thin layer chromatography (TLC) coupled with gas-liquid chromatography (GLC).

RESULTS

Identification of two QTLs for the photosynthesis response to increased irradiance

Using 344 accessions, Φ_{PSII} was measured repeatedly three times a day in a climate chamber where the growth irradiance was increased from 100 to 550 µmol m^{-2} s^{-1}, at the onset of the photoperiod, on day 25 after sowing. The first measurement in high light was performed one hour after the irradiance increase and the second measurement 3.5 hours after the irradiance increase. Genome wide association studies (GWAS) were performed to associate these first two high light measurements with 215,000 SNPs spread over the genome of Arabidopsis. By setting the significance threshold for association peaks to a -10log(p)=4, thirteen peaks of association were identified one hour after the irradiance increase and seventeen peaks 3.5 hours after the irradiance increase, with an overlap of 6 peaks (Fig. 1A and 1B). All association peaks are specific for high light, none of them appeared before the irradiance increase (Fig. S2).

In order to select the QTLs for further analysis, two GWAS accessions (S96 and SLSP30) were crossed that were polymorphic for all SNPs above our association threshold. One F1-plant was self-fertilized, and the F2 population was grown under the same conditions as the GWAS population and Φ_{PSII} values were measured at the same time points. A genetic map was created for the F2 population (Supplementary Fig S1), and QTLs for Φ_{PSII} values at the same time points as in the GWAS were mapped using family mapping (Fig 1C and 1D).
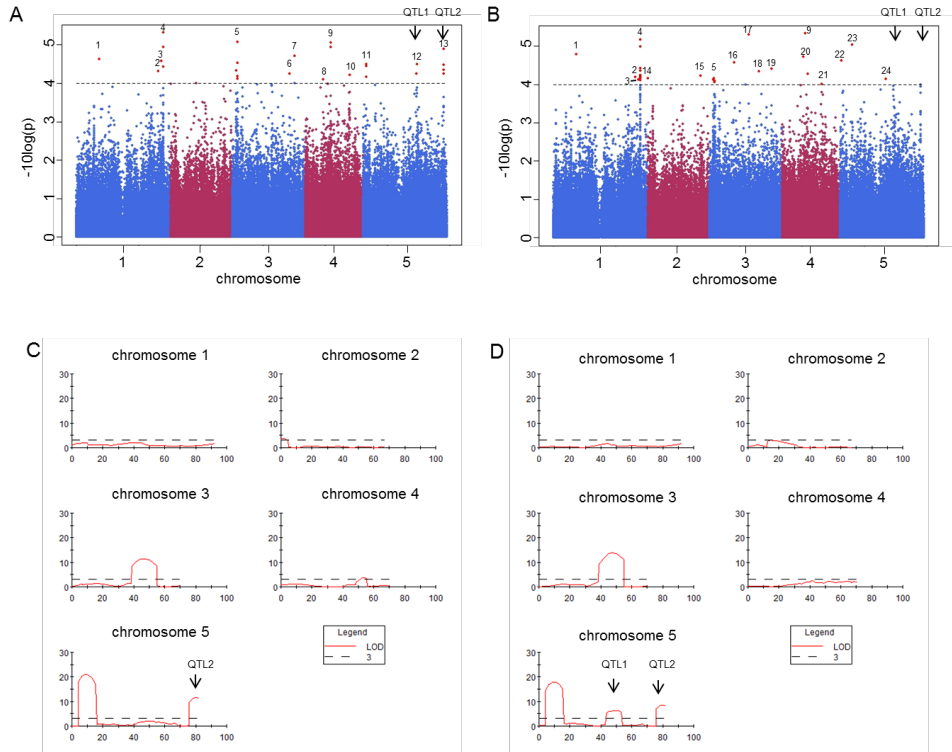
Figure 1. Mapping of photosynthesis response to excess irradiance in Arabidopsis thaliana
(A + B) -log$_{10}$(Pvalue) for 215,000 single nucleotide polymorphisms (SNPs) in a genome-wide association mapping panel of 344 natural accessions (A) one hour after increased growth irradiance, and (B) three and a half hours after increased growth irradiance. The colours blue and pink distinguish the 5 chromosomes from left to right, the black dotted line represents a significance threshold arbitrarily set at -log$_{10}$(Pvalue)=4, the red dots are SNPS that are associated with the phenotype at -log$_{10}$(Pvalue)≥4, the numbers indicate distinct association peaks; (C + D) LOD scores of 384 SNPs represented as a red line though each chromosome in an F2 mapping population arisen from a cross between two natural accessions S96 and SLSP30 (C) one hour after increased growth irradiance, and (D) three and a half hours after increased growth irradiance. The black dotted line represents a significance threshold set with a permutation test at LOD=3.

At one hour after the irradiance increase, the F2 population QTL map showed five QTLs. The QTL on chromosome 2 and the QTL on chromosome 4 were unstable when comparing the one hour time-point to the 3.5 hour time-point; the QTL on chromosome 3 and the other QTL on chromosome 5 were also found when Φ_{PSII} was measured before the irradiance increase (Fig. S3). Only the QTL at the end of chromosome five is specific for high light and is stable when compared to 3.5 hours after the increase (QTL2, Fig. 1C). At 3.5 hours after the irradiance increase, one more QTL on chromosome 5 was

associated with Φ_{PSII}, also specific for high light (QTL1, Fig. 1D). QTL1 disappeared on day 2 after the irradiance increase and QTL2 disappeared on day 3 after the irradiance increase (Fig. S3). QTL1 and 2 were both also found in the GWAS-profiles (Fig. 1A and 1B); with the notification that 3.5 hours after the irradiance increase these two peaks were just below our arbitrary threshold of -10log(p)=4 (Fig. 1B). However, both QTLs reappeared in subsequent time-points (Fig. S2). The location of the associated SNPs above –log10(p)=4 in GWAS or above LOD=3 in F2 family mapping for both QTLs are shown in Table 1.

Table 1. Location of the associated SNPs above –log10(p)=4 in GWAS or above LOD=3 in F2 family mapping for (A) QTL1 and (B) QTL2

A

QTL1	
Location of associated SNPs on chromosome 5	
above -log10(p)=4 in GWAS	above LOD=3 in family mapping
17,186,178	14,853,688
17,187,071	16,105,691
17,187,390	16,428,797
	16,947,516
	17,154,448
	17,612,157
	17,675,463
	17,675,844
	18,241,308
	20,391,591
	20,898,095

B

QTL2	
Location of associated SNPs on chromosome 5	
above -log10(p)=4 in GWAS	above LOD=3 in family mapping
25,956,134	25,149,877
25,963,073	25,802,730
25,967,700	26,203,511
25,968,943	26,420,670
25,975,808	26,621,481
25,976,943	

The LD region in GWAS around the associated SNPs of QTL1 is 8 kb (Kim et al., 2007), which encompasses three genes according to TAIR10 (www.arabidopsis.org), which are At5g42860, At5g42870, and At5g42880. Of these three genes, only at5g42870 has a described gene function, encoding *PHOSPHATIDIC PHOSPHOHYDROLASE 2 (PAH2)*. Haplotype analysis and mutant analysis was performed for *PAH2* to prove its involvement in natural variation for photosynthesis efficiency, as described in the next paragraphs.

The LD region in GWAS around the associated SNPs of QTL2 is 50 kb (Kim et al., 2007), which encompasses twenty genes according to TAIR10, ranging from At5g64855 until At5g65020. This association peak also arose after performing GWAS in a time-course manner (Chapter 3 of this thesis). *In silico* prioritization of these twenty candidate genes

172

based on gene ontology, gene co-expression, gene expression in the vegetative rosette, and the presence of segregating polymorphisms in the coding sequence followed by mutant analysis highlighted At5g65010, encoding *ASPARGINE SYNTHETASE 2 (ASN2)*, as the best candidate underlying QTL2 (Chapter 3 of this thesis). Haplotype analysis and functional analysis was performed for *ASN2* to prove its involvement in photosynthesis efficiency.

Haplotype analysis

Haplotype analysis among 173 re-sequenced accessions for the *PAH2* gene resulted in 8 different alleles with allele frequencies ≥ 4% (Fig. 2A). No clear difference in photosynthesis efficiency response to increased irradiance was discovered between these alleles (Fig. 2B). Sequence analysis revealed several polymorphisms were common among alleles 1, 2, 3, 5, and 6, indicated by the blue arrows in Fig. 2A. Additionally, alleles 7 and 8 showed sequence similarity (Fig. 2A). Allele 4 showed distinct from either of the other alleles, indicated by the red arrows in Fig. 2A. Grouping the 173 re-sequenced accessions according to their *PAH2* alleles based on this observation (*PAH2-1,2,3,5,6* versus *PAH2-7,8* versus *PAH2-4*) revealed higher photosynthesis efficiency in response to increased irradiance for accession with the *PAH2-1,2,3,5,6* allele (Fig. 2C).

Haplotype analysis among 173 re-sequenced accessions for *ASN2* resulted in 7 different alleles with allele frequencies ≥ 4% (Fig. 2D), of which allele 2 resulted in significantly lower photosynthesis efficiency compared to the other alleles (Fig. 2E). In addition, also allele 4 has lower photosynthesis efficiency specifically at later time points (Fig. 2E). Close analysis of the sequences of alleles led to the hypothesis that the following two polymorphisms in *ASN2* are associated to the observed photosynthesis differences: the guanine (G) of alleles 5, 6 and 7 (*ASN2-5,6,7*) in the fifth intron of the coding sequence (position 25,970,333 bp) led to relatively high photosynthesis efficiency; and the cytosine (C) of alleles 2 and 3 (*ASN2-2,3*) in the tenth exon of the coding sequence (position 25,971,571 bp), leads to relatively low photosynthesis efficiency (Fig. 2D). We did not observe genotypes in which both polymorphisms were present together. Grouping the 173 re-sequenced accessions according to their *ASN2* alleles based on this observation (*ASN2-1,4* versus *ASN2-2,3* versus *ASN2-5,6,7*) revealed different photosynthesis efficiency in response to increased irradiance between accessions with the *ASN2-2,3* compared to accessions with the *ASN2-5,6,7* allele (Fig. 2F).

Figure 2 (on next page). In silico analysis of 173 re-sequenced Arabidopsis accessions (1001 genomes)

(A) Eight most abundant alleles and frequency (%) for the PAH2 gene. Gene orientation is 3' to 5'; two splice variants are indicated. SNPs differing from the Col-0 reference genome sequence (allele 8) are marked. Polymorphisms indicative of possible association with natural variation in photosynthesis efficiency are marked in red and blue; (B) Average photosynthesis efficiencies (Φ_{PSII}) (±SE) of accessions grouped by the eight alleles of PAH2 before and after an increase in irradiance; (C) Median Φ_{PSII} one hour after increased irradiance of accessions grouped by the identity of the two SNPs that represent best the different alleles in the PAH2 gene (N=118 for PAH2-1,2,3,5,6; N=23 for PAH2-7,8; N=32 for PAH2-4). Box = 25th and 75th percentiles; bars = min and max values; letter over bar indicates significant differences between groups in T-test series; (D) Seven most abundant alleles and frequency (%) for the ASN2 gene. Gene orientation is 5' to 3'; two splice variants are indicated. SNPs differing from the Col-0 reference genome sequence (allele 1) are marked. Polymorphisms associated with natural variation in photosynthesis efficiency are marked in red (E) Average photosynthesis efficiencies (Φ_{PSII}) (±SE) of accessions grouped by the seven alleles of ASN2 before and after an increase in irradiance. (F) Median Φ_{PSII} one hour after increased irradiance of accessions grouped by the identity of the two causative SNPs in the ASN2 gene (N=79 for ASN2-1,4; N=27 for ASN2-2,3; N=67 for ASN2-5,6,7). Box = 25th and 75th percentiles; bars = min and max values; letter over bar indicates significant differences between groups in T-test series.
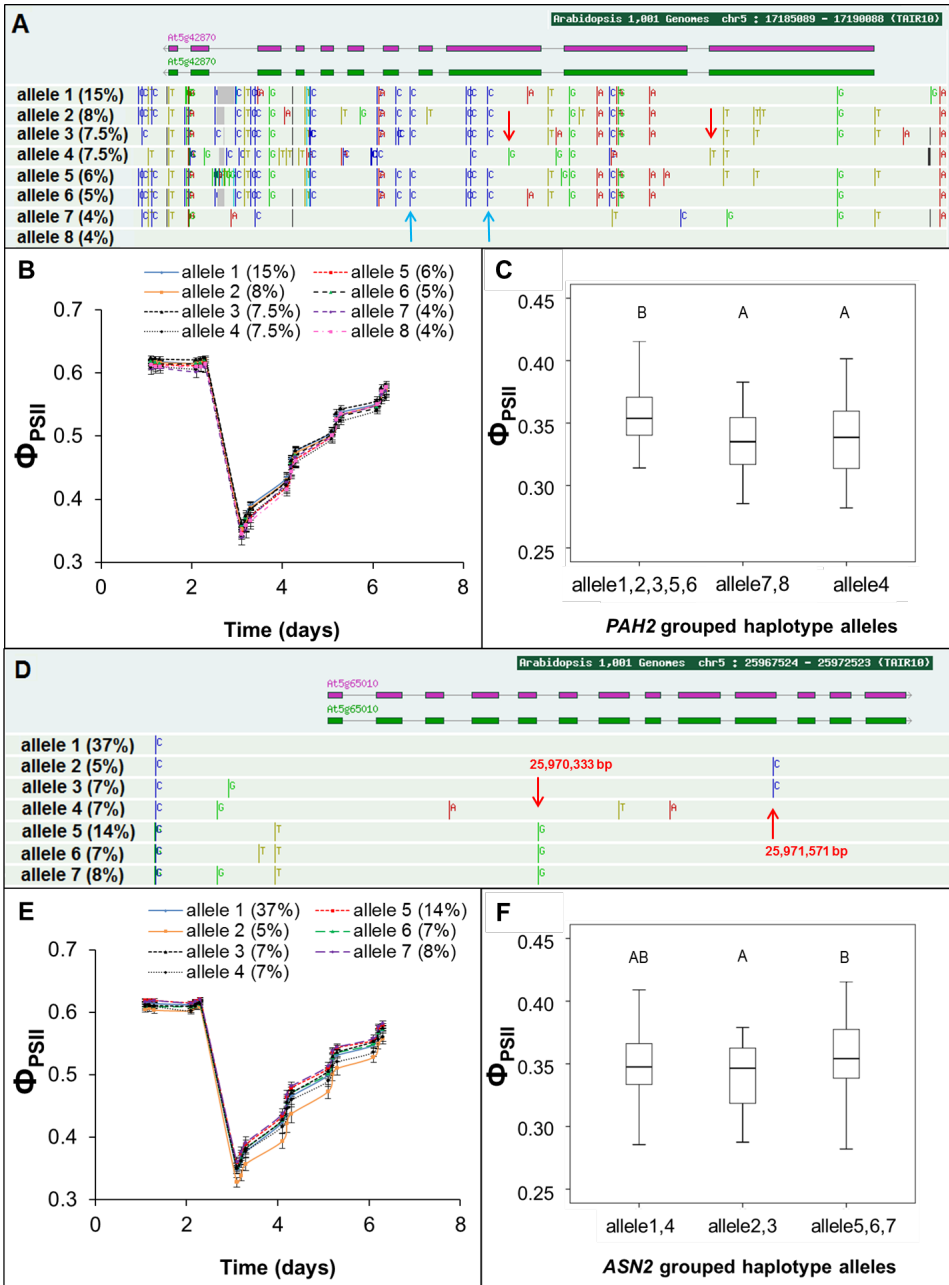
Epistasis

Analysis of the effect of the different *PAH2* and *ASN2* alleles revealed that the variation at the *PAH2* gene only affected photosynthesis efficiency in high light when *ASN2-2,3* was present (Fig. 3A). Oppositely, the variation at the *ASN2* gene only affected photosynthesis efficiency in high light when *PAH2-4* was present (Fig. 3A). The same epistatic relation was observed in the F3 population arisen from five F2 plants grouped by their genotypes concerning the *PAH2* and *ASN2* alleles (Fig. 3B).
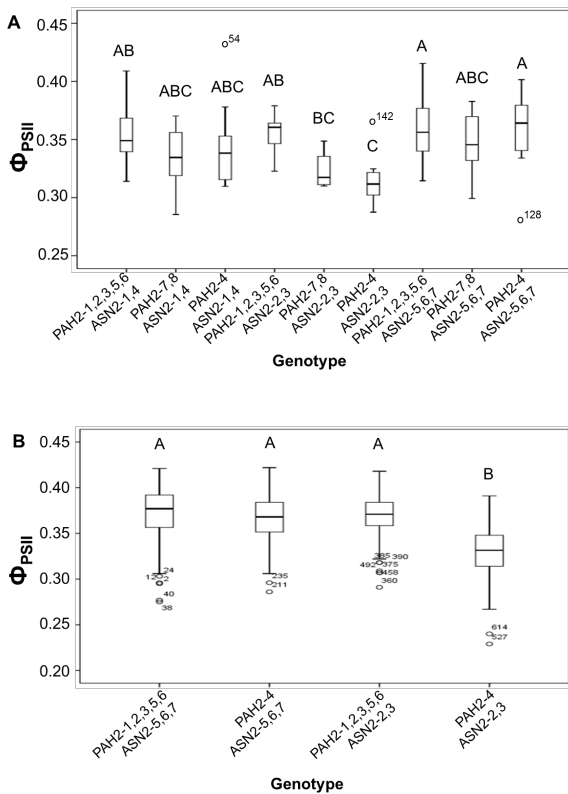
Figure 3. Epistasis

Median Φ_{PSII} one hour after increased irradiance of (A) the natural accessions; and (B) the F3-families arisen from the F2 population, grouped by their genotypes concerning the PAH2 and ASN2 alleles; Box = 25th and 75th percentiles; bars = min and max values; number over or under bar indicates statistical outliers; letter over bar indicates significant differences between groups in ANOVA.

Mutant analysis

For both the *PAH2* as the *ASN2* gene T-DNA insertion knock-out mutants are available. These were studied to further investigate the involvement of *PAH2* and *ASN2* in photosynthesis efficiency. A knock-out of *ASN2* in the Col-0 background (*asn2-1*) affected photosynthesis efficiency at the first two days after the increase in growth irradiance (Fig. 4). A knock-out of *PAH2* is expected to have no obvious phenotype as *PAH2* is known to be redundant with *PAH1*, and both genes need to be mutated to disrupt their function (Eastmond et al., 2010). The double knock-out *pah1pah2* did not affect photosynthesis efficiency on the first two days after increased growth irradiance, but after the third and fourth day it acclimated less than control (Fig. 4). The lines *asn2-1* and *pah1pah2* were crossed and the triple mutant *asn2-1pah1pah2* was selected in its progeny using mutant specific markers. The triple mutant did not affect photosynthesis efficiency in any time point compared to Col-0 (Fig. 4). To confirm the effect of the different natural alleles identified in haplotype analysis, quantitative complementation was tried for the *asn2-1* mutant, but failed to identify *ASN2* as causal for the identified QTL (Chapter 3 of this thesis).
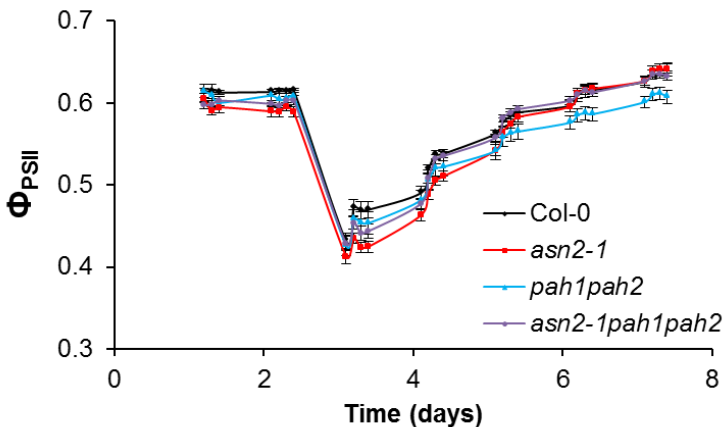

Figure 4. Mutant analysis of asn2-1, pah1pah2, and asn2-1pah1pah2.
Representative photosynthetic (Φ_{PSII}) phenotypes for Arabidopsis Col-0, and the mutants asn2-1, pah1pah2, and asn2-1pah1pah2, grown for 24 days in 100 µmol m^{-2} s^{-1} growth irradiance and subsequently 6 days in 550 µmol m^{-2} s^{-1} growth irradiance, measured from day 23 (first day of measurement) until day 31, at four time-points per day; AV±SE .

Gene expression

Gene expression of *PAH2* and *ASN2* in natural accessions as well as in T-DNA knock-out insertion lines was studied to provide evidence for the involvement of both genes as underlying the two QTLs found for photosynthesis efficiency, as well as to find an explanation for the epistatic interaction between these two QTLs. There is no difference in expression of *ASN2* when comparing *ASN2-567* vs *ASN2-23* under LL, whereas *ASN2-567* is higher expressed than *ASN2-23* under HL (Fig. 5A). Additionally, the presence of the *PAH2-1,2,3,5,6* allele leads to down-regulation of *ASN2* in response to increased irradiance (Fig. 5A). Expression of *PAH1* nor *PAH2* in response to increased irradiance could not be associated to any allelic combination (Fig 5B and 5C).

In the double mutant *pah1pah2*, the expression response to increased irradiance of *ASN2* is similar as in Col-0 (Fig 6A). When *ASN2* is no longer functional (in the *asn2-1* mutant), the expression of *PAH2* is increased in response to increased irradiance, whereas the expression of *PAH1* is not (Fig 6B and 6C). In the double mutant *pah1pah2,* there is still some *PAH1* expression implying *pah1* is not a knock-out, but a knock-down. In the triple mutant *asn2-1pah1pah2*, the expression response to increased irradiance of *PAH1* is increased compared to Col-0 (Fig 6B).
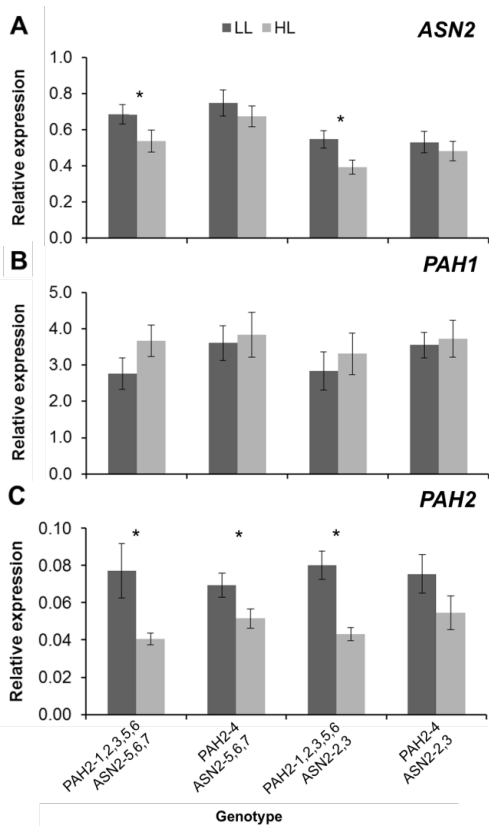
Figure 5. Expression analysis of ASN2, PAH1, and PAH2 in natural Arabidopsis accessions

*Expression of (A) ASN2, (B) PAH1, and (C) PAH2 measured as relative expression to the averaged value of the housekeeping genes (± SE) by qRT-PCR three hours after excess irradiance induction (HL) as well as in control conditions (LL), in natural Arabidopsis accessions grouped by their genotypes concerning the PAH2 and ASN2 alleles. Expression was measured in four accessions randomly chosen per genotype (Baa-1, Ga-0, S96, Uk-1, and Got-7 to represent the genotype 'PAH2-1,2,3,5,6-ASN2-5,6,7'; Ra-0, Old-1, Yo-0, Faeb-4, and Broet1-6 to represent the genotype "PAH2-4- ASN2-5,6,7"; Fei-0, Kin-0, Ren-1, and Chat-1 to represent the genotype "PAH2-1,2,3,5,6-ASN2-2,3"; and Ts-1, LL-0, Com-1, and SLSP30 to represent the genotype 'PAH2-4- ASN2-2,3'; four biological replications were used per accessions, two plants were pooled per biological replication. The * indicates significant (P=0.05) difference between expression in high light conditions (HL) versus expression in control conditions (LL).*

HL response affects membrane lipid remodelling

PAH1 and *PAH2* convert phosphatidic acid into di-acyl-glycerol (DAG), releasing orthophosphate as by-product (Eastmond et al., 2010). This is a small step in the complex physiological process of remodelling phospholipids to the galactolipids monogalactosyl diacylglycerol (MGDG) and digalactosyl diacylglycerol (DGDG) (Nakamura et al., 2009). The lipid remodelling functions in releasing orthophosphate (Pi) from phospholipids to overcome phosphate starvation (Moellering and Benning, 2011), as well as to acclimate photosynthesis efficiency to excess light (Nilsson et al., 2011). *PAH2* and *ASN2* were hypothesized to epistatically function in balancing the intracellular Pi concentrations.

Gene expression of MGDG and DGDG synthase genes in the *asn2-1* and *pah1pah2* T-DNA knock-out insertion lines was studied to test if *ASN2* can take over the lipid remodelling function of *PAH1/2* in providing balanced Pi concentrations. No effect of increased irradiance (HL) was observed after three hours on expression of the MGDG and DGDG synthase genes compared to control conditions (LL) in Col-0, nor in the single mutant *asn2-1* or the double mutant *pah1pah2* (Fig 6D, 6E, 6F, 6G, and 6H), while all tested MGDG and DGDG synthase genes were upregulated after three hours in response to increased irradiance in the triple mutant *asn2-1pah1pah2* (Fig 6D, 6E, 6F, 6G, and 6H). The absent induction of the MGDG and DGDG synthase genes in Col-0 implies that three hours after irradiance increase is too short to activate the process of lipid remodelling to release orthophosphate. The induction of the MGDG and DGDG synthase genes in the triple mutant is correlated with the induction of *PAH1* in the triple mutant (Fig. 6B), implying *PAH1* activates lipid remodelling within three hours after the irradiance increase only when both *ASN2* and *PAH2* are knocked-out, indicating the significance of the lipid remodelling process in acclimation to increase irradiance.

To confirm the significance of lipid remodelling, lipid profiling in the *asn2-1* and *pah1pah2* T-DNA knock-out insertion lines as well as in two natural accessions with contrasting *ASN2* and *PAH2* genotypes was performed. Additionally, it was still not clear if *ASN2* could take over the lipid remodelling function of *PAH1/2*. Four lipids were quantified, two of which are galactolipids (monogalactosyldiacylglycerol [MGDG] and digalactosyldiacylglycerol [DGDG]) and two are phospholipids (phosphatidylcholine [PC] and phosphatidylglycerol [PG]). The molar ratios (the share of one class of lipids in the total amount of lipids) of MGDG were similar in the double mutant *pah1pah2* and the triple mutant *asn2-1pah1pah2*, both were lower than in Col-0 (Fig. 7A). This observation

confirms the lipid remodelling function of *PAH1* and *PAH2*, and implies *ASN2* cannot take over the lipid remodelling function of *PAH1/2*. The molar ratio of DGDG was similar in all genotypes measured (Fig. 7B), implying the effect of *PAH1/2* on lipid remodelling does not affect DGDG synthesis. Of the phospholipids, the molar ratios of PC were similar in the double mutant *pah1pah2* and the triple mutant *asn2-1pah1pah2*, both were higher than in Col-0 (Fig. 7A). The molar ratios of PG were similar in all genotypes measured. No differences were measured between Col-0 and the natural Arabidopsis accessions representing the 'PAH2-1,2,3,5,6-ASN2-5,6,7' and 'PAH2-4-ASN2-2,3' genotypes (Fig. 7).
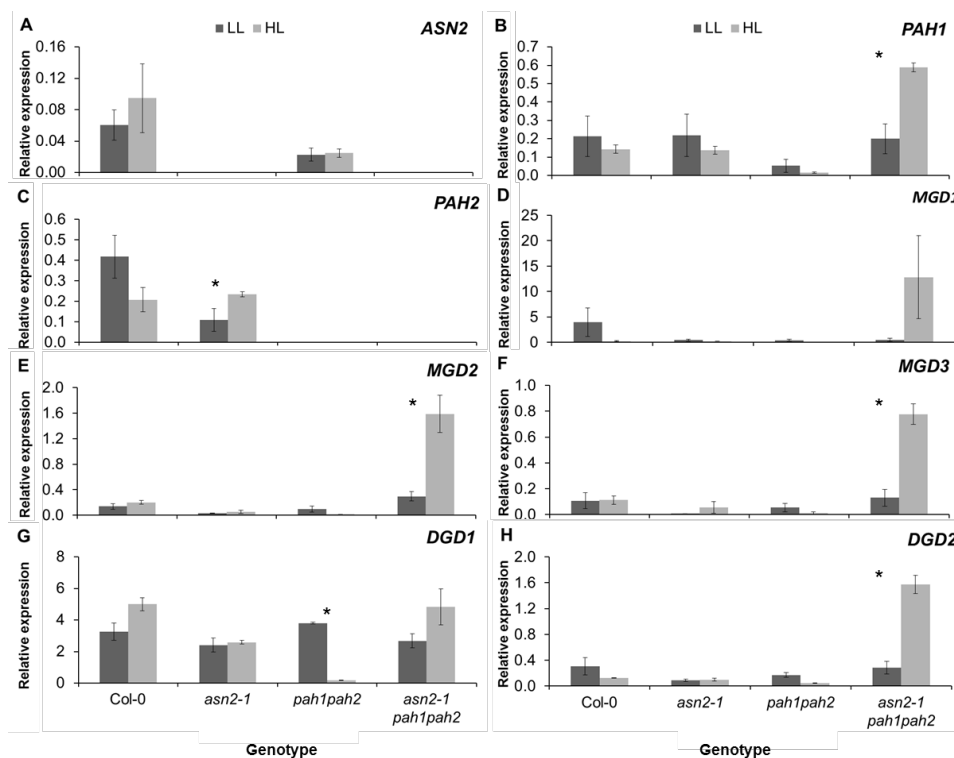
Figure 6. Expression analysis of ASN2, PAH1, PAH2, MGD1, MGD2, MGD3, DGD1, and DGD2 in Col-0, asn2-1, pah1pah2, and asn2-1pah1pah2.

Expression of (A) ASN2, (B) PAH1, (C) PAH2, (D) MGD1, (E) MGD2, (F) MGD3, (G) DGD1, (H) DGD2 measured as relative expression to the averaged value of the housekeeping genes (± SE) by qRT-PCR three hours after increased irradiance induction (HL) as well as in control conditions (LL), in Col-0, and in the T-DNA knock-out mutant lines asn2-1, pah1pah2, and asn2-1pah1pah2. The * indicates significant (P=0.05) difference between expression in high light conditions (HL) versus expression in control conditions (LL).
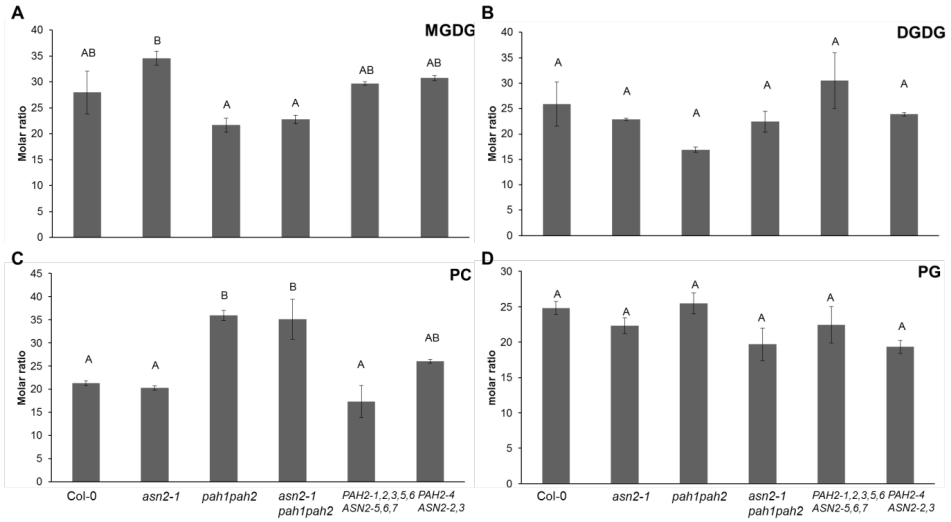
Figure 7. Molar ratios of major lipid classes in Arabidopsis mutants and in natural accessions grown for 33 days in 600 µmol m^{-2} s^{-1} growth irradiance.

Molar ratio of (A) monogalactosyldiacylglycerol (MGDG); (B) digalactosyldiacylglycerol (DGDG); (C) phosphatidylcholine (PC); and (D) phosphatidylglycerol (PG) in whole rosettes of Arabidopsis Col-0, in the T-DNA knock-out mutant lines asn2-1, pah1pah2*, and* asn2-1pah1pah2, *and in one natural accession representing the '*PAH2-1,2,3,5,6-ASN2-5,6,7*' genotype and one natural accession representing the '*PAH2-4-ASN2-2,3*' genotype, grown for 3 days in 600 µmol m^{-2} s^{-1} growth irradiance, (AV ±SE; N=3) . Letter above bars indicate significant differences.*

Geographic distribution

In order to find any pattern of evolutionary adaptation, the coordinates of the GWAS accessions were mapped according to their genotypes concerning the *PAH2* and *ASN2* alleles (Fig. 8). The geographical distribution of European GWAS accessions grouped by the identity of the *ASN2* and *PAH2* alleles shows an east-west gradient with the photosynthetically best performing combination of alleles '*PAH2-1,2,3,5,6-ASN2-5,6,7*' (green) in central and eastern Europe, the two combinations of one positive and one negative photosynthetically performing allele '*PAH2-4-ASN2-5,6,7*' and '*PAH2-1,2,3,5,6-ASN2-2,3*' (combined in one colour: yellow) are mainly found in France and Spain and the photosynthetically worst performing '*PAH2-4-ASN2-2,3*' (red) found in France and Spain as well as in Britain (Fig. 9).
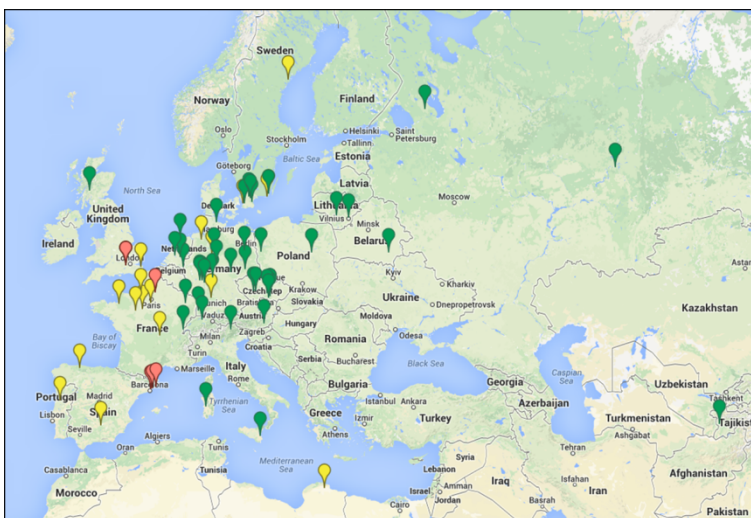
Map data ©2014 Geobasis-DE/BKG (©2009), Google

Figure 8. Geographic distribution.

Geographic distribution of European GWAS accessions grouped by grouped by their genotypes concerning the PAH2 and ASN2 alleles: 'PAH2-1,2,3,5,6-ASN2-567' (green) and 'PAH2-4-ASN2-2,3' (red), plus the two heterozygous alleles 'PAH2-4-ASN2-567' and 'PAH2-1,2,3,5,6-ASN2-2,3' (combined in one colour: yellow).

DISCUSSION

By combining GWAS and F2 family mapping, we identified two QTLs on chromosome 5, which have an epistatic interaction for photosynthesis efficiency response to increased irradiance. Using the high resolution of GWAS we identified the underlying genes *ASPARAGINE SYNTHASE 2* (*ASN2*) and *PHOSPHATIDIC ACID PHOSPHOHYDROLASE 2* (*PAH2*) as the best candidates associated to natural variation in photosynthesis efficiency response to increased irradiance.

Epistatic interaction and allelic variation for *PAH2* and *ASN2* underlying two QTLs for photosynthesis response to increased irradiance

In the GWAS, the association peak for *PAH2* (QTL1) as well as the peak for *ASN2* (QTL2) came above our arbitrary threshold at one hour after the irradiance increase (Fig. 1A), both were below the threshold at 3.5 hours after the irradiance increase (Fig. 1B), and both re-appeared in subsequent time-points (Fig. S2), revealing the QTLs depend on the environment. In the F2 family mapping, the QTL for *ASN2* appeared within one hour after the irradiance increase and it was still present after 3.5 hours, whereas the QTL for *PAH2* appeared only 3.5 hours after the increase in irradiance (Fig. 1C and 1D). Similar as in GWAS, also in the F2 family mapping the two QTLs re-appeared in subsequent time-points (Fig. S3), revealing 'genotype x environment' interaction (El-Soda et al., 2014).

Both for *ASN2* and *PAH2*, haplotype analysis revealed three distinct alleles (Fig. 2). The *PAH2-1,2,3,5,6* and the *PAH2-4* alleles reveal distinct polymorphisms compared to the *PAH2-7,8* allele (the Col-0 allele). The combination of the polymorphismics SNPs of the *PAH2-1,2,3,5,6* allele and the polymorphisms of the *PAH2-4* allele does not occur in the population. Similarly, the *ASN2-5,6,7* and *ASN2-2,3* alleles reveal distinct polymorphisms compared to the *ASN2-1,4* allele (the Col-0 allele), and the combination of polymorphisms does not occur in the population. The fact that some combinations of polymorphisms do not occur suggests that two independent mutational events happened one after the other (Fig. 9). The combination of the *PAH2-4* and *ASN2-2,3* allele is photosynthetically unfavourable (Fig 2), probably leading their low frequency in the population (Fig 9). Many more polymorphisms are present in *PAH2* than in *ASN2*, suggesting *PAH2* is functionally less important than *ASN2*, as functionally less important loci evolve at a faster rate (Kimura and Ohta, 1974). The fact that there is another gene with similar function as *PAH2*, which is *PAH1*, supports this suggestion.
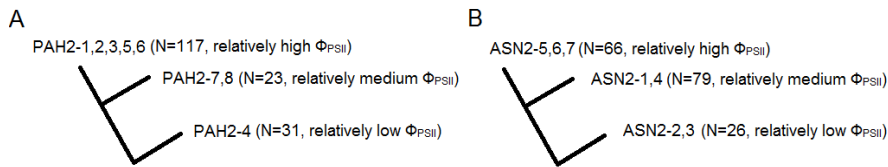
A

PAH2-1,2,3,5,6 (N=117, relatively high Φ_{PSII})

PAH2-7,8 (N=23, relatively medium Φ_{PSII})

PAH2-4 (N=31, relatively low Φ_{PSII})

B

ASN2-5,6,7 (N=66, relatively high Φ_{PSII})

ASN2-1,4 (N=79, relatively medium Φ_{PSII})

ASN2-2,3 (N=26, relatively low Φ_{PSII})

Figure 9. Overview of (A) PAH2 and (B) ASN2 alleles

The occurrence in the population (N) and the effects on photosynthesis efficiency (Φ_{PSII}) of the alleles relative to each other are shown.

The combination of GWAS mapping and F2 family mapping allowed the discovery of an epistatic relationship between the two loci covering the *PAH2* and *ASN2* genes (Fig. 3). The epistasis was more pronounced in the F2 population than in the GWAS population (Fig. 3), explained by the less allelic diversity of the two loci in the F2 population. In the F2 population both loci have two possible alleles (either parent A or parent B), whereas in the GWAS population there are at least three alleles per locus (Fig. 2). Epistasis limits the effect of genetic variation in one locus to the presence of a specific allele at another locus, reducing the amount of accessions to determine the effect size of the QTL, limiting the genetic signal. Additionally, when the two loci are on the same chromosome there is genetic linkage, lowering the recombination events between the two loci, distorting the distribution of frequencies of allelic combinations of the two loci. Both these limitations contributes to epistasis often being seen as a limiting factor in performing GWAS, as it lowers the association of QTLs (Korte and Farlow, 2013). The epistatic effect results in the combination of two alleles (*PAH2-4* and *ASN2-2,3*) that gives a less favourable photosynthesis efficiency, which indicates that although the other alleles function sufficiently to take over the effect of a less functional allele at the other locus, this is not the case when a less functional allele occurs at both loci, implying both genes function in a similar way in photosynthesis.

PAH2 and *ASN2* balance intracellular Pi concentrations for maintaining high photosynthesis efficiency

PAH1 and *PAH2*, which act redundantly (Eastmond et al., 2010), are needed for remodelling phospholipids to galactolipids (Nakamura et al., 2009). The lipid remodelling functions in releasing orthophosphate (Pi) from phospholipids to overcome phosphate starvation (Moellering and Benning, 2011), as well as to acclimate photosynthesis efficiency to excess light. In photosynthesis, Pi is necessary for ATP synthesis, activation

185

of Rubisco, and for export of triose phosphate (Dietz and Foyer, 1986). Within the process of lipid remodelling *PAH1* and *PAH2* convert phosphatidic acid into di-acyl-glycerol (DAG), releasing orthophosphate as by-product (Eastmond et al., 2010). DAG is the direct substrate for synthesis of monogalactosyl diacylglycerol (MGDG), MGDG being a substrate for the synthesis of digalactosyl diacylglycerol (DGDG). DGDG is important for the integrity of the chloroplast protein-import apparatus (Chen and Li, 1998), explaining the significance of the lipid remodelling process for keeping high photosynthetic efficiencies. However, MGDG but not DGDG molar ratios were affected in the *asn2-1* and *pah1pah2* mutants, suggesting not DGDG but another galactolipid is significant for the response to increased irradiance (Fig 7). It is suggested the MGDG is converted to the negatively charged sulfoquinvosyl diacyldiglycerol (SQDG), that creates a charge balance to the photosynthetic membranes that is overcharged as a result of the excess light (Chapter 4 of this thesis).

ASN2 is one of three members of the small asparagine synthetase gene family in Arabidopsis (Lam et al., 1998), which converts the amino acid aspartic acid (Asp) to asparagine (Asn). Asn acts as an important nitrogen storage and transport compound in plants, particularly when carbon supplies are limited (Lam et al., 1998). The expression of *ASN2* is absent in dark-adapted plants, and is induced after a switch from dark to light in an ammonium-dependent way (Lam et al., 1998; Wong et al., 2004). Oxidative stress following excess irradiance increases the cellular concentrations of ammonium by either increased rates of photorespiration or induced rates of proteolytic activity, breaking down oxidatively damaged proteins (Sweetlove et al., 2002; Foyer et al., 2003; Kumagai et al., 2011; Bittsánszky et al., 2015). Genotypic variation for increased rates of ammonia emission in relation to photorespiration has been found in rice (Kumagai et al., 2011), but this relationship could not be found in Arabidopsis (Gaufichon et al., 2013). However, the proteolytic activity that results from oxidative stress does increase ammonia levels in Arabidopsis (Sweetlove et al., 2002). As excess ammonium is toxic to plants, the produced ammonium is normally immediately re-used for new organic and amino acid biosynthesis (Foyer et al., 2003). Ammonium levels were found to accumulate in high light irradiance in *asn2*-knock-out lines but not in Col-0 wild type, indicating that ASN2 is needed for proper removal of excess ammonium upon high light irradiance, either by degradation or by reallocation (Wong et al., 2004; Gaufichon et al., 2013). ASN2 is particularly known to play a role in the export of nitrogen from source organs to sink organs via the phloem (Gaufichon et al., 2013). Our study identifies genetic variation in the *ASN2* gene to explain part of the natural variation for photosynthesis efficiency in response to increased irradiance, suggesting that balancing nitrogen metabolism is

186

closely associated to the efficiency of photosynthesis acclimation. We explain the significance of balancing nitrogen metabolism for keeping high photosynthetic efficiencies by the need of removing of excess ammonium levels that rise in source organs in response to oxidative stress (Britto and Kronzucker, 2002; Bittsánszky et al., 2015).

ASN2 was found to have an epistatic interaction with *PAH2* regarding its effect on photosynthesis efficiency. The ASN2 protein is an ATP-pyrophosphatase, which means its synthetase domain binds Mg^{2+}-ATP and aspartate to catalyse the production of an β-aspartyl-AMP intermediate and pyrophosphate (PPi), (Larsen et al., 1999). The β-aspartyl-AMP intermediate is subsequently converted into asparagine via a chemical reaction with ammonia, and the PPi is hydrolysed into two orthophosphate (Pi) molecules (Larsen et al., 1999). Also PAH1 and PAH2 release Pi as by-product when converting phosphatidic acid into di-acyl-glycerol (DAG) (Eastmond et al., 2010). We hypothesize the epistatic relation between ASN2 and PAH2 is explained by the fact that both genes catalyse reactions where Pi molecules are released as by-products. We suggest *ASN2* and *PAH2* are redundant in their role of balancing intracellular Pi concentrations to maintain high photosynthesis efficiency in response to increased irradiance. The epistatic effect between *ASN2* and *PAH2* explains the unsuccessful quantitative complementation test to confirm the effect of the *ASN2* natural alleles on photosynthesis efficiency (Chapter 3 of this thesis). The use of quantitative complementation is ambiguous because of the confounding effects of epistasis (Service, 2004; Turner, 2014). Transgenic complementation is needed to confirm to allelic effects of *PAH2* and *ASN2* on photosynthesis efficiency response to increased irradiance.

PAH2 is known to be redundant to *PAH1* (Eastmond et al., 2010). There is still some *PAH1* expression in the double mutant *pah1pah2,* implying *pah1* is not a knock-out, but a knock-down (Fig. 6B). In the triple mutant *asn2-1pah1pah2*, the expression response to increased irradiance of *PAH1* is increased compared to Col-0 (Fig 6B). The induction of the MGDG and DGDG synthase genes in the triple mutant (Fig 6D, 6E, 6F, 6G, and 6H) is correlated with the induction of *PAH1* in the triple mutant (Fig. 6B), implying *PAH1* activates lipid remodelling within three hours after the irradiance increase only when both *ASN2* and *PAH2* are knocked-out. This suggests *PAH1* function is only needed when both *PAH2* and *ASN2* are knocked-out, confirming the redundant role of *ASN2* and *PAH2* in acclimation to increased irradiance.

Several observations lead to the conclusion that *ASN2* acts earlier in the acclimation response to increased irradiance than does *PAH2*, i.e. the QTL for *ASN2* appears earlier

in the F2 family mapping (Fig. 1), the knock out mutant *asn2-1* mainly affects photosynthesis efficiency on the first two days after increase in irradiance whereas the double knock-out mutant *pah1pah2* mainly affects photosynthesis efficiency on the last few days after increase in irradiance (Fig. 4), and the MGDG and DGDG synthase genes were not induced yet after 3 hours (Fig 6). The triple mutant *asn2-1pah1pah2* does not affect photosynthesis efficiency compared to wild type Col-0 (Fig. 4), suggesting a third pathway for photosynthetic acclimation takes over when the first two are knocked out.

Both the expression of *ASN2* and *PAH2* are not induced in expression after irradiance increase (Fig. 5), implying their individual effects are on translational or functional level. However, the epistatic relation between them is expression-based, as accessions that have *PAH2-1,2,3,5,6* allele show reduced *ASN2* expression three hours after increased irradiance (Fig. 5A), leading to the conclusion that PAH2 downregulates the expression of *ASN2* when *PAH2* gets functional after the irradiance increase by taking over the function of *ASN2* in photosynthetic acclimation to increased irradiance. This expression-based relation is supported by the observation that *PAH2* expression in response to irradiance increase is induced when *ASN2* is knocked out (Fig. 6C), i.e. when one functional pathway is omitted another takes over. The fact that *ASN2* expression is not induced to compensate when *PAH2* is knocked-out, can explained by the fact that the pathway in which ASN2 acts functions earlier in time than the pathway in which PAH2 acts. We explain this by the fast rise of reactive oxygen species and subsequently ammonia, that has to be dissipated and transported to sink organs by ASN2 (producing Pi as side product). When the formation of reactive oxygen species are being prevented by subsequent metabolism such as formation of anthocyanins (Asada, 2006), the release of Pi needed for higher photosynthetic rates gets taken over by PAH2. *PAH2* gets activated for the release of extra Pi, as well as for keeping the integrity of the photosynthetic membranes by providing galactolipids.

Allelic effects on the epistatic interaction between *PAH2* and *ASN2*

We conclude the *ASN2-5,6,7* allele, leading to relatively high photosynthesis efficiency acclimation (Fig. 2), is capable of providing enough Pi so that lipid remodelling by *PAH2* for extra Pi remobilization is not needed. The *ASN2-1,4* allele (the Col-0 allele) is not capable of providing enough Pi so that lipid remodelling is needed, as seen in reduced conversion of phospholipids to galactolipids in the *pah1pah2* double mutant where the *ASN2-1,4* allele cannot take over the lipid remodelling function of mutant PAH2 (Fig. 7). The *ASN2-2,3* allele is also not capable of providing enough Pi, as seen in apparent

effects of *PAH2* allelic variation only when the *ASN2-2,3* allele is present (Fig. 3). The observation of PAH2 allelic variation only being apparent when the *ASN2-2,3* allele is present, suggests the *ASN2-3* allele is less functional that the *ASN2-1,4* allele Oppositely, the *PAH2-1,2,3,5,6* allele, leading to relatively high photosynthesis efficiency acclimation (Fig. 2), provides enough Pi, leading to down-regulation of *ASN2* (Fig. 5A). Both the *PAH2-4* allele and the *PAH2-7,8* allele (the Col-0 allele) do not show this effect, being less functional (Fig. 5A and Fig. 6A). The observation of *ASN2* allelic variation only being apparent when the *PAH2-4* allele is present, suggest the *PAH2-4* allele is less functional than the *PAH2-7,8* allele (the Col-0 allele).

The European geographic distribution of natural accessions grouped according to the presence of the allelic combinations for *ASN2* and *PAH2*, shows a longitudinal gradient with the photosynthetically best performing allelic combination (*PAH2-1,2,3,5,6* and *ASN2-5,6,7*) found more in eastern Europe (Fig. 8). This is indicative of a selective force acting on photosynthesis regulation; future evolutionary ecological studies are necessary to find out what this force is.

This study shows strong indications for the involvement of *PAH2* and *ASN2* in keeping high photosynthesis efficiencies in response to increased irradiance. Ultimate proof of the *PAH2-1,2,3,5,6* allelic effects and the *ASN2-5,6,7* allelic effects for increasing photosynthesis efficiencies should be gained by future transgenic complementation studies.

ACKNOWLEDGEMENT

SUPPLEMENTARY TABLES AND FIGURES

Table S1. Primers used for qRT-PCR

| Name	Gene	Forward Primer	Reverse Primer
ASN2	at5g65010	TTGCATCGACAACTCTCAAG	CTCCAATCAGGACCTCTG
PAH1	at3g09560	CCTGTTGCCACTTCTCCCTT	TACAACCCGTTCTATGCCGG
PAH2	at5g42870	CCATTCTTCAAAACCCCTTG	AGGTCCGTTTCATCCATTTG
MGD1	at4g31780	GTTTTGGGTGAGGAGGGATT	CAGAAGCTCTGTGACCACCA
MGD2	at5g20410	CCGTCATACCCATCATCACA	CCGATCTGGATAAGCTCCAA
MGD3	at2g11810	ATTAATGGGAGGGGGTGAAG	GGCCGCATATGACAATCAA
DGD1	at3g11670	TTCCTTCCTCCCTCTCCATT	ATCTCTCTTGGGAAGCAGCA
DGD2	at4g00550	CCTGGAGCTTCTGCTGTTCT	GCTGCGACTCAAGAATACCC
UBQ7	at2g35635	GCAGCGACACCATCGACAAT	AGGTCCGGCCATCTTCCAAT
CB5-E	at5g53560	TTGCAGTGTCGCTGTGACCA	TGATCATCCTGGAGGCGATG
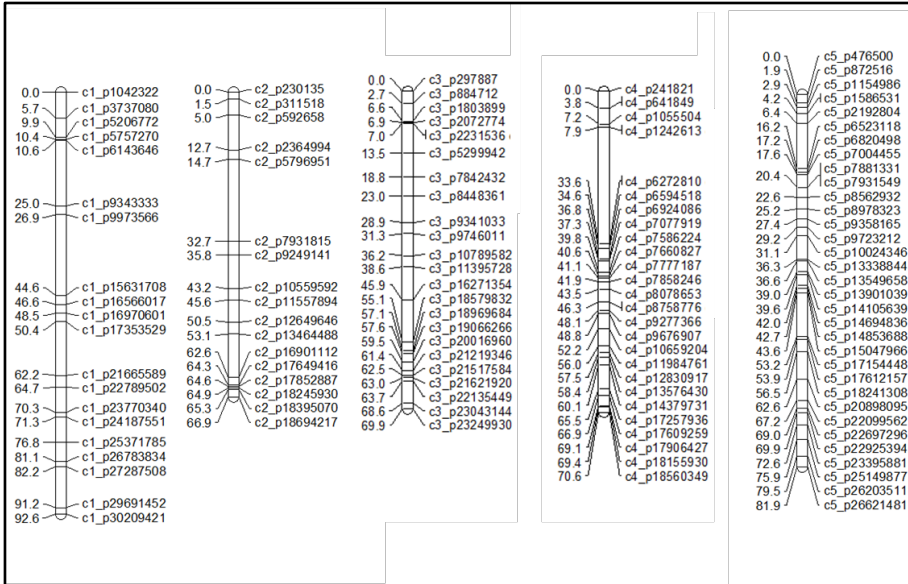
Figure S1. Genetic map of F2 population

The five chromosomes of Arabidopsis thaliana are shown from left to right.
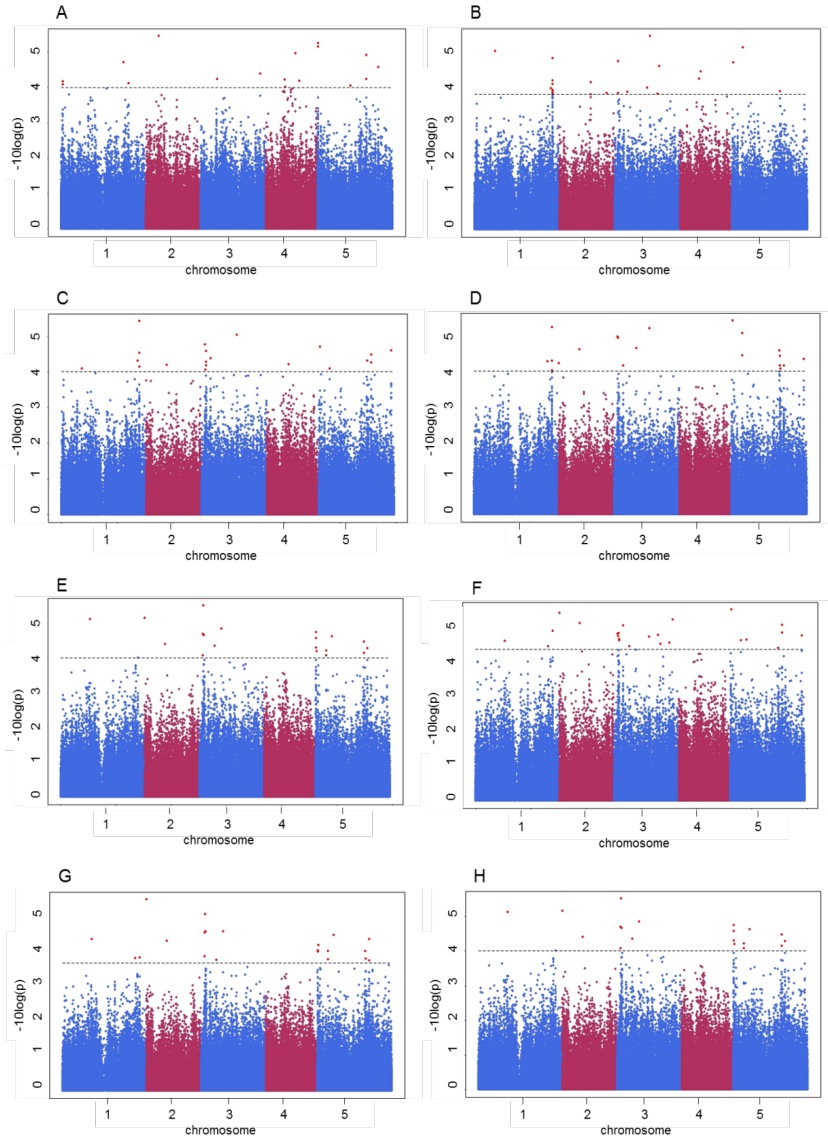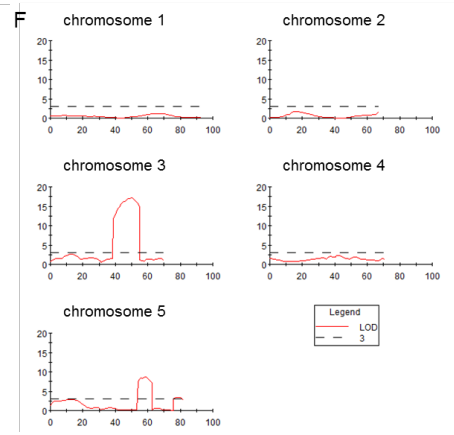
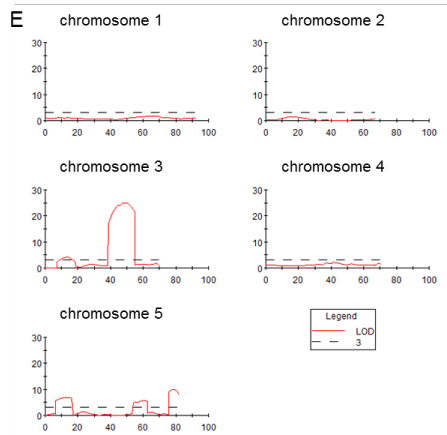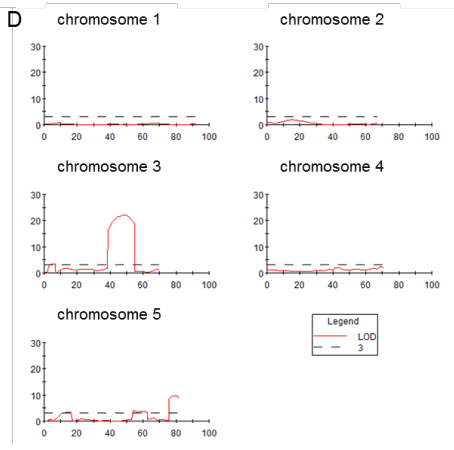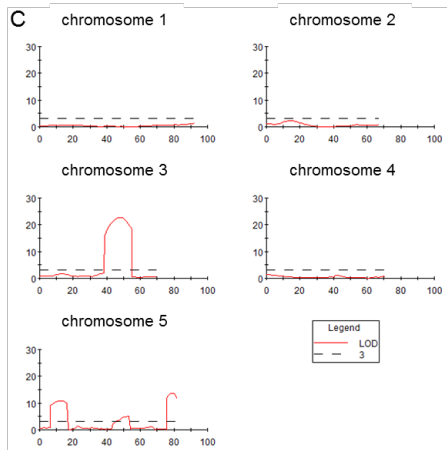**Figure S2. Genetic mapping in the GWAS population with Φ_{PSII} values measured (A) before; (B) 6.5 hours; (C) 25 hours; (D) 28.5 hours; (E) 31.5 hours; (F) 49 hours; (G) 52.5 hours; and (H) 55.5 hours after the increase in growth irradiance.**

-log₁₀(Pvalue) for 215,000 single nucleotide polymorphisms (SNPs) in a genome-wide association mapping panel of 344 natural accessions. The colours blue and pink distinguish the 5 chromosomes from left to right, the black dotted line represents a significance threshold arbitrarily set at -log₁₀(Pvalue)=4, the red dots are SNPS that are associated with the phenotype at -log₁₀(Pvalue)≥4
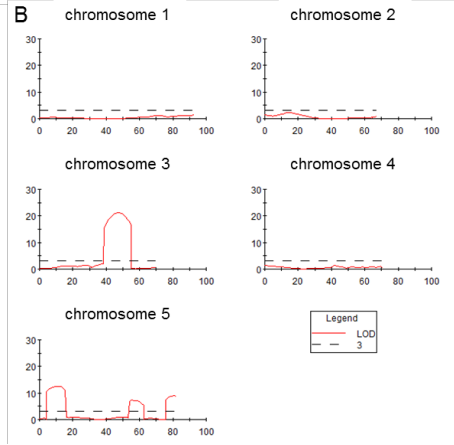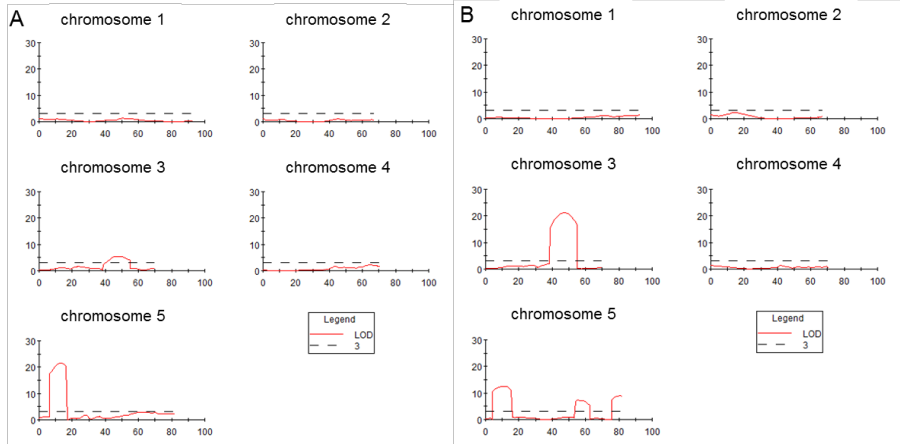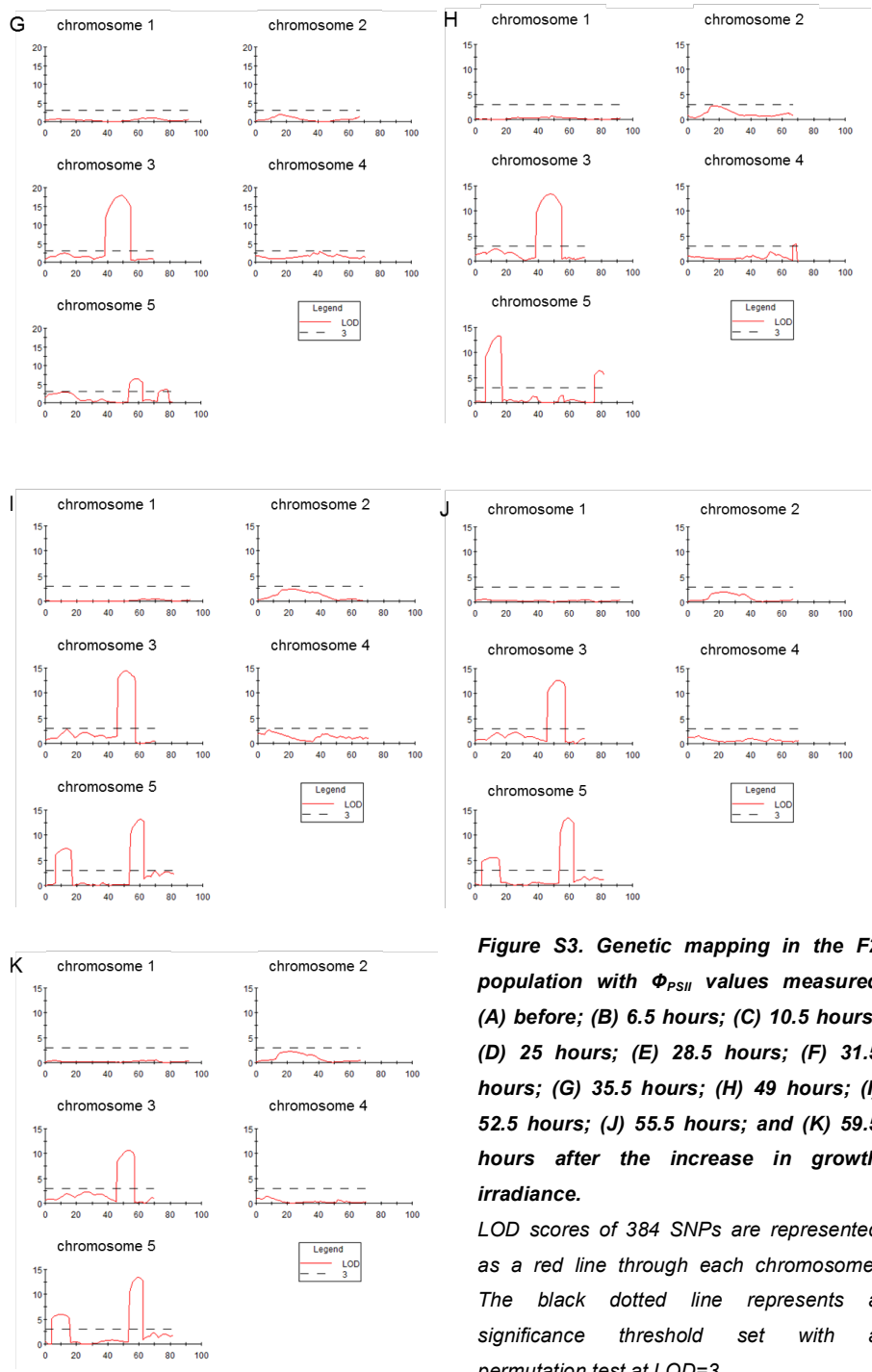
Figure S3. Genetic mapping in the F2 population with Φ_{PSII} values measured (A) before; (B) 6.5 hours; (C) 10.5 hours; (D) 25 hours; (E) 28.5 hours; (F) 31.5 hours; (G) 35.5 hours; (H) 49 hours; (I) 52.5 hours; (J) 55.5 hours; and (K) 59.5 hours after the increase in growth irradiance.

LOD scores of 384 SNPs are represented as a red line through each chromosome. The black dotted line represents a significance threshold set with a permutation test at LOD=3.

Chapter 6

General Discussion

Photosynthesis efficiency variation under light stress

Improving the efficiency of photosynthesis is a grand opportunity to increase food and climate security in a world with ever increasing population and rising CO_2 levels (Zhu et al., 2010; Lawson et al., 2012; Long et al., 2015). Photosynthesis is the basis of all life on earth, it provides carbohydrates for plant growth, and through the edible plants indirectly also for animal and human growth. Additionally, it provides the oxygen to the air we all so desperately need to breathe, thereby using CO_2 as a substrate, reducing the rising atmospheric CO_2 concentrations.

Photosynthesis is a complex process both on the physiological as well as the molecular level. Many possible targets have been identified to manipulate for increasing photosynthetic efficiency. These targets range from the canopy level to the level of enzymatic kinetic properties, and from light harvesting to CO_2 conductances (Evans, 2013). However, improving the maximum efficiency of light energy conversion seems surprisingly difficult (Zhu et al., 2008), resulting in the idea that plant photosynthesis has been optimized during evolution (Leister, 2012). This thesis negates this idea, as it reveals several genetic targets for direct improvement of light use efficiency of photosystem II (Φ_{PSII}).

The success of manipulations for enhancing photosynthetic efficiency depends on the environmental conditions in which it is measured. In the laboratory, photosynthesis is usually measured in stable environmental conditions, i.e. the plant has completely acclimated to its environment. In nature, environments are more dynamic due to the daily moving of the sun and clouds, as well as seasonal temperature changes. Extensive regulation is known for photosynthetic responses to such environmental fluctuations (Walters, 2005; Minagawa, 2013; Dietz, 2015). In this thesis, a broader phenotypic distribution for photosynthesis efficiency was found among Arabidopsis accessions under light stress, as opposed to stable conditions (Chapter 2). However, the light stress effect on photosynthesis efficiency did not influence the heritability of the trait (Chapter 2), and QTLs could be found for photosynthesis efficiency both in low light conditions as well as in stressful high light conditions, although the number of quantitative trait loci (QTLs) increased after the onset of light stress (Chapter 3). The increase in phenotypic variation could have different biological reasons, first of which is that every accession has adapted its genome to the dynamic growth environment it was growing in the field, leading to more variation for responses to fluctuating environmental conditions as opposed to stable laboratory conditions. Furthermore, a step-wise increase in irradiance moves the leaf

from light limitation to light saturation, which is known to provoke regulatory physiological responses. The extra regulatory mechanisms are an additional source for potential variation. Plant photosynthesis has originated in a marine ecosystem lacking light and oxygen (Ting et al., 2002). Only when plants colonized land, they needed to evolve mechanisms to use and protect the photosynthesis system from damage by high light (Alboresi et al., 2010). As a result, less variation exists among land pants for photosynthetic functioning in low light, as opposed to high light, possibly explaining the observations on genetic variation. An additional explanation is the lack of genetic information of chloroplast genomes among the genotype data used in the genome-wide association studies (GWAS) approach, although the extent of natural variation in chloroplast genes is still unknown. Many genes encoding the structural components of the photosystems and light harvesting complexes are on the chloroplast genome, whereas the regulatory genes for photosynthetic responses are mainly encoded on the nuclear genome (Berry et al., 2013).

The use of natural variation to uncover the genetics of photosynthesis

Traditional plant breeding strategies depend on the existence of natural genetic variation for any trait of interest, which is exploited by intercrossing available germplasm, which can include wild relatives. Photosynthesis efficiency is a phenotypic trait not yet bred for specifically, mainly because it is difficult to measure and because of its genetic complexity. Before the start of the project of which the results are described in this thesis, significant efforts have been made to develop a high-throughput phenotyper for photosynthesis efficiency (Harbinson et al., 2012), solving the phenotyping issue. This photosynthesis phenotyper exists of a camera moving over a platform of growing plants, imaging the plants top view. Because it is a non-destructive measurement, plants can repeatedly be measured throughout the experiment, allowing the construction of time courses through development (Flood et al., 2016) or through a stress response (Chapter 3).

The identification of the true genes causal for a quantitative phenotypic trait such as photosynthesis efficiency, to potentially use for introducing beneficial new alleles crossing into commercial varieties, remains a difficult task. Entire germplasms could be screened for the presence of favourable alleles for a trait of interest by the use of marker assisted selection. For genetically complex traits, such as plant photosynthesis, it is difficult to select the underlying genes with the beneficial alleles because the phenotypic effect of

variations in sequence of a candidate gene are usually very small as one gene plays only a small part in the entire process (small effect size). Natural genetic variation for the major regulators of a process is uncommon, as their big effect size causes selection on these loci, resulting in the presence of only one allele in the population. Genetic mapping studies try to find associations between the phenotypes of interest and genetic loci (Quantitative Trait Loci, QTLs) throughout the entire genome. These studies usually reveal multiple QTLs per mapping experiment, reflecting the genetic variation present for the process that is studied. The underlying causal genes can be identified by mutagenesis and overexpression studies. Different mapping strategies have been developed over the years, using populations with different genetic layouts. These strategies range from family mapping in the progeny of a cross between two accessions (F2 or RIL populations), to a more genetically complex situation in the progeny of a cross between multiple accessions (Ampril population or Magic population), to an even more complex genetics in a population of natural accessions (GWAS population), (Kover et al., 2009; Atwell et al., 2010; Bergelson and Roux, 2010; Huang et al., 2011; Keurentjes et al., 2011). Chapter 5 of this thesis shows that the combination of family mapping (crossing two accessions and genetically and phenotypically analysing the offspring of this cross) and GWAS mapping (exploiting multiple alleles and thousands of years of recombination events) allowed the discovery and explanation of an epistatic relationship between two loci (Chapter 5). Epistasis is often seen as a limiting factor in performing genetic mapping, as it lowers the association of QTLs (Korte and Farlow, 2013). Combining the two mapping approaches overcomes this problem, helping to dissect the genetic complexity of a trait with many different and connecting parts, such as photosynthesis efficiency.

In order to proceed from the QTL to the underlying causal gene, it is essential to know if the observed phenotypic differences are caused by expression differences in the causal gene or by structural differences in the encoded protein. Genome-wide transcriptomic analysis complements the mapping analysis in this (Chapter 4). Not much overlap was found between the QTLs found in the mapping study (Chapter 3) and the genes responsive to increased irradiance found in transcriptomic analysis (Chapter 4). However, they did point to candidates functioning in similar physiological pathways. The *YELLOW SEEDING 1* (*YS1)* gene found in Chapter 3 acts in anterograde signalling between the nucleus and the chloroplast, regulating expression of chloroplast encoded genes. RNA metabolism and signalling between the nucleus and chloroplast was found as biological process to which many responsive genes to increased irrdiance belong (Chapter 4). Additionally, many genes acting in the lipid remodelling process were upregulated by this

treatment (Chapter 4), to which also the gene encoding for phosphatidic acid hydrolase (*PAH2*), found to act epistatically to the gene encoding for asparagine synthetase (*ASN2*), (Chapter 5), belongs. None of the three genes that we characterized as genes underlying natural variation for photosynthesis response to increased growth irradiance (*YS1, ASN2, PAH2*), were found to be transcriptionally responsive to the irradiance increase themselves. However, finding enrichment of the same biological processes for these three genes in transcriptomics suggests the complementarity of the two approaches, which can be explained by the fact that associated polymorphisms in mapping studies are linked to underlying genes in the LD region, whereas transcriptional variation for a gene can be caused either *in cis* or *in trans*. Transcriptional variation caused *in trans* would not be uncovered in mapping studies, which apparently is the case for the photosynthetic regulatory genes. A proper confirmation study on this would be to do expression QTL (eQTL) mapping (Gibson and Weir, 2005; Gilad et al., 2008).

The journey from QTL to QTN

The huge advantage of GWAS over other mapping approaches is its high resolution as only few candidate genes underlie a QTL because of the small region of linkage disequilibrium (LD), (Korte and Farlow, 2013). In most of the published GWAS, the best associated single nucleotide polymorphism (SNP) from the dataset is not the causal SNP, however it does associate with the causal SNP through the LD. It is challenging to find the causal SNPs, as the SNPs in GWAS datasets are chosen because both of their alleles are common, and so cannot be in complete LD with a causal SNP driven to low frequency by selection (Wray et al., 2013), frequently referred to as hidden or missing heritability (Gibson, 2010; Brachi et al., 2011; Zuk et al., 2014). Whole genome re-sequence data for Arabidopsis (Weigel and Mott, 2009) solves this problem as it allows analysis of LD between the rare variant SNPs (absent in GWAS datasets) and the associated SNPs arisen from GWAS (Service et al., 2014), as seen in Chapter 3 and Chapter 5.

In quantitative genetics, different prioritizing methods for gene candidate lists have been developed (Huang et al., 2009; Feltus, 2014). A pathway-based expression set analysis is a way to examine for each candidate gene whether it is co-expressed with genes in the same functional pathway (Wang et al., 2007; Wang et al., 2010). In addition for each candidate gene it can be checked if the expression is mapped to the developmental stage and part of the plant under study (Schmid et al., 2005). Gene function prediction is a

method to determine the functional relation for each candidate gene by examining the gene ontology terms (Ashburner et al., 2000; Bargsten et al., 2014). All these approaches have their limitations, i.e. LD is calculated in a pre-determined group of re-sequenced accessions; transcriptomics is studied on certain time points/conditions; sequencing is done on a limited number of accessions. Therefore, even when a gene is causal in GWAS, it will never comply to all the selection criteria described above. However, the selective power of the different approaches can be improved by adding them together and prioritize the gene candidates by counting the number of selection approaches the candidate gene does comply to, as achieved in Chapter 3 of this thesis.

The use of T-DNA insertion lines to knock-out candidate genes is widely used in Arabidopsis to analyse gene functions (Alonso and Ecker, 2006). Its use in quantitative genetics is valuable to confirm the involvement of the gene candidate in the trait of study (Verslues et al., 2014). However, its use is not undisputed as there are limitations to its effectiveness (Wang, 2008), mainly because screening a large library of T-DNA homozygous lines for phenotypes of interest limits the researchers to only find effective knockouts of genes that have no redundancy and/or epistasis in the genome of the reference accession Columbia (Col), as most knock-outs are in the Col background.

The use of quantitative complementation is ambiguous because of the confounding effects of epistasis (Service, 2004; Turner, 2014). However, it has been applied successfully in Arabidopsis (Motte et al., 2014; Sanchez-Bermejo et al., 2014). Because of these confounding effects of epistasis, it is difficult to conclude if the absence of a successful complementation test is because the alleles are not causal, or because there is an epistatic effect (as for the *ASN2* gene in Chapter 3 and Chapter 5). However, as argued by (Turner, 2014), this problem can be surmounted by producing knock-outs in the accession under study instead of in Columbia-0 background. By using artificial micro RNAs (amiRNAs), we can reach this goal by knocking out the gene of interest in any genomic background (Weigel, 2012). In addition to amiRNAs, the CRISPR-Cas technological breakthrough in genomic manipulation facilitates the exact reproduction of natural alleles of a causal gene in different genomic backgrounds (Cong et al., 2013). Additionally, besides strengthening the quantitative complementation test, the CRISPR-Cas technology will also surmount the limitations of T-DNA insertion lines (mutation possible in different background breaking redundant/epistatic effects, multiple insertions in one genome, incomplete knockout, etc), (Voytas, 2013; Xing et al., 2014; Kumar and Jain, 2015).

The role of anterograde signalling in photosynthetic response to excess light

All the changes during photosynthetic acclimation are the result of signal-induced changes in gene expression, in a tight co-ordinated regulation between nuclear and chloroplast genes. This co-ordinated regulation is termed anterograde signalling in cases where nuclear signalling affects chloroplast gene expression and retrograde signalling in cases where chloroplast signalling affects nuclear gene expression. The anterograde signals are coming from trans-acting regulatory factors determining when and where in the chloroplast gene activation occurs. There are many distinct types and classes of trans-acting factors, ranging from nuclear factors interacting with light responsive gene promoters (such as the *YS1* promoter, Chapter 3), to nuclear encoded transcription factors controlling transcription of plastid encoded genes, and nuclear encoded proteins involved in post-transcriptional modification of chloroplast transcribed RNAs, such as the pentatrico-repeat (PPR) protein family to which YS1 belongs. For chloroplast encoded photosynthesis genes, post-transcriptional regulation is the major regulatory mechanisms that determines the timing and location of expression (Berry et al., 2013). A very large number of nuclear-encoded RNA-binding proteins are present in plastids (Berry et al., 2013), and some of these are found to be responsive to light irradiance increase (Chapter 4). Several types of plastid-targeted RNA-binding proteins exist in plants, of which the class of PPR proteins is most enriched: the Arabidopsis genome encodes ~450 of them (Berry et al., 2013). PPR proteins are defined by the presence of a 35-amino-acid motif repeated in tandem up to 30 times (Schmitz-Linneweber and Small, 2008). They are separated into two major classes, the P- and PLS-class, based on the nature of their PPR motifs. The PLS-class is separated into two smaller subclasses, the E- and DYW-subclass, based on the presence of characteristic C-terminal motifs (Schmitz-Linneweber and Small, 2008). PPR proteins function in RNA translation, RNA editing, RNA splicing, and RNA stability of chloroplast and mitochondrial encoded genes (Schmitz-Linneweber and Small, 2008).

The chloroplast genome includes around 100 genes, the expression of which is essential for chloroplast development and photosynthetic functioning. Two types of RNA polymerases transcribe these genes: the nuclear-encoded polymerase (NEP) and the plastid-encoded polymerase (PEP). NEP transcribes the chloroplast housekeeping genes, whereas PEP transcribes the photosynthesis genes. PEP has a catalytic core consisting of RpoA, RpoB, RpoC1 and RpoC2, all encoded for by the chloroplast

genome. Additionally to the core, PEP associates with variable signalling factors determining its promoter specificity. These are known as sigma factors, and are all encoded by the nuclear genome (Hanaoka et al., 2003). The *YS1* gene encoding a PPR protein with a DYW motif is such a sigma factor, editing the *RpoB* transcript in the chloroplast, indirectly affecting transcription of chloroplast encoded photosynthesis genes and, remarkably, many chloroplast transfer-RNAs (tRNAs), (Zhou et al., 2009; Kindgren et al., 2012). The significance of PEP-transcribed tRNAs for photosynthetic functioning has been noted before, but remains elusive to date (Williams-Carrier et al., 2014).

High light induced photosynthetic activity has a strong effect on PEP-dependent plastid gene expression, generating a retrograde signal from the chloroplast to the nucleus (Kindgren et al., 2012). In response to increased irradiance, the plant thus can synchronize the expression of nuclear- and chloroplast-encoded photosynthetic via PEP, necessary to acclimate to environmental fluctuations. The identification of the *YS1* gene in this thesis as a genetic factor causing differences in photosynthetic efficiency (Chapter 3) and the finding of many RNA associated genes up-regulated in response to light increase of which some associated with photosynthetic efficiency (Chapter 4), reveals the significance of this regulatory mechanism in nature.

The role of internal phosphate levels in photosynthetic acclimation to excess light

In photosynthesis, orthophosphate (Pi) is necessary for ATP synthesis, activation of Rubisco, and for export of triose phosphate (Dietz and Foyer, 1986). As a consequence, P-starved leaves have low photosynthetic rates per unit leaf area, and high P-levels are needed for high photosynthetic rates. Increased rates of photosynthesis need a balance between the concentration of free Pi and phosphorylated intermediates (Stitt et al., 2010). When the release of Pi and the regeneration of ATP and NADPH lag behind the capture of light energy, i.e. in the case of excess irradiance, the imbalance leads to enhanced overreduction of the photosystems (Nilsson et al., 2011).

The internal Pi levels are regulated by the uptake of phosphate by the roots, as well as by internal mobilisation through (de)phosphorylation of internal structures (Abel et al., 2002). Pi is one of the least mobile macronutrients in the soil, due to precipitation with metal ions and binding to soil particles. As a result, high photosynthetic P-use efficiency in response to increased irradiance is gained from remobilizing Pi from internal structures, as shown in Chapters 4 and 5 of this thesis. This thesis shows that a major process for releasing Pi

to meet the increased photosynthetic rates in response to excess light, is the remodelling of chloroplast and cellular membranes, where phospholipids get converted to galactolipids (Chapters 4 and 5). An additional process working epistatically with the lipid remodelling is the removal of excess ammonium, thereby releasing Pi as a side product (Chapter 5). Different processes acting in concert to balance internal Pi levels, associated with different photosynthetic efficiencies in response to excess light, reveals the significance of this regulatory mechanism in nature.

Future prospective

Within biological research more and more focus is put on identifying genes, because with the genes in hand society believes we can not only improve crop production, but also animal and human health. This thesis contributes in finding genes underlying natural variation in photosynthesis efficiency in *Arabidopsis thaliana*, the genetic model organism for plants. As a model organism, Arabidopsis is significant for improving crop production, because it can act as an example for identifying molecular and physiological pathways that could potentially be modified in crops for their improvement. Understanding natural genetic variation in Arabidopsis is most interesting for breeding, as those genes are likely to be variable also in the germplasm of crops. Next step would now be to screen the germplasm of commercial crops for the presence of beneficial alleles of the genes causal for natural variation in photosynthesis efficiency response to increased growth irradiance identified in this thesis, by the use of marker assisted selection. Subsequent crossing of these beneficial alleles into commercial lines will allow analysis of its effect on photosynthesis in crops, as well as crop yield.

Additionally to improving photosynthesis efficiency, and ultimately crop yield, this thesis serves as an example for the dissection of complex genetics. Photosynthesis is a multi-step process for which many genes work together. This thesis shows also that the regulation of photosynthesis to light stress consists of many physiological and molecular pathways. This was already known, though at the genetic level, this thesis contributes to new insights. The combined use of GWAS, family mapping, and transcriptomics has helped in getting these results. These three approaches together yield huge and very rich datasets to analyse for a biologist, a task that a PhD student cannot completely fulfil within the provided time; the datasets provided in this thesis are still full with information not analysed in detail. Anyhow, I have shown the possibility of dissecting part of this complexity by a well-structured and targeted approach.

References

Abel S, Ticconi CA, Delatorre CA (2002) Phosphate sensing in higher plants. Physiologia Plantarum **115**: 1-8.

Alboresi A, Gerotto C, Giacometti GM, Bassi R, Morosinotto T (2010) Physcomitrella patens mutants affected on heat dissipation clarify the evolution of photoprotection mechanisms upon land colonization. PNAS **107**: 11128-33.

Albrecht-Borth V, Kauss D, Fan D, Hu Y, Collinge D, Marri S, Liebers M, Apel K, Pfannschmidt T, Chow WS, Pogson BJ (2013) A Novel Proteinase, SNOWY COTYLEDON4, Is Required for Photosynthetic Acclimation to Higher Light Intensities in Arabidopsis. Plant Physiology **163**: 732-745.

Allen JF (1992) How does protein phosphorylation regulate photosynthesis? Trends in Biochemical Science **17**: 12-17.

Alonso-Blanco C, Aarts MGM, Bentsink L, Keurentjes JJB, Reymond M, Vreugdenhil D, Koornneef M (2009) What has natural variation taught us about plant development, physiology, and adaptation? The Plant Cell **21**: 1877-1896.

Alonso-Blanco C, Méndez-Vigo B (2014) Genetic architecture of naturally occurring quantitative traits in plants: an updated synthesis. Current Opinion in Plant Biology **18**: 37-43.

Alonso JM, Ecker JR (2006) Moving forward in reverse: genetic technologies to enable genome-wide phenomic screens in Arabidopsis. Nature Reviews Genetics **7**: 524-536.

Alter P, Dreissen A, Luo F-L, Matsubara S (2012) Acclimatory responses of Arabidopsis to fluctuating light environment: comparison of different sunfleck regimes and accessions. Photosynthesis Research **113**: 221-237.

Apel K, Hirt H (2004) Reactive oxygen species: metabolism, oxidative stress, and signal transduction. Annu Rev Plant Biol **55**: 373-99.

Asada K (1999) The water-water cycle in chloroplasts: scavenging of active oxygens and dissipation of excess photons. Annual Review of Plant Physiology and Plant Molecular Biology **50**: 601-639.

Asada K (2006) Production and scavenging of reactive oxygen species in chloroplasts and their functions. Plant Physiology **141**: 391-396.

Ashburner M, Ball CA, Blake JA, Botstein D, Butler H, Cherry JM, Davis AP, Dolishki K, Dwight SS, Eppig JT, Harris MA, Hill DP, Issel-Tarver L, Kasarskis A, Lewis S, Matese JC, Richardson JE, Ringwald M, Rubin GM, Sherlock G (2000) Gene Ontology: tool for the unification of biology. Nature Genetics **25**: 25-29.

Athanasiou K, Dyson BC, Webster RE, Johnson GN (2010) Dynamic Acclimation of Photosynthesis Increases Plant Fitness in Changing Environments. Plant Physiology **152**: 366-373.

Atwell S, Huang YS, Vilhjalmsson BJ, Willems G, Horton M, Li Y, Meng D, Platt A, Tarone AM, Hu TT, Jiang R, Muliyati NW, Zhang X, Amer MA, Baxter I, Brachi B, Chory J, Dean C, Debieu M, de Meaux J, Ecker JR, Faure N, Kniskern JM, Jones JDG, Michael T, Nemri A, Roux F, Salt DE, Tang C, Todesco M, Traw MB, Weigel D, Marjoram P, Borevitz JO, Bergelson J, Nordborg M (2010) Genome-wide association study of 107 phenotypes in Arabidopsis thaliana inbred lines. Nature **465**: 627-631.

Bac-Molenaar JA, Vreugdenhil D, Granier C, Keurentjes JJB (2015) Genome-wide association mapping of growth dynamics detects time-specific and general quantitative trait loci. Journal of Experimental Botany **66**: 5567-5580.

Bailey S, Horton P, Walters RG (2004) Acclimation of Arabidopsis thaliana to the light environment: the relationship between photosynthetic function and chloroplast composition. Planta **218**: 793-802.

Bailey S, Walters RG, Jansson S, Horton P (2001) Acclimation of Arabidopsis thaliana to the light environment: the existence of separate low light and high light responses. Planta **213**: 794-801.

Baker NR (2008) Chlorophyll fluorescence: a probe of photosynthesis in vivo. Annual Review of Plant Biology **59**: 89-113.

Balaguer L, Martinez-Ferri E, Valladares F, Perez-Corona ME, Baquedano FJ, Castillo FJ, Manrique E (2001) Population divergence in the plasticity of the response of Quercus coccifera to the light environment. Functional Ecology **15**: 124-135.

Ballottari M, Dall'Osto L, Morosinotto T, Bassi R (2007) Contrasting behavior of higher plant photosystem I and II antenna systems during acclimation. The Journal of Biological Chemistry **282**: 8947-8958.

Bargsten JW, Nap J-P, Sanchez-Perez GF, van Dijk ADJ (2014) Prioritization of candidate genes in QTL regions based on associations between traits and biological processes. BMC Plant Biology **14**: 330.

Barton NH, Keightley PD (2002) Understanding Quantitative Genetic Variation. Nature Reviews Genetics **3**: 11-21.

Bateson W (1909) Mendel's principles of heredity. Cambridge: Cambridge University Press.

Benjamini Y, Hochberg Y (1995) Controlling the false discovery rate: a practical and powerful approach to multiple testing. Journal of the Royal Statistical Society, Series B (Methodological): 289-300.

Bergelson J, Roux F (2010) Towards identifying genes underlying ecologically relevant traits in *Arabidopsis thaliana*. Nature Reviews Genetics **11**: 867- 879.

206

Berry JO, Yerramsetty P, Zielinski AM, Mure CM (2013) Photosynthetic gene expression in higher plants. Photosynthesis Research **117**: 91-120.

Bittsánszky A, Pilinszky K, Gyulai G, Komives T (2015) Overcoming ammonium toxicity. Plant Science **231**: 184-190.

Björkman O (1981) Responses to different quantum flux denisities. In Springer-Verlag (ed), Physiological Plant Ecology. I. Responses to the Physical Environment. New York: 57-107.

Björkman O, Demmig B (1987) Photon yield of O2 evolution and chlorophyll fluorescence characteristics at 77 K among vascular plants of diverse origins. Planta **170**: 489-504.

Brachi B, Morris GP, Borevitz JO (2011) Genome-wide association studies in plants: the missing heritability is in the field. Genome Biology **12**: 232.

Britto DT, Kronzucker HJ (2002) NH4+ toxicity in higher plants: a critical review. Journal of Plant Physiology **159**: 567-584.

Bustos R, Castrillo G, Linhares F, Puga MI, Rubio V, Pérez-Pérez J, Solano R, Leyva A, Paz-Ares J (2010) A Central Regulatory System Largely Controls Transcriptional Activation and Repression Responses to Phosphate Starvation in Arabidopsis. Plos Genetics **6**: e1001102.

Butler WL (1978) Energy distribution in the photochemical apparatus of photosynthesis. Annual Review of Plant Physiology **29**: 345-378.

Chao D-Y, Silva A, Baxter I, Huang YS, Nordborg M, Danku J, Lahner B, Yakubova E, Salt DE (2012) Genome-wide association studies identify heavy metal ATPase3 as the primary determinant of natural variation in leaf cadmium in Arabidopsis thaliana. Plos Genetics **8**: e1002923.

Chen L-J, Li H-M (1998) A mutant deficient in the plastid lipid DGD is defective in protein import into chloroplasts. The Plant Journal **16**: 33-39.

Cheng Y, Zhou W, El Sheery NI, Peters C, Li M, Wang X, Huang J (2011) Characterization of the Arabidopsis glycerophosphodiester phosphodiesterase (GDPD) family reveals a role of the plastid-localized AtGDPD1 in maintaining cellular phosphate homeostasis under phosphate starvation. The Plant Journal **66**: 781-795.

Cong L, Ran FA, Cox D, Lin S, Barretto R, Habib N, Hsu PD, Wu X, Jiang W, Marraffini LA, Zhang F (2013) Multiplex Genome Engineering Using CRISPR/Cas Systems. Science **339**: 819-823.

Dekker JP, Boekema EJ (2005) Supramolecular organization of thylakoid membrane proteins in green plants. Biochimica et Biophysica Acta **1706**: 12-39.

Demarsy E, Schepens I, Okajima K, Hersch M, Bergmann S, Christie J, Shimazaki K-i, Tokutomi S, Fankhauser C (2012) Phytochrome Kinase Substrate 4 is phosphorylated by the phototropin 1 photoreceptor. The EMBO Journal **31**: 3457-3467.

Demmig-Adams B, Adams WW (1992) Photoprotection and other responses of plants to high light stress. Annual Review of Plant Physiology **43**: 599-626.

Demmig-Adams B, Adams WW (2006) Photoprotection in an ecological context: the remarkable complexity of thermal energy dissipation. New Phytologist **172**: 11-21.

Demmig B, Winter K, Kruger A, Czygan F (1987) Photoinhibition and zeaxanthin formation in intact leaves. A possible role of the xanthophyll cycle in the dissipation of excess light energy. Plant Physiology **84**: 218-224.

Dietz K-J (2015) Efficient high light acclimation involves rapid processes at multiple mechanistic levels. Journal of Experimental Botany **66**: 2401-2414.

Dietz K, Foyer C (1986) The relationship between phosphate status and photosynthesis in leaves - Reversibility of the effects of phosphate deficiency on photosynthesis. Planta **167**: 376-381.

Driever SM, Lawson T, Andralojc PJ, Raines CA, Parry MAJ (2014) Natural variation in photosynthetic capacity, growth, and yield in 64 field-grown wheat genotypes. Journal of Experimental Botany **65**: 4959-4973.

Eastmond PJ, Quettier A-L, Kroon JT, Craddock C, Adams N, Slabas AR (2010) PHOSPHATIDIC ACID PHOSPHOHYDROLASE1 and 2 Regulate Phospholipid Synthesis at the Endoplasmic Reticulum in Arabidopsis. The Plant Cell **22**: 2796-2811.

Eberhard S, Finazzi G, Wollman F-A (2008) The Dynamics of Photosynthesis. Annual Review of Genetics **42**: 463-515.

Efron B, Tibshirani R (2002) Empirical Bayes methods and false discovery rates for microarrays. Genetic Epidemiology **23**: 70-86.

El-Lithy ME, Rodrigues GC, van Rensen JJS, Snel JFH, Dassen HJHA, Koornneef M, Jansen MAK, Aarts MGM, Vreugdenhil D (2005) Altered photosynthetic performance of a natural Arabidopsis accession is associated with atrazine resistance. Journal of Experimental Botany **56**: 1625–1634.

El-Soda M, Malosetti M, Zwaan BJ, Koornneef M, Aarts MGM (2014) Genotype X environment interaction QTL mapping in plants: lessons from Arabidopsis. Trends in Plant Science **19**: 390-398.

Evans JR (2013) Improving Photosynthesis. Plant Physiology **162**: 1780-1793.

Evans JR, Poorter H (2001) Photosynthetic acclimation of plants to growth irradiance: the relative importance of specific leaf area and nitrogen partitioning in maximizing carbon gain. Plant, Cell & Environment **24**: 755-767.

Falke KC, Frisch M (2011) Power and false-positive rate in QTL detection with near-isogenic line libraries. Heredity **106**: 576-584.

Fellerer C, Schweiger R, Schöngruber K, Soll J, Schwenkert S (2011) Cytosolic HSP90 cochaperones HOP and FKBP interact with freshly synthesized chloroplast preproteins of Arabidopsis. Molecular Plant **4**: 1133-1145.

Feltus A (2014) Systems genetics: A paradigm to improve discovery of candidate genes and mechanisms underlying complex traits. Plant Science **223**: 45-48.

Filiault DL, Maloof JN (2012) A genome-wide association study identifies variants underlying the Arabidopsis thaliana shade avoidance response. Plos Genetics **8**: e1002589.

Flood PJ, Harbinson J, Aarts MGM (2011) Natural genetic variation in plant photosynthesis. Trends in Plant Science **16**: 327-335.

Flood PJ, Kruijer W, Schnabel SK, van der Schoor R, Jalink H, Snel JFH, Harbinson J, Aarts MGM (2016) Phenomics for photosynthesis, growth and reflectance in Arabidopsis thaliana reveals circadian and long-term fluctuations in heritability. Plant Methods **12**: 14.

Foyer CH, Neukermans J, Queval G, Noctor G, Harbinson J (2012) Photosynthetic control of electron transport and the regulation of gene expression. Journal of Experimental Botany **63**: 1637-1661.

Foyer CH, Parry M, Noctor G (2003) Markers and signals associated with nitrogen assimilation in higher plants. Journal of Experimental Botany **54**: 585-593.

Gaude N, Nakamura Y, Scheible WR, Ohta H, Dörmann P (2008) Phospholipase C5 (NPC5) is involved in galactolipid accumulation during phosphate limitation in leaves of Arabidopsis. The Plant Journal **56**: 28-39.

Gaufichon L, Masclaux-Daubresse C, Tcherkez G, Reisdorf-Cren M, Sakakibara Y, Hase T, Clement G, Avice J-C, Grandjean O, Marmagne A, Boutet-Mercey S, Azzopardi M, Soulay F, Suzuki A (2013) Arabidopsis thaliana ASN2 encoding asparagine synthetase is involved in the control of nitrogen assimilation and export during vegetative growth. Plant, Cell & Environment **36**: 328-342.

Gentleman R, Carey V, Bates D, Bolstad B, Dettling M, Dudoit S, Ellis B, Gautier L, Ge Y, Gentry J, Hornik K, Hothorn T, Huber W, Iacus S, Irizarry R, Leisch F, Li C, Maechler M, Rossini A, Sawitzki G, Smith C, Smyth G, Tierney L, Yang J, Zhang J (2004) Bioconductor: open software development for computational biology and bioinformatics. Genome Biology **5**: R80.

Genty B, Briantais JM, Baker NR (1989) The relationship between the quantum yield of photosynthetic electron transport and quenching of chlorophyll fluorescence. Biochimica et Biophysica Acta **990**: 87-92.

Genty B, Harbinson J (1996) Regulation of Light Utilization for Photosynthetic Electron Transport. In NR Baker (ed), Photosynthesis and the Environment. Springer, Dordrecht, the Netherlands: 67-99.

Gibson G (2010) Hints of hidden heritability in GWAS. Nature Genetics **42**: 558-560.

Gibson G (2012) Rare and common variants: twenty arguments. Nature Reviews Genetics **13**: 135-145.

Gibson G, Weir B (2005) The quantitative genetics of transcription. Trends Genet **21**: 616-23.

Gilad Y, Rifkin SA, Pritchard JK (2008) Revealing the architecture of gene regulation: the promise of eQTL studies. Trends Genet **24**: 408-15.

Gilmartin PM, Chua N-H (1990) Spacing between GT-1 binding sites within a light-responsive element is critical for transcriptional activity. The Plant Cell **2**: 447-455.

Gilmartin PM, Sarokin L, Memelink J, Chua N-H (1990) Molecular Light Switches for Plant Genes. The Plant Cell **2**: 369-378.

Green PJ, Yong MH, Cuozzo M, Kano-Murakami Y, Silverstein P, Chua NH (1988) Binding site requirements for pea nuclear protein factor GT-1 correlate with sequences required for light-dependent transcriptional activation of the rbcS-3A gene. The EMBO Journal **7**: 4035-4044.

Hajdukiewicz PT, Allison LA, Maliga P (1997) The two RNA polymerases encoded by the nuclear and the plastid compartments transcribe distinct groups of genes in tobacco plastids. The EMBO Journal **16**: 4041-4048.

Hanaoka M, Kanamaru K, Takahashi H, Tanaka K (2003) Molecular genetic analysis of chloroplast gene promoters dependent on SIG2, a nucleus-encoded sigma factor for the plastid-encoded RNA polymerase, in Arabidopsis thaliana. Nucleic Acids Research **31**: 7090-7098.

Harbinson J, Genty B, Baker NR (1989) Relationship between the Quantum Efficiencies of Photosystems I and II in Pea Leaves. Plant Physiology **90**: 1029-1034.

Harbinson J, Prinzenberg AE, Kruijer W, Aarts MGM (2012) High throughput screening with chlorophyll fluorescence imaging and its use in crop improvement. Current Opinion in Plant Biotechnology **23**: 221-226.

Härtel H, Dörmann P, Benning C (2000) DGD1-independent biosynthesis of extraplastidic galactolipids after phosphate deprivation in Arabidopsis. PNAS **97**: 10649-10654.

Hill J (2012) Early pioneers of photosynthesis research. In JJ Eaton-Rye *et al* (ed), Photosynthesis. Springer Netherlands **34**

Hogewoning SW, Wientjes E, Douwstra P, Trouwborst G, van Ieperen W, Croce R, Harbinson J (2012) Photosynthetic Quantum Yield Dynamics: From Photosystems to Leaves. The Plant Cell **24**: 1921-1935.

Holm M, Ma LG, Qu LJ, Deng XW (2002) Two interacting bZIP proteins are direct targets of COP1-mediated control of light-dependent gene expression in Arabidopsis. Genes and Development **16**: 1247-1259.

Holm S (1979) A Simple Sequentially Rejective Multiple Test Procedure. Scandinavian Journal of Statistics **6**: 65-70.

Horton MW, Bodenhausen N, Beilsmith K, Meng D, Muegge BD, Subramanian S, Vetter MM, Vilhjalmsson BJ, Nordborg M, Gordon JI, Bergelson J (2014) Genome-wide association study of Arabidopsis thaliana leaf microbial community. Nature Communications **5**: 5320.

Horton P, Hague A (1988) Studies on the induction of chlorophyll fluorescence in isolated barley protoplasts. IV. Resolution of non-photochemical quenching. Biochimica et Biophysica Acta **932**: 107-115.

Hruz T, Laule O, Szabo G, Wessendorp F, Bleuler S, Oertle L, Widmayer P, Gruissem W, Zimmermann P (2008) Genevestigator V3: A Reference Expression Database for the Meta-Analysis of Transcriptomes. Advances in Bioinformatics **2008**: 420-747.

Hruz T, Wyss M, Docquier M, Pfaffl MW, Masanetz S, Borghi L, Verbrugghe P, Kalaydjieva L, Bleuler S, Laule O, Descombes P, Gruissem W, Zimmermann P (2011) RefGenes: identification of reliable and condition specific reference genes for RT-qPCR data normalization. BMC Genomics **12**: 156.

Huang DW, Sherman BT, Lempicki RA (2009) Bioinformatics enrichment tools: paths toward the comprehensive functional analysis of large gene lists. Nucleic Acids Research **37**: 1-13.

Huang X, Paulo M-J, Boer M, Effgen S, Keizer P, Koornneef M, van Eeuwijk FA (2011) Analysis of natural allelic variation in Arabidopsis using a multiparent recombinant inbred line population. PNAS **108**: 4488-4493.

Irizarry RA, Hobbs B, Collin F, Beazer-Barclay YD, Antonellis KJ, Scherf U, Speed TP (2003) Exploration, normalization, and summaries of high density oligonucleotide array probe level data. Biostatistics **4**: 249-264.

Jin H, Liu B, Luo L, Feng D, Wang P, Liu J, Da Q, He Y, Qi K, Wang J, Wang H-B (2014) HYPERSENSITIVE TO HIGH LIGHT1 Interacts with LOW QUANTUM YIELD OF PHOTOSYSTEM II1 and Functions in Protection of Photosystem II from Photodamage in Arabidopsis. The Plant Cell **26**: 1213-1229.

Johnson G, Murchie EH (2011) Gas exchange measurements for the determination of photosynthetic efficiency in Arabidopsis leaves. In RP Jarvis (ed), Chloroplast Research in Arabidopsis: Methods and Protocols, Volume II, Methods in Molecular Biology, vol. 775.

Jung H-S, Crisp PA, Estavillo GM, Cole B, Hong F, Mockler TC, Pogson BJ, Chory J (2013) Subset of heat-shock transcription factors required for the early response of Arabidopsis to excess light. PNAS **110**: 14474-14479.

Jung H-S, Niyogi KK (2009) Quantitative Genetic Analysis of Thermal Dissipation in Arabidopsis. Plant Physiology **150**: 977-986.

Kasahara M, Kagawa T, Oikawa K, Suetsugu N, Miyao M, Wada M (2002) Chloroplast avoidance movement reduces photodamage in plants. Nature **420**: 829-32.

Keurentjes JJB, Willems G, Eeuwijk FAv, Nordborg M, Koornneef M (2011) A comparison of population types used for QTL mapping in *Arabidopsis thaliana*. Plant Genetic Resources: Characterization and Utilization **9**: 185-188.

Kim S, Plagnol V, Hu TT, Toomajian C, Clark RM, Ossowski S, Ecker JR, Weigel D, Nordborg M (2007) Recombination and linkage disequilibrium in Arabidopsis thaliana. Nature Genetics **39**: 1151-1155.

Kimura M, Ohta T (1974) On some principles governing molecular evolution. PNAS **71**: 2848-2852.

Kindgren P, Kremnev D, Blanco NE, de Dios Barajas Lopez J, Fernandez AP, Tellgren-Roth C, Kleine T, Small I, Strand A (2012) The plastid redox insensitive 2 mutant of Arabidopsis is impaired in PEP activity and high light-dependent plastid redox signalling to the nucleus. Plant J **70**: 279-91.

Kleine T, Kindgren P, Benedict C, Hendrickson L, Strand A (2007) Genome-wide gene expression analysis reveals a critical role for CRYPTOCHROME1 in the response of Arabidopsis to high irradiance. Plant Physiology **144**: 1391-1406.

Kobayashi K, Fujii S, Sasaki D, Baba S, Ohta H, Masuda T, Wada H (2014) Transcriptional regulation of thylakoid galactolipid biosynthesis coordinated with chlorophyll biosynthesis during the development of chloroplasts in Arabidopsis. Frontiers in Plant Science **5**: 272.

Korte A, Farlow A (2013) The advantages and limitations of trait analysis with GWAS: a review. Plant Methods **9**: 29.

Kouřil R, Dekker JP, Boekema EJ (2012) Supramolecular organization of photosystem II in green plants. Biochimica et Biophysica Acta **1817**: 2-12.

Kouřil R, Wientjes E, Bultema JB, Croce R, Boekema EJ (2013) High-light vs. low-light: Effect of light acclimation on photosystem II composition and organization in Arabidopsis thaliana. Biochimica et Biophysica Acta **1827**: 411-419.

Kover PX, Valdar W, Trakalo J, Scarcelli N, Ehrenreich IM, Purugganan MD, Durrant C, Mott R (2009) A Multiparent Advanced Generation Inter-Cross to Fine-Map Quantitative Traits in Arabidopsis thaliana. Plos Genetics **5**: e1000551.

Kramer DM, Johnson G, Kiirats O, Edwards GE (2004) New fluorescence parameters for the determination of Q_A redox state and excitation energy fluxes. Photosynthesis Research **79**: 209-218.

Kruijer W, Boer MP, Malosetti M, Flood PJ, Engel B, Kooke R, Keurentjes JJB, van Eeuwijk FA (2015) Marker-based estimation of heritability in immortal populations. Genetics **199**: 379-398.

Kumagai E, Araki T, Hamaoka N, Ueno O (2011) Ammonia emission from rice leaves in relation to photorespiration and genotypic differences in glutamine synthetase activity. Ann Bot **108**: 1381-6.

Kumar V, Jain M (2015) The CRISPR–Cas system for plant genome editing: advances and opportunities. Journal of Experimental Botany **66**: 47-57.

Lam H-M, Hsieh M-H, Coruzzi G (1998) Reciprocal regulation of distinct asparagine synthetase genes by light and metabolites in Arabidopsis thaliana. The Plant Journal **16**: 345-353.

Lander ES, Botstein D (1989) Mapping medelian factors underlying quantitative traits using RFLP linkage maps. Genetics **121**: 185-199.

Larcher W (2003) Physiological plant ecology. Springer Science & Business Media.

Larsen TM, Boehlein SK, Schuster SM, Richards NGJ, Thoden JB, Holden HM, Rayment I (1999) Three-Dimensional Structure of Escherichia coli Asparagine Synthetase B: A Short Journey from Substrate to Product. Biochemistry **38**: 16146-16157.

Lawson T, Kramer DM, Raines CA (2012) Improving yield by exploiting mechanisms underlying natural variation of photosynthesis. Current Opinion in Biotechnology **23**: 215-220.

Leakey ADB, Press MC, Scholes JD (2003) Patterns of dynamic irradiance affect the photosynthetic capacity and growth of dipterocarp tree seedlings. Oecologia **135**: 184-193.

Lee J, He K, Stolc V, Lee H-J, Figueroa P, Gao Y, Tongprasit W, Zhao H, Lee I, Deng XW (2007) Analysis of Transcription Factor HY5 Genomic Binding Sites Revealed Its Hierarchical Role in Light Regulation of Development. The Plant Cell **19**: 731-749.

Leister D (2012) How can the light reactions of photosynthesis be improved in plants? Frontiers in Plant Science **3**: 199.

Li XP, Gilmore AM, Caffarri S, Bassi R, Golan T, Kramer D, Niyogi KK (2004) Regulation of photosynthetic light harvesting involves intrathylakoid lumen pH sensing by the PsbS protein. J Biol Chem **279**: 22866-74.

Li Y, Huang Y, Bergelson J, Nordborg M, Borevitz JO (2010) Association mapping of local climate-sensitive quantitative trait loci in Arabidopsis thaliana. PNAS **107**: 21199–21204.

Li Z, Wakao S, Fischer BB, Niyogi KK (2009) Sensing and responding to excess light. Annual Review of Plant Biology **60**: 239-260.

Long AD, Mullaney SL, Mackay TFC, Langley CH (1996a) Genetic interactions between naturally occuning alleles at quantitative trait loci and mutant alleles at candidate loci affecting bristle number in Drosophila melanogaster Genetics **144**: 1497-1510.

Long SP, Farage PK, Garcia RL (1996b) Measurement of leaf and canopy photosynthetic CO2 exchange in the field. Journal of Experimental Botany **47**: 1629-1642.

Long SP, Humphries SW, Falkowski PG (1994) Photoinhibition of photosynthesis in nature. Annual Review of Plant Physiology and Plant Molecular Biology **45**: 633-662.

Long SP, Marshall-Colon A, Zhu X-G (2015) Meeting the global food demand of the future by engineering crop photosynthesis and yield potential. Cell **161**: 56-66.

Maxwell K, Johnson GN (2000) Chlorophyll fluorescence - a practical guide. Journal of Experimental Botany **51**: 659-668.

Mehler AH, Brown AH (1952) Studies on reactivities of illuminated chloroplasts. III. Simultaneous photoproduction of and consumption of oxygen studied with oxygen isotopes. Archives of Biochemistry and Biophysics **38**: 365-370.

Meijón M, Satbhai SB, Tsuchimatsu T, Busch W (2014) Genome-wide association study using cellular traits identifies a new regulator of root development in Arabidopsis. Nature Genetics **46**: 77-81.

Minagawa J (2013) Dynamic reorganization of photosynthetic supercomplexes during environmental acclimation of photosynthesis. Frontiers in Plant Science **4**: 513.

Mitchell-Olds T, Schmitt J (2006) Genetic mechanisms and evolutionary significance of natural variation in Arabidopsis. Nature **441**: 947-952.

Moellering ER, Benning C (2011) Galactoglycerolipid metabolism under stress: a time for remodeling. Trends in Plant Science **16**: 98-107.

Moore CR, Johnson LS, Kwak I-Y, Livny M, Broman KW, Spalding EP (2013) High-throughput computer vision introduces the time axis to a quantitative trait map of a plant growth response. Genetics **195**: 1077-1086.

Moore M, Vogel M, Dietz K (2014) The acclimation response to high light is initiated within seconds as indicated by upregulation of AP2/ERF transcription factor network in Arabidopsis thaliana. Plant Signalling & Behavior **9**: 976479.

Mori T, Yoshimura K, Nosaka R, Sakuyama H, Koike Y, Tanabe N, Maruta T, Tamoi M, Shigeoka S (2012) Subcellular and Subnuclear Distribution of High-Light Responsive Serine/Arginine-Rich Proteins, atSR45a and atSR30, in Arabidopsis thaliana. Bioscience Biotechnology Biochemistry **76**: 2075-2081.

Motte H, Vercauteren A, Depuydt S, Landschoot S, Geelen D, Werbrouck S, Goormachtig S, Vuylsteke M, Vereecke D (2014) Combining linkage and association mapping identifies RECEPTOR-LIKE PROTEIN KINASE1 as an essential Arabidopsis shoot regeneration gene. PNAS **111**: 8305-8310.

Muller P, Li X-P, Niyogi KK (2001) Non-Photochemical Quenching. A Response to Excess Light Energy. Plant Physiology **125**: 1558-1566.

Müller R, Morant M, Jarmer H, Nilsson L, Hamborg Nielsen T (2007) Genome-Wide Analysis of the Arabidopsis Leaf Transcriptome Reveals Interaction of Phosphate and Sugar Metabolism. Plant Physiology **143**: 156-171.

Munekage Y, Hashimoto M, Miyake C, Tomizawa K-I, Endo T, Tasaka M, Shikanai T (2004) Cyclic electron flow around photosystem I is essential for photosynthesis. Nature **429**: 579-582.

Munekage YN, Inoue S, Yoneda Y, Yokota A (2015) Distinct palisade tissue development processes promoted by leaf autonomous signalling and long-distance signalling in Arabidopsis thaliana. Plant Cell Environ **38**: 1116-26.

Murakawa M, Shimojima M, Shimomura Y, Kobayashi K, Awai K, Ohta H (2014) Monogalactosyldiacylglycerol synthesis in the outer envelope membrane of chloroplasts is required for enhanced growth under sucrose supplementation. Frontiers in Plant Science **5**: 280.

Murchie EH, Horton P (1997) Acclimation of photosynthesis to irradiance and spectral quality in British plant species: chlorophyll content, photosynthetic capacity and habitat preference. Plant, Cell & Environment **20**: 438-448.

Murchie EH, Niyogi KK (2011) Manipulation of Photoprotection to Improve Plant Photosynthesis. Plant Physiology **155**: 86-92.

Nakamura Y, Koizumi R, Shui G, Shimojima M, Wenk MR, Ito T, Ohta H (2009) Arabidopsis lipins mediate eukaryotic pathway of lipid metabolism and cope critically with phosphate starvation. PNAS **106**: 20978-20983.

Nguyen XC, Kim SH, Lee K, Kim KE, Liu XM, Han HJ, Hoang MH, Lee SW, Hong JC, Moon YH, Chung WS (2012) Identification of a C2H2-type zinc finger transcription factor (ZAT10) from Arabidopsis as a substrate of MAP kinase. Plant Cell Rep **31**: 737-45.

Nilsson L, Lundmark M, Jensen PE, Nielsen TH (2011) The Arabidopsis transcription factor PHR1 is essential for adaptation to high light and retaining functional photosynthesis during phosphate starvation. Physiologia Plantarum **144**: 35-47.

Niyogi KK (1999) PHOTOPROTECTION REVISITED: Genetic and Molecular Approaches. Annual Review of Plant Physiology and Plant Molecular Biology **50**: 333-359.

Oguchi R, Hikosaka K, Hirose T (2003) Does the photosynthetic light-acclimation need change in leaf anatomy? Plant, Cell & Environment **26**: 505-512.

Ogura T, Busch W (2015) From phenotypes to causal sequences: using genome wide association studies to dissect the sequence basis for variation of plant development. Current Opinion in Plant Biology **23**: 98-108.

Okuda K, Chateigner-Boutin A-L, Nakamura T, Delannoy E, Sugita M, Myouga F, Motohashi R, Shinozaki K, Small I, Shikanai T (2009) Pentatricopeptide repeat proteins with the DYW motif have distinct molecular functions in RNA editing and RNA cleavage in Arabidopsis chloroplasts. The Plant Cell **21**: 146-156.

Onate-Sánchez L, Vicente-Carbajosa J (2008) DNA-free RNA isolation protocols for *Arabidopsis thaliana*, including seeds and siliques. BMC Research Notes **1**: 93.

Ouwerkerk PB, Trimborn TO, Hilliou F, Memelink J (1999) Nuclear factors GT-1 and 3AF1 interact with multiple sequences within the promoter of the Tdc gene from Madagascar periwinkle: GT-1 is involved in UV light-induced expression. Molecular General Genetics **261**: 610-622.

Oxborough K, Baker NR (1997) Resolving chlorophyll a fluorescence images of photosynthetic efficiency into photochemical and non-photochemical components – calculation of qP and Fv'/Fm' without measuring Fo'. Photosynthesis Research **54**: 135-142.

Pérez-Pérez JM, Serrano-Cartagena J, Micol JL (2002) Genetic Analysis of Natural Variations in the Architecture of Arabidopsis thaliana Vegetative Leaves. Genetics **162**: 893-915.

Pigliucci M (1998) Ecological and evolutionary genetics of Arabidopsis. Trends in Plant Science **3**: 485-489.

Portes MT, Alves TH, Souza GM (2008) Time-course of photosynthetic induction in four tropical woody species grown in contrasting irradiance habitats. Photosynthetica **46**: 431-440.

Powles SB (1984) Photoinhibition of photosynthesis induced by visible-light. Annual Review of Plant Physiology **35**: 15-44.

Ptushenko VV, Ptushenko EA, Samoilova OP, Tikhonov AN (2013) Chlorophyll fluorescence in the leaves of Tradescantia species of different ecological groups: Induction events at different intensities of actinic light. Biosystems **114**: 85-97.

Puga MI, Mateos I, Charukesi R, Wang Z, Franco-Zorrilla JM, de Lorenzo L, Irigoyen ML, Masiero S, Bustos R, Rodriguez J, Leyva A, Rubio V, Sommer H, Paz-Ares J (2014) SPX1 is a phosphate-dependent inhibitor of Phosphate Starvation Response 1 in Arabidopsis. PNAS **111**: 14947-14952.

Quick WP, Stitt M (1989) An examination of factors contributing to non-photochemical quenching of chlorophyll fluorescence in barley leaves. Biochimica et Biophysica Acta **977**: 287-296.

Rabinowitch E (1951) Photosynthesis. New York: Interscience Publishers, Inc.

Rintamäki E, Salonen M, Suoranta UM, Carlberg I, Andersson B, Aro EM (1997) Phosphorylation of Light-harvesting Complex II and Photosystem II Core Proteins Shows Different Irradiance-dependent Regulation *in Vivo*. The Journal of Biological Chemistry **272**: 30476-30482.

Rossel JB, Wilson IW, Pogson BJ (2002) Global changes in gene expression in response to high light in Arabidopsis. Plant Physiology **130**: 1109-1120.

Rossel JB, Wilson PB, Hussain D, Woo NS, Gordon MJ, Mewett OP, Howell KA, Whelan J, Kazan K, Pogson BJ (2007) Systemic and Intracellular Responses to Photooxidative Stress in Arabidopsis. The Plant Cell **19**: 4091-4110.

Ruelland E, Djafi N, Zachowski A (2013) The phosphoinositide dependent-phospholipase C pathway differentially controls the basal expression of DREB1 and DREB2 genes. Plant Signalling & Behavior **8**: e26895.

Ruelland E, Kravets V, Derevyanchuk M, Martinec J, Zachowski A, Pokotylo I (2015) Role of phospholipid signalling in plant environmental responses. Environmental and Experimental Botany **114**: 129-143.

Sakuma Y, Maruyama K, Qin F, Osakabe Y, Shinozaki K, Yamaguchi-Shinozaki K (2006) Dual function of an Arabidopsis transcription factor DREB2A in water-stress-responsive and heat-stress-responsive gene expression. PNAS **103**: 18822-18827.

Sanchez-Bermejo E, Castrillo G, del Llano B, Navarro C, Zarco-Fernandez S, Martinez-Herrera DJ, Leo-del Puerto Y, Munoz R, Camara C, Paz-Ares J, Alonso-Blanco C, Leyva A (2014) Natural variation in arsenate tolerance identifies an arsenate reductase in Arabidopsis thaliana. Nature Communications **5**: 4617.

Scheibe R, Backhausen JE, Emmerlich V, Holtgrefe S (2005) Strategies to maintain redox homeostasis during photosynthesis under changing conditions. J Exp Bot **56**: 1481-9.

Schepens I, Duek P, Fankhauser C (2004) Phytochrome-mediated light signalling in Arabidopsis. Current Opinion in Plant Biology **7**: 564-569.

Schmid M, Davison TS, Henz SR, Pape UJ, Demar M, Vingron M, Schölkopf B, Weigel D, Lohmann JU (2005) A gene expression map of Arabidopsis thaliana development. Nature Genetics **37**: 501-506.

Schmitz-Linneweber C, Small I (2008) Pentatricopeptide repeat proteins: a socket set for organelle gene expression. Trends Plant Sci **13**: 663-70.

Seemann JR (1989) Light adaptation/acclimation of photosynthesis and the regulation of ribulose-1, 5-bisphosphate carboxylase activity in sun and shade plants. Plant Physiology **91**: 379-386.

Seren U, Vilhjalmsson BJ, Horton MW, Meng D, Forai P, Huang YS, Long Q, Segura V, Nordborg M (2012) GWAPP: A Web Application for Genome-Wide Association Mapping in Arabidopsis. The Plant Cell **24**: 4793-4805.

Service PM (2004) How Good Are Quantitative Complementation Tests? Science Aging Knowledge Environment **12**: pe13.

Service SK, Teslovich TM, Fuchsberger C, Ramensky V, Yajnik P, Koboldt DC, Larson DE, Zhang Q, Lin L, Welch R, Ding L, McLellan MD, O'Laughlin M, Fronick C, Fulton LL, Magrini V, Swift A, Elliott P, Jarvelin MR, Kaakinen M, McCarthy MI, Peltonen L, Pouta A, Bonnycastly LL, Collins FS, Narisu N, Stringham HM, Tuomilehto J, Ripatti S, Fulton RS, Sabatti C, Wilson RK, Boehnke M, Freimer NB (2014) Re-sequencing Expands Our Understanding of the Phenotypic Impact of Variants at GWAS Loci. Plos Genetics **10**: e1004147.

Seták Z, Catský J, Jarvis PG (1971) Plant photosynthetic production: manual of methods. The Hague: Dr. W. Junk.

Sims DA, Pearcy RW (1993) Sunfleck frequency and duration affects growth-rate of understorey plant, Alocasia macrorrhiza. Functional Ecology **7**: 683-689.

Sinclair TR, Muchow RC (1999) Radiation use efficiency. Advances in Agronomy. **65**: 5-265.

Stitt M, Lunn J, Usadel B (2010) Arabidopsis and primary photosynthetic metabolism - more than the icing on the cake. Plant J **61**: 1067-91.

Suorsa M, Järvi S, Grieco M, Nurmi M, Pietrzykowsk M, Rantala M, Kangasjärvi S, Paakkarinen V, Tikkanen M, Jansson S, Aro EM (2012) PROTON GRADIENT REGULATION5 Is Essential for Proper Acclimation of Arabidopsis Photosystem I to Naturally and Artificially Fluctuating Light Conditions. The Plant Cell **24**: 2934-2948.

Suzuki N, Koussevitzky S, Mittler R, Miller G (2012) ROS and redox signalling in the response of plants to abiotic stress. Plant, Cell & Environment **35**: 259-270.

Sweetlove LJ, Heazlewood JL, Herald V, Holtzapffel R, Day DA, Leaver CJ, Millar AH (2002) The impact of oxidative stress on Arabidopsis mitochondria. The Plant Journal **32**: 891-904.

Swindell WR, Huebner M, Weber AP (2007) Transcriptional profiling of Arabidopsis heat shock proteins and transcription factors reveals extensive overlap between heat and non-heat stress response pathways. BMC Genomics **8**: 125.

Sylak-Glassman EJ, Malnoë A, De Re E, Brooks MD, Lee Fisher A, Niyogi KK, Fleming GR (2014) Distinct roles of the photosystem II protein PsbS and zeaxanthin in the regulation of light harvesting in plants revealed by fluorescence lifetime snapshots. PNAS **111**: 17498-17503.

Tanabe N, Yoshimura K, Kimura A, Yabuta Y, Shigeoka S (2007) Differential Expression of Alternatively Spliced mRNAs of Arabidopsis SR Protein Homologs, atSR30 and atSR45a, in Response to Environmental Stress. Plant and Cell Physiology **48**: 1036-1049.

Tikkanen M, Grieco M, Kangasjarvi S, Aro EM (2010) Thylakoid protein phosphorylation in higher plant chloroplasts optimizes electron transfer under fluctuating light. Plant Physiology **152**: 723-735.

Tikkanen M, Suorsa M, Gollan PJ, Aro EM (2012) Post-genomic insight into thylakoid membrane lateral heterogeneity and redox balance. FEBS Letters **586**: 2911-2916.

Ting CS, Rocap G, King J, Chisholm SW (2002) Cyanobacterial photosynthesis in the oceans: the origins and significance of divergent light-harvesting strategies. Trends in Microbiology **10**: 134-142.

Trontin C, Tisne S, Bach L, Loudet O (2011) What does Arabidopsis natural variation teach us (and does not teach us) about adaptation in plants? Current Opinion in Plant Biology **14**: 225-231.

Turner TL (2014) Fine-mapping natural alleles: quantitative complementation to the rescue. Molecular Ecology **23**: 2377-2382.

Valladares F, Allen MT, Pearcy RW (1997) Photosynthetic responses to dynamic light under field conditions in six tropical rainforest shrubs occuring along a light gradient. Oecologia **111**: 505-514.

van Ooijen JW (2006) JoinMap 4, Software for the calculation of genetic linkage maps in experimental populations. Wageningen, the Netherlands: Kyazma B.V.

van Ooijen JW (2009) MapQTL 6, Software for the mapping of quantitative trait loci in experimental populations of diploid species. Wageningen, the Netherlands: Kyazma B.V.

van Rooijen R, Aarts MGM, Harbinson J (2015) Natural genetic variation for acclimation of photosynthetic light use efficiency to growth irradiance in Arabidopsis. Plant Physiology **167**: 1412-1429.

Vanderauwera S, Zimmerman P, Rombauts S, Vandenabeele S, Langebartels C, Gruissem W, Inzé D, Van Breusegem F (2005) Genome-Wide Analysis of Hydrogen Peroxide-Regulated Gene Expression in Arabidopsis Reveals a High Light-Induced Transcriptional Cluster Involved in Anthocyanin Biosynthesis. Plant Physiology **139**: 806-821.

Vass I (2012) Molecular mechanisms of photodamage in the Photosystem II complex. Biochim Biophys Acta **1817**: 209-17.

Verslues PE, Lasky JR, Juenger TE, Liu T-W, Kumar MN (2014) Genome-wide association mapping combined with reverse genetics identifies new effectors of low water potential-induced proline accumulation in Arabidopsis. Plant Physiology **164**: 144-159.

Visscher PM, Hill WG, Wray NR (2008) Heritability in the genomics era — concepts and misconceptions. Nature Reviews Genetics **9**: 255-266.

Vogel MO, Moore M, König K, Pecher P, Alsharafa K, Lee J, Dietz K-J (2014) Fast Retrograde Signaling in Response to High Light Involves Metabolite Export, MITOGEN-ACTIVATED PROTEIN KINASE6, and AP2/ERF Transcription Factors in Arabidopsis. The Plant Cell **26**: 1151-1165.

Von Caemmerer S, Farquhar GD (1981) Some relationships between the biochemistry of photosynthesis and the gas exchange of leaves. Planta **153**: 376-387.

Voytas DF (2013) Plant Genome Engineering with Sequence-Specific Nucleases. Annual Review of Plant Biology **64**: 327-350.

Walters RG (2005) Towards an understanding of photosynthetic acclimation. Journal of Experimental Botany **56**: 435-447.

Walters RG, Horton P (1991) Resolution of components of non-photochemical chlorophyll fluorescence quenching in barley leaves. Photosynthesis Research **27**: 121-133.

Walters RG, Shephard F, Rogers JJM, Rolfe SA, Horton P (2003) Identification of Mutants of Arabidopsis Defective in Acclimation of Photosynthesis to the Light Environment. Plant Physiology **131**: 472–481.

Wang K, Li M, Bucan M (2007) Pathway-Based Approaches for Analysis of Genomewide Association Studies. American Journal of Human Genetics **81**: 1278-1283.

Wang K, Li M, Hakonarson H (2010) Analysing biological pathways in genome-wide association studies. Nature Reviews Genetics **11**: 843-854.

Wang YH (2008) How effective is T-DNA insertional mutagenesis in Arabidopsis? Journal of Biochemical Technology **1**: 11-20.

Waters MT, Wang P, Korkaric M, Capper RG, Saunders NJ, Langdale JA (2009) GLK Transcription Factors Coordinate Expression of the Photosynthetic Apparatus in Arabidopsis. The Plant Cell **21**: 1109-1128.

Weigel D (2012) Natural Variation in Arabidopsis: From Molecular Genetics to Ecological Genomics. Plant Physiology **158**: 2-22.

Weigel D, Mott R (2009) The 1001 Genomes Project for Arabidopsis thaliana. Genome Biology **10**: 107.

Wientjes E, Van Amerongen H, Croce R (2013) LHCII is an antenna of both photosystems after long-term acclimation. Biochimica et Biophysica Acta **1827**: 420-426.

Williams-Carrier R, Zoschke R, Belcher S, Pfalz J, Barkan A (2014) A major role for the plastid-encoded RNA polymerase complex in the expression of plastid transfer RNAs. Plant Physiol **164**: 239-48.

Wong H-K, Chan H-K, Coruzzi GM, Lam H-M (2004) Correlation of ASN2 Gene Expression with Ammonium Metabolism in Arabidopsis. Plant Physiology **134**: 332-338.

Wray NR, Yang J, Hayes BJ, Price AL, Goddard ME, Visscher PM (2013) Pitfalls of predicting complex traits from SNPs. Nature Reviews Genetics **14**: 507-515.

Wunder T, Liu Q, Aseeva E, Bonardi V, Leister D, Pribil M (2013) Control of STN7 transcript abundance and transient STN7 dimerisation are involved in the regulation of STN7 activity. Planta **237**: 541-558.

Xing H-L, Dong L, Wang Z-P, Zhang H-Y, Han C-Y, Liu B, Wang X-C, Chen Q-J (2014) A CRISPR/Cas9 toolkit for multiplex genome editing in plants. BMC Plant Biology **14**: 327.

Yamamoto Y, Shimada Y, Kimura M, Manabe K, Sekine Y, Matsui M, Ryuto H, Fukunishi N, Abe T, Yoshida S (2004) Global classification of transcriptional responses to light stress in Arabidopsis thaliana. Endocytobiosis Cell Research **15**: 438-452.

Yin L, Fristedt R, Herdean A, Solymosi K, Bertrand M, Andersson MX, Mamedov F, Vener AV, Schoefs B, Spetea C (2012) Photosystem II Function and Dynamics in Three Widely Used Arabidopsis thaliana Accessions. Plos One **7**: e46206.

Yoshimura K, Mori T, Yokoyama K, Koike Y, Tanabe N, Sato N, Takahashi H, Maruta T, Shigeoka S (2011) Identification of alternative splicing events regulated by an Arabidopsis serine/arginine-like protein, atSR45a, in response to high-light stress using a tiling array. Plant and Cell Physiology **52**: 1786-1805.

Zhou W, Cheng Y, Yap A, Chateigner-Boutin A-L, Delannoy E, Hammani K, Small I, Huang J (2009) The Arabidopsis gene YS1 encoding a DYW protein is required for editing of rpoB transcripts and the rapid development of chloroplasts during early growth. The Plant Journal **58**: 82-96.

Zhu X, Long SP, Ort DR (2008) What is the maximum efficiency with which photosynthesis can convert solar energy into biomass? Current Opinion in Biotechnology **19**: 153-159.

Zhu X, Long SP, Ort DR (2010) Improving Photosynthetic Efficiency for Greater Yield. Annual Review of Plant Biology **61**: 235-261.

Zuk O, Schaffner SF, Samocha K, Do R, Hechter E, Kathiresan S, Daly MJ, Neale BM, Synyaev SR, Lander ES (2014) Searching for missing heritability: Designing rare variant association studies. PNAS **111**: E455-E464.

Summary

The efficiency of photosynthesis results from the composition and organization of the plant's internal structural components as well as the capability of response to environmental fluctuations. This thesis aims at identifying the genetic loci that are regulating the (sub-) processes in photosynthetic acclimation to increased irradiance levels, in order to obtain the genetic information useful to breed for photosynthetic performance. It uses genome wide association studies (GWAS) to reveal which genetic loci are being exploited in nature for keeping good photosynthetic performances in natural conditions. Phenotypic variation among natural accessions in photosynthetic light use efficiency response to increased growth irradiance is related to its variation in genetics in order to identify the associated genetic loci. In Chapter 2 is described which light environment reveals most natural variation in photosynthetic performance and for which photosynthetic parameter this is. It shows different Arabidopsis accessions display different photosynthetic responses to various light environments, well relatable to genetic differences. A candidate gene list for the direct response to increased growth irradiance was revealed after performing genome wide association analysis. Chapter 3 elaborates on the genome wide association results by visualizing the dynamics of the associated genetic loci over the time course of the photosynthetic response to increased irradiance. It shows it is possible to simplify the complexity of photosynthetic physiology as well as the genetic analysis in such way to confirm the causal genes underlying the associated loci, by confirming this for the *YELLOW SEEDLING 1 (YS1)* gene, a gene encoding a Pentatrico-Peptide-Repeat (PPR) protein involved in RNA editing of plastid-encoded genes essential for photosystems I and II. Genetic variation for any trait can be on the transcriptional level or on the functional level. In Chapter 4, the gene regulation in three Arabidopsis accessions with contrasting photosynthesis efficiency responses to increased irradiance is studied. These differences in photosynthesis efficiency are associated to differences in activation extents of heat responsive genes as well as to differences in the presence of a gene activation pathway acting on membrane lipid remodelling, suggested to maintain balanced cellular phosphate concentrations. Chapter 5 confirms the significance of maintaining balanced cellular phosphate concentrations for photosynthesis efficiency responses to increased irradiance. It describes how genome wide association mapping and linkage mapping combine to reveal genetic epistatic interactions between *PHOSPHATIDIC ACID PHOPSPHOHYDROLASE 2 (PAH2,* phosphate metabolism gene) and *ASPARAGINE SYNTHETASE 2 (ASN2,* nitrogen metabolism gene), both

acting in the delivery of orthophosphate in the chloroplast. In conclusion this thesis contributes new insights into the physiological and molecular pathways underlying photosynthesis responses to increased growth irradiances.

Samenvatting

De efficiëntie van fotosynthese is het gevolg van de compositie en organisatie van de interne structurele onderdelen van de plant, als wel het reactievermogen van de plant op veranderingen in omgevingsomstandigheden. Dit proefschrift heeft als doel genetische loci te identificeren die de (sub-) processen voor het acclimatiseren van fotosynthese in reactie op verhoogde licht intensiteit reguleren, ten einde deze verkregen genetische informatie te gebruiken voor het veredelen van fotosynthese prestaties binnen gewassen. Het onderzoek maakt gebruik van zogeheten genoom-wijde associatie studies (GWAS) om de genetische loci te onthullen die door de natuur binnen een soort variabel gehouden worden voor het ten alle tijde behouden van goede fotosynthese prestaties in afwisselende natuurlijke omgevingsomstandigheden. Fenotypische variatie tussen natuurlijke accessies (dezelfde soort planten afkomstig uit, en dus aangepast aan, een ander ecosysteem) in de reactie van fotosynthese efficiëntie op verhoogde licht intensiteit is voor dit onderzoek gerelateerd aan de genetisch variatie tussen deze accessies ten einde de geassocieerde genetische loci te identificeren. In hoofdstuk 2 wordt beschreven welke lichtomstandigheden de meeste waar te nemen variatie in fotosynthese efficiëntie onthullen en voor welke specifieke fotosynthese parameter dit is. Het laat verschillend reactievermogen met betrekking tot fotosynthese efficiëntie zien voor verschillende accessies van *Arabidopsis thaliana*, en laat zien dat deze verschillen goed te relateren zijn aan genetische variatie tussen deze accessies. Na het uitvoeren van GWAS, wordt een lijst met kandidaatgenen die verantwoordelijk kunnen zijn voor het initiële reactievermogen op verhoogde lichtintensiteit gegeven. In hoofdstuk 3 wordt verder ingegaan op de resultaten van de GWAS door de dynamica van geassocieerde genetische loci te analyseren tijdens een tijdsspanne waarin fotosynthese acclimatiseert aan de verhoogde lichtintensiteit. Het laat zien dat het mogelijk is om de fysiologische en genetische complexiteit van fotosynthese te simplificeren wat leidt tot het identificeren van de genen onderliggende de geassocieerde genetische loci. Dit is bevestigd voor het *YELLOW SEEDLING 1 (YS1)* gen, een gen wat codeert voor een Pentatrico-Peptide-Repeat (PPR) eiwit betrokken bij het aanpassen van het RNA afkomstig van genen gecodeerd op het chloroplast DNA die essentieel zijn voor het functioneren van fotosysteem I en II. Genetische variatie voor iedere eigenschap kan voorkomen op het gebied van gen expressie of op het gebied van functionele eigenschappen van het gecodeerde eiwit. In hoofdstuk 4 wordt de gen expressie regulatie bestudeerd van drie Arabidopsis accessies met contrasterende reactievermogens betreffende fotosynthese

efficiëntie op verhoogde lichtintensiteit. De verschillen in reactievermogen betreffende fotosynthese efficiëntie worden geassocieerd met verschillen in activatie van genen betrokken bij reactie op hitte, als wel met verschillen in het aanwezig zijn van een gen activatie reactieroute leidende tot het her-modelleren van membraan lipiden, wat wordt gesuggereerd belangrijk te zijn voor het behouden van gebalanceerde cellulaire fosfaat concentraties. Hoofdstuk 5 bevestigd het belang van het behouden van gebalanceerde cellulaire fosfaat concentraties voor de reactie van fotosynthese efficiëntie op verhoogde lichtintensiteit. Het beschrijft hoe een genoom-wijde associatie studie in natuurlijke accessies en een gen karteringsstudie in genetisch uitsplitsende nakomelingen uit een kruising tussen twee accessies elkaar aanvullen in het onthullen van een genetische epistatische interactie tussen het gen *PHOSPHATIDIC ACID PHOPSPHOHYDROLASE 2* (*PAH2*, een gen betrokken bij fosfaat metabolisme) en het gen *ASPARAGINE SYNTHETASE 2* (*ASN2*, een gen betrokken bij nitraat metabolisme), beide handelend in het vrijmaken van orthofosfaat in de chloroplast. In conclusie draagt dit proefschrift bij aan nieuwe inzichten in de mogelijke fysiologische en moleculaire routes voor de reactie van fotosynthese efficiëntie op verhoogde lichtintensiteit.

Acknowledgement / Dankwoord

Als eerste wil ik mijn co-promoter Mark Aarts bedanken voor het aanbieden van dit zeer uitdagende promotie onderzoek. Daarnaast ook bedankt voor alle goede adviezen en de begeleiding bij de uitvoering van de experimenten en het opschrijven van de resultaten.

I would like to thank my co-promoter Jeremy Harbinson for giving me the chance to do this PhD research under his supervision. Thank you for all your advice and guidance throughout the process.

Bedankt aan mijn promoter Maarten Koornneef voor alle adviezen die je mij gegeven hebt betreffende het doen van genetisch onderzoek.

I would like to thank the whole research group of Genetics for being such a welcoming and inspiring group of people. I have always enjoyed talking to all of you and hearing about the different research you were doing.

Although my desk was in the research group of Genetics, I was also part of the research group of Horticulture & Product Physiology (HPP). Although I was not around much in the department, I would like to thank the whole research group of HPP as well. Many of you gave me inspiration especially during the research seminars on Monday afternoons.

Bedankt aan de mensen van Unifarm voor het zorgen voor mijn planten in de klimaatcellen en in de kassen.

Thanks to Aina Prinzenberg for advising me and always helping me in the experiments and most of all for becoming my friend during my PhD time. Thanks for being my paranimph!

Bedankt aan René Boesten voor het zijn van de beste MSc student die ik mij kon wensen en voor het afmaken van de laatste experimenten toen ik het lab al had verlaten om in Düsseldorf te gaan werken. Bedankt ook dat je mijn paranimf wil zijn!

Graag wil ik ook mijn ouders bedanken voor de onvoorwaardelijke steun die zij mij bieden. Dankjewel dat jullie zijn wie jullie zijn en dat ik mag zijn wie ik ben.

Meeste dank gaat naar mijn vriend en geliefde Jan Knippenbergh. Dankjewel dat je er altijd voor mij bent en dat je zo goed kunt luisteren. Dankjewel ook dat je vier jaar lang werkdagen hebt gedraaid van meer dan 9 uur per dag totdat ik jou weer kwam ophalen in Boxmeer, zonder daar ooit over te klagen. Zelfs niet als ik weer eens in de file stond en chagrijnig bij jou aankwam. Jij bent echt een topper, en ik hoop dat we nog heel lang gelukkig samen mogen zijn.

Curriculum Vitae

Roxanne van Rooijen was born on March 31st 1987 in Venlo, the Netherlands. In 2005 she decided to study Biology at the Radboud University in Nijmegen, where she completed her research Master of Science in 2010 and an extra educational master in 2011. During her research master she completed a thesis in the laboratory of Plant Genetics of Radboud University under the supervision of Dr. Janny Peters and a research internship in Nunhems Netherlands (now Bayer Crop Science) in the laboratory of Seed Physiology under the supervision of Dr. Ruud Nabben. After that in 2011 she started her PhD research at Wageningen University under the supervsion of Prof. Dr. Maarten Koornneef, Dr. Mark G.M. Aarts, and Dr. Jeremy Harbinson, of which the result is lying in front of you. When her PhD-contract finished in 2015, she started a Postdoc position at Heinrich-Heine Universität in Düsseldorf in the laboratory of Developmental and Molecular Plant Biology under supervision of Prof. Dr. Peter Westhoff, where she currently works.

Publications

van Rooijen R, Aarts MGM, Harbinson J (2015) Natural genetic variation for acclimation of photosynthetic light use efficiency to growth irradiance in Arabidopsis. Plant Physiology **167**: 1412-1429.

Van Rooijen R, Boesten R, Kruijer W, van Eeuwijk FA, Harbinson J., Aarts MGM (*in preparation*) A regulator in anterograde signalling underlies natural variation for plant photosynthesis

Education Statement of the Graduate School

Experimental Plant Sciences

Issued to: **Roxanne van Rooijen**

Date: **5 July 2016**

Group: **Laboratory of Genetics**

University: **Wageningen University & Research**

1) Start-up phase	*date*
►	
First presentation of your project Genetic variation in Arabidopsis thaliana of photosynthesis parameters in response to abiotic stress	Sep 13, 2011
►	
Writing or rewriting a project proposal Genetic variation in Arabidopsis thaliana of photosynthesis parameters in response to abiotic stress	2012
►	
Writing a review or book chapter	
►	
MSc courses	
►	
Laboratory use of isotopes	

Subtotal Start-up Phase   7.5 credits*

2) Scientific Exposure	*date*
►	
EPS PhD student days 6th European Plant Science Retreat for PhD students in Experimental Plant Sciences, Amsterdam	Jul 03, 2014
EPS PhD Get2Gether, Soest	Jan 29-30, 2015
►	
EPS theme symposia	
EPS Theme 4 symposium 'Genome Biology', Wageningen University	Dec 09 2011
EPS Theme 3 symposium 'Metabolism and Adaptation', Utrecht University	Apr 26, 2012
EPS Theme 3 symposium 'Metabolism and Adaptation', University of Amsterdam	Mar 15, 2013
EPS Theme 4 symposium 'Genome Biology', Wageningen University	Dec 13 2013
►	
Lunteren days and other National Platforms Annual meeting 'Experimental Plant Sciences', Lunteren (NL)	Apr 02-03, 2012
Annual meeting 'Experimental Plant Sciences', Lunteren (NL)	Apr 22-23, 2013
Annual meeting 'Experimental Plant Sciences', Lunteren (NL)	Apr 14-15, 2014

▶	Annual meeting 'Experimental Plant Sciences', Lunteren (NL)	Apr 13-14, 2015

Seminars (series), workshops and symposia

seminars of invited spekers

Robert Furbank: 'Plant Phenomics, photosynthesis and the global food security challenge'	Sep 02, 2011
Neil Baker: 'Evaluation of the role of the water-water cycle as a mechanism for protecting the photosynthetic apparatus from high light'	Dec 06, 2011
Jennifer McElwain: "Impacts of global warming on plant biodiversity and ecosystem function"	Jan 20, 2012
Lauren McIntyre: 'Genotype to Phenotype mapping in a post-GWAS world'	Sep 17, 2012
Roy Wigger (BioRad): 'An introduction to qPCR and gene expression'	Oct 30, 2012
Tom Mitchell-Olds: 'Strong selection on the genes controlling complex traits in complex environments"	Dec 10, 2012
Nicole van Dam: 'Multiple-stress management: what we learn from plants?"	Dec 20, 2012
Andrew Sugden: 'Writing for high impact journals'	Feb 08, 2013
Detlef Weigel: "Arabidopsis thaliana as a model system for the study of evolutionary questions"	Feb 27, 2013
Graham Farquhar: "Integrating photosynthetic carbon assimilation from the leaf to the canopy"	Mar 13, 2013
Onno Muller: "Plant growth at cool temperature and bottlenecks of photosynthesis"	Jul 08, 2013
Plant Science seminar: "Plant Metabolomics"	Oct 08, 2013
Plant Science seminar: "Global Nutrient Cycles and Food security"	Nov 12, 2013
Eric Schranz: 'Whole genome duplications as drivers of evolutionary innovations and radiation"	Nov 21, 2013
Joy Bergelson; "Maintaining an ancient balanced polymorphism for resistance amidst diffuse interactions"	Sep 26, 2014
Ortrun Mittelsten Scheid:"Genetics and epigenetics: a complex relationship"	Nov 19, 2014
George Coupland: 'Seasonal flowering in annual and perennial plants'	Jan 19, 2015
Yves van de Peer: 'The evolutionary significance of gene and genome duplications'	Feb 03, 2015

Symposia

EPS Mini Symposium Plant breeding in the genomics era	Nov 25, 2011
Start symposium Plant Developmental Biology	Oct 14, 2013
Wageningen PhD Symposium	Dec 10, 2013
Symposium Measuring the Photosynthetic phenome	Jul 07-09, 2014
EPS Symposium "Omics Advances for Academia and Industry- Towards True Molecular Plant Breeding"	Dec 11, 2014

Workshops

Workshop "Bioinformatics, statistical genetics and genomics"	Mar 08, 2012
Workshop "Understanding the impact of crop characteristics on yield through crop growth modelling"	Mar 09, 2012

► **Seminar plus**	
► **International symposia and congresses**	
Honours class: Hacking the biological clock: circadian rhytm and photosynthesis, Lorentz Center, Leiden, NL	Apr 10-13, 2012
Next Generation Plant Science Symposium, Max Planck Institute, Cologne, Germany	Sep 26-28,2012
Workshop: Photosynthesis from Science to Industry, Noordwijkerhout, NL	Oct 08-11,2012
16th International Congress on Photosynthesis Research, St. Louis MO, USA	Aug 11-16, 2013
Plant Biology Europe FESPB/EPSO 2014 Congress, Dublin, Ireland	Jun 22-26, 2014
26th International Congress on Arabidopsis Research, Paris, France	Jul 05-09, 2015
►	
Presentations	
Annual meeting 'Experimental Plant Sciences', Lunteren - Title: 'Genetic variation for photosynthesis parameters in response to high light stress in Arabidopsis thaliana' (Poster)	Apr 02-03, 2012
Next Generation Plant Science Symposium, Cologne - Title: 'A genome-wide association study of the photosynthetic response to a light intensity increase in Arabidopsis thaliana' (Poster)	Sep 26-28,2012
Workshop: Photosynthesis from Science to Industry, Noordwijkerhout, NL (Talk)	Oct 11, 2012
EPS Theme 3 symposium 'Metabolism and Adaptation', Utrech, NL (Talk)	Mar 15, 2013
16th International Congress on Photosynthesis Research, St. Louis MO, USA - Title: 'Identifying genes in Arabidopsis thaliana for photosynthetic acclimation to increased irradiance' (Poster)	Aug 11-16, 2013
Annual meeting 'Experimental Plant Sciences', Lunteren, NL (Talk)	Apr 15, 2014
Plant Biology Europe FESPB/EPSO 2014 Congress, Dublin, Ireland (Talk)	Jun 23, 2014
6th European Plant Science Retreat for PhD students, Amsterdam, NL (Talk)	Jul 03, 2014
Annual meeting 'Experimental Plant Sciences', Lunteren, NL (Talk)	Apr 14, 2015
26th International Congress on Arabidopsis Research, Paris, France - Title: 'Natural genetic variation for photosynthetic acclimation to inceased irradiance in Arabidopsis' (Poster)	Jul 05-09, 2015
►	
IAB interview	
Meeting with a member of the International Advisory Board of EPS	Jan 05, 2015
Excursions	

Subtotal Scientific Exposure   *27.5 credits**

3) In-Depth Studies	*date*
►	
EPS courses or other PhD courses	
Postgraduate course Increasing Photosynthesis in Plants	Aug 21-26, 2011
Training course Association mapping	Feb 23, 2012

Summer School Natural Variation of Plants	Aug 20-24, 2012
Postgraduate Course Microscopy and Spectroscopy in Food and Plant Sciences	May 06-09, 2014
Postgraduate Course Introduction to R for statistical analysis	Oct 23-24, 2014
Postgraduate Course Genome Assembly	Apr 28-29, 2015
► **Journal club**	
Literature discussion group, Laboratory of Genetics	2011-2015
Literature and manuscript discussion group, Horticulture & Product Physiology Group	2011-2013
► **Individual research training**	

Subtotal In-Depth Studies   *8.4 credits**

4) Personal development	*date*
► **Skill training courses**	
Competence assessment	Jan 24 & Mar 27, 2012
Techniques for writing and presenting a scientific paper	Dec 04-07, 2012
Mobilising your scientific network	Jun 12 & 19, 2013
Data management	Feb 24, 2014
Reviewing a scientific paper	Jun 10, 2014
► **Organisation of PhD students day, course or conference**	
► **Membership of Board, Committee or PhD council**	

Subtotal Personal Development   *3.0 credits**

TOTAL NUMBER OF CREDIT POINTS*	**46,4**

Herewith the Graduate School declares that the PhD candidate has complied with the educational requirements set by the Educational Committee of EPS which comprises of a minimum total of 30 ECTS credits

* A credit represents a normative study load of 28 hours of study.